博士論文番号：1541025
(Doctoral student number)

Development of S-Glycosylated Porphyrins for Photodynamic Therapy Photosensitizers

(光線力学療法剤としてのチオグルコース連結ポルフィリン類の開発)

Arif Fadlan

Nara Institute of Science and Technology
Graduate School of Materials Science
Synthetic Organic Chemistry Laboratory

Supervisor: Prof. Kiyomi Kakiuchi

(Submitted on 2018/03/16)

Table of Contents

Arif Fadlan
January 2018
Graduate School of Materials Science

Development of S-Glycosylated Porphyrins

for Photodynamic Therapy Photosensitizers

(光線力学療法剤としてのチオグルコース連結ポルフィリン類の開発)

Abstract

Photodynamic therapy (PDT) is a regimen for cancer, age-related macular degeneration, and localized infections which combines photosensitizer (PS), a light source, and molecular oxygen for producing toxic reactive oxygen species (ROS) to kill the targeted cells in tissues. Recently, development for better PSs is an emerging and active research area. A chemical modification of PSs using sugars often called glycoconjugation has attracted considerable attention due to the beneficial structure of carbohydrates and their roles in many biological metabolisms. In line with this, here we report the development of S-glycosylated tetrakis(pentafluorophenyl)-porphyrin (TFPP)s for PDT PSs application.

In preparation of glycoconjugation, deoxythiolated D-glucose at the 2-, 3-, 4-, and 6-positions were synthesized. Starting with D-mannose, tetraacetyl 2-thio glucose (2-Ac-S-AcGlc) as β-anomer was obtained in 84% yield from tetraacetyl mannose 2-triflate which was prepared through orthoester formation of D-mannose and introduction of an acethylthio group by an S_N2 reaction. 3-Thiolated derivative was synthesized from commercially available diacetone D-glucose by oxidation and reduction followed by triflation, and acetylthiolation. And finally, the tetraacetyl 3-thio glucose (3-Ac-S-AcGlc) was afforded as α/β-anomeric mixture through transformation of furanose ring into the pyranose form. The tetraacetyl 4-thio glucose (4-Ac-S-AcGlc) as α/β-

anomeric mixture from D-galactose was synthesized in 55% yield from 4-triflated sugar derivative through its acetyl thiolation. The tetraacetyl 6-thio glucose (6-Ac-S-AcGlc) as β-anomer was obtained in 86% yield from the prepared tetraacetyl 6-tosyl D-glucose.

Conjugation of the obtained 2-, 3-, 4-, 6-Ac-S-AcGlcs with TFPP was performed by utilizing the S_NAr reactions to give the acetylated TFPP-glucose conjugates **2Ac** and **6Ac** as a β-anomer and **3Ac** and **4Ac** as α/β-anomeric mixture. Four mono-conjugated TFPP-glucose conjugates **2–4OH**, and **6OH** were obtained after removal of the acetyl groups and chromatographic purification in 11%, 20%, 31%, and 5% yield, respectively.

Scheme 1. Synthesis of TFPP-glucose conjugates

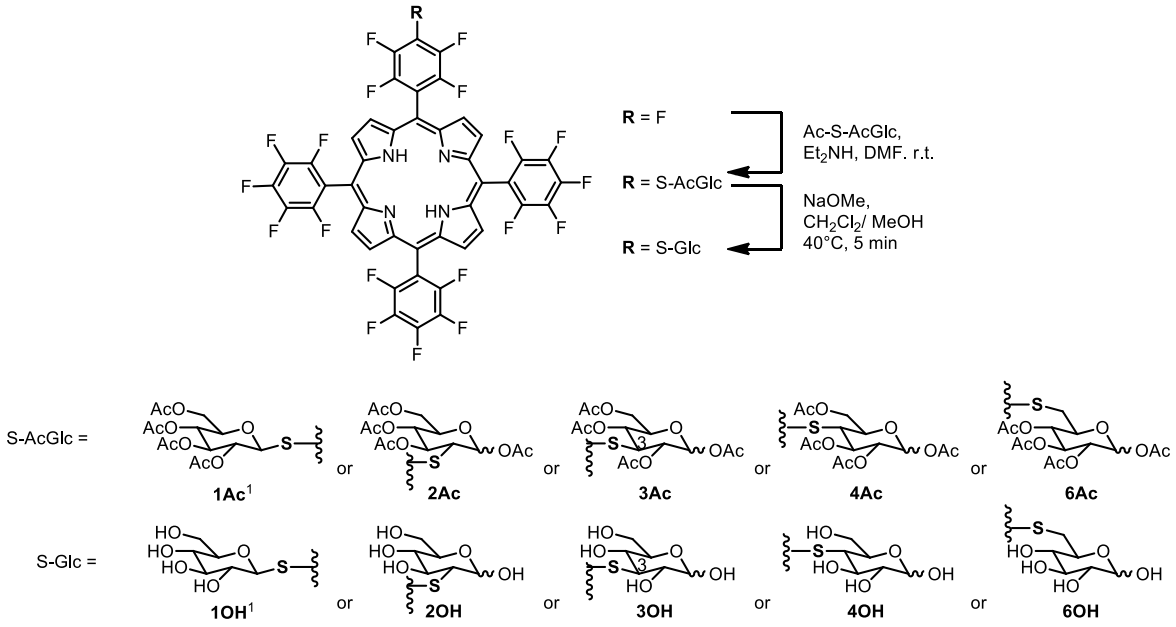

The relative quantum yields of $^1O_2$ generation (Φ_Δ) of **2–4OH**, and **6OH** illustrate no contrast of hydroxyphenyl fluorescein (HPF) fluorescence. However, similar to previously synthesized **1OH**, these conjugates generated higher •OHs compared to hematoporphyrin (HP). The order of

$\Phi_{\bullet OH}$ values was **2OH** < **1OH** < **4OH** < **3OH** << **6OH**. These conjugates prefer to produce ROS by the type I reaction. The cellular uptake evaluated by using an RGK gastric carcinoma mucosal cell line (RGK cells) indicated that the quantity of the conjugates linearly correlates with the increasing incubation time. Among them, **4OH** shows a significant activity. The cellular uptake investigation combining the RGK cells with cytochalasin B, an inhibitor of membrane-bound glucose transporter (GLUT1), notified slight inhibition with **2OH**, **3OH**, and **4OH**, indicating that these conjugates are partially affected by GLUT1. The photocytotoxicity in Human cervical cell line (HeLa cells) showed no cytotoxicity in the dark, but potent under photoirradiation with a 100 W halogen lamp except for **2OH**. A detailed photocytotoxicity evaluation performed in the concentration range from 0.1 to 1.0 μM revealed that **1OH**, **3OH**, and **4OH** showed a slight higher photocytotoxicity with lower concentration for 50% cell death (EC_{50}) compared to those of **2OH** and **6OH**. Further photocytotoxicity test using human glioblastoma cell line (U251 cells) and RGK cells displayed identical results to those in HeLa cells.

The multiconjugated TFPP-glucose conjugates including *cis*- and *trans*-disubstituted, trisubstituted, and tetrasubstituted compounds through sulfide bonds were synthesized by conjugation of TFPP with 3-Ac-S-AcGlc and 4-Ac-S-AcGlc. This conjugation was performed by controlling the ratio of 3-Ac-S-AcGlc and 4-Ac-S-AcGlc to TFPP.

List of Figures

List of Tables

List of Schemes

List of Abbreviations

ε	molar extinction coefficient
λ_{max}	maximum absorption wavelength
ALA	5-aminolevulinic acid
CL	cycloleucine
DEA	diethylamine
DLS	dynamic light scattering
DMF	dimethylformamide
DMPC	dimyristoylphosphatidylcholine
DMSO	dimethyl sulfoxide
EC_{50}	concentration inducing 50% cell death
GLUT1	membrane-bound glucose transporter
HP	hematoporphyrin
HPLC	high-performance liquid chromatography
HSV-1 and HSV-2	herpes simplex virus
HeLa cells	human cervical cell line
HPF	hydroxyphenyl fluorescein
HRMS	high-resolution mass spectrometry
$ID_{50}T$	dose for 50% decrease in CL transport
$ID_{50}G$	dose for 50% decrease in growth rate
J	coupling constant
K562 cells	human chronic myelogenous leukemia

Log *P*	hydrophobicity parameter
MALDI-TOF	matrix-assisted laser desorption/ionization time-of-flight
MDA-MB-231 cells	breast cancer cell
NMR	nuclear magnetic Resonance
PBS	phosphate buffer saline
PDC	pyridinium dichromate
PDT	photodynamic therapy
PSs	photosensitizers
RGK cells	gastric carcinoma mucosal cell line
ROS	reactive oxygen species
RP-TLC	reverse-phase thin layer chromatography
R_f	retention indices
S_0	ground singlet state
S_1	excited singlet state
S_NAr	aromatic nucleophilic substitution reaction
T_1	excited triplet state
TFPP	tetrakispentafluorophenyl porphyrin
TLC	thin-layer chromatography
TPPS	tetraphenylporphyrin sulfonic acid
U251	human glioblastoma cell line
k'	capacity factor
Φ_{1O2}	the relative quantum yield of singlet oxygen generation
$\Phi_{\bullet OH}$	the relative quantum yields of •OH

CHAPTER 1 General Introduction

1.1 Photodynamic Therapy: Principle and Mechanism

Photodynamic therapy (PDT) is an anticancer therapy. PDT combines photosensitizers (PSs), a light source, and tissue oxygen which produce toxic reactive oxygen species (ROS) for killing the targeted cells in tissues by apoptosis or necrosis [1-5]. Compared to conventional surgery, chemotherapy, and radiotherapy, PDT is a low-cost and simple treatment. Moreover, PDT is free from severe toxic side effects because the PSs itself is well-tolerated by the cells without cytotoxic effect in the absence of light. Additionally, PDT only disrupts the malignant cells by the cytotoxic PSs upon photoirradiation while keeps the normally cells [6-8]. These advantages bring PDT as a promising cancer treatment in the future.

Light source is one of the important factors in PDT. Light source for PDT including laser and non-laser sources/lamps determines the efficacy of PDT which reaches its peak when light is delivered in homogenous, adequate, and penetrate deep into the targeted tissues [9]. After photosensitizers are injected to the organ and a drug-to-light time interval, the irradiation is conducted on the targeted tissue [9,10]. In this step, oxygen in the targeted tissue is important for PDT processes. With light irradiation, the PSs are converted into the excited singlet state (S_1) from the ground state (S_0) followed by the excited triplet state (T_1) through intersystem crossing. This T_1 state form generates the two different photochemical reactions. In Type I reaction, T_1 form reacts directly with biological components like plasma membrane, peptides, proteins, and nucleic acids to generate their radicals or radical ions which can interact with triplet state of oxygen ($^3O_2$) and water to produce superoxide anions ($O_2^{\bullet -}$) and hydroxyl radicals (HO•). On the other hand, the T_1 form participates in the energy transfer of $^3O_2$ into the cytotoxic singlet oxygen ($^1O_2$) in Type

II reaction [8,10]. These two types of reactions take place instantaneously and deliver their cytotoxic effect to the locally-irradiated area due to the short lifetime of the generated reactive oxygen species (ROS) and their diffusion distance [9]. These all cytotoxic reactive oxygen species damage the cell organelles including membrane, mitochondria, lysosome, etc. and finally kill the cells. This mechanism is shown in the Figure 1.1.

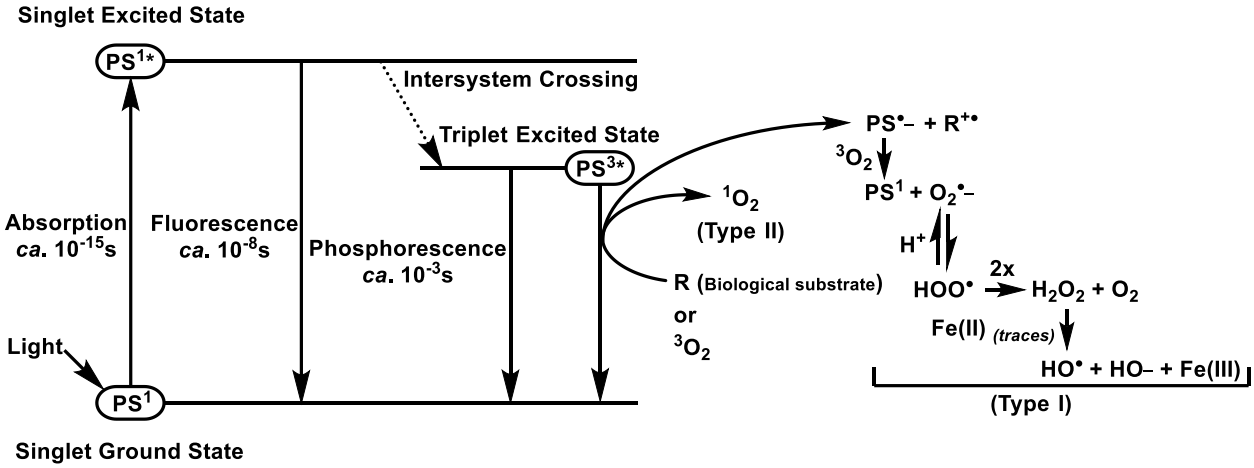

Figure 1.1 Scheme of Type I and Type II PDT

1.2 Photosensitizers (PSs)

PSs are (natural or synthetic) molecules that absorb light and transfer the energy to other species or to trigger the photochemical reactions in order to produce ROS [11,12]. The ideal PS involves the following : availability of PSs produced from an efficient and reproducible synthetic route in pure form; no or low toxicity in the dark; stable and soluble in aqueous media; rapid selective accumulation and fast clearance; high-molar extinction coefficient in the 600-1000 nm range of wavelength; high quantum yield for ROS generation [13-15]. PSs include porphyrin or non-porphyrin based structures. Phthalocyanines, chlorins, bacteriochlorin, and protoporhyrin IX obtained from 5-aminolevulinic acid (ALA) through biosynthetic process are PSs with porphyrin

1) General

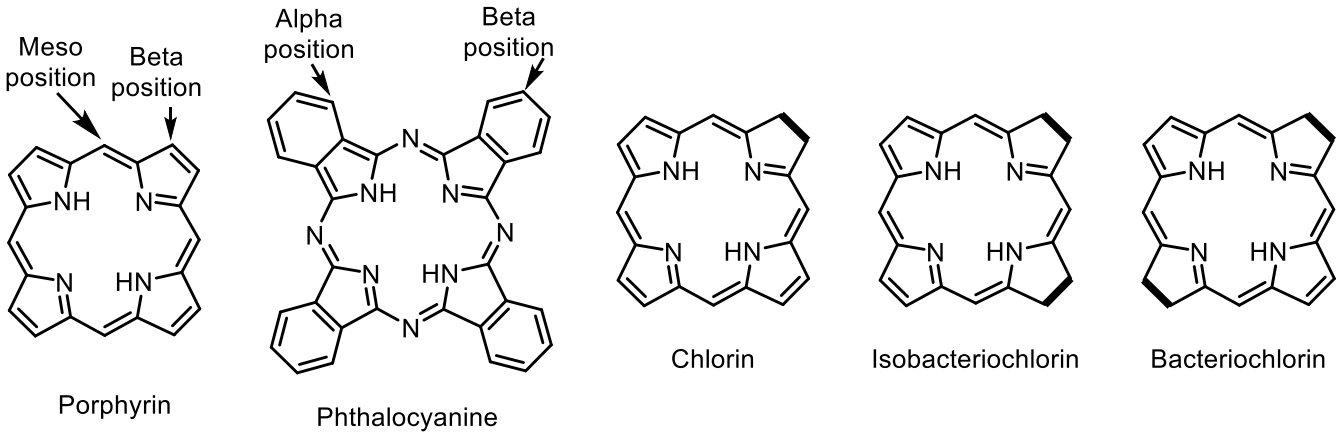

2) Porphyrin based

a) First generation

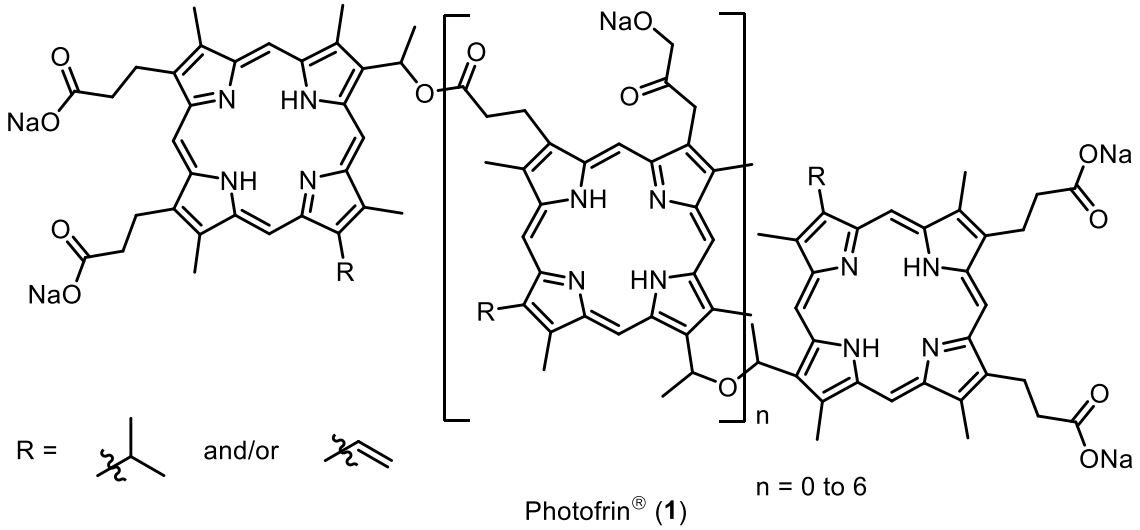

Photofrin® (**1**)

b) Second generation

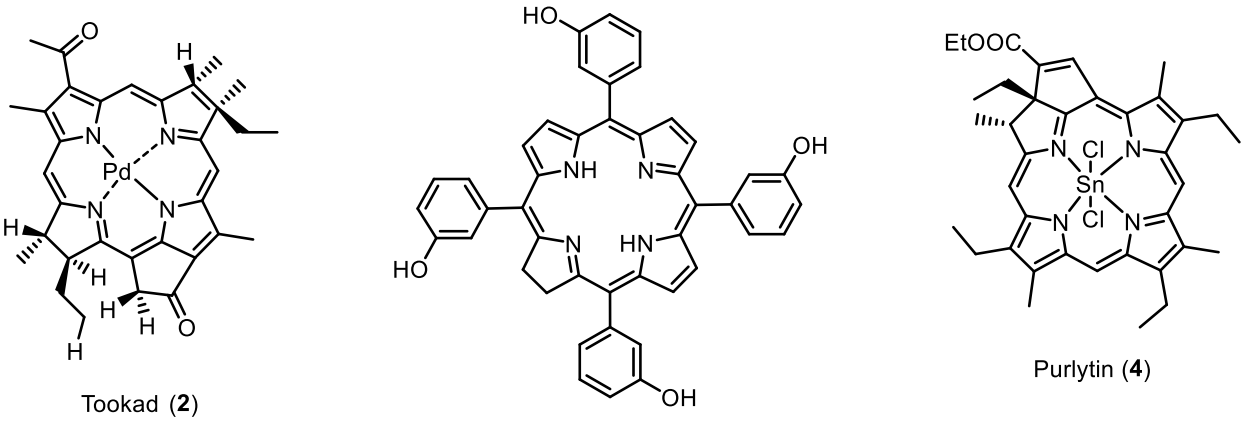

Tookad (**2**) Foscan (**3**) Purlytin (**4**)

Figure 1.2 Structure of PDT photosensitizers

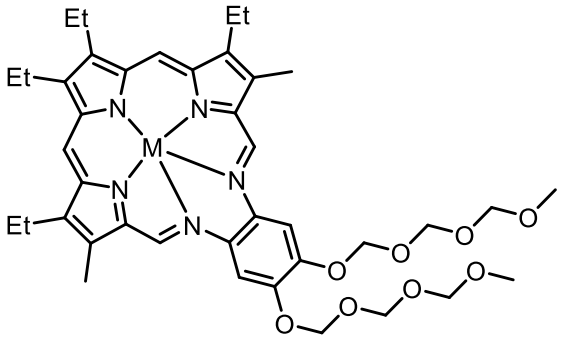

Lutrin (**5**)

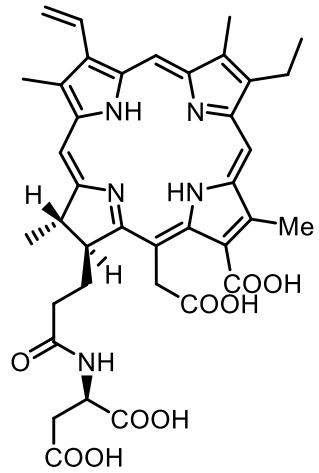

Laserphyrin (**6**)

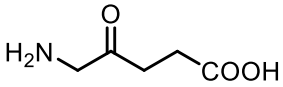

5-Aminolevulinic acid (Levulan, **7**)

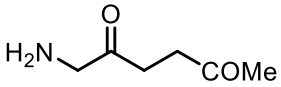

Metvix (**8**)

3) Non-porphyrin based

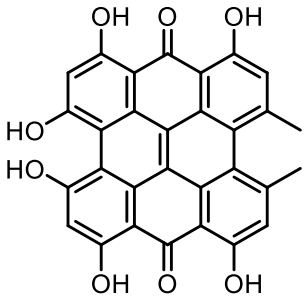

Hypericin (**9**)

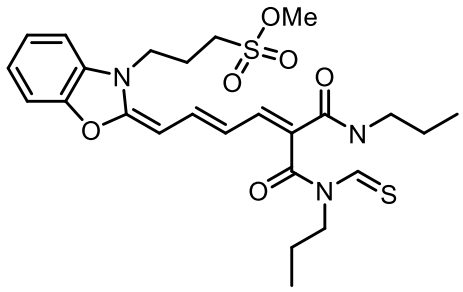

Merocyanine 540 (**10**)

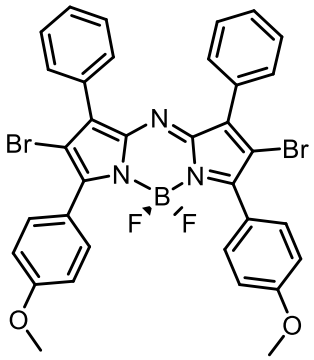

ADPM06 (**11**)

Figure 1.2 Structure of PDT photosensitizers (continued)

Table 1.1 Characteristics of several photosensitizers [21]

Photosensitizer	First generation	Second generation						
	Photofrin (**1**)	Tookad (**2**)	Foscan (**3**)	Purlytin (**4**)	Lutrin (**5**)	Laser-Phyrin(**6**)	Levulan (**7**)	Metvix (**8**)
Absorption (nm)	630	763	652	664	732	664	635	635
Localization	Golgi apparatus, plasma membrane	Vasculature	Endoplasmic reticulum (ER), mitochondria	Mitochondria, lysosomes	Lysosome	Lysosome, endosome	Mitochondria, cytosol, cytosolic membranes	Mitochondria, cytosol, cytosolic membranes
Primary mechanism of action	Vascular damage and ischemic tumor cell necrosis	Vascular damage	Vascular damage and direct tumor cytotoxicity	Direct tumor cytotoxicity	Vascular damage and direct tumor cytotoxicity	Vascular stasis and direct tumor cytotoxicity	Direct tumor cytotoxicity	Direct tumor cytotoxicity
Most commonly employed drug-light interval	24-48 h	15 min	96 h	24 h	3 h	2-4 h	4-6 h	3 h
Clinical/ preclinical application	Approved: Esophageal cancer, lung cancer, microinvasive endobronchial cancer, gastric and pappilary bladder, cervical, dysplasia and cancer	Clinical trials: Prostate cancer	Approved: Head and neck cancer	Clinical trials: Metastatic breast cancer, AIDS-related Kaposis sarcoma, basal cell carcinomas	Clinical trials: Recurrent prostate cancer, cervical cancer Preclinical testing: Recurrent breast cancer	Approved (Japan): Early lung cancer Clinical trials: Hepatocellular cancer, Liver metastatis	Approved: Actinic keratosis	Approved: Actinic keratosis, basal cell carcinoma
Most common local side effects	Mild to moderate erythema		Swelling, bleeding, ulceration, scarring				Stinging, burning, itching, erythema	Burning sensation, redness, scabbing
Most common systemic side effects	Photosensitivity, mild constipation	–	Photosensitivity	Photosensitivity	Photosensitivity (minima)	–	–	–
Clinically approved?	Yes	No	Yes	No	No	Yes (Japan)	Yes	Yes

Table 1.1 Characteristics of several photosensitizers (continued) [21]

Photosensitizer	Hypericin (**9**)	Phenothiazinium dye-methylene Blue	Phenothiazinium dye-toluidine Blue	Merocyanine 540 (**10**)	ADPM06 (**11**)
Absorption (nm)	595	666	626,632	535-574	680
Localization	Membrane of endoplasmic reticulum (ER), membranes of Golgi	Lysosome	ER, Golgi apparatus	Mitochondria, plasma membrane	ER, mitochondria
Primary mechanism of action	Tumor cell cytotoxicity and vascular damage	Tumor cell and cytotoxicity	Tumor cell and cytotoxicity	Tumor cell and cytotoxicity	Vascular-targeted
Most commonly employed drug-light interval	0.5-6 h	1-4 h	1 h	1 h	< 5 min
Clinical/ preclinical application	Preclinical testing: Bladder cancer, nasopharyngeal cancer	Preclinical testing: Bladder cancer, colon cancer, AIDS-related Kaposi's sarcoma	Preclinical testing: AIDS-related Kaposi's sarcoma, T-cell sarcoma	Preclinical testing: Leukimia, lymphoma	Preclinical testing: Breast cancer, mouse lung cancer
Most common local side effects	Slight damage to surrounding normal tissue	–	–	–	–
Most common systemic side effects	–	–	Minimal side effects	Minimal side effects	–
Clinically approved?	No	No	No	No	No

based structure, while psoralens, anthracyclines, hypericin, hypocrellins, cyanines, and phenothiazinium compounds i.e. methylene blue, Nile blue analogs, toluidine blue, rhodamines, triarylmethanes, and acridine are examples of PSs with non-porphyrin based structure [16-21]. Porphyrin-based PSs are mainly divided into the first, second, and third generations. Hematoporphyrin (HpD) and its derivatives, HpD, and partially-purified of hematoporphyrin, porfimer sodium (Photofrin®) are the first generation PSs which have been approved to be used in several cancers and is widely used in PDT treatment up to this day. However, several problems arise from the usage of this first generation i.e. use as mixtures of various porphyrins, low selectivity, and slow clearance results in the long-lasting photosensitivity [1,22-27]. To resolve these problems, the second generation PSs were developed. These include verteporfin, visudyne, and Foscan®. The third generation PSs were established for enhancing the selectivity, bioavailability, and targeting the tumor tissue by conjugation of the first and second generation PSs to biomolecules, like carbohydrates, proteins, peptides, cholesterol, antibodies, and liposomes [12,14]. Figure 1.2 shows the structures of several PSs and Table 1.1 summarizes the characteristics of the PSs.

1.3 Glycoconjugated Porphyrin Derivatives

Searching for new PSs is an emerging and active research area nowadays because of the limited number of PSs clinically approved. The low selectivity of PSs in tumor cells gives the chance to modify the first or second generation PSs by attaching them to vectors/carriers that deliver PSs to tumor cells precisely [14,15,28]. Among other conjugation of PSs to biologically active materials, glycoconjugation has attracted attention since carbohydrates are the major natural compounds [29-31] and it includes in several diseases such as cancer, immune dysfunction, congenital disorders,

and infectious diseases [29,30,32,33]. Furthermore, carbohydrates can accurately lead the binding process to the receptors on the cell surface [34-40] and tune the amphiphilic features to regulate the biodistribution [28]. This new class of PSs which are often called glycoporphyrins covers the coupling of one or more carbohydrate units to the porphyrin cores by glycosidic or other bonding with or without spacers/linkers [28]. The spacers/linkers between the porphyrin and the carbohydrate units can be positioned at either *meso* or β positions in porphyrin structures and the carbohydrate units can be linked to the porphyrins through heteroatoms bonding like nitrogen, sulfur, carbon, and oxygen. (Figure 1.3). The glycosides themselves can act as spacers/linkers. The glycoporphyrins can be obtained by the following methods: (1) cyclization of glycosylated benzaldehydes with pyrroles to form the desired porphyrin macrocycles by the Lindsey, Adler, McDonald or Little methods; (2) glycosylation of pre-made porphyrins from various benzaldehydes with spacers/linkers or carbohydrate units; (3) acylation of amino groups or hydroxy group with carboxylic acids to obtain the conjugates through stable amide bonds; (4) direct nucleophilic substitution to the porphyrin cores. A number of different *meso*-substituted porphyrins can be afforded from the method (1) by modification of the structure of benzaldehydes, but it usually gives low yields. The method (2) offers building small libraries of compounds. This can evaluate the effect of the numbers and the collecting positions of carbohydrate units on their activities. This is also advantageous on a clean reaction regarding the cyclization step of porphyrins [41,42]. Through these synthetic methods, numerous glycoporphyrins have been studied along with their photophysical characteristics, *in vitro* cytotoxicity, and cellular uptake. The structures of reported glycoporphyrins is presented in the Figure 1.3 and their properties are tabulated in the Table 1.2.

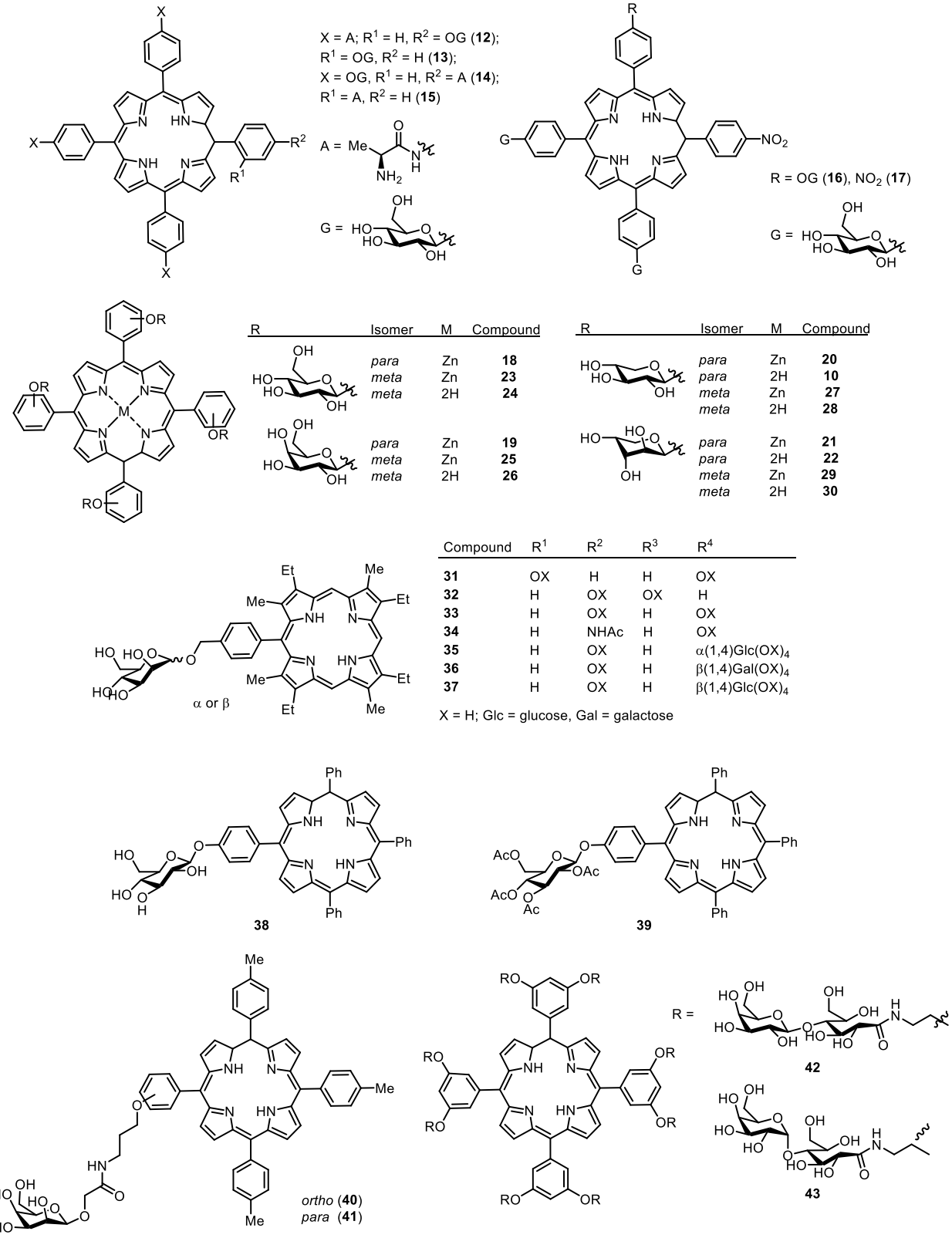

Figure 1.3 Structures of some glycoporphyrins

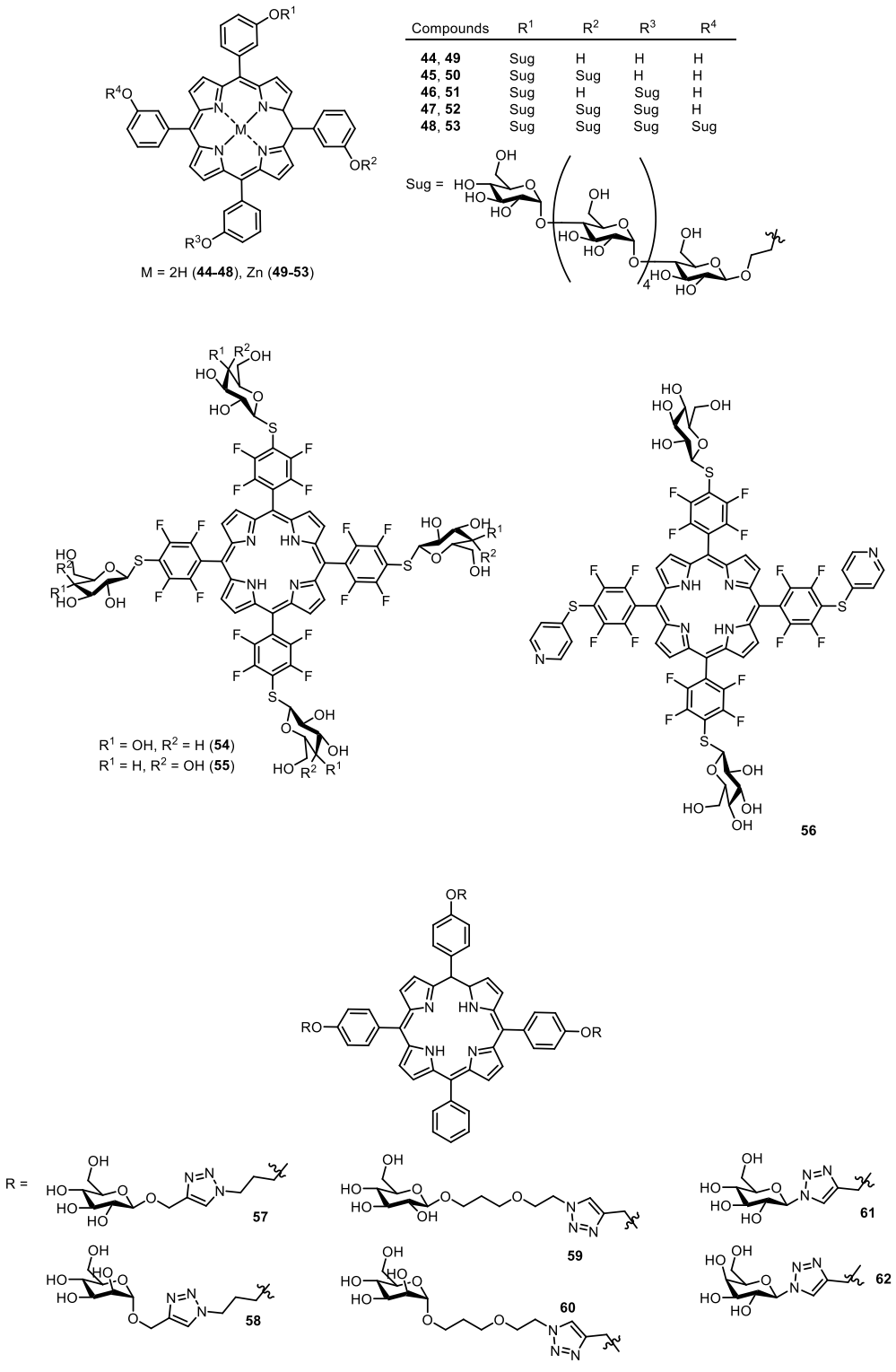

Figure 1.3 Structures of some glycoporphyrins (continued)

Table 1.2 Characteristics of some glycoporphyrins

Compound	Preparation	*in vitro*	Comments	Ref.
12-**15**	Lindsey method	Human chronic myelogenous leukemia (K562 cells)	The percentage of cell survival is low (< 10%) at a concentration 2 μM and under irradiation for 100 min. The percentage of cell survival is 10% with **15** after 24 h irradiation	52
16,**17**	Lindsey method	*Staphylococcus aureus*, *Escherichia coli*	The conjugates **16** and **17** are bactericidal to *S. aureus*	53
18-**30**	Template synthesis and a modified Lindsey method	HeLa cells	None of these conjugates shows cytotoxicity in the dark, in contrast almost all of these conjugates shows photocytotoxicity (except for **18**, **27**). The conjugates have identical electronic absorption spectra in DMSO, but have different one in phosphate buffer containing 10%w/w of bovine serum albumin (BSA).	54, 55, 56, 57, 58
31-**37**	Glycosylation	Phosphatidylethanolamine (PE) liposomes and dimyristoylphosphatidylcholine (DMPC) liposomes.	The binding constant for DMPC liposomes is lower than for PE liposomes. The conjugate **37** shows the highest binding constant with PE.	59
38,**39**	Glycosylation	Vero cells infected with the herpes simplex virus (HSV-1 and HSV-2)	The maximum concentration of **38**,**39** for non-infected cells is 15-30 ppm, and 100 ppm and 1000 ppm for Acyclovir and Foscarnet as standard, respectively.	60
40,**41**	Acylation	K562 cells	The cell survival evaluation for **40** is higher than **41**.	61
42,**43**	Acylation	RLC-16 hepatocytes	The conjugate **42** is attached to the cells, but not for **43**.	62
44-**53**	Nucleophilic substitution	HeLa cells	All conjugates show no cytotoxicity in the dark. The conjugates **44** and **49** show the highest photocytotoxicity upon irradiation. The cis- conjugate **45** displays higher photocytotoxicity compared to trans- conjugate **46**.	63
54-**56**	Nucleophilic substitution	Breast cancer cell (MDA-MB-231 cells), rat fibroblasts (3Y1, $3Y1^{c\text{-}Src}$, $3Y1^{v\text{-}Src}$)	The cellular uptake of **54** is higher 2 times than **55**. The conjugate **54** show minimal affinity to healthy 3Y1 cells, but high for $3Y1^{v\text{-}Src}$. The cellular uptake increases with increasing incubation time. The cell survival after 24 h of incubation reaches 20%.	50, 64
57-**62**	Microwave-assisted 1,3-dipolar cycloaddition	Y79 cells, HT-29 cells	None of these conjugates show cytotoxicity in the dark. The photocytotoxicity of **57**-**62** to Y79 cells is 10-20 times higher than that for HT-29 cells. The conjugate **61** is the best.	65

1.4 Object and Outline of The Thesis

As one of key components in PDT, photosensitizers determine the performance of PDT treatment. Porphyrin-based photosensitizers lead in PDT application, but the first generation photosensitizers show various problems as shown in section 1.2. Thus, second generation as well as third generation photosensitizers rise to respond this fact. Manipulation of photochemotherapeutic properties of photosensitizers can be accomplished by structural modification of photosensitizers. Sugar-conjugated photosensitizers have been developed and a considerable amount of this photosensitizers have been synthesized. A study of *in vitro* and *in vivo* photocytotoxicity along with photophysical properties and cellular uptake of sugar-conjugated photosensitizers indicate that sugar moiety affects the high cellular uptake and photocytotoxicity [41,43-45].

Kessel and co-workers reported their work on conjugation of tetraphenylporphyrin (TPP) with sulfonic acid (i.e. mono-, bis *cis*-, bis *trans*-, tri-, and tetra-sulfonic acids) (**63**-**67**) (Figure 1.4). Photocytotoxicity data in cycloleucine (CL) clearly say that when intracellular drug concentrations in the dose for 50% decrease in CL transport ($ID_{50}T$) upon irradiation were compared, the bis *cis*-sulfonic acid product (**64**) to be the most potent of the analogs, with bis *trans*- (**65**), tri- (**66**), tetra- (**67**), and mono-sulfonic acid (**63**) progressively less effective. The external and corresponding intracellular drug concentrations which mediate a 50% decrease in cell growth ($ID_{50}G$) upon irradiation also gave the same trend with the $ID_{50}G$ concentration of bis *cis*- product (**64**) was only slightly greater than the $ID_{50}T$ [46]. Furthermore, in order to explore the effect of substitution patterns on the photocytotoxicity of glycoconjugated porphyrins, a 'complete set' of tetrakis(pentafluorophenyl)porphyrins (TFPP) (namely, mono-, bis *cis*-, bis *trans*-, tri-, and tetra-glucoses) (**68**-**72**) having 1-β-D-glucopyranosylthio group obtained from tetraacetyl-1-β-D-thioglucopyranose (**73**) on the phenyl ring have been synthesized and characterized (Figure 1.4).

The results indicating a close correlation between photocytotoxicity and cellular uptake revealed that bis *trans*- product (**70**) showed an uptake and phototcytotoxicity that was three-fold and twenty-fold greater than those of the other conjugates (**68**,**69**,**71**,**72**). This finding imply that the substitution number and pattern greatly influence the overall effect of the photosensitizers [47].

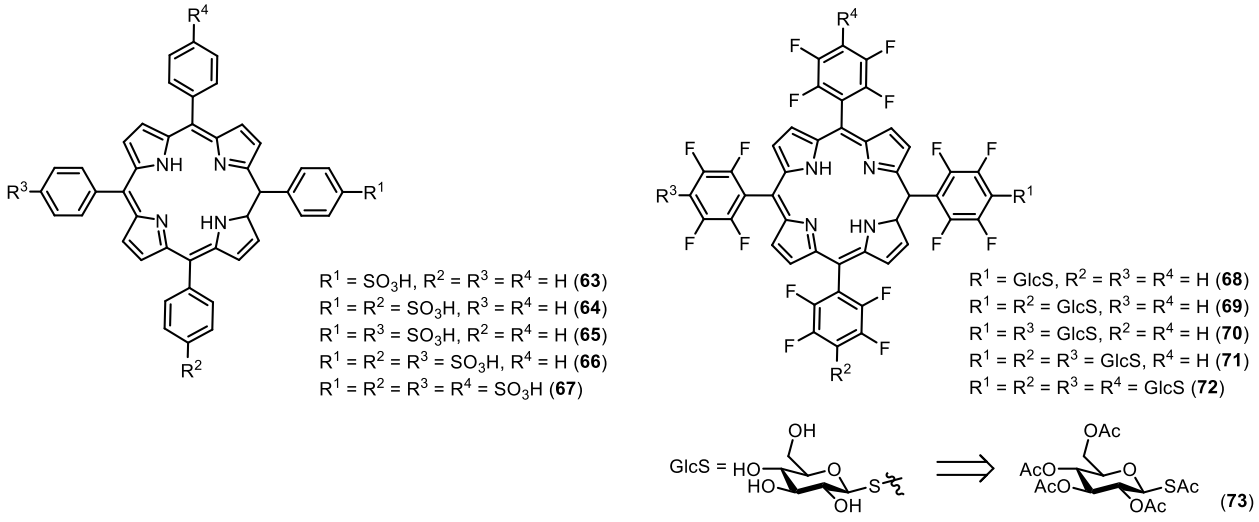

Figure 1.4 Previous reported glycoconjugated porphyrins (46,47)

In line with this fact, this thesis reports the study on the development of S-glycosylated porphyrins for PDT photosensitizers. As for porphyrin system, tetrakis(pentafluorophenyl)-porphyrins (TFPP) was chosen due to the reactivity of fluorine at the *para*- position of pentafluorophenyl group [48-50]. Also, to enhance the biochemical stability and enzymatic resistance as well as give better selectivity and specificity of the resulted photosensitizers [50,51], *S*-glycoside linkage is used instead of *O*-glycoside in this study. Sulfur has lower tendency to form acid conjugate for hydrolysis due to its weaker Lewis base properties and lower affinity for proton compared to oxygen [50].

Previous studies noted that only 1-β-D-thioglucopyranose obtained from tetraacetyl-1-β-D-

thioglucopyranose (**73**) was reported and there were no records on the other thioglucoses [47]. This fact strongly motivates this research and the development of PDT photosensitizers in this research is expanded by using 2-, 3-, 4-, and 6-thioglucopyranoses resulted from tetraacetyl-2-thioglucopyranose (**2-Ac-S-AcGlc**), tetraacetyl-3-thioglucopyranose (**3-Ac-S-AcGlc**), tetraacetyl-4-thioglucopyranose (**4-Ac-S-AcGlc**), and tetraacetyl-6-thioglucopyranose (**6-Ac-S-AcGlc**) (Figure 1.5). The development includes mono-glycoconjugated porphyrins of positional isomer of 2-,3-,4-,6-thioglucoses (**2-4OH**, **6OH**) and multi-glycoconjugated porphyrins of promising thioglucose resulted from monoconjugation (**3-TFPP(SGlc)$_{trans\text{-}2}$**, **3-TFPP(SGlc)$_{cis\text{-}2}$**, **3-TFPP(SGlc)$_3$**, **3-TFPP(SGlc)$_4$**, **4-TFPP(SGlc)$_{trans\text{-}2}$**, **4-TFPP(SGlc)$_{cis\text{-}2}$**, **4-TFPP(SGlc)$_3$**, and **4-TFPP(SGlc)$_4$**). The first object in this research, mono-glycoconjugated porphyrins of positional isomer of 2-,3-,4-,6-thioglucoses, is addressed to understand the effect of thioglucose positional isomers on their photophysical properties, cellular uptake, and photocytotoxicity. Whereas the multi-glycoconjugated porphyrins as the second object are to direct the systematic study on the photophysical properties, cellular uptake, and photocytotoxicity of a complete set of glycoconjugated porphyrins.

Figure 1.5 Structure of **2-Ac-S-AcGlc**, **3-Ac-S-AcGlc**, **4-Ac-S-AcGlc**, and **6-Ac-S-AcGlc**

In order to achieve that research motivation, a strategy is applied to this research. The mono-glycoconjugated porphyrins (**2-4OH**, **6OH**) is converted to intermediate acetylated mono-glycoconjugated porphyrins (**2-4Ac**, **6Ac**), first, and then they are should be constructed from

tetrakis(pentafluorophenyl)-porphyrins (TFPP) and tetraacetyl-2-, 3-, 4-, and 6-thioglucopyranose (**2-Ac-S-AcGlc**, **3-Ac-S-AcGlc**, **4-Ac-S-AcGlc**, and **6-Ac-S-AcGlc**). The strategy in this research is broken down as follow : 1) synthesis of tetraacetyl-2-, 3-, 4-, and 6-thioglucopyranose (**2-Ac-S-AcGlc**, **3-Ac-S-AcGlc**, **4-Ac-S-AcGlc**, and **6-Ac-S-AcGlc**) which is introduction of acetylthio group by S_N2 reaction, 2) synthesis of mono-glycoconjugated porphyrins (**2-4OH**, **6OH**) by utilizing aromatic S_N reaction and deprotection, 3) *in vitro* study of mono glycoconjugated porphyrins which includes photophysical properties, cellular uptake, and photocytotoxicity, and 4) synthesis of multi-glycoconjugated porphyrins (**3-TFPP(SGlc)$_{trans\text{-}2}$**, **3-TFPP(SGlc)$_{cis\text{-}2}$**, **3-TFPP(SGlc)$_3$**, **3-TFPP(SGlc)$_4$**, **4-TFPP(SGlc)$_{trans\text{-}2}$**, **4-TFPP(SGlc)$_{cis\text{-}2}$**, **4-TFPP(SGlc)$_3$**, and **4-TFPP(SGlc)$_4$**) by harnessing aromatic S_N reaction and deprotection (Figure 1.6).

This thesis is outlined as follow. In Chapter 2, the preparation of tetraacetyl-2-, 3-, 4-, and 6-thioglucopyranose (**2-Ac-S-AcGlc**, **3-Ac-S-AcGlc**, **4-Ac-S-AcGlc**, and **6-Ac-S-AcGlc**) toward porphyrin conjugation through sulfide bonding is presented. Chapter 3 explains the conjugation of these tetraacetyl-2-, 3-, 4-, and 6-thioglucopyranose (**2-Ac-S-AcGlc**, **3-Ac-S-AcGlc**, **4-Ac-S-AcGlc**, and **6-Ac-S-AcGlc**) with tetrakis(pentafluorophenyl)-porphyrins (TFPP) giving the mono-glycoconjugated porphyrins (**2-4OH**, **6OH**). The photophysical properties, cellular uptake, ROS generation, and *in vitro* photocytotoxicity experiments of the obtained conjugates (**2-4OH**, **6OH**) are displayed in Chapter 4. Chapter 5 informs the conjugation experiment of tetraacetyl-3-, and 4-thioglucopyranose (**3-Ac-S-AcGlc**, **4-Ac-S-AcGlc**) with tetrakis(pentafluorophenyl)-porphyrins (TFPP) producing the intermediate acetylated multi-glycoconjugated porphyrins (**3-TFPP(SAcGlc)$_{trans\text{-}2}$**, **3-TFPP(SAcGlc)$_{cis\text{-}2}$**, **3-TFPP(SAcGlc)$_3$**, **4-TFPP(SAcGlc)$_{trans\text{-}2}$**, **4-TFPP(SAcGlc)$_{cis\text{-}2}$**, **4-TFPP(SAcGlc)$_3$**, and **4-TFPP(SAcGlc)$_4$**). Lastly, Chapter 6 summarizes the results of the this study.

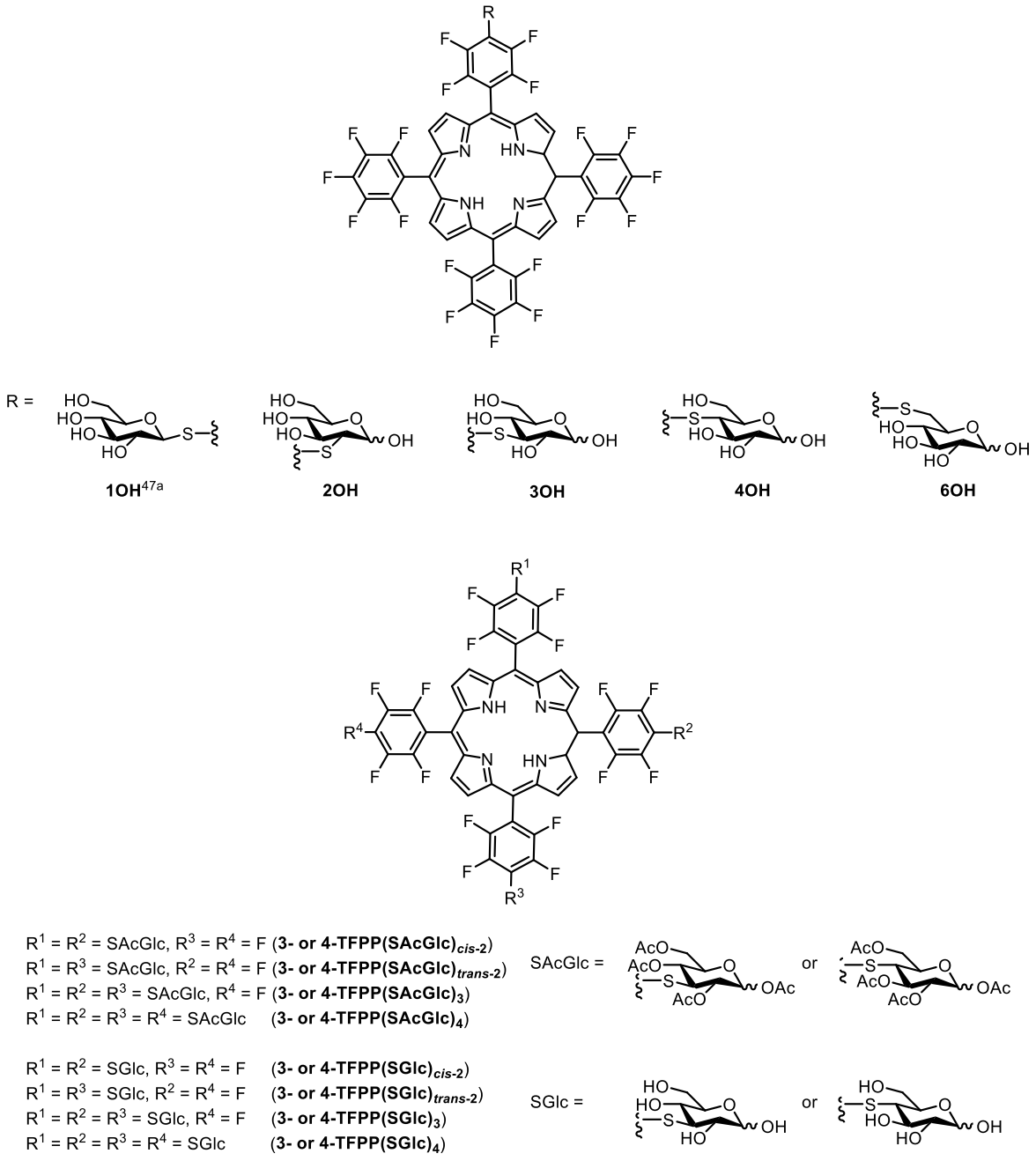

Figure 1.6 The objects of this research

1.5 References

1. Kessel, D. *Photodiagn. Photodyn. Ther.* **2004**, *1*, 3.

2. Abdel-Kader, M. H. *History of Photodynamic Therapy in Photodynamic Therapy From Theory to Application*.; Ed. Abdel-Kader. Springer-Verlag Berlin 2014. p. 3-24.
3. Luo, Y.; Kessel, D. *Photochem. Photobiol.* **1997**, *66*, 479.
4. Mroz, P.; Yaroslavsky, A.; Kharkwal, G. B.; Hamblin, M. R. *Cancers* **2011**, *3*, 2516.
5. Soriano, J.; Mora-Espí, I.; Alea-Reyes, M. E.; Péres-García, L.; Barrios, L.; Ibánez, E.; Nogues, C. *Sci. Rep.* **2017**, *7*, 41340.
6. Pandey, R. K. *J. Porphyrins Phthalocyanines* **2000**, *4*, 368.
7. Hammerer, F.; Garcia, G.; Chen, S.; Poyer, F.; Achelle, S.; Fiorini-Debuisschert, C.; Teulade-Fichou, M-P.; Mailard, P. *J. Org. Chem.* **2014**, *79*, 1406.
8. Fan, W.; Huang, P.; Chen, X. *Chem. Soc. Rev.* **2016**, *45*, 6488.
9. Debele, T. A.; Peng, S.; Tsai, H-C. *Int. J. Mol. Sci.* **2015**, *16*, 22094.
10. Dąbrowski, J. M.; Arnaut, L. G. *Photochem. Photobiol. Sci.* **2015**, *14*, 1765.
11. Allison, R.R.; Moghissi, K. *Clin. Endosc.* **2013**, *46*, 24.
12. Deda, D. K. Araki, K. *J. Braz. Chem. Soc.* **2015**, *26*, 2448.
13. Mehraban, N.; Freeman, H. S. *Materials* **2015**, *8*, 4421.
14. Yoon, I.; Li, J. Z.; Shim, Y. K. *Clin. Endosc.* **2013**, *46*, 7.
15. Ethirajan, M.; Chen, Y.; Joshi, P.; Pandey, R. K. *Chem. Soc. Rev.* **2011**, *40*, 340.
16. Allison, R. R.; Sibata, C. H. *Photodiagn. Photodyn. Ther.* **2010**, *7*, 61.
17. Ormond, A. B.; Freeman, H. S. *Materials* **2013**, *6*, 817.
18. Zhu, T. C.; Finlay, J. C. *Med. Phys.* **2008**, *35*, 3127.
19. Wainwright, M. *Chem. Soc. Rev.* **1996**, *25*, 351.
20. Sternberg, E. D.; Dolphin, D. *Tetrahedron* **1998**, *54*, 4151.
21. O'Connor, A. E.; Gallagher, W. M.; Byrne, A. T. *Photochem. Photobiol.* **2009**, *85*, 1053.

22. Boyle, R. W.; Dolphin, D. *Photochem. Photobiol.* **1996**, *64*, 469.

23. Zhang, Y.; Lovell, J. F. *Theranostics* **2012**, *2*, 905.

24. Bonnett, R. *Chemical Aspects of Photodynamic Therapy*; Gordon and Breach Science Publishers, CRC Press: Boca Raton, FL, 2000.

25. Yano, S.; Hirohara, S.; Obata, M.; Hagiya, Y.; Ogura, S.; Ikeda, A.; Kataoka, H.; Tanaka, M.; Joh, T. *J. Photochem. Photobiol. C: Photohem. Rev.* **2011**, *12*, 46.

26. Moser, J. G. Definition and General Properties of 2nd and 3rd Generation Photosensitizers. In *Photodynamic Tumor Therapy, 2nd and 3rd Generation Photosensitizers*; Moser, J. G., Ed.; Harwood Academic Publishers: The Netherlands, 1998.

27. Wu, J.; Han, H.; Jin, Q.; Li, Z.; Li, H.; Ji, J. *ACS Appl. Mater. Interfaces* **2017**, *9*, 14596.

28. Titov, D. V.; Gening, M. L.; Tsvetkov, Y. E.; Nifantiev, N. E. *Russ. Chem. Rev.* **2014**, *83*, 523.

29. Waki, A.; Fujibayashi, Y.; Yokoyama, A. *Nucl. Med. Biol.* **1998**, *25*, 589.

30. Calvaresi, E. C.; Hergenrother, P. J. *Chem. Sci.* **2013**, *4*, 2319.

31. Zheng, G.; Graham, A.; Shibata, M.; Missert, J. R.; Oseroff, O. R.; Dougherty, T. J.; Pandey, R. K. *J. Org. Chem.* **2001**, *66,* 8709.

32. Comellas-Aragones, M.; Chowdhury, S.; Bentley, P.; Kaczanowska, K.; BenMohamed, L.; Gildersleeve, J. C.; Finn, M. G.; Huang, X. *ACS Chem. Biol.* **2013**, *8*, 1253.

33. Orlean, P. *J. Clin. Invest.* **2000**, *105*, 131.

34. Ballut, S.; Makky, A.; Chauvin, B.; Michel, J-P.; Kasselouri, A.; Maillard, P.; Rosilio, V. *Org. Biomol. Chem.* **2012**, *10*, 4485.

35. Lafonta, D.; Zorlub, Y.; Savoiec, H.; Albrieuxd, F.; Ahsenb, V.; Boylec, R. W.; Dumoulin, F. *Photodiagnosis Photodyn. Ther.* **2013**, 10, 252.

36. MacDonald, I. J.; Dougherty, T. J. *J. Porphyrins Phthalocyanines* **2001**, *5*, 105.

37. Liu, J-Y.; Lo, P-C.; Fong, W-P.; Ng, D. K. P. *Org. Biomol. Chem.* **2009**, *7*, 1583.

38. Daly, R.; Vaz, G.; Davies, A. M.; Senge, M. O.; Scanlan, E. M. *Chem. Eur. J.* **2012**, *18*, 14671.

39. Sears, P.; Wong, C. H. *Angew. Chem., Int. Ed.* **1999**, *38*, 2300.

40. Lee, Y. C.; Lee, R. T. C. *Acc. Chem. Res.* **1995**, *28*, 321.

41. Singh, S.; Aggarwal, A.; Bhupathiraju, N. V. S. D. K.; Arianna, G.; Tiwari, K.; Drain, C. M. *Chem. Rev.* **2015**, *115*, 10261.

42. Moylan, C.; Scanlan, E. M.; Senge, M. O. *Curr. Med. Chem.* **2015**, *22*, 2238.

43. Hirohara, S.; Oka, C.; Totani, M.; Obata, M.; Yuasa, J.; Ito, H.; Tamura, M.; Matsui, H.; Kakiuchi, K.; Kawai, T.; Kawaichi, M.; Tanihara, M. *J. Med. Chem.* **2015**, *58*, 8658.

44. (a) Hirohara, S.; Kawasaki, Y.; Funasako, R.; Yasui, N.; Totani, M.; Alitomo, H.; Yuasa, J.; Kawai, T.; Oka, C.; Kawaichi, M.; Obata, M.; Tanihara, M. *Bioconjugate Chem.* **2012**, *23*, 1881. (b) Zheng, X.; Morgan, J.; Pandey, S. K.; Chen, Y.; Tracy, E.; Baumann, H.; Missert, J. R.; Batt, C.; Jackson, J.; Bellnier, D. A.; Henderson, B. W.; Pandey, R. K. *J. Med. Chem.* **2009**, *52*, 4306.

45. Tanaka, M.; Kataoka, H.; Mabuchi, M.; Sakuma, S.; Takahashi, S.; Tujii, R.; Akashi, H.; Ohi, H.; Yano, S.; Morita, A.; Joh, T. *Anticancer Res.* **2011**, *31*, 763.

46. Kessel, D.; Thompson, P.; Saatio, K.; Nantwi, K. D. *Photochem. Photobiol.* **1987**, *45*, 787.

47. (a) Hirohara, S.; Nishida, M.; Sharyo, K.; Obata, M.; Ando, T. Tanihara, M. *Bioorg. Med. Chem.* **2010**, *18,* 1526.; (b) Hirohara, S.; Sharyo, K.; Kawasaki, Y.; Totani, M.; Tomotsuka, A.; Funasako, R.; Yasui, N.; Hasegawa, Y.; Yuasa, J.; Nakashima, T.; Kawai, T.; Oka, C.; Kawaichi, M.; Obata, M.; Tanihara, M. *Bull. Chem. Soc. Jpn.* **2013**, *86*, 1295

48. Hirohara, S.; Obata, M.; Alitomo, H.; Sharyo, K.; Ando, T.; Tanihara, M.; Yano, S. *J. Photochem. Photobiol. B: Biol* **2009**, 97, 22.

49. Pasetto, P.; Chen, X.; Drain, C. M.; Franck, R. W. *Chem. Commun.* **2001**, 81.

50. Chen, X.; Hui, L.; Foster, D. A.; Drain, C. M. *Biochemistry* **2004**, *43*, 10918.

51. Megia-Fernandez, A.; Torre-Gonzalez, D.; Parada-Aliste, J.; Lopez-Jaramillo, F. X.; Hernandez-mateo, F.; Santoyo-Gonzalez, F. *Chem. Asian J.* **2014**, *9*, 620.

52. Sol, V.; Blais, J. C.; Bolbach, G.; Carre, V.; Granet, R.; Guilloton, M.; Spiro, M.; Krausz, P. *Tetrahedron Lett.* **1997**, *38*, 6391.

53. Sol, V.; Branland, P.; Granet, R.; Kaldapa, C.; Verneuil, B.; Krausz, P. *Bioorg. Med. Chem. Lett.* **1998**, *8*, 3007.

54. Hirohara, S.; Obata, M.; Saito, A.; Ogata, S.; Ohtsuki, C.; Higashida, S.; Ogura, S.; Okura, I.; Sugai, Y.; Mikata, Y.; Tanihara, M.; Yano, S. *Photochem. Photobiol.* **2004**, *80*, 301.

55. Hirohara, S.; Obata, M.; Ogura, S.; Okura, I.; Higashida, S.; Ohtsuki, C.; Ogata, S.; Nishikawa, Y.; Takenaka, M.; Ono, H.; Mikata, Y.; Yano, S. *J. Porphyrins Phthalocyanines* **2004**, *8*, 1289.

56. Hirohara, S.; Obata, M.; Alitomo, H.; Sharyo, K.; Ogata, S.; Ohtsuki, C.; Yano, S.; Ando, T.; Tanihara, M. *Biol. Pharm. Bull.* **2008**, *31*, 2265.

57. Hirohara, S.; Obata, M.; Ogata, S.; Ohtsuki, C.; Higashida, S.; Ogura, S.; Okura, I.; Takenaka, M.; Ono, H.; Sugai, Y.; Mikata, Y.; Tanihara, M.; Yano, S. *J. Photochem. Photobiol. B* **2005**, *78*, 7.

58. Obata, M.; Hirohara, S.; Sharyo, K.; Alitomo, H.; Kajiwara, K.; Ogata, S.; Tanihara, M.; Ohtsuki, C.; Yano, S. *Biochem. Biophys. Acta* **2007**, *1770*, 1204.

59. Schell, C.; Hombrecher, H. K. *Chem.: Eur. J.* **1999**, *5*, 587.

60. Tome, J. P. C.; Neves, M. G. P. M. S.; Tome, A. C.; Cavaleiro, J. A. C.; Mendona, A. F.; Pegado, I. N.; Duarte, R.; Valdeira, M. L. *Bioorg. Med. Chem.* **2005**, *13*, 3878.

61. Sol, V.; Charmot, A.; Krausz, P.; Trombotto, S.; Queneau, Y. *J. Carbohydr. Chem.* **2006**, *25*, 345.

62. Fujimoto, K.; Miyata, T.; Aoyama, Y. *J. Am. Chem. Soc.* **2000**, *122*, 3558.

63. Mikata, Y.; Shibata, M.; Baba, Y.; Kakuchi, T.; Nakai, M.; Yano, S. *J. Porphyrins Phthalocyanines* **2012**, *16*, 1177.

64. Samaroo, D.; Vinodu, M.; Chen, X.; Drain, C. M. *J. Comb. Chem.* **2007**, *9*, 998.

65. Garcia, G.; Naud-Martin, D.; Carrez, D.; Croisy, A.; Maillard, P. *Tetrahedron* **2011**, *67*, 4924.

CHAPTER 2 Synthesis of Tetraacetyl Thioglucopyranoses

2.1 Introduction

Thiosugars have been applied in the conjugation with porphyrins to give porphyrin glycoconjugates. A series of porphyrin glycoconjugates have been synthesized with thioglucose such as thiomannose, and thiogalactose, and they showed their stability and photoactivity [1,2]. Thioglucose, namely 2,3,4,6-tetra-*O*-acetyl-*S*-acetyl-1-thio-β-D-glucopyranose, also has been used in the synthesis of tetrakis(pentafluorophenyl)-porphyrin (TFPP)-glucose conjugates [3]. This chapter describes the preparation of glucosyl thiols i.e. deoxythiolated D-glucose at the 2-, 3-, 4-, and 6-positions for porphyrin glycocojugates tethered by sulfide linkages. The tetraacetyl 2-thio glucose (**2-Ac-S-AcGlc**), tetraacetyl 3-thio glucose (**3-Ac-S-AcGlc**), tetraacetyl 4-thio glucose (**4-Ac-S-AcGlc**), and tetraacetyl 6-thio glucose (**6-Ac-S-AcGlc**) are synthesized from D-mannose, diacetone D-glucose, D-galactose, and D-glucose, respectively, following previously reported procedures, with some modifications.

2.2 Results and Discussion

2.2.1 Synthesis of Tetraacetyl 2-Thioglucopyranose (**2-Ac-S-AcGlc**)

The preparation of **2-Ac-S-AcGlc** was started from pentaacetyl mannose (**75**) which was obtained through iodine-promoted acetylation of D-mannose (**74**). **75** was brominated by 33% solution of hydrogen bromide in acetic acid. Due to the instability, the obtained acetobromomannose (**76**) was directly reacted with ethanol in the presence of 2,4,6-collidine to afford orthoester (**77**) as a diastereomeric mixture. Hydrolysis of **77** was performed with 1M hydrochloric acid in acetone to yield 1,3,4,6-tetra-O-acetyl-β-D-mannopyranose (**78**). Triflation of **78** was accomplished using

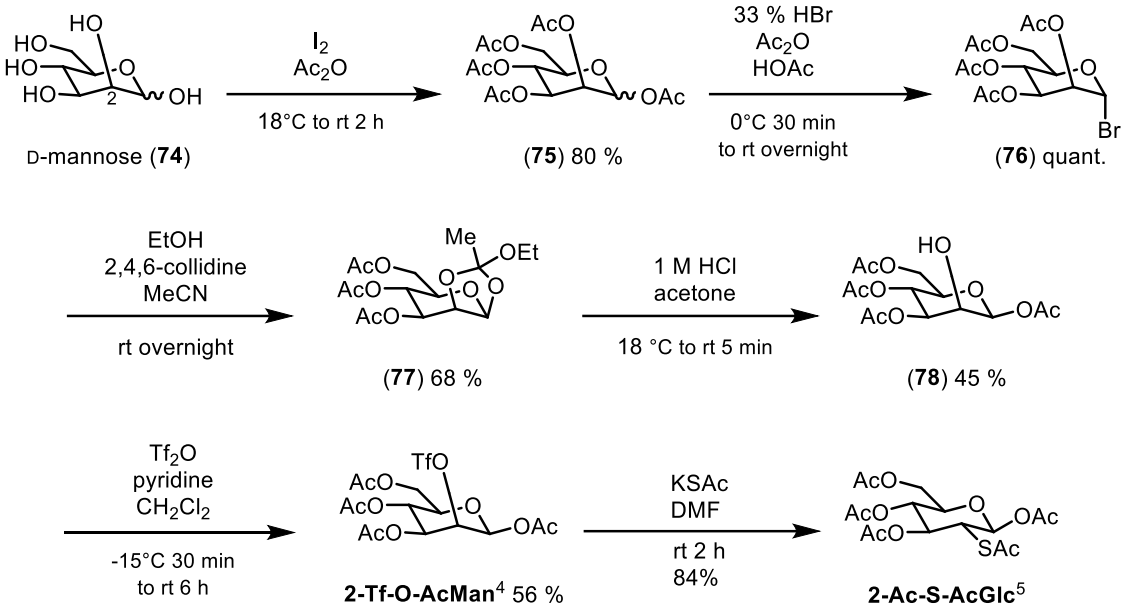

Scheme 2.1 Synthesis of **2-Ac-S-AcGlc**

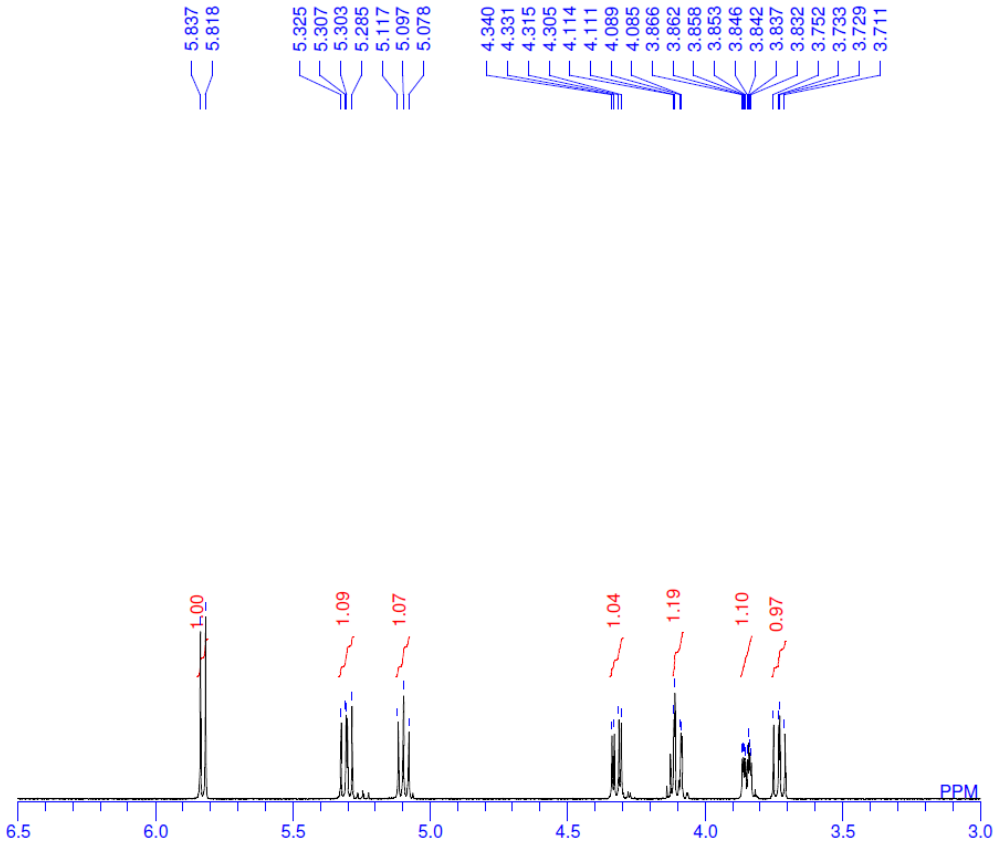

Figure 2.1 Selected ^{1}H NMR of **2-Ac-S-AcGlc**

triflic anhydride to yield the mannose triflate (**2-Tf-O-AcMan**) as reported [4]. Finally, an acetylthio group was introduced by an S_N2 reaction with potassium thioacetate to afford tetraacetyl 2-thio glucose (**2-Ac-S-AcGlc**) as colorless solids in 12 % total yield (Scheme 2.1). The structure of **2-Ac-S-AcGlc** determined unambiguously by spectral data which was same as those reported [5] indicated that **2-Ac-S-AcGlc** in a β-anomer form as shown by doublet peaks at 5.8 ppm (J = 8.0 Hz) in ^{1}H NMR (Figure 2.1) [6]. Fortunately, the single crystal of **2-Ac-S-AcGlc** was obtained and the analysis result supported this β-anomer form (Figure 2.2).

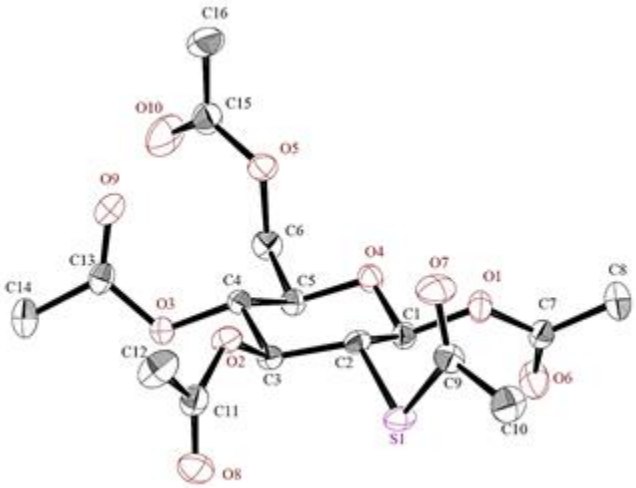

Figure 2.2 Structure of **2-Ac-S-AcGlc**

2.2.2 Synthesis of Tetraacetyl 3-Thioglucopyranose (**3-Ac-S-AcGlc**)

The preparation of 3-thio sugar (**3-Ac-S-AcGlc**) (Scheme 2.2) was started by oxidation of commercial diacetone D-glucose (**79**) with pyridinium dichromate (PDC) followed by reduction of the derived ketone by sodium borohydride to give epimerized **79**, 1,2;5,6-di-isopropylidene-α-D-allofuranose (**80**) [7]. Triflation of **80** in dichloromethane at -15 °C gave 1,2:5,6-di-*O*-isopropyidene-3-*O*-trifyl-D-allofuranose (**81**) [8]. Next, substitution of triflate (**81**) by thioacetate

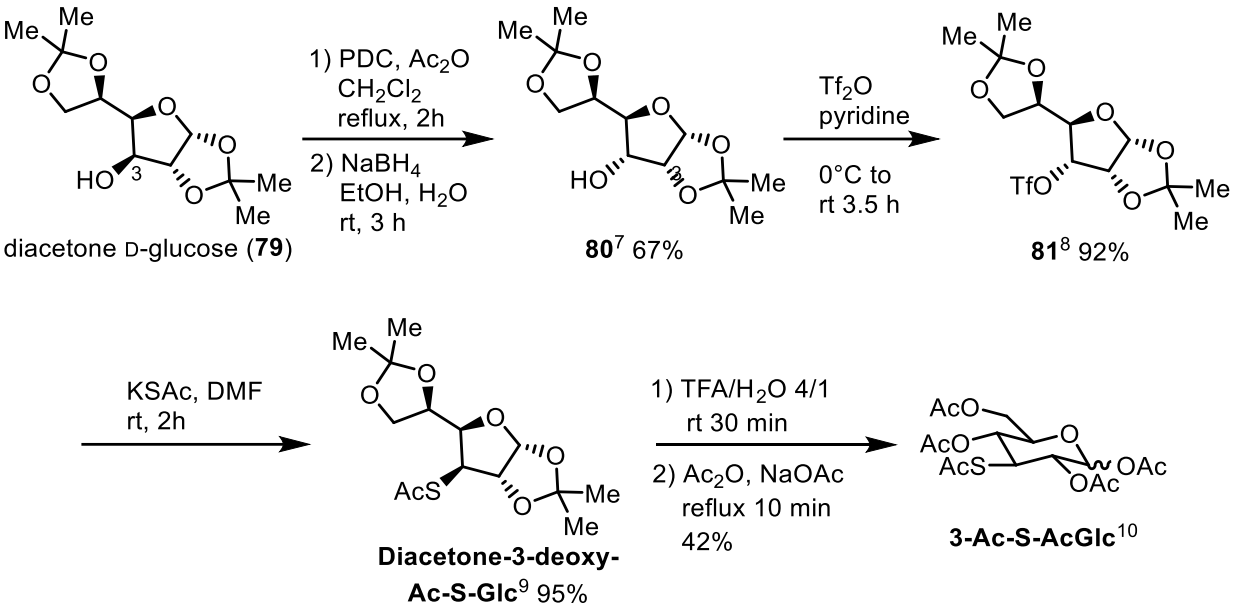

Scheme 2.2 Synthesis of **3-Ac-S-AcGlc**

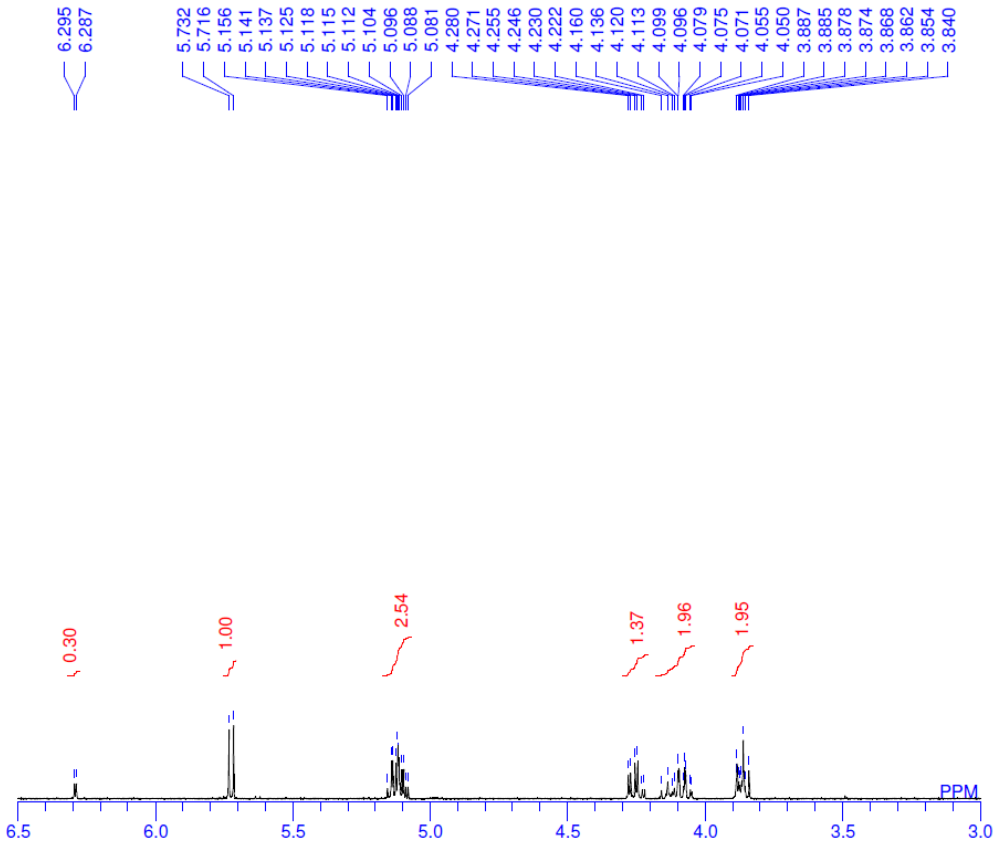

Figure 2.3 Selected ^{1}H NMR of **3-Ac-S-AcGlc**

ion yielded 3-*S*-acetyl-1,2:5,6-di-*O*-isopropylidene-3-thio-D-glucofuranose (**Diacetone-3-deoxy-Ac-S-Glc**) [9]. Finally, the furanose structure was transformed into pyranose by acid treatment followed by acetylation to obtain an α/β anomeric mixture (0.3:1.0) of **3-Ac-S-AcGlc** as yellowish oil in 25 % total yield where the structure were identical with those already reported (Figure 2.3) [10]. **3-Ac-S-AcGlc** showed two doublet peaks that were assigned to the α-anometic proton (J = 4.0 Hz) at 6.3 ppm and the β-anomeric one (J = 8.0 Hz) at 5.7 ppm [6].

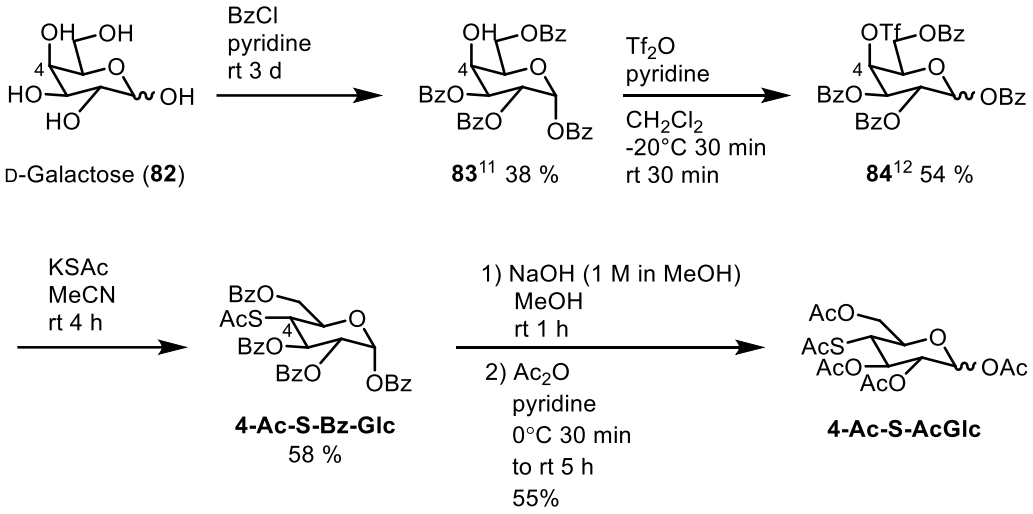

Scheme 2.3. Synthesis of **4-Ac-S-AcGlc**

2.2.3 Synthesis of Tetraacetyl 4-Thioglucopyranose (**4-Ac-S-AcGlc**)

The synthesis tetraacetyl 4-thio glucose (**4-Ac-S-AcGlc**) was commenced with D-galactose (**82**) (Scheme 2.3). Global benzoylation of **82** except for the axial 4-hydroxy group gave 1,2,3,6-tetra-*O*-benzoyl-α-D-galactopyranose (**83**) [11] which was triflated to give **84** [12]. Next, substitution of **84** by thioacetate yielded 1,2,3,6-tetra-*O*-benzoyl-4-acetyl-4-thio-α-D-glucopyranose (**4-Ac-S-Bz-Glc**). Finally, global exchange of protecting group from benzoyl to acetyl by hydrolysis and acetylation afforded an α/β anomeric mixture (0.3:1.0) the desired and known **4-Ac-S-AcGlc** as

white solids in 7 % total yield (Figure 2.4). The two doublet peaks at 6.4 ppm (J = 4.0 Hz) and at 5.7 ppm (J = 8.5 Hz) were assigned for the α-and β-anomeric proton [6].

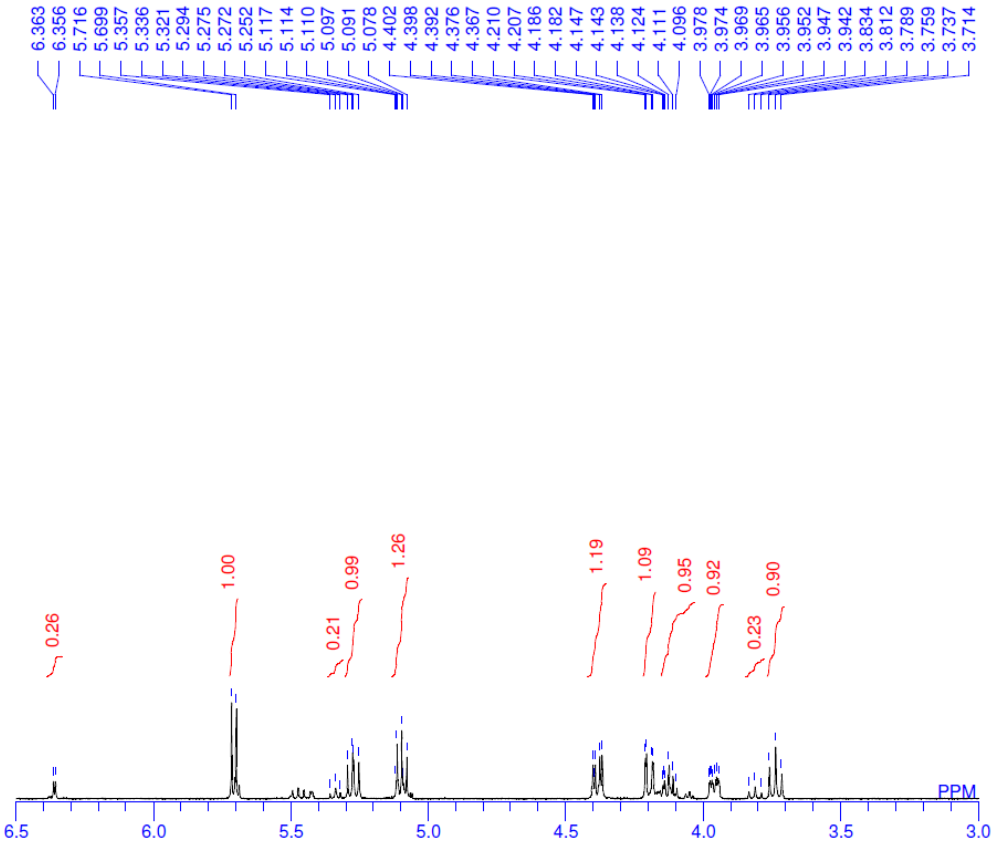

Figure 2.4 Selected ^{1}H NMR of **4-Ac-S-AcGlc**

2.2.4 Synthesis of Tetraacetyl 6-Thioglucopyranose (**6-Ac-S-AcGlc**)

Pentaacetate of 6-deoxy-6-thioglucose (**6-Ac-S-AcGlc**) was prepared from D-glucose (**85**) in accordance of the literature [13] by one-pot regioselective tosylation/tetraacetylation [14] (Scheme 2.4) followed by acetylthiolation was accomplished to synthesize a β- anomer of the known **6-Ac-S-AcGlc** in 34 % total yield as white solids [14]. The doublet peaks at 5.7 ppm (J = 8.0 Hz) in ^{1}H NMR indicated that **6-Ac-S-AcGlc** in a β-anomer form (Figure 2.5) [6].

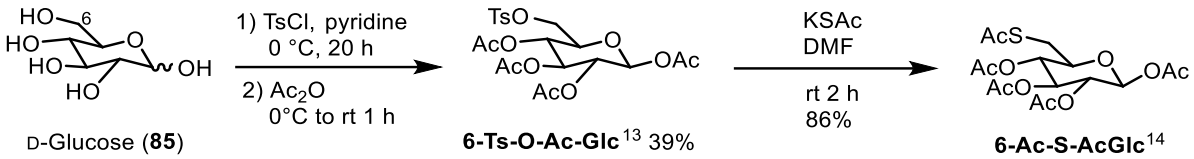

Scheme 2.4. Synthesis of **6-Ac-S-AcGlc**

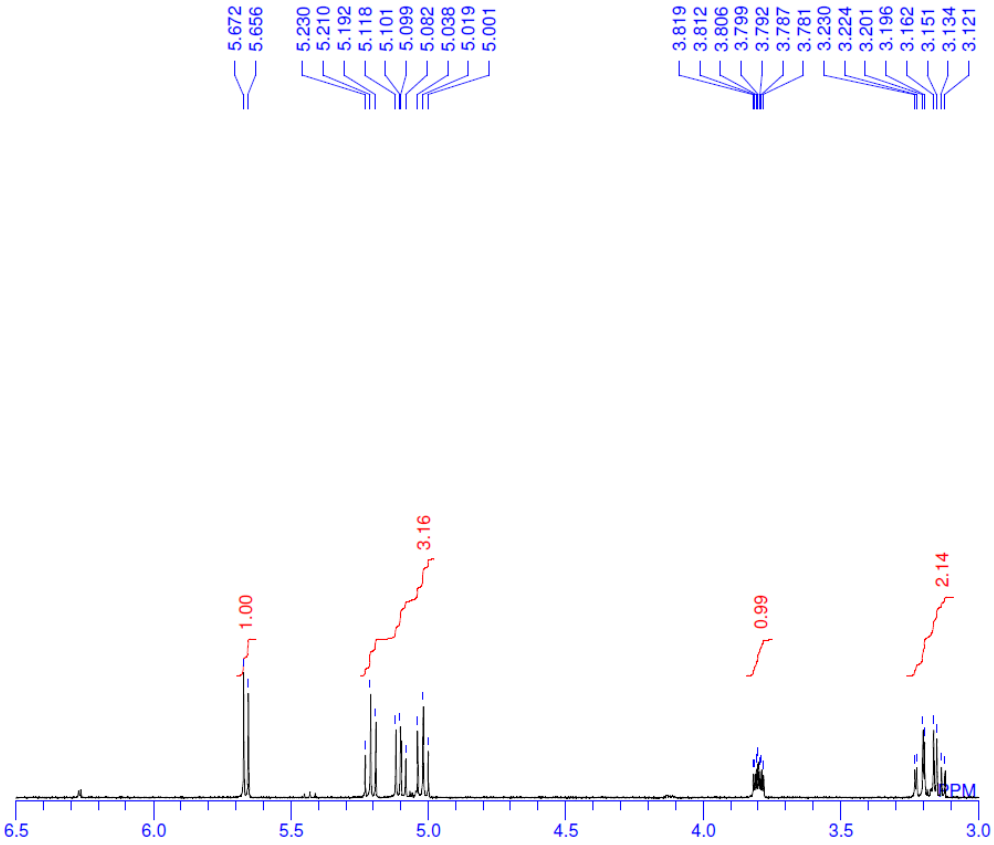

Figure 2.5 Selected ^{1}H NMR of **6-Ac-S-AcGlc**

2.3 Summary

Commenced with commercially available carbohydrates, deoxy 2-, 3-, 4-, and 6-thioglucoses with acetyl group protection were synthesized. Starting with D-mannose, tetraacetyl 2-thio glucose (**2-Ac-S-AcGlc**) as a β-anomer was obtained. 3-Thiolated derivative (**3-Ac-S-AcGlc**) was synthesized from diacetone D-glucose as an α/β-anomeric mixture. The 4-thio glucose (**4-Ac-S-**

AcGlc) as an α/β-anomeric mixture was prepared from D-galactose. The 6-thio glucose (**6-Ac-S-AcGlc**) as an β-anomer was obtained from D-glucose. Introduction of acetylthio groups were performed by S_N2 reaction with the appropriate surfonylated carbohydrates.

2.4 Experiments

Materials and Measurements

All chemicals were of analytical grade. ^1H and ^{13}C NMR spectra were recorded using a JEOL JNM-ECX500 spectrometer (500 MHz for ^1H NMR and 126 MHz for ^{13}C NMR) (JEOL Ltd., Tokyo, Japan). Chemical shifts are reported as δ values in ppm and calibrated with respect to the residual solvent peak ($CDCl_3$: δ 7.26 for ^1H NMR and δ 77.00 for ^{13}C NMR) or tetramethylsilane (δ 0 for ^1H NMR). The abbreviation used is as follows: s (singlet), d (doublet), dd (doublet of doublets), ddd (doublet of doublet of doublet), t (triplet), m (multiplet). Melting points were measured using a Yanaco Micro melting point apparatus (Yanako Corporation, Tokyo, Japan). Infrared spectra were measured using a JASCO FT-IR-4200 spectrometer (Jasco Co., Ltd., Tokyo, Japan). Mass spectra were recorded using a JEOL JMS-700 MStation [EI (70 eV), CI, FAB, and ESI], Bruker Autoflex II, and JEOL spiral TOF JMS-S3000 (MALDI-TOF) (JEOL Ltd., Tokyo, Japan). Flash column chromatography was performed using Merck silica gel 60 (Merck, Germany). The progress of the reactions was monitored by silica-gel thin-layer chromatography (TLC) (Merck TLC Silica gel 60 F254) (Merck, Germany).

Synthesis of 2-Ac-S-AcGlc

*2,3,4,6-Tetra-O-acetyl-α-D-mannopyranosyl bromide (**76**)*[4]

The oily penta-*O*-acetyl-D-mannopyranose **75** (~6.9 g) obtained from acetylation of D-mannose **74**

(4 g, 22 mmol) using iodine (51 mg, 200 µmol) in acetic anhydride (Ac_2O, 20 mL) was dissolved in glacial acetic acid (AcOH, 6.3 mL) containing Ac_2O (0.5 mL) with vigorous stirring. The solution was cooled to 0 °C under an argon atmosphere and a precooled 33% hydrogen bromide (HBr) in acetic acid (6.7 mL) was added dropwise for 25 minutes with vigorous stirring. The mixture was then stirred at room temperature overnight and diluted with chloroform ($CHCl_3$, 35 mL). The organic layer was washed successively with pre-cooled saturated aqueous sodium hydrogen carbonate ($NaHCO_3$, 3 × 20 mL) and water (20 mL). The $CHCl_3$-layer was dried over anhydrous sodium sulfate (Na_2SO_4), filtered, and concentrated on a rotary evaporator to yield tetra-*O*-acetyl-α-D-mannopyranosyl bromide **76** as a brown oil (7.2 g, quant.). R_f value 0.5 (hexane : ethyl cetate (EtOAc) = 1 : 1). HRMS (ESI): *m/z* for $C_{14}H_{19}BrNaO_9$ ($[M+Na]^+$) calcd 433.01101, found 433.01125 (error 0.23 mmu, 0.54 ppm). IR (NaCl, neat) ν_{max} 1750, 1432, 1371, 1222, 1166, 1129, 1052, 1015, 984, 910, 734 cm^{-1}. ^1H NMR ($CDCl_3$, 500.16 MHz, $Si(CH_3)_4$ = 0 ppm) δ (ppm) = 6.29 (1H, d, J_2 = 1.5 Hz, 1-Glc*H*), 5.72 (1H, dd, J_4 = 10.0 Hz, J_2 = 3.5 Hz, 3-Glc*H*), 5.44 (1H, dd, J_3 = 3.5 Hz, J_1 = 2.0 Hz, 2-Glc*H*), 5.37 (1H, dd, J_5 = 10.0 Hz, J_3 = 10.0 Hz, 4-Glc*H*), 4.33 (1H, dd, $J_{6'}$ = 12.5 Hz, J_5 = 5.0 Hz, 6-Glc*H*), 4.22 (1H, ddd, J_4 = 7.0 Hz, J_6 = 5.0 Hz, $J_{6'}$ = 2.0 Hz, 5-Glc*H*), 4.14 (1H, dd, J_6 = 12.5 Hz, J_5 = 2.5 Hz, 6'-Glc*H*), 2.18 (3H, s, $CO\mathit{C}H_3$), 2.11 (3H, s, $CO\mathit{C}H_3$), 2.08 (3H, s, $CO\mathit{C}H_3$), 2.01 (3H, s, $CO\mathit{C}H_3$). ^{13}C NMR ($CDCl_3$, 125.77 MHz, $CDCl_3$ = 77.0 ppm): δ (ppm) = 170.5 ($\mathit{C}OCH_3$), 169.7 ($\mathit{C}OCH_3$), 169.6 ($\mathit{C}OCH_3$), 83.0 (1-Glc*C*), 72.8 (2-Glc*C*), 72.1 (3-Glc*C*), 68.0 (4-Glc*C*), 65.2 (5-Glc*C*), 61.4 (6-Glc*C*), 20.8 ($CO\mathit{C}H_3$), 20.7 ($CO\mathit{C}H_3$), 20.6 ($CO\mathit{C}H_3$), 20.6 ($CO\mathit{C}H_3$). $[\alpha]_D^{22}$ +120.4 (*c* 1.00 in $CHCl_3$).

3,4,6-Tri-O-acetyl-1,2,-O-(1-ethoxyethylidene)-β-D-mannopyranose (77)[4]

The oily tetra-*O*-acetyl-α-D-mannopyranosyl bromide **76** was dissolved in anhydrous acetonitrile (MeCN, 2.5 mL) containing 2,4,6-collidine (3.5 mL, 27 mmol). To this solution was added

anhydrous ethanol (EtOH, 4 mL, 69 mmol) in one portion with vigorous stirring. The stirring was continued at room temperature in the dark overnight. The heterogeneous mixture was diluted with $CHCl_3$ (50 mL) and washed with water (3 × 35 mL). The combined water layers were re-extracted with $CHCl_3$ (35 mL). The combined organic layer was dried over anhydrous Na_2SO_4, filtered, and concentrated on a rotary evaporator. The residue was triturated with hexane and recrystallized from EtOH to yield the orthoester **77** (4.4 g, 68%) as a white solid. R_f value 0.47 (hexane : EtOAc = 1 : 1). m.p. 84–86°C. HRMS (ESI): *m*/*z* for $C_{16}H_{24}NaO_{10}$ ($[M+Na]^+$) calcd 399.12672, found 399.12694 (error 0.22 mmu, 0.56 ppm). IR (NaCl, neat) ν_{max} 1747, 1434, 1372, 1228, 1118, 1050, 979, 897 cm^{-1}. ^1H NMR ($CDCl_3$, 500.16 MHz, $Si(CH_3)_4$ = 0 ppm) δ (ppm) = 5.47 (1H, d, J_2 = 2.5 Hz, 1-Glc*H*), 5.30 (1H, dd, 1H, J_5 = 10.0 Hz, J_3 = 10.0 Hz, 4-Glc*H*), 5.15 (1H, dd, J_4 = 10.0 Hz, J_2 = 4.0 Hz, 3-Glc*H*), 4.60 (1H, dd, J_3 = 4.0 Hz, J_1 = 2.5 Hz, 2-Glc*H*), 4.23 (1H, dd, $J_{6'}$ = 12.0 Hz, J_5 = 4.5 Hz, 6-Glc*H*), 4.14 (1H, dd, J_6 = 12.0 Hz, J_5 = 2.0 Hz, 6'-Glc*H*), 3.67 (1H, m, 5-Glc*H*), 3.55 (2H, m, CH_3CH_2O), 2.12 (3H, s, $COCH_3$), 2.08 (3H, s, $COCH_3$), 2.05 (3H, s, $COCH_3$), 1.75 (3H, s, CH_3CO_3), 1.18 (3H, t, CH_3CH_2O). ^{13}C NMR ($CDCl_3$, 125.77 MHz, $CDCl_3$ = 77.0 ppm): δ (ppm) = 170.7 ($COCH_3$), 170.4 ($COCH_3$), 169.4 ($COCH_3$), 124.2 (CH_3CO_3), 97.3 (1-Glc*C*), 76.3 (2-Glc*C*), 71.2 (3-Glc*C*), 70.6 (4-Glc*C*), 65.5 (5-Glc*C*), 62.3 (6-Glc*C*), 58.1 (CH_3CH_2O), 24.7 (CH_3CO_3), 20.7 ($COCH_3$), 20.7 ($COCH_3$), 20.7 ($COCH_3$), 15.0 (CH_3CH_2O). $[\alpha]_D^{22}$ -7.5 (*c* 1.00 in $CHCl_3$).

*1,3,4,6-Tetra-O-acetyl-β-D-mannopyranose (**78**)*[4]

To a solution of the orthoester **77** (4.4 g, 12 mmol) in anhydrous acetone (27 mL) was added 1M hydrochloric acid (HCl) aq. (2.7 mL) in one portion with vigorous stirring (~18 °C, water bath). After being stirred for an additional 5 min at room temperature, the reaction mixture was concentrated on a rotary evaporator below 20 °C. The resulting solid was dissolved in $CHCl_3$ (25

mL) and washed with water (2 × 10 mL). The organic layer was dried over anhydrous Na_2SO_4, filtered, and concentrated on a rotary evaporator. The residue was triturated with diethyl ether (Et_2O) and recrystallized from EtOH to yield the tetraacetyl mannose **78** (1.9 g, 45%) as a white solid. R_f value 0.13 (hexane : EtOAc = 1 : 1). m.p. 134–136°C. HRMS (ESI): *m*/*z* for $C_{14}H_{20}NaO_{10}$ ($[M+Na]^+$) cacld 371.09542, found 71.09581 (error 0.39 mmu, 1.06 ppm). IR (NaCl, neat) ν_{max} 3466, 1747, 1432, 1371, 1230, 1176, 1080, 1050, 936 cm^{-1}. ^1H NMR ($CDCl_3$, 500.16 MHz, $Si(CH_3)_4$ = 0 ppm) δ (ppm) = 5.80 (1H, d, J_2 = 1.0 Hz, 1-Glc*H*), 5.40 (1H, dd, J_5 = 10.0 Hz, J_3 = 10.0 Hz, 4-Glc*H*), 5.04 (1H, dd, J_4 = 10.5 Hz, J_2 = 3.5 Hz, 3-Glc*H*), 4.31 (1H, dd, $J_{6'}$ = 12.5 Hz, J_5 = 5.5 Hz, 6-Glc*H*), 4.20 (1H, dt, J_3 = 7.0 Hz, J_{OH} = 4.0 Hz, J_1 = 1.5 Hz, 2-Glc*H*), 4.13 (1H, dd, J_6 = 13.0 Hz, J_5 = 2.5 Hz, 6'-Glc*H*), 3.78 (1H, ddd, J_4 = 10.0 Hz, J_6 = 5.5 Hz, $J_{6'}$ = 2.5 Hz, 5-Glc*H*), 2.18 (3H, s, CO*C*H_3), 2.12 (3H, s, CO*C*H_3), 2.10 (3H, s, CO*C*H_3), 2.05 (3H, s, CO*C*H_3). ^{13}C NMR ($CDCl_3$, 125.77 MHz, $CDCl_3$ = 77.0 ppm): δ (ppm) = 170.7 (*C*OCH_3), 170.1 (*C*OCH_3), 169.5 (*C*OCH_3), 168.4 (*C*OCH_3), 91.6 (1-Glc*C*), 73.1 (2-Glc*C*), 72.8 (3-Glc*C*), 68.4 (4-Glc*C*), 65.1 (5-Glc*C*), 62.0 (6-Glc*C*), 21.0 (CO*C*H_3), 20.8 (CO*C*H_3), 20.8 (CO*C*H_3), 20.7 (CO*C*H_3). $[\alpha]_D^{18}$ -22.7 (*c* 1.00 in $CHCl_3$).

*1,3,4,6-Tetra-O-acetyl-2-O-trifluoromethylsulfonyl-β-D-mannopyranose (**2-Tf-O-AcMan**)*[4]

The tetraacetyl mannose **78** (1.8 g, 5 mmol) was dissolved in anhydrous CH_2Cl_2 (14 mL) containing dry pyridine (0.9 mL, 11 mmol). This solution was cooled to -15 °C and trifluoromethanesulfonic anhydride (triflic anhydride) (0.9 mL, 5.2 mmol) was added dropwise over a period of 25 min under a nitrogen atmosphere with vigorous stirring. The mixture was then allowed to reach room temperature overnight. The reaction mixture was successively washed with ice-cold saturated aqueous $NaHCO_3$ (50 mL) and water (50 mL). The organic layer was dried over anhydrous Na_2SO_4, filtered, and concentrated on a rotary evaporator. **2-Tf-O-AcMan** was isolated

by column chromatography on silica with hexane : EtOAc = 1 : 1 as the eluant as white solid (1.4 g, 56%). R_f value 0.5 (hexane : EtOAc = 1 : 1). m.p. 118–120 °C. HRMS (ESI): *m*/*z* for $C_{15}H_{19}F_3NaO_{12}S$ ($[M+Na]^+$) cacld 503.04470, found 503.04470 (error 0.00 mmu, 0.00 ppm). IR (NaCl, neat) ν_{max} 1758, 1418, 1371, 1215, 1142, 1091, 1057, 934, 734 cm^{-1}; ^1H NMR ($CDCl_3$, 500.16 MHz, $Si(CH_3)_4$ = 0 ppm) δ (ppm) = 5.90 (1H, d, J_2 = 1.0 Hz, 1-Glc*H*), 5.30 (1H, dd, J_5 = 10.5 Hz, J_3 = 10.5 Hz, 4-Glc*H*), 5.18 (1H, dd, J_4 = 9.5 Hz, J_2 = 3.0 Hz, 3-Glc*H*), 5.14 (1H, dd, J_3 = 7.0 Hz, J_1 = 2.5 Hz, 2-Glc*H*), 4.25 (1H, dd, $J_{6'}$ = 12.5 Hz, J_5 = 5.0 Hz, 6-Glc*H*), 4.18 (1H, dd, J_6 = 12.5 Hz, J_5 = 2.0 Hz, 6'-Glc*H*), 3.83 (1H, ddd, J_4 = 10.0 Hz, J_6 = 5.5 Hz, $J_{6'}$ = 3.0 Hz, 5-Glc*H*), 2.17 (3H, s, $COCH_3$), 2.12 (3H, s, $COCH_3$), 2.10 (3H, s, $COCH_3$), 2.07 (3H, s, $COCH_3$). ^{13}C NMR ($CDCl_3$, 125.77 MHz, $CDCl_3$ = 77.0 ppm): δ (ppm) = 170.6 ($COCH_3$), 169.8 ($COCH_3$), 169.1 ($COCH_3$), 167.9 ($COCH_3$), 118.4 (CF_3, $J_{C\text{-}F}$ = 320.9 Hz), 89.1 (1-Glc*C*), 81.2 (2-Glc*C*), 73.5 (3-Glc*C*), 69.6 (4-Glc*C*), 64.5 (5-Glc*C*), 61.6 (6-Glc*C*), 20.7 ($COCH_3$), 20.6 ($COCH_3$), 20.5 ($COCH_3$), 20.4 ($COCH_3$). $[\alpha]_D^{23}$ -14.9 (*c* 1.00 in $CHCl_3$).

*1,3,4,6-Tetra-O-acetyl-2-S-acetyl-2-thio-β-D-glucopyranose (**2-Ac-S-AcGlc**)*[5]

A 0.05 M solution of **2-Tf-O-AcMan** (501 mg, 1 mmol) in dimethylformamide (DMF, 21 mL) was treated with potassium thioacetate (KSAc, 1.2 g, 10 mmol) at room temperature under nitrogen atmosphere. The reaction mixture was stirred for 2h and was partitioned between diethyl ether (Et_2O) and water. The organic phase was dried, filtered, and concentrated in vacuo. Purification by column chromatography on silica with hexane : ethyl acetate (EtOAc) = 3 : 1 as the eluant followed by recrystallization from Et_2O gave **2-Ac-S-AcGlc** as colorless solids (354 mg, 84%). R_f value 0.46 (hexane : EtOAc = 1 : 1). m.p. 117–119 °C. HRMS (ESI) : *m*/*z* for $C_{16}H_{22}NaO_{10}S$ $[M+Na]^+$ calcd 429.08314, found 429.08357 (error 0.43 mmu, 1.00 ppm). IR (NaCl, neat) ν_{max} 1755, 1707, 1369, 1221, 1103, 1049 cm^{-1}. ^1H NMR ($CDCl_3$, 500.16 MHz, $Si(CH_3)_4$ = 0 ppm): δ

(ppm) = 5.83 (1H, d, J_2 = 9.0 Hz, 1-Glc*H*), 5.31 (1H, dd, J_2 = 11.5 Hz, J_4 = 9.0 Hz, 3-Glc*H*), 5.10 (1H, dd, J_5 = 10.0 Hz, J_3 = 9.0 Hz, 4-Glc*H*), 4.32 (1H, dd, $J_{6'}$ = 12.5 Hz, J_5 = 4.5 Hz, 6-Glc*H*), 4.10 (1H, dd, J_6 = 12.5 Hz, J_5 = 1.5 Hz, 6'-Glc*H*), 3.85 (1H, ddd, J_4 = 10.0 Hz, J_6 = 4.5 Hz, $J_{6'}$ = 1.5 Hz, 5-Glc*H*), 3.73 (1H, dd, J_3 = 11.0 Hz, J_1 = 9.5 Hz, 2-Glc*H*), 2.34 (3H, s, SCO*C*H_3), 2.09 (6H, s, 2CO*C*H_3), 2.017 (3H, s, CO*C*H_3), 2.015 (3H, s, CO*C*H_3). ^{13}C NMR ($CDCl_3$, 125.77 MHz, $CDCl_3$ = 77.0 ppm): δ (ppm) = 192.3 (S*C*OCH$_3$), 170.7 (O*C*OCH$_3$), 170.0 (O*C*OCH$_3$), 169.5 (O*C*OCH$_3$), 169.0 (O*C*OCH$_3$), 92.0 (1-Glc*C*), 72.6 (3-Glc*C*), 71.0 (4-Glc*C*), 68.8 (5-Glc*C*), 61.5 (6-Glc*C*), 47.1 (2-Glc*C*), 30.7 (SCO*C*H_3), 20.7 (OCO*C*H_3), 20.6 (OCO*C*H_3), 20.5 (OCO*C*H_3). $[\alpha]_D^{30}$ +15.9 (*c* 1.00 in $CHCl_3$).

Synthesis of 3-Ac-S-AcGlc

*1,2;5,6-Di-O-isopropylidene-D-allofuranose (**80**)*[7]

A solution of diacetone D-glucose **79** (100 mg, 0.4 mmol) in dichloromethane (0.6 mL) was added to a mixture of pyridinium dichromate (108 mg, 0.3 mmol) and Ac_2O (0.1 mL, 1.2 mmol) in dichloromethane (1.2 mL) at room temperature under nitrogen. The whole mixture was refluxed for 2h, then cooled to room temperature, and the solvent was evaporated under reduced pressure. EtOAc (1 mL) was added to dissolve the solid residue, and the resulting solution was filtered through short-column of silica gel. The filtrate was concentrated in vacuo and the resulted ketone was dissolved in 56% EtOH aq. (0.4 mL). A solution of sodium borohydride (15 mg, 0.4 mmol) in water (0.4 mL) was added at room temperature to this solution. After stirring for 3h, the mixture was extracted with dichloromethane (CH_2Cl_2, 3 × 5 mL), and the combined organic layers were dried over magnesium sulfate ($MgSO_4$), filtered, and concentrated in vacuo. The residue was recrystallized from diethyl ether-hexane to afford the product **80** (68 mg, 67%) as colorless solid.

R_f value 0.33 (hexane : EtOAc = 1 : 1). m.p. 72–73 °C. HRMS (ESI): *m*/*z* for $C_{12}H_{20}NaO_6$ ($[M+Na]^+$) cacld 283.11576, found 283.11508 (error -0.68 mmu, -2.40 ppm). IR (NaCl, neat) ν_{max} 3465, 2987, 1648, 1377, 1215, 1165, 1061, 1016, 870 cm^{-1}. ^1H NMR ($CDCl_3$, 500.16 MHz, $Si(CH_3)_4$ = 0 ppm) δ (ppm) = 5.82 (1H, d, J_2 = 4.0 Hz, 1-Glc*H*), 4.62 (1H, dd, J_3 = 5.0 Hz, J_1 = 4.0 Hz, 2-Glc*H*), 4.31 (1H, ddd, $J_{6'}$ = 6.5 Hz, J_6 = 6.5 Hz, J_4 = 5.0 Hz, 5-Glc*H*), 4.00-4.10 (3H, m, 3-,6-,6'-Glc*H*), 3.82 (1H, dd, J_3 = 8.5 Hz, J_5 = 5.0 Hz, 4-Glc*H*), 1.58 (3H, s, CH_3), 1.47 (3H, s, CH_3), 1.40 (3H, s, CH_3), 1.37 (3H, s, CH_3). ^{13}C NMR ($CDCl_3$, 125.77 MHz, $CDCl_3$ = 77.0 ppm): δ (ppm) = 112.8 (OO*C*CH_3CH_3), 109.9 (OO*C*CH_3CH_3), 103.9 (1-Glc*C*), 79.7 (2-Glc*C*), 78.9 (3-Glc*C*), 75.5 (4-Glc*C*), 72.5 (5-Glc*C*), 65.9 (6-Glc*C*), 26.6 (*C*H_3), 26.5 (*C*H_3), 26.3 (*C*H_3), 25.3 (*C*H_3). $[\alpha]_D^{31}$ +32.9 (*c* 1.00 in $CHCl_3$).

*1,2;5,6-Di-O-isopropylidene-3-O-trifyl-D-allofuranose (**81**)*[8]

To a cooled (0 °C) solution of 1,2:5,6-di-*O*-isopropyidene-D-allofuranose **80** (0.3 g, 1.3 mmol) in pyridine (0.4 mL), triflic anhydride (0.4 mL, 2 mmol) was slowly added. After stirring 3.5h at room temperature, the reaction mixture was diluted with CH_2Cl_2, washed with saturated $NaHCO_3$ and brine, dried. The resulting residue after evaporation under reduced pressure was purified by column chromatography (hexane : EtOAc = 5 : 1) to afford the title compound **81** (0.5 g, 92%) as a colorless oil. R_f value 0.75 (hexane : EtOAc = 1 : 1). HRMS (FAB): *m*/*z* for $C_{13}H_{20}F_3O_8S$ ($[M+H]^+$) cacld 393.0831, found 393.0829 (error -0.20 mmu, -0.50 ppm). IR (NaCl, neat) ν_{max} 1417, 1379, 1213, 1146, 1018, 877 cm^{-1}. ^1H NMR ($CDCl_3$, 500.16 MHz, $Si(CH_3)_4$ = 0 ppm) δ (ppm) = 5.84 (1H, d, J_2 = 4.0 Hz, 1-Glc*H*), 4.91 (1H, dd, J_4 = 7.5 Hz, J_2 = 5.0 Hz, 3-Glc*H*), 4.77 (1H, dd, J_3 = 5.0 Hz, J_1 = 4.0 Hz, 2-Glc*H*), 4.23-4.16 (2H, m, 4-,6-Glc*H*), 4.12 (1H, dd, J_5 = 8.5 Hz, J_6 = 6.0 Hz, 6'-Glc*H*), 3.91 (1H, dd, J_6 = 8.5 Hz, $J_{6'}$ = 4.5 Hz, 5-Glc*H*), 1.58 (3H, s, CH_3), 1.45 (3H, s, CH_3), 1.39 (3H, s, CH_3), 1.35 (3H, s, CH_3). ^{13}C NMR ($CDCl_3$, 125.77 MHz, $CDCl_3$ =

77.0 ppm): δ (ppm) = 118.3 (*C*F_3, $J_{C\text{-}F}$ = 319.0 Hz), 114.4 (OO*C*CH_3CH_3), 110.3 (OO*C*CH_3CH_3), 104.1 (1-Glc*C*), 82.8 (2-Glc*C*), 77.8 (3-Glc*C*), 77.6 (4-Glc*C*), 75.1 (5-Glc*C*), 66.2 (6-Glc*C*), 26.8 (*C*H_3), 26.5 (*C*H_3), 26.2 (*C*H_3), 24.7 (*C*H_3). $[\alpha]_D^{32}$ +67.4 (*c* 1.00 in $CHCl_3$).

*3-S-Acetyl-1,2;5,6-di-O-isopropylidene-3-thio-D-glucofuranose (**Diacetone-3-deoxy-Ac-S-Glc**)*[9]

A 0.05 M solution of 1,2:5,6-di-*O*-isopropyidene-3-*O*-trifyl-D-allofuranose **81** (0.5 g, 1.2 mmol) in dimethylformamide (24 mL) was treated with potassium thioacetate (KSAc, 1.4 g, 12 mmol) at room temperature under nitrogen atmosphere. The reaction mixture was stirred for 2h and was partitioned between diethyl ether and water. The organic phase was dried, filtered, and concentrated in vacuo. **Diacetone-3-deoxy-Ac-S-Glc** was isolated by column chromatography on silica with hexane : ethyl acetate = 5 : 1 as the eluant as colorless oil (0.4 g, 95%). R_f value 0.73 (hexane : EtOAc = 1 : 1). HRMS (ESI): *m/z* for $C_{14}H_{22}NaO_6S$ ($[M+Na]^+$) calcd 341.10348, found 341.10369 (error 0.21 mmu, 0.62 ppm). IR (NaCl, neat) ν_{max} 2985, 2937, 1701, 1375, 1255, 1209, 1163, 1068, 1014 cm^{-1}. ^{1}H NMR ($CDCl_3$, 500.16 MHz, $Si(CH_3)_4$ = 0 ppm) δ (ppm) = 5.80 (1H, d, J_2 = 3.5 Hz, 1-Glc*H*), 4.55 (1H, d, J_1 = 3.5 Hz, 2-Glc*H*), 4.30 (1H, m, 4-Glc*H*), 4.13 (1H, d, J_4 = 4.0 Hz, 5-Glc*H*), 4.07-4.11 (2H, m, 6-,6'-Glc*H*), 3.97-4.01 (1H, m, 3-Glc*H*), 2.39 (3H, s, SCO*C*H_3), 1.53 (3H, s, C*H*$_3$), 1.41 (3H, s, C*H*$_3$), 1.33 (3H, s, C*H*$_3$), 1.31 (3H, 3H, s, C*H*$_3$). ^{13}C NMR ($CDCl_3$, 125.77 MHz, $CDCl_3$ = 77.0 ppm): δ (ppm) = 193.4 (S*C*OCH_3), 112.3 (OO*C*CH_3CH_3), 109.7 (OO*C*CH_3CH_3), 104.7 (1-Glc*C*), 86.4 (2-Glc*C*), 78.8 (3-Glc*C*), 74.2 (5-Glc*C*), 67.6 (6-Glc*C*), 50.2 (4-Glc*C*), 31.2 (SCO*C*H_3), 26.9 (*C*H_3), 26.6 (*C*H_3), 26.2 (*C*H_3), 25.2 (*C*H_3). $[\alpha]_D^{24}$ -43.2 (*c* 1.00 in $CHCl_3$).

*1,2,4,6-Tetra-O-acetyl-3-S-acetyl-3-thio-D-glucopyranose (**3-Ac-S-AcGlc**)*[10]

A solution of **Diacetone-3-deoxy-Ac-S-Glc** (330 mg, 1 mmol) in CF_3COOH/H_2O (4:1, 1.4 mL) was stirred at room temperature under nitrogen atmosphere for 30 min. Concentration of the

mixture gave a colorless residue, which was dissolved in acetic anhydride (Ac_2O, 1.9 mL) containing sodium acetate (NaOAc, 48 mg, 0.6 mmol). This mixture was heated at reflux (10 min) before being poured into ice/water. Standard work-up (EtOAc) and column chromatography on silica with hexane : EtOAc = 3 : 1 as eluant gave **3-Ac-S-AcGlc** as a yellowish oil (180 mg, 42%). R_f value 0.40 (hexane : EtOAc = 1 : 1). HRMS (ESI): *m/z* for $C_{16}H_{22}NaO_{10}S$ $[M+Na]^+$ calcd 429.08314, found 429.08323 (error 0.09 mmu, 0.22 ppm). IR (NaCl, neat) ν_{max} 1753, 1702, 1373, 1221, 1068 cm^{-1}. ^1H NMR ($CDCl_3$, 500.16 MHz, $Si(CH_3)_4$ = 0 ppm): δ (ppm) = 6.29 (0.3 H, d, J_2 = 4.0 Hz, 1α-Glc*H*), 5.72 (1H, d, J_2 = 8.0 Hz, 1β-Glc*H*), 5.16-5.08 (2.6H, m, 2α/β-,6α/β-Glc*H*), 4.28-4.22 (1.3H, m, 4α/β-Glc*H*), 4.16-4.05 (1.9H, m, 5α/β-,3α-,6'α-Glc*H*), 3.86 (2H, m, 3β-,6'β-Glc*H*), 2.34 (3.9H, s, SCO*C*H_3), 2.10 (3.9H, s, CO*C*H_3), 2.08 (3.9H, s, CO*C*H_3), 2.03 (7.8H, s, 2CO*C*H_3). ^{13}C NMR ($CDCl_3$, 125.77 MHz, $CDCl_3$ = 77.0 ppm): δ (ppm) = 193.1 (S*C*OCH$_3$), 170.7 (O*C*OCH$_3$), 169.3 (O*C*OCH$_3$), 169.2 (O*C*OCH$_3$), 169.0 (O*C*OCH$_3$), 93.1 (1-Glc*C*), 75.3 (2-Glc*C*), 69.1 (4-Glc*C*), 66.7 (5-Glc*C*), 61.7 (6-Glc*C*), 47.7 (3-Glc*C*), 30.6 (SCO*C*H_3), 20.8 (OCO*C*H_3), 20.7 (OCO*C*H_3), 20.52 (OCO*C*H_3), 20.51 (OCO*C*H_3). $[\alpha]_D^{28}$ +17.8 (*c* 1.00 in $CHCl_3$).

Synthesis 4-Ac-S-AcGlc

*1,2,3,6-Tetra-O-benzoyl-α-D-galactopyranose (**83**)*[11]

A solution of benzoyl chloride (2.6 mL, 23 mmol) in pyridine (1 mL) was added dropwise to a stirred suspension of D-galactose **82** (1 g, 5.6 mmol) in pyridine (20 mL) at 18°C under nitrogen atmosphere. After 3 days, ice was added and the mixture was extracted with CH_2Cl_2. The organic layer was washed with 1 M HCl aq., saturated $NaHCO_3$ aq. and water, dried under Na_2SO_4, filtered, and concentrated. Column chromatography on silica with hexane : EtOAc = 5 : 1 as eluant gave the compound **83** as a white solid (1.3 g, 38%). R_f value 0.60 (hexane : EtOAc = 1 : 1). HRMS

(ESI): *m*/*z* for $C_{34}H_{28}NaO_{10}$ ([M+Na]$^+$) cacld 619.15802, found 619.15702 (error -1.00 mmu, -1.61 ppm). IR (NaCl, neat) ν_{max} 3500, 1726, 1268, 1110, 1069, 1023, 708 cm^{-1}. ^{1}H NMR ($CDCl_3$, 500.16 MHz, Si(CH_3)$_4$ = 0 ppm) δ (ppm) = 8.09-8.11 (2H, dd, J_{ortho} = 9.0 Hz, J_{meta} = 1.0 Hz, Ar*H*), 8.00-8.03 (4H, m, Ar*H*), 7.85-7.87 (2H, dd, J_{ortho} = 8.0 Hz, J_{meta} = 1.0 Hz, Ar*H*), 7.39-7.65 (12H, m, Ar*H*), 6.82 (1H, d, J_2 = 4.0 Hz, 1-Glc*H*), 6.06 (1H, dd, J_3 = 10.5 Hz, J_1 = 4.0 Hz, 2-Glc*H*), 5.88 (1H, dd, J_4 = 10.5 Hz, J_2 = 4.0 Hz, 3-Glc*H*), 4.79 (1H, dd, J_5 = 11.0 Hz, J_6 = 7.0 Hz, 6'-Glc*H*), 4.46-4.55 (3H, m, 4-,5-,6-Glc*H*), 2.76 (1H, d, J_4 = 4.0 Hz, O*H*). ^{13}C NMR ($CDCl_3$, 125.77 MHz, $CDCl_3$ = 77.0 ppm): δ (ppm) = 166.6, 165.9, 165.5, 164.6 (OBz), 133.8, 133.6, 133.4, 133.3, 129.9, 129.82, 129.79, 129.7, 129.2, 129.1, 128.93, 128.85, 128.1, 128.5, 128.4, 128.3 (Ph of Bz), 90.8 (1-Glc*C*), 70.8 (2-Glc*C*), 70.4 (3-Glc*C*), 67.4 (4-Glc*C*), 67.1 (5-Glc*C*), 62.4 (6-Glc*C*). $[\alpha]_D^{23}$ +136.8 (*c* 1.00 in $CHCl_3$).

*1,2,3,6-Tetra-O-benzoyl-4-O-trifluoromethylsulfonyl-D-galactopyranose (**84**)*[12]

To a solution of 1,2,3,6-tetra-*O*-benzoyl-α-D-galactopyranose **83** (1 g, 1.7 mmol) in 50 mL anhydrous CH_2Cl_2 and 10 mL anhydrous pyridine was added dropwise triflic anhydride (1.1 mL, 6.5 mmol) at -20°C under a nitrogen atmosphere. After 30 min the reaction mixture was allowed to reach room temperature, stirred for additional 30 min, diluted with 40 mL of CH_2Cl_2, and the resulting solution poured onto ice. The aqueous layer was separated and extracted twice with 50 mL of CH_2Cl_2. The combined organic layers were washed with saturated $NaHCO_3$ solution, dried, concentrated under reduced pressure, and purified by column chromatography on silica with hexane : ethyl acetate = 5 : 1 to give the product **84** as white solid (0.7 g, 54%). R_f value 0.625 (hexane : EtOAc = 1 : 1). m.p. 67–69 °C. HRMS (ESI): *m z* for $C_{35}H_{27}F_3NaO_{12}S$ ([M+Na]$^+$) cacld 751.10730, found 751.10714 (error -0.16 mmu, -0.21 ppm). IR (NaCl, neat) ν_{max} 1734, 1416, 1265, 1216, 1143, 1110, 1070, 1023, 915, 709 cm^{-1}. ^{1}H NMR ($CDCl_3$, 500.16 MHz, Si(CH_3)$_4$ = 0 ppm)

δ (ppm) = 8.16 (0.5H, dd, J_{ortho} = 8.5 Hz, J_{meta} = 1.0 Hz, Ar*H*), 8.08 (2H, dd, J_{ortho} = 3.5 Hz, J_{meta} = 1.0 Hz, Ar*H*), 8.06 (2H, dd, J_{ortho} = 3.0 Hz, J_{meta} = 1.5 Hz, Ar*H*), 7.95-8.03 (3.5H, m, Ar*H*), 7.85 (2H, d, Ar*H*), 7.39-7.66 (15H, m, Ar*H*), 6.94 (0.25H, d, J_2 = 4.0 Hz, 1α-Glc*H*), 6.88 (1H, d, J_2 = 4.0 Hz, 1β-Glc*H*), 6.24 (0.25H, dd, J_4 = 4.0 Hz, J_2 = 2.0 Hz, 3α-Glc*H*), 6.06 (1H, dd, J_4 = 11.0 Hz, J_2 = 3.0 Hz, 3β-Glc*H*), 5.92-5.97 (1.25H, m, 2α-,2β-Glc*H*), 5.70-5.73 (1.25H, m, 4α-,4β-Glc*H*), 4.80 (1H, dd, $J_{6',\beta}$ = 11.5 Hz, $J_{5\beta}$ = 6.5 Hz, 6β-Glc*H*), 4.71-4.74 (1.25H, m, 6α-,6'β-Glc*H*), 4.61 (0.25H, dd, $J_{6',\alpha}$ = 11.5 Hz, $J_{5\alpha}$ = 6.5 Hz, 6α-Glc*H*), 4.39 (0.25H, dd, $J_{6\alpha}$ = 11.5 Hz, $J_{6',\alpha}$ = 7.0 Hz, 5α-Glc*H*), 4.32 (1H, dd, $J_{6\beta}$ = 11.5 Hz, $J_{6',\beta}$ = 8.0 Hz, 5β-Glc*H*). ^{13}C NMR ($CDCl_3$, 125.77 MHz, $CDCl_3$ = 77.0 ppm): δ (ppm) = 165.8 (OBz), 165.6 (OBz), 165.1 (OBz), 164.2 (OBz), 134.1, 134.0, 133.6, 133.5, 130.1, 129.9, 129.72, 129.7, 128.8, 128.6, 128.5, 128.4 (Ph of Bz), 118.3 (*C*F_3, $J_{C\text{-}F}$ = 319.7Hz), 90.1 (1-Glc*C*), 81.7 (4-Glc*C*), 68.3 (2-Glc*C*), 67.6 (3-Glc*C*), 66.5 (5-Glc*C*), 60.7 (6-Glc*C*). $[\alpha]_D^{23}$ +132.8 (*c* 1.00 in $CHCl_3$).

*1,2,3,6-Tetra-O-benzoyl-4-acetyl-4-thio-α-D-glucopyranose (**4-Ac-S-Bz-Glc**)*

A 0.05 M solution of 1,2,3,6-tetra-*O*-benzoyl-4-*O*-trifluoromethanesulfonyl-α-D-galactopyranose **84** (1.5 g, 2 mmol) in dry MeCN (41 mL) was treated with potassium thioacetate (2.4 g, 20 mmol) at room temperature under nitrogen atmosphere. The reaction mixture was stirred for 4h and was partitioned between chloroform and water. The organic phase was dried over Na_2SO_4, filtered, and concentrated in vacuo. **4-Ac-S-Bz-Glc** was isolated by column chromatography on silica with hexane : EtOAc = 5 : 1 as white solid (0.8 g, 58%). R_f value 0.65 (hexane : EtOAc = 1 : 1). m.p. 68–69 °C. HRMS (ESI): *m*/*z* for $C_{36}H_{30}NaO_{10}S$ ($[M+Na]^+$) cacld 677.14574, found 677.14511 (error -0.63 mmu, -0.93 ppm). IR (NaCl, neat) ν_{max} 1731, 1451, 1267, 1109, 1068, 1021, 709 cm^{-1}. ^{1}H NMR ($CDCl_3$, 500.16 MHz, $Si(CH_3)_4$ = 0 ppm) δ (ppm) = 8.15 (2H, d, Ar*H*), 8.10 (2H, d, Ar*H*), 7.95 (2H, dd, J_{ortho} = 8.5 Hz, J_{meta} = 1.5 Hz, Ar*H*), 7.86 (2H, dd, J_{ortho} = 8.5 Hz, J_{meta} = 1.0

Hz, Ar*H*), 7.37-7.65 (12H, m, Ar*H*), 6.84 (1H, d, J_2 = 4.0 Hz, 1-Glc*H*), 6.18 (1H, t, J_4 = 10.5 Hz, J_2 = 10.5 Hz, 3-Glc*H*), 5.61 (1H, dd, J_3 = 10.0 Hz, J_1 = 4.0 Hz, 2-Glc*H*), 4.57-4.66 (3H, m, 5-,6-,6'-Glc*H*), 4.25 (1H, t, J_5 = 11.5 Hz, J_3 = 11.5 Hz, 4-Glc*H*), 2.23 (3H, s, C*H*$_3$). ^{13}C NMR ($CDCl_3$, 125.77 MHz, $CDCl_3$ = 77.0 ppm): δ (ppm) = 192.3 (SAc), 166.2, 165.8, 165.3, 164.4 (OBz), 133.8, 133.5, 133.4, 133.2, 130.0, 129.8, 129.7, 128.9, 128.86, 128.8, 128.5, 128.4, 128.37, (Ph of Bz), 90.2 (1-Glc*C*), 71.5 (2-Glc*C*), 71.0 (3-Glc*C*), 69.0 (5-Glc*C*), 63.3 (6-Glc*C*), 43.9 (4-Glc*C*), 30.7 (Me of Ac). $[\alpha]_D^{24}$ +180.9 (*c* 1.00 in $CHCl_3$).

*1,2,3,6-Tetra-O-acetyl-4-S-acetyl-4-thio-D-glucopyranose (**4-Ac-S-AcGlc**)*

4-Ac-S-BzGlc (20 mg, 30 μmol) was debenzoylated in methanol (MeOH, 0.6 mL) with sodium methoxide (MeONa, 0.1 M, 31 μL). After stirring at room temperature for 60 min, the mixture was neutralized with acetic acid (AcOH) and concentrated. The resulted residue was dissolved in anhydrous pyridine (83 μL), cooled to 0 °C and Ac_2O (24 μL, 26 μmol) was added. After 30 min the reaction mixture was allowed to reach room temperature, stirred for additional 5h, solvent was removed under reduced pressure and the residue was dissolved in dichloromethane (CH_2Cl_2, 10 mL). The solution was washed with saturated sodium hydrogen carbonate ($NaHCO_3$) solution followed by 0.2 M hydrochloric acid (HCl) aq. and water, dried, concentrated under reduced pressure, and purified by column chromatography on silica with hexane : EtOAc = 5 : 1 to give the product **4-Ac-S-AcGlc** as white solids (6.8 mg, 55%). R_f value 0.38 (hexane : EtOAc = 1 : 1). m.p. 30–32 °C. HRMS (ESI): *m*/*z* for $C_{16}H_{22}NaO_{10}S$ $[M+Na]^+$ calcd 429.08314, found 429.08333 (error 0.19 mmu, 0.45 ppm). IR (NaCl, neat) ν_{max} 1754, 1707, 1369, 1223, 1073, 1046, 918, 732 cm^{-1}. ^{1}H NMR ($CDCl_3$, 500.16 MHz, Si(C*H*$_3$)$_4$ = 0 ppm): δ (ppm) = 6.36 (0.3H, d, $J_{2\alpha}$ = 4.0 Hz, 1α-Glc*H*), 5.71 (1H, d, $J_{2\beta}$ = 8.5 Hz, 1β-Glc*H*), 5.34 (0.3H, dd, $J_{2\alpha}$ = 10.5 Hz, $J_{4\alpha}$ = 7.5 Hz, 3α-Glc*H*), 5.27 (1H, dd, $J_{2\beta}$ = 11.0 Hz, $J_{4\beta}$ = 9.5 Hz, 3β-Glc*H*), 5.08-5.12 (1.3H, m, 2α-,2β-Glc*H*),

4.38 (1H, dd, $J_{6',\beta}$ = 13.0 Hz, $J_{5\beta}$ = 5.0 Hz, 6β-Glc*H*), 4.20 (1H, dd, $J_{6\beta}$ = 12.0 Hz, $J_{5\beta}$ = 1.5 Hz, 6'β-Glc*H*), 4.10-4.15 (0.9H, m, 6α-,6'α-,5α-Glc*H*), 3.96 (1H, ddd, $J_{4\beta}$ = 11.0 Hz, $J_{6\beta}$ = 4.5 Hz, $J_{6',\beta}$ = 2.5 Hz, 5β-Glc*H*), 3.81 (0.3H, dd, $J_{5\alpha}$ = 11.0 Hz, $J_{3\alpha}$ = 11.0 Hz, 4α-Glc*H*), 3.74 (1H, dd, $J_{5\beta}$ = 11.0 Hz, $J_{3\beta}$ = 11.0 Hz, 4β-Glc*H*), 2.33 (3H, s, SCO*C*H$_3$), 2.11 (3H, s, CO*C*H$_3$), 2.09 (3H, s, CO*C*H$_3$), 2.02 (6H, s, CO*C*H$_3$). ^{13}C NMR ($CDCl_3$, 125.77 MHz, $CDCl_3$ = 77.0 ppm): δ (ppm) = 192.4 (S*C*OCH$_3$), 170.7 (O*C*OCH$_3$), 169.9 (O*C*OCH$_3$), 169.4 (O*C*OCH$_3$), 168.9 (O*C*OCH$_3$), 91.5 (1-Glc*C*), 73.6 (2-Glc*C*), 71.4 (3-Glc*C*), 71.1 (5-Glc*C*), 62.6 (6-Glc*C*), 43.3 (4-Glc*C*), 30.7 (SCO*C*H$_3$), 20.8 (OCO*C*H$_3$), 20.7 (OCO*C*H$_3$), 20.54 (OCO*C*H$_3$), 20.50 (OCO*C*H$_3$). $[\alpha]_D^{20}$ +22.8 (*c* 1.00 in $CHCl_3$).

Synthesis of 6-Ac-S-AcGlc

*1,2,3,4-Tetra-O-acetyl-6-O-p-toluenesulfonyl-β-D-glucopyranose (**6-Ts-O-Ac-Glc**)*[14]

D-Glucose **85** (500 mg, 2.8 mmol) was added to a solution of *p*-toluenesulfonyl chloride (TsCl, 534 mg, 2.8 mmol) in anhydrous pyridine (7.5 mL) at 0 °C under nitrogen atmosphere and the solution was stirred overnight. Then, Ac_2O (2.2 mL) was added dropwise and the solution was allowed to warm to room temperature. After 1h the solvent was removed in reduced pressure and the residue was dissolved in CH_2Cl_2. The solution was washed several times with saturated $NaHCO_3$ aq., 0.2 M HCl aq. and water, dried under Na_2SO_4, and concentrated. The resulted crude 1,2,3,4-tetra-*O*-acetyl-6-*O*-*p*-toluenesulfonyl-β-D-glucopyranose (**6-Ts-O-Ac-Glc**) was crystallized from EtOH (0.54 g, 39%) as white solid. R_f value 0.41 (hexane:EtOAc = 1:1). m.p. 178–179 °C. HRMS (ESI): *m*/*z* for $C_{21}H_{26}NaO_{12}S$ ($[M+Na]^+$) cacld 525.10427, found 525.10401 (error -0.26 mmu, -0.49 ppm). IR (NaCl, neat) ν_{max} 1759, 1367, 1216, 1177, 1077, 1038 cm^{-1}. ^{1}H NMR ($CDCl_3$, 500.16 MHz, Si(C*H*$_3$)$_4$ = 0 ppm) δ (ppm) = 7.77 (2H, d, *J* = 8.0 Hz, ArTs), 7.35 (2H, d, *J*

= 8.0 Hz, ArTs), 5.64 (1H, d, J_2 = 8.0 Hz, 1-Glc*H*), 5.19 (1H, dd, J_4 = 9.0 Hz, J_2 = 9.0 Hz, 3-Glc*H*), 5.06 (1H, dd, J_3 = 8.0 Hz, J_1 = 4.0 Hz, 2-Glc*H*), 5.03 (1H, dd, J_5 = 4.0 Hz, J_3 = 4.0 Hz, 4-Glc*H*), 4.15 (1H, dd, J_5 = 11.5 Hz, $J_{6'}$ = 4.0 Hz, 6-Glc*H*), 4.10 (1H, dd, J_5 = 11.5 Hz, J_6 = 4.0 Hz, 6'-Glc*H*), 3.84 (1H, ddd, J_6 = 9.5 Hz, $J_{6'}$ = 4.0 Hz, J_5 = 3.0 Hz, 5-Glc*H*), 2.45 (s, 3H, MeTs), 2.09 (s, 3H, CO*C*H$_3$), 2.02 (s, 3H, CO*C*H$_3$), 2.00 (s, 3H, CO*C*H$_3$), 1.99 (s, 3H, CO*C*H$_3$). ^{13}C NMR ($CDCl_3$, 125.77 MHz, $CDCl_3$ = 77.0 ppm): δ (ppm) = 170.1, 169.3, 169.1, 168.8, (OAc), 145.1, 132.3, 129.8, 128.1 (Ph of Ts), 91.5 (1-Glc*C*), 72.5 (2-Glc*C*), 72.1 (3-Glc*C*), 69.9 (4-Glc*C*), 67.8 (5-Glc*C*), 66.6 (6-Glc*C*), 21.7 (Me of Ts), 20.7, 20.6, 20.52, 20.49 (OAc). $[\alpha]_D^{23}$ +25.7 (*c* 1.00 in $CHCl_3$).

*1,2,3,4-Tetra-O-acetyl-6-S-acetyl-6-thio-β-D-glucopyranose (**6-Ac-S-AcGlc**)*[13]

A 0.05 M solution of **6-Ts-OAcGlc** (450 mg, 890 μmol) in DMF (18 mL) was treated with KSAc (1.0 g, 8.9 mmol) at room temperature under nitrogen atmosphere. The reaction mixture was stirred for 2h and was partitioned between Et_2O and water. The organic phase was dried, filtered, and concentrated in vacuo. The product **6-Ac-SAcGlc** was isolated by column chromatography on silica with hexane : EtOAc = 2 : 1 as the eluant as white solids (312 mg, 86%). R_f value 0.55 (hexane : EtOAc = 1 : 1). m.p. 126–127 °C. HRMS (ESI): *m*/*z* for $C_{16}H_{22}NaO_{10}S$ $[M+Na]^+$ calcd 429.08314, found 429.08333 (error 0.19 mmu, 0.45 ppm). IR (NaCl, neat) ν_{max} 1757, 1695, 1369, 1215, 1074, 1037 cm^{-1}. ^{1}H NMR ($CDCl_3$, 500.16 MHz, Si(C*H*$_3$)$_4$ = 0 ppm): δ (ppm) = 5.66 (1H, d, J_2 = 8.0 Hz, 1-Glc*H*), 5.21 (1H, dd, J_2 = 9.5 Hz, J_4 = 9.5 Hz, 3-Glc*H*), 5.10 (1H, dd, J_1 = 8.0 Hz, J_3 = 9.5 Hz, 2-Glc*H*), 5.02 (1H, dd, J_3 = 9.5 Hz, J_5 = 9.5 Hz, 4-Glc*H*), 3.80 (1H, ddd, J_4 = 9.5 Hz, J_6 = 6.0 Hz, $J_{6'}$ = 3.0 Hz, 5-Glc*H*), 3.21 (1H, dd, $J_{6'}$ = 14.5 Hz, J_5 = 3.0 Hz, 6-Glc*H*), 3.14 (1H, dd, J_6 = 14.5 Hz, J_5 = 6.0 Hz, 6'-Glc*H*), 2.34 (3H, s, SCO*C*H$_3$), 2.11 (3H, s, CO*C*H$_3$), 2.08 (3H, s, CO*C*H$_3$), 2.02 (3H, s, CO*C*H$_3$), 2.00 (3H, s, CO*C*H$_3$). ^{13}C NMR ($CDCl_3$, 125.77 MHz, $CDCl_3$ =

77.0 ppm): δ (ppm) = 194.6 (S*C*OCH$_3$), 170.1 (O*C*OCH$_3$), 169.7 (O*C*OCH$_3$), 169.2 (O*C*OCH$_3$), 168.9 (O*C*OCH$_3$), 91.5 (1-Glc*C*), 73.7 (2-Glc*C*), 72.7 (3-Glc*C*), 70.2 (4-Glc*C*), 69.7 (5-Glc*C*), 30.4 (SCO*C*H$_3$), 29.6 (6-Glc*C*), 20.8 (OCO*C*H$_3$), 20.7 (OCO*C*H$_3$), 20.6 (OCO*C*H$_3$), 20.5 (OCO*C*H$_3$). $[\alpha]_D^{25}$ -11.4 (*c* 1.00 in CHCl$_3$).

2.5 References

1. Sylvain, I.; Benhaddou, R.; Carre, V.; Cottaz, S.; Driguez, H.; Granet, R.; Guilloton, M.; Krausz, P. *J. Porphyrins Phthalocyanines* **1999**, *3*, 1.
2. Sylvain, I.; Zerrouki, R.; Granet, R.; Huang, Y. M.; Lagorce, J-F.; Guilloton, M.; Blais, J-C.; Krausz, P. *Bioorg. Med. Chem.* **2002**, *10*, 57.
3. Hirohara, S.; Nishida, M.; Sharyo, K.; Obata, M.; Ando, T. Tanihara, M. *Bioorg. Med. Chem.* **2010**, *18*, 1526.
4. Toyokuni, T.; Kumar, J. S. D.; Gunawan, P.; Basarah, E. S.; Liu, J.; Barrio, J. R.; Satyamurthy, N. *Mol. Imaging. Biol.* **2004**, *6*, 324.
5. Knapp, S.; Kirk, B. A. *Tetrahedron Lett.* **2003**, *44*, 7601.
6. Roslund MU, Tähtinen P, Niemitz M, Sjöholm R. *Carbohydr. Res.* 2008; 343: 101.
7. Lee, J.-C.; Chang, S.-W.; Liao, C.-C.; Chi, F.-C.; Chen, C.-S.; Wen, Y.-S.; Wang, C.-C.; Kulkarni, S. S.; Puranik, R.; Liu, Y.-H.; Hung, S.-C. *Chem. Eur. J.* **2004**, *10*, 399.
8. Hall, L. D.; Miller, D. C. *Carbohydr. Res.* **1976**, *47*, 299.
9. Contour-Galcera, M-O.; Guillot, J-M.; Ortiz-Mellet, C.; Pflieger-Carrara, F.; Defaye, J.; Gelas. J. *Carbohydr. Res.* **1996**, *81*, 99.
10. Stick, R. V.; Stubbs, K. A. *Tetrahedron: Asymmetry* **2005**, *16*, 321.
11. Garegg, P. J.; Hultberg, H. *Carbohydr. Res.* **1982**, *110*, 261.

12. Leon, B.; Liemann, S.; Klaffke, W. *J. Carbohydr. Chem.* **1993**, *12*, 597.

13. Akagi, M.; Tejima, S.; Haga, M. *Chem. Pharm. Bull*. **1962**, *10*, 562.

14. Maschauer, S.; Haubner, R.; Kuwert, T.; Prante, O. *Mol. Pharmaceutics* **2014**, *11*, 505.

CHAPTER 3 Synthesis of Mono-Glycoconjugated Porphyrins

3.1 Introduction

As mentioned in Chapter 1, Photofrin® is a common PS used in PDT and provides its cyclic core and peripheral substituent for PDT effect [1]. However, Photofrin® exhibits several problems, i.e. it is a complex mixture of dimeric and oligomeric porphyrins [2-8]. Therefore, advancing PSs properties is needed, and conjugation of sugars to porphyrins have been developed [9-18]. A number of porphyrins-sugar conjugates have been developed including the use of sulfur linkage between porphyrins and sugar, and their PDT effects have been evaluated [19-27]. This chapter describes the conjugation of TFPP with peracetylated glucopyranoses followed by global deprotection to afford the desired mono-glycoconjugated porphyrins as well as their characterization. The further research goal for these mono-glycoconjugated porphyrins of positional isomer of 2-,3-,4-,6-thioglucoses is addressed to understand the effect of thioglucose positional isomers on their photophysical properties, cellular uptake, and photocytotoxicity.

3.2 Results and Discussion

3.2.1 Synthesis of Glycoconjugated 5,10,15,20-Tetrakis(pentafluorophenyl)porphyrin

The acetylated TFPP-glucose conjugates **2-4Ac**, and **6Ac** were prepared by utilizing the S_NAr reactions of TFPP with peracetylated thioglucopyranoses **2-4-Ac-S-AcGlc**, and **6-Ac-S-AcGlc** according to the similar procedure for preparing the TFPP-glucose conjugate **1Ac** (Scheme 3.1) [28]. The reactions were carried out in *N*,*N*-dimethylformamide (DMF) in the presence of diethylamine at ambient temperature except for the reaction of TFPP with **6-Ac-S-AcGlc** which requires higher temperature (40 ~ 50 ºC) or longer reaction times (3 days or more) than other thioglucose materials.

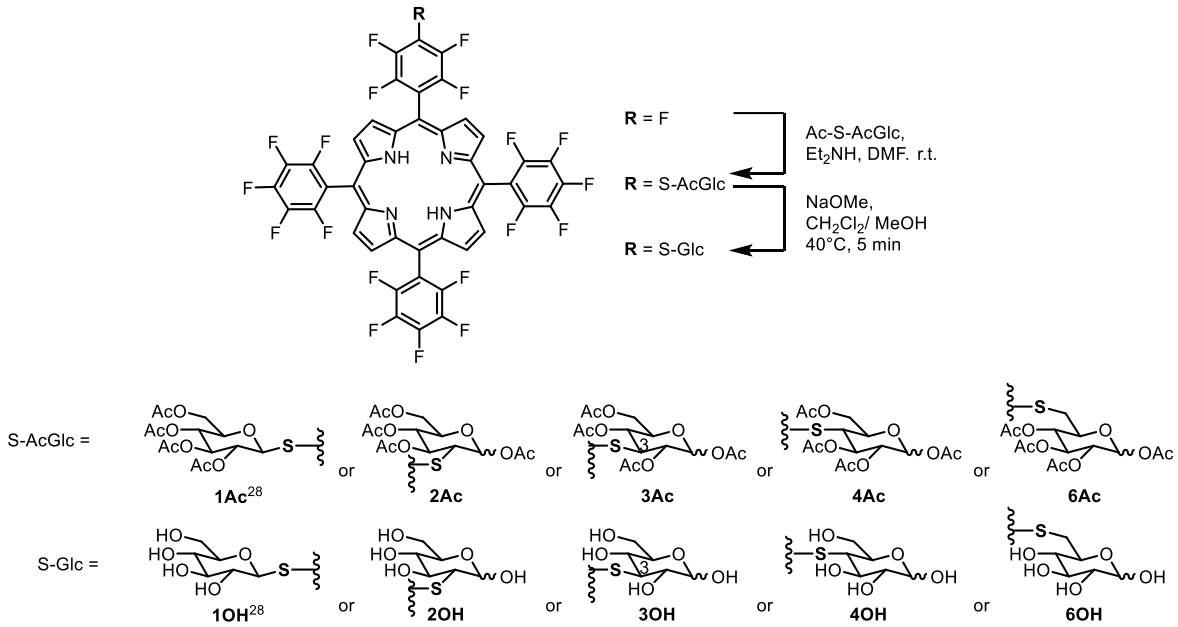

Scheme 3.1 Synthesis of TFPP-glucose conjugates

It was found that all pentaacetyl thioglucopyranoses in this research reacted slowly compared to previous **1-Ac-S-AcGlc** (deduced from the TLC profile of the reaction mixture) due to different reactivity of C2, C3, C4, and C6 positions contrasted to anomeric position (C1) [29]. This different reactivity may be due to the slow generation of thiolate ions in **2-4-Ac-S-AcGlc**, and **6-Ac-S-AcGlc** which affected in the ability to bind with the TFPP. Moreover, this fact is also supported by the recovery of the starting sugars from the reaction mixture after chromatographic purification. **2-4Ac**, and **6Ac** were isolated as deep purplish red solids in 6 ~ 54% yields after chromatographic purification. The structure of **2-4Ac**, and **6Ac** was confirmed by means of matrix-assisted laser desorption/ionization time-of-flight (MALDI-TOF) high-resolution mass spectrometry (HRMS) and ^{1}H and ^{19}F NMR. **2-4Ac**, and **6Ac** were detected as $[M]^{+}$ species with error 0.73–0.98 ppm. Further study on the ^{1}H NMR revealed that **2Ac** and **6Ac** were obtained only in a β-anomeric form,

while **3Ac** and **4Ac** were afforded as an anomeric mixture, respectively. However, the anomeric stereochemistry does not matter because this will be epimerized after removal of acetyl group. At this stage, the purity of these products including the anomeric product of **3Ac** and **4Ac** was 99% to more than 99% as evaluated by HPLC method. Based on this fact, these products were used for the next reaction.

The removal of acetyl groups was performed by alkaline hydrolysis using sodium methoxide in a mixture of MeOH and dichloromethane (DCM) [30-33] to give mono-glycoconjugated porphyrins **2-4OH**, and **6OH** as anomeric mixtures in 37 % – 81 % yields. The purity evaluation of all TFPP-glucose conjugate products by HPLC method using 99% of silica gel packed column indicated that the purities were over 99%. MALDI-TOF HRMS, ^{1}H and ^{19}F NMR were used to affirm the structure of **2-4OH**, and **6OH**. **2-4OH**, and **6OH** were detected as $[M]^{+}$ species with error -0.85–0.39 ppm by using MALDI-TOF HRMS.

3.2.2 NMR Spectra of Mono-Glycoconjugated TFPPs

The NMR spectroscopy (^{1}H, ^{19}F, ^{13}C, COSY, HSQC, and ^{1}H-^{19}F HOESY) was used to confirm the structure of all TFPP-glucose conjugates. The ^{1}H NMR spectra of **2-4Ac**, and **6Ac** recorded in $CDCl_3$ indicates two peaks centered at 8.9 ppm correspond for the β-pyrrole protons similar to that for **1Ac** [28]. A number of peaks around 6.44 ~ 3.35 ppm together with singlet peaks and a broad singlet peak in the range of 1.87 ~ 2.29 ppm and -2.92 ppm are attributable for glucose protons, acetyl groups, and the inner pyrrole protons, respectively. **3Ac** and **4Ac** as an α/β anomeric mixtures can be distinguished by the coupling constant of the anomeric proton. The two doublet peaks of anomeric proton located at 6.4 ppm with J = 4.0 Hz and at 5.8 ppm with J = 8.0 Hz as the α- anomer and the β- anomer separately (Figure 3.1) [34,35]. At the same time, the characteristic

peaks of porphyrin ring of **2-4Ac**, and **6Ac** can be recognized by ^{13}C NMR. The ^{13}C NMR spectra of these conjugates show peaks at 147.45 ~ 145.48, 130.98 ~ 131.27, and 103.57 ~ 103.87 ppm correspond to α position (resemble with 2,6-PhC and 3,5-PhC), β-pyrrole, and *meso* position, proportionately. Further investigation on the ^{19}F NMR reveals that **3Ac** and **4Ac** gave two set of distinctly-separated two peaks which correlates for the 2,6- and 3,5-F nucleus of glucose-substituted perfluorophenyl group resulted from the stereochemical difference of α- and β-anomeric positions (Figure 3.2).

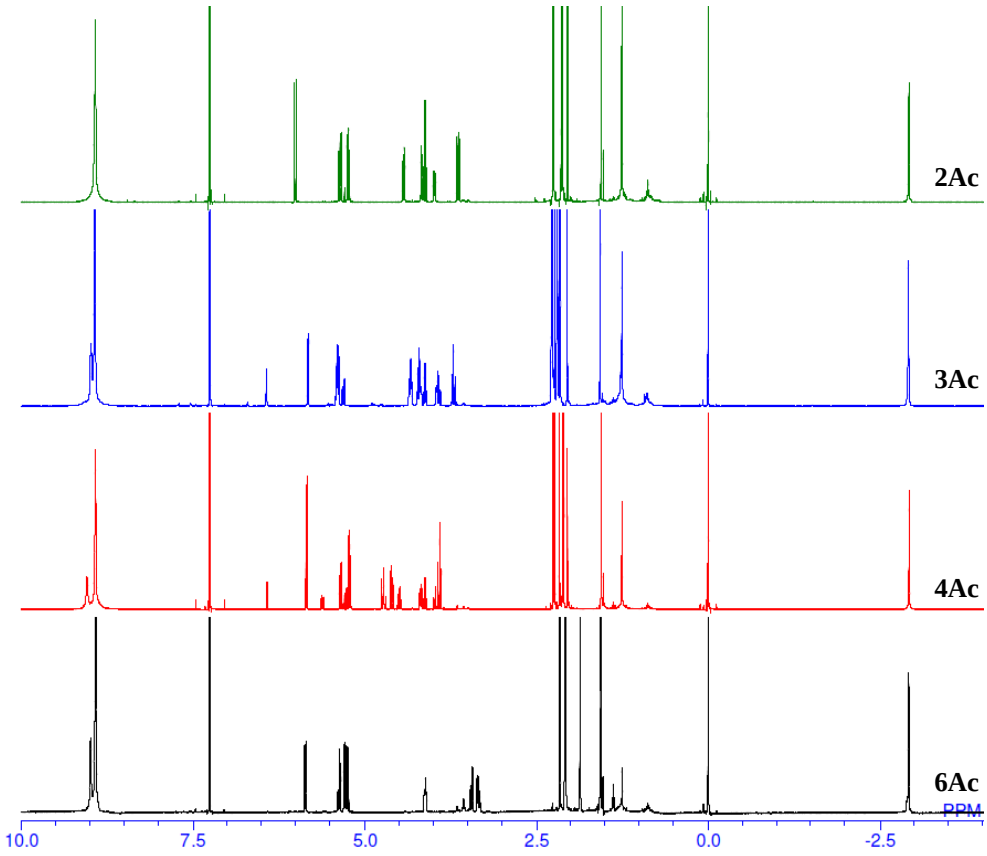

Figure 3.1 Selected ^{1}H NMR of **2-4Ac**, **6Ac**

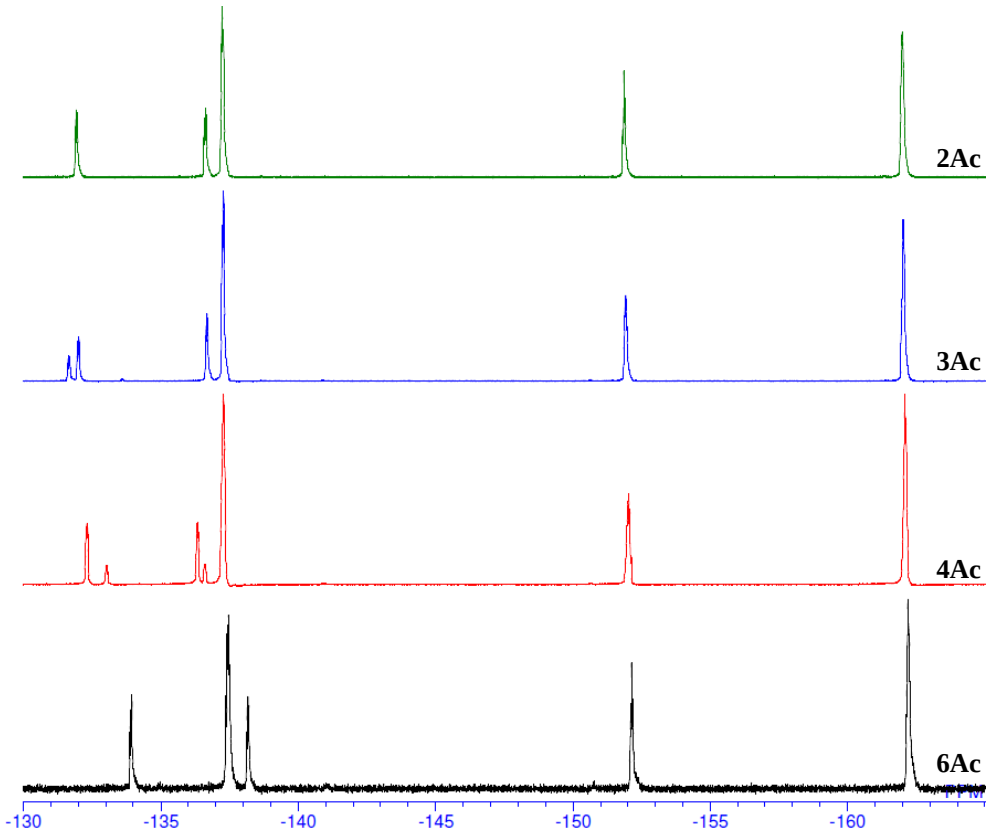

Figure 3.2 Selected ^{19}F NMR of **2-4Ac**, **6Ac**

The ^{1}H NMR spectra of **2-4OH** and **6OH** indicate that all peaks featured for acetyl groups on **2-4Ac**, and **6Ac** disappeared. The ^{1}H NMR spectra also imply that **2-4OH**, and **6OH** is in an α/β anomeric mixtures illustrated from the two doublet peaks with different coupling constant in the range 5.7 ~ 4.62 ppm (Figure 3.3). This is supported by ^{19}F NMR spectra which show two sets of two peaks conforming the 2,6- and 3,5-F nucleus of glucose-conjugated perfluorophenyl group. Detailed study on the ^{19}F NMR spectra of **2-4OH**, and **6OH** clearly indicates that the 4-F nucleus of the pentafluorophenyl groups remains in the porphyrin ring (Figure 3.4).

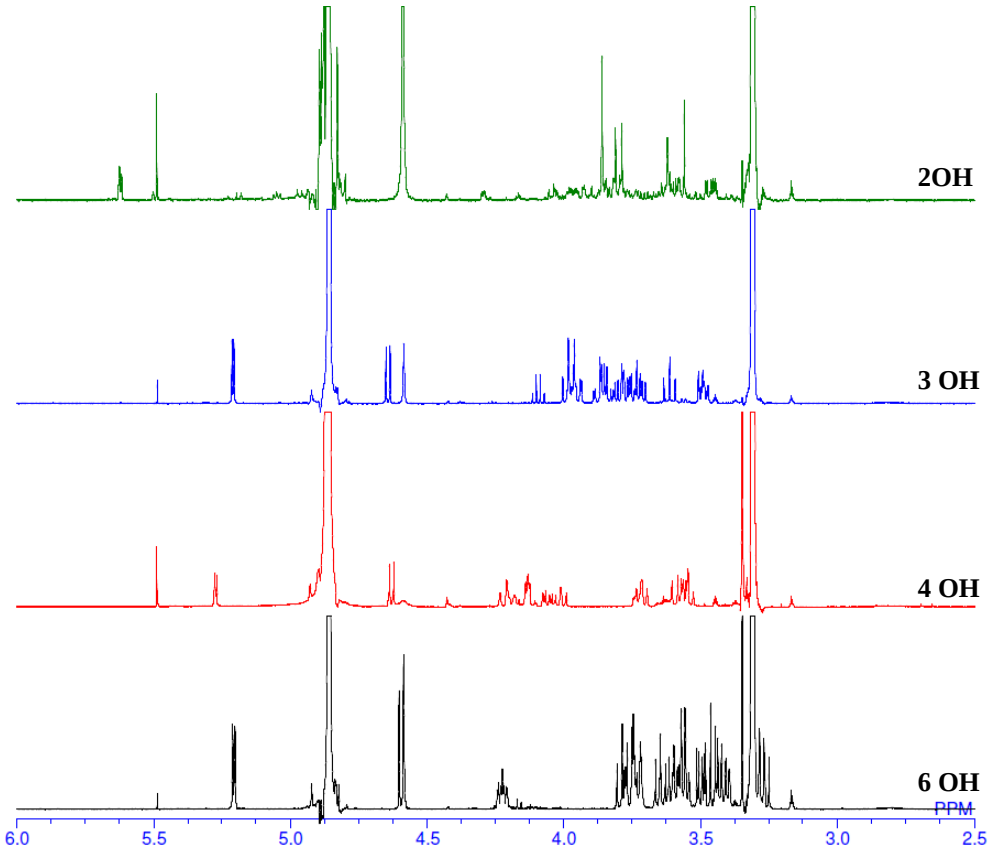

Figure 3.3 Selected ^{1}H NMR of **2-4OH**, **6OH**

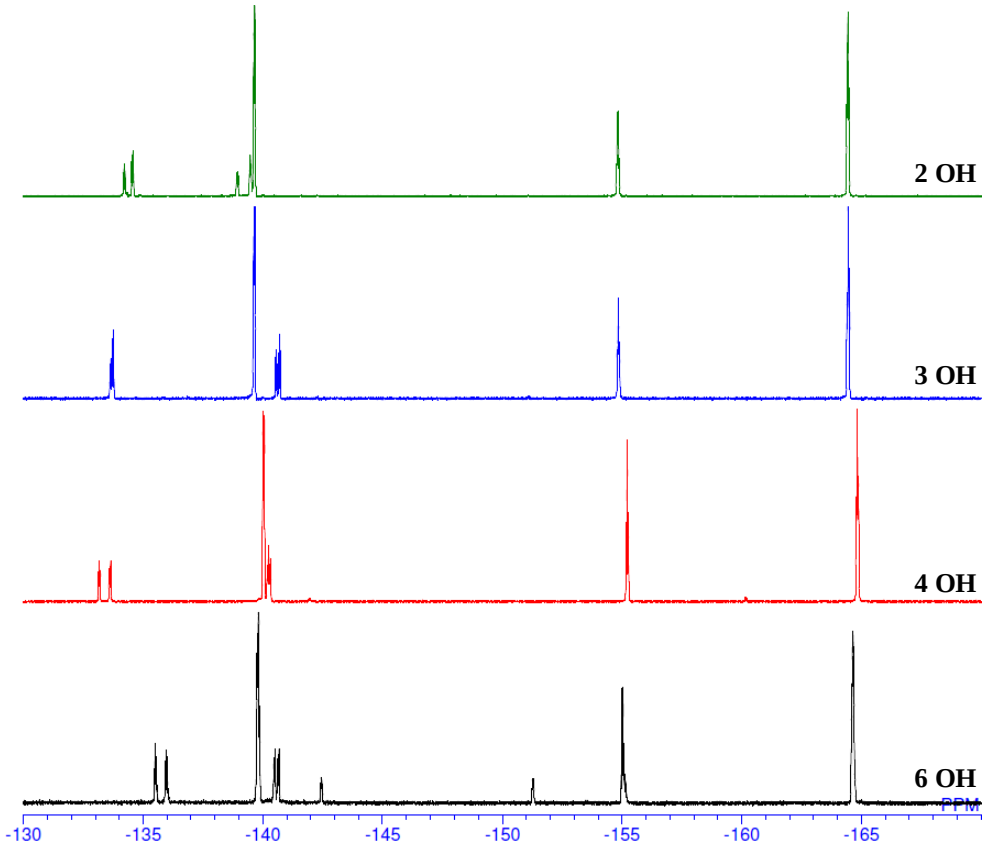

Figure 3.4 Selected ^{19}F NMR of **2-4OH**, **6OH**

3.2.3 Electronic Absorption Spectra of Mono-Glycoconjugated TFPPs

Light is a critical factor in PDT as it is known that PDT is a light-based treatment. The light's wavelength range typically used for PDT relies 600-800 nm is called "therapeutic window". The energy in this wavelength range is sufficient enough to excite the photosensitizers and allows the light to appropriately penetrate the tissue [36,37]. In order to study the aggregation behaviour of **2-4OH**, and **6OH**, their electronic absorption was measured in dimethylsulfoxide (DMSO) and in phosphate buffer saline (PBS). Figure 3.5 shows the electronic absorption of **2-4OH**, and **6OH** recorded in DMSO, and Table 3.1 summarizes their maximum absorption wavelengths (λ_{max}) and molar extinction coefficients (ε). **2-4OH**, and **6OH** have one intense peak of Soret band at

approximately 413 nm and three vibronic peaks (Q bands) around 505 to 648 nm typical for phyllo-type UV-vis spectra of porphyrins with *meso*-position are occupied by substituents [38]. An intense Soret band in this UV-vis spectra documented in DMSO is characteristic of the monomeric form of mono-glycoconjugated porphyrins. No detectable differences informed by Figure 3.5 means the electronic absorption measured in DMSO did not depend on the positional isomer of D-glucose. Meanwhile, the UV-vis spectra of **2-4OH**, and **6OH** measured in phosphate buffer saline (PBS) containing 1 vol% DMSO afford a distinct decrease in the intensity and broadening of the Soret band as shown in Figure 3.6 and are listed in Table 3.2 for their maximum absorption wavelengths (λ_{max}) and molar extinction coefficients (ε), respectively. These results parallel to the spectrum of **1OH** that was reported previously [28]. The four mono-glycoconjugates displayed a red-shifted Soret bands in PBS solution as clearly indicated from Table 3.2 imply the formation of J-aggregates [39] similar to **1OH** in PBS [28]. Table 3.2 also informed the order of molar extinction coefficients (ε) of **2-4OH**, and **6OH** for their Soret band is **2OH** > **6OH** > **4OH** > **1OH** > **3OH**. This order means **3OH** more aggregated than other mono-glycoconjugated prophyrins. The differences in the aggregation behavior of these mono-glycoconjugated porphyrins **2-4OH**, and **6OH** with different in positional isomer of 2-4, 6 thioglucopyranoses are not easy to be explained. It is known that the aggregation of porphyrins as indicated by wavelength shift and absorption changes are dependent upon such factors as pH, temperature, solvent change [38]. A detail investigation i.e. dynamic light scattering (DLS) for the number of molecules or size of an aggregate in solution is needed in order to gain the information about this aggregation behaviour.

Further, the oscillator strength as an important parameter representing the light absorbing ability and the photoexcitation probability was evaluated in the wavelength over 500 nm ($f_{>500nm}$). The $f_{>500nm}$ becomes an important factor for the next photocytotoxicity evaluation (a 100 W halogen

lamp equipped with a Y-50 cut-off filter (λ > 500 nm)). The calculated oscillator strengths (Table 1 and Table 2) indicate the constant values for all TFPP-glucose conjugates which is around 0.03-0.04 in DMSO and is about 0.05-0.06 in PBS containing 1%vol DMSO.

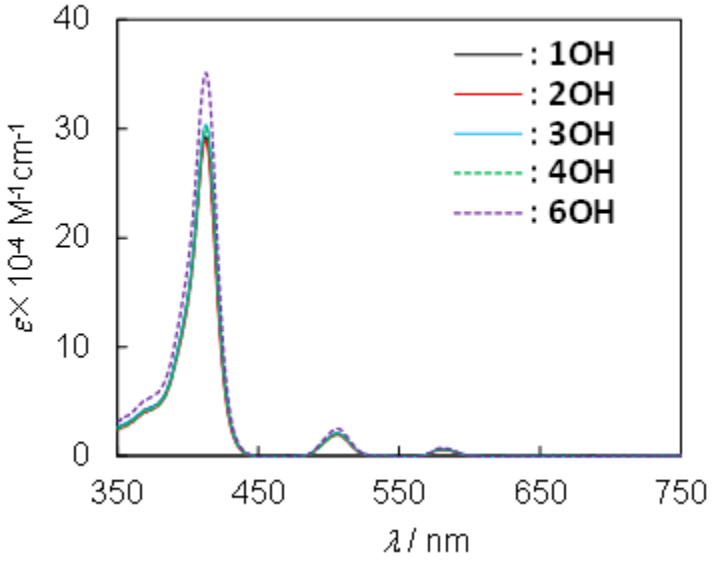

Figure 3.5 UV-vis spectra of **1-4OH** and **6OH** in DMSO at 25 °C. [**1-4OH**, and **6OH**]= 5.00 µM.

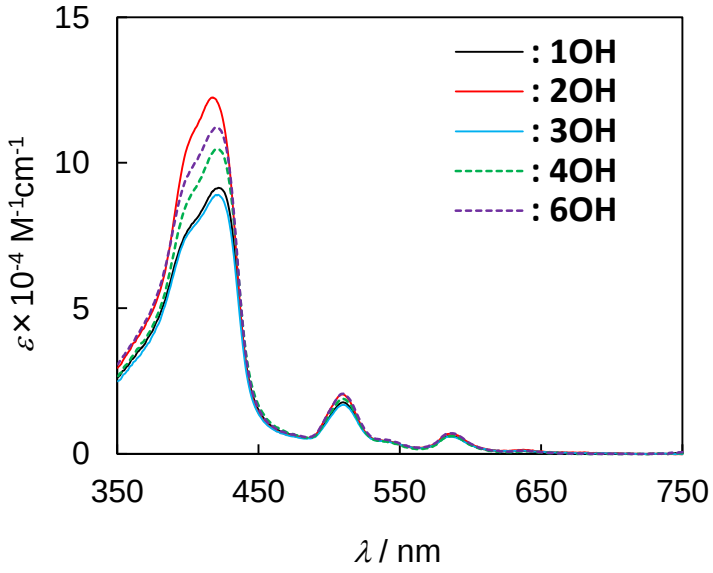

Figure 3.6 UV-vis spectra of **1-4OH**, and **6OH** in PBS (1% DMSO) at 25°C.

Table 3.1 UV-Vis and Photoluminescence Spectral Data of **1-4OH**, and **6OH** in DMSO at 25°C.[a]

	UV-vis					Luminescence
	λ_{max} / nm ($\varepsilon \times 10^{-4}$ / M^{-1} cm^{-1})				$f_{>500\ nm}$[b]	λ_{max} / nm[c]
	Soret	Q bands				
1OH	412.5 (29.3)	505.5 (2.09)	537.5 (0.07)	582.0 (0.61)	0.03	637.5, 702.5
2OH	412.5 (28.9)	506.0 (1.93)	537.5 (0.03)	582.0 (0.55)	0.03	637.5, 702.5
3OH	413.0 (30.4)	505.5 (2.13)	537.5 (0.06)	581.0 (0.63)	0.03	637.5, 703.0
4OH	413.0 (30.2)	506.0 (2.01)	537.5 (0.02)	582.0 (0.57)	0.03	637.5, 703.0
6OH	412.5 (35.1)	505.5 (2.52)	536.5 (0.06)	581.0 (0.71)	0.04	637.5, 702.5

[a] [**1OH**] = 5.00 μM, [**2OH**] = 4.44 μM, [**3OH**] = 4.48 μM, [**4OH**] = 4.05 μM, [**6OH**] = 4.19 μM. [b] Oscillator strength in the range above 500 nm estimated as $4.32 \times 10^{-9} \int \varepsilon(\nu) d\nu$. [c] The excitation wavelength was adjusted to the maximum absorption wavelength of the Soret band.

Table 3.2 UV-Vis and Photoluminescence Spectral Data of **1-4OH**, and **6OH** in PBS (1% DMSO) at 25°C.[a]

	UV-vis					Luminescence
	λ_{max} / nm ($\varepsilon \times 10^{-4}$ / M^{-1} cm^{-1})				$f_{>500\ nm}$[b]	λ_{max} / nm[c]
	Soret	Q bands				
1OH	421.5 (9.1)	509.5 (1.77)	557.0 (0.23)	586.5 (0.60)	0.06	645.0, 709.0
2OH	417.5 (12.2)	509.0 (2.04)	556.5 (0.23)	586.0 (0.69)	0.06	646.5, 662.0, 702.5
3OH	421.5 (8.90)	509.0 (1.67)	557.0 (0.23)	586.0 (0.58)	0.05	645.5, 663.0, 703.0
4OH	421.5 (10.5)	510.0 (1.90)	557.0 (0.21)	586.5 (0.61)	0.06	646.0, 662.5, 703.0

6OH	421.0 (11.2)	510.0 (2.06)	557.0 (0.25)	586.0 (0.70)	0.06	645.5, 702.5

[a] [**1OH**] = 5.00 μM, [**2OH**] = 4.44 μM, [**3OH**] = 4.48 μM, [**4OH**] = 4.05 μM, [**6OH**] = 4.19 μM. [b] Oscillator strength in the range above 500 nm estimated as $4.32 \times 10^{-9} \int \varepsilon(\nu) d\nu$. [c] The excitation wavelength was adjusted to the maximum absorption wavelength of the Soret band.

The study of aggregation behavior of porphyrins are usually conducted by two spectroscopic techniques i.e. UV-Vis absorption and fluorescence spectroscopy due to their peculiar spectroscopic properties [38]. Figure 3.7 and Figure 3.8 shows fluorescence spectra of mono-glycoconjugated porphyrins **1-4OH**, and **6OH** recorded in DMSO and in PBS (1% DMSO). The fluorescence spectral data in DMSO and in PBS (1% DMSO) are listed in Table 3.1 and Table 3.2. In DMSO, **1-4OH**, and **6OH** display two emission bands which is characteristics of porphyrins [40] and they show a very small difference in intensities. In PBS (1% DMSO), **1-4OH** showed three emission bands, while **1OH** and **6OH** have two emission bands. All mono-glycoconjugated porphyrin **1-4OH**, and **6OH** exhibited a red-shift which correlates with the formation of J-aggregates [41].

The UV-Vis absorption and fluorescence spectroscopy studies indicate that mono-glycoconjugated porphyrins **1-4OH**, and **6OH** have an amphiphilic character where they are bearing hydrophilic and hydrophobic groups. These amphiphilic molecules are capable of forming micellar colloidal aggregates in aqueous solutions as displayed both by UV-Vis and fluorescence spectroscopy recorded in PBS (1%DMSO) solution. The driving force for micellar colloidal aggregates formation comes from the hydrophobic interaction accompanied by the desolvation process [41].

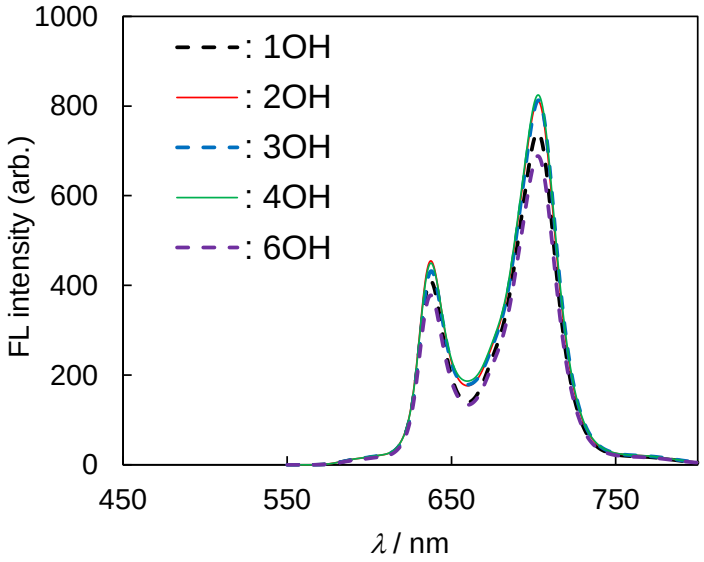

Figure 3.7 Steady-state luminescence spectra of **1-4OH** and **6OH** in DMSO at 25 °C. [**1-4OH**, and **6OH**]= 5.00 μM.

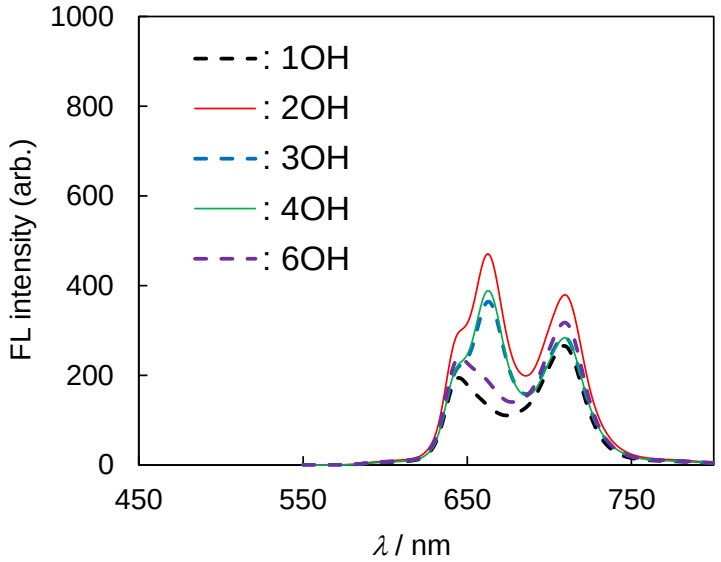

Figure 3.8 Steady-state luminescence spectra of **1-4OH**, and **6OH** in PBS (1% DMSO) at 25°C. [**1-4OH**, and **6OH**]= 5.00 μM.

3.3 Summary

The S_NAr reactions of TFPP with peracetylated thioglucopyranoses **2-Ac-S-AcGlc**, **3-Ac-S-AcGlc**, **4-Ac-S-AcGlc**, and **6-Ac-S-AcGlc** gave acetylated TFPP-glucose conjugates **2-4Ac** and **6Ac**. The

purity of these conjugates was 99% to more than 99% determined by HPLC analysis. Deprotection of acetyl groups produces the TFPP-glucose conjugates **2OH**, **3OH**, **4OH**, and **6OH** with >99% purities and are in the anomeric mixtures. While **2-4OH**, and **6OH** has phyllo-type UV-vis spectra with one intense peak of Soret band and three Q bands in DMSO, they have a broad peak in the UV-vis spectra recorded in PBS containing 1 vol% DMSO and displayed a red-shifted Soret band. The ^{1}H, ^{13}C, and ^{19}F NMR spectra establish the structure of all conjugates.

3.4 Experiments

Materials and Measurements

The purities of peracetyrated TFPP-Glucose conjugates **2Ac**, **3Ac**, **4Ac** and **6Ac** were determined to be >99% on an HPLC system (Jasco PU-2086 Plus Intelligent pump, Jasco Co., Ltd., Tokyo, Japan) equipped with a UV-vis detector (UV-2075 Plus, Jasco Co., Ltd.) and a silica gel column (COSMOSIL 5SL-II packed column, 4.6 mmϕ × 150 mm, Nacalai Tesque, Inc., Kyoto, Japan) using a mixture of dichloromethane (CH_2Cl_2) and ethyl acetate (9/1, v/v) at 30°C. The purities of TFPP-Glucose conjugates **2OH**, **3OH**, **4OH** and **6OH** were determined to be >97% on an HPLC system (Jasco PU-2086 Plus Intelligent pump) equipped with a UV-vis detector (UV-2075 Plus) and a silica gel column (COSMOSIL 5SL-II packed column, 4.6 mmϕ× 150 mm, Nacalai Tesque, Inc.) using a mixture of CH_2Cl_2 and CH_3OH (9/1, v/v) at 30°C. Mass spectra were recorded using JEOL spiral TOF JMS-S3000 (MALDI-TOF) (JEOL Ltd., Tokyo, Japan). UV-vis spectra were recorded on UV-2550 spectrophotometer (Shimadzu Co., Kyoto, Japan) and V-570 spectrophotometer (JASCO Co., Ltd., Tokyo, Japan). Steady-state fluorescence (FL) spectra were recorded on FP-6300 spectrofluorometer (JASCO Co., Ltd., Tokyo, Japan). NMR spectra were recorded using an AVANCE III HD (500 MHz; Bruker Biospin K.K., Yokohama, Japan) and a

NMR-DD2 500PS (500 MHz; Agilent Technologies, CA, USA). Luminescence spectra of singlet oxygen sensitized by each compound's solution was recorded using a spectrometer (Jobin Yvon SPEX fluorolog3, HORIBA, Ltd., Kyoto, Japan) equipped with a photomultiplier (NIR-PMT R5509-72, Hamamatsu Photonics K.K., Shizuoka, Japan) cooled to 193 K. The absorbance and the fluorescence intensity of each well were determined using plate readers (Multiscan JX and Fluoroskan Ascent, Thermo Fisher Scientific Co., Yokohama, Japan).

5-[4-(1,3,4,6-Tetra-*O*-acetyl-2-thio-β-D-glucopyranos-2-*S*-yl)-2,3,5,6-tetrafluoro-phenyl)]-10,15,20-tris(2,3,4,5,6-pentafluorophenyl)porphyrin (2Ac). TFPP (192.2 mg, 197 μmol), **2-Ac-S-AcGlc** (117.8 mg, 290 μmol), and diethylamine (DEA, 60 μL, 580 μmol) were dissolved in DMF (40 mL). The reaction mixture was stirred at room temperature for 24h, diluted with CH_2Cl_2 (15 mL) and washed with distilled water (15 mL × 5). The extract was dried over Na_2SO_4 and the solvent was removed under reduced pressure. The crude product was purified by column chromatography (silica gel, CH_2Cl_2 to CH_2Cl_2/EtOAc = 100–90:10) to give TFPP-glucose conjugate **2Ac** (41.2 mg, yield 15.8%) as deep purplish red solids. Purity (HPLC): 98.7%. MALDI-TOF high resolution mass spectrometry (HRMS): *m*/*z* for $C_{58}H_{29}N_4O_9F_{19}S$ ($[M]^+$) cacld 1318.13560, found 1318.13464 (error 0.97 mmu, 0.73 ppm). ^{1}H NMR ($CDCl_3$, 499.91 MHz, Si(CH_3)$_4$ = 0 ppm): δ (ppm) = 8.93 (8H, br s, 2,3,7,8,12,13,17,18-β-pyrrole*H*), 6.02 (1H, d, *J* = 9.0 Hz, 1'-Glc*H*), 5.36 (1H, dd, *J* = 10.0 Hz and 9.0 Hz, 3'-Glc*H*), 5.24 (1H, dd, *J* = 10.0 Hz and 10.0, 4'-Glc*H*), 4.44 (1H, dd, *J* = 12.0 Hz and 4.0 Hz, 6'-Glc*H*), 4.17 (1H, dd, *J* = 12.0 Hz and 2.00 Hz, 6-Glc*H*), 3.99 (1H, ddd, *J* = 12.0 Hz, 4.0 Hz and 2.0 Hz, 5'-Glc*H*), 3.64 (1H, dd, *J* = 9.0 Hz and 9.0 Hz, 2'-Glc*H*), 2.26 (3H, s, C*H*$_3$), 2.25 (3H, s, C*H*$_3$), 2.14 (3H, s, C*H*$_3$), 2.12 (3H, s, C*H*$_3$), −2.92 (2H, br s, N*H*). ^{13}C NMR ($CDCl_3$, 125.72 MHz, $CDCl_3$ = 77.0 ppm): δ (ppm) = 170.64 (*C*=O),

170.26 (*C*=O), 169.64 (*C*=O), 169.55 (*C*=O), 147.48−145.48 (2,6-Ph*C*, 3,5-Ph*C*, α-pyrrole*C*), 130.98 (β-pyrrole*C*), 122.35 (4-Ph*C*), 115.47 (1-Ph*C*), 103.84 (meso*C*), 94.17 (1'-Glc*C*), 72.72 (5'-Glc*C*), 71.58 (3'-Glc*C*), 68.94 (4'-Glc*C*), 61.45 (6'-Glc*C*), 52.82 (2'-Glc*C*), 20.78 (*C*H_3), 20.69 (*C*H_3), 20.68 (*C*H_3), 20.61 (*C*H_3). ^{19}F NMR ($CDCl_3$, 470.34 MHz, C*F*$_3$CO_2H = −76.05 ppm): δ (ppm) = −131.85 (2F, dd, $J_{F\text{-}F}$ = 25.9 Hz, $J_{F\text{-}F}$ = 13.3 Hz, 3,5-Ph*F*Glc), −136.54 (2F, dd, $J_{F\text{-}F}$ = 25.8 Hz, $J_{F\text{-}F}$ = 12.4 Hz, 2,6-Ph*F*Glc), −137.18 (6F, dd, $J_{F\text{-}F}$ = 15.2 Hz, $J_{F\text{-}F}$ = 6.7 Hz, 3,5-Ph*F*), −151.78 (3F, dd, $J_{F\text{-}F}$ = 20.0 Hz, $J_{F\text{-}F}$ = 20.0 Hz, 4-Ph*F*), −161.92 (6F, dd, $J_{F\text{-}F}$ = 14.3 Hz, $J_{F\text{-}F}$ = 6.7 Hz, 2,6-Ph*F*). UV-Vis (c = 5.00 μM, DMSO, path length = 1 cm, 25 °C): λ/nm ($\varepsilon \times 10^{-4}$/M^{-1} cm^{-1}) = 412 (33.96), 505 (2.44), 532 (0.34), 580 (0.80), 631 (0.10).

5-[4-(1,2,4,6-Tetra-*O*-acetyl-3-thio-D-glucopyranos-3-*S*-yl)-2,3,5,6-tetrafluoro-phenyl)]-10,15,20-tris(2,3,4,5,6-pentafluorophenyl)porphyrin (3Ac). A procedure similar to that described for TFPP-glucose conjugate **2Ac** was applied to TFPP (112.8.mg, 116 μmol), **3-Ac-S-AcGlc** (91.7 mg, 226 μmol), and DEA (40 μL, 387 μmol) to give TFPP-glucose conjugate **3Ac** (83.0 mg, yield 54.4%) as a deep purplish red solids. Purity (HPLC): >99%. MALDI-TOF high resolution mass spectrometry (HRMS): *m*/*z* for $C_{58}H_{29}N_4O_9F_{19}S$ ([M]$^+$) cacld 1318.13569, found 1318.13464 (error 1.05 mmu, 0.80 ppm). ^{1}H NMR ($CDCl_3$, 499.91 MHz, Si(C*H*$_3$)$_4$ = 0 ppm): δ (ppm) = 8.99 (2H, br s, 3,7-β-pyrrole*H*), 8.93 (6H, br s, 2,8,12,13,17,18-β-pyrrole*H*), 6.44 (0.5H, d, J = 4.0 Hz, 1'α-Glc*H*), 5.83 (1H, dd, J = 8.0 Hz, 1'β-Glc*H*), 5.42-5.37 (2.5H, m, 2'α-,2'β-,6"β-Glc*H*), 5.32 (0.5H, m, 6"α-Glc*H*), 4.36-4.31 (1.5H, m, 4'αβ-Glc*H*), 4.23-4.18 (2H, m, 3'α-,5'αβ-Glc*H*), 3.97-3.90 (1.5H, m, 6'α-,3'β-Glc*H*), 3.71 (1H, dd, J = 10.0 Hz, 6'β-Glc*H*), 2.29 (3H, s, C*H*$_3$), 2.28 (3H, s, C*H*$_3$), 2.27 (3H, s, C*H*$_3$), 2.23 (3H, s, C*H*$_3$), 2.21 (3H, s, C*H*$_3$), 2.20 (3H, s, C*H*$_3$), 2.159 (3H, s, C*H*$_3$), 2.156 (3H, s, C*H*$_3$), −2.91 (2H, br s, N*H*). ^{13}C NMR ($CDCl_3$, 125.72 MHz, $CDCl_3$ = 77.0 ppm): δ (ppm) = 170.74 (*C*=O), 169.45 (*C*=O), 169.16 (*C*=O), 169.12 (*C*=O),

147.45−145.45 (2,6-Ph*C*, 3,5-Ph*C*, α-pyrrole*C*), 131.26 (β-pyrrole*C*), 122.03 (4-Ph*C*), 115.48 (1-Ph*C*), 103.87 (meso*C*), 93.13 (1'α-Glc*C*), 88.88 (1'β-Glc*C*), 75.40 (6'α-Glc*C*), 71.28 (5'αβ-Glc*C*), 70.73 (2'αβ-Glc*C*), 70.33 (6"α-Glc*C*), 68.20 (6"β-Glc*C*), 62.00 (4'αβ-Glc*C*), 61.91 (3'α-Glc*C*), 54.18 (6'β-Glc*C*), 50.33 (3'β-Glc*C*), 20.92 (*C*H_3), 20.80 (*C*H_3), 20.63 (*C*H_3), 20.58 (*C*H_3). ^{19}F NMR ($CDCl_3$, 470.34 MHz, C*F*$_3$CO$_2$H = −76.05 ppm): δ (ppm) = −131.74 (2F, dd, $J_{F\text{-}F}$ = 25.8 Hz, $J_{F\text{-}F}$ = 12.4 Hz, 3,5-Ph*F*Glc), −136.59 (2F, dd, $J_{F\text{-}F}$ = 25.8 Hz, $J_{F\text{-}F}$ = 12.4 Hz, 2,6-Ph*F*Glc), −137.18 (6F, dd, $J_{F\text{-}F}$ = 22.0 Hz, $J_{F\text{-}F}$ = 22.0 Hz, 3,5-Ph*F*), −151.84 (3F, dd, $J_{F\text{-}F}$ = 32.4 Hz, $J_{F\text{-}F}$ = 19.0 Hz, 4-Ph*F*), −161.94 (6F, dd, $J_{F\text{-}F}$ = 12.4 Hz, $J_{F\text{-}F}$ = 6.9 Hz, 2,6-Ph*F*). UV-Vis (*c* = 5.00 μM, DMSO, path length = 1 cm, 25 °C): λ/nm ($\varepsilon \times 10^{-4}$/M^{-1} cm^{-1}) = 412 (33.62), 505 (2.46), 532 (0.36), 580 (0.82), 631 (0.12).

5-[4-(1,2,3,6-Tetra-O-acetyl-4-thio-D-glucopyranos-4-*S*-yl)-2,3,5,6-tetrafluoro-phenyl)]-10,15,20-tris(2,3,4,5,6-pentafluorophenyl)porphyrin (4Ac). A procedure similar to that described for TFPP-glucose conjugate **2Ac** was applied to TFPP (111.9 mg, 115 μmol), **4-Ac-S-AcGlc** (20.9 mg, 52 μmol), and DEA (37 μL, 358 μmol) to give TFPP-glucose conjugate **4Ac** (59.2 mg, yield 39.1%) as a deep purplish red solids. Purity (HPLC): >99%. MALDI-TOF high resolution mass spectrometry (HRMS): *m*/*z* for $C_{58}H_{29}N_4O_9F_{19}S$ ([M]$^+$) cacld 1318.13565, found 1318.13464 (error 1.01 mmu, 0.77 ppm). ^{1}H NMR ($CDCl_3$, 499.91 MHz, Si(CH_3)$_4$ = 0 ppm): δ (ppm) = 9.05 (2H, br s, 3,7-β-pyrrole*H*), 8.92 (6H, br s, 2,8,12,13,17,18-β-pyrrole*H*), 6.43 (0.3H, d, *J* = 4.0 Hz, 1'α-Glc*H*), 5.85 (1H, dd, *J* = 8.0 Hz, 1'β-Glc*H*), 5.62 (0.3H, dd, *J* = 10.0 Hz, 3'α-Glc*H*), 5.35 (1H, dd, *J* = 11.0 Hz, 9.0 Hz, 3' β-Glc*H*), 5.20-5.27 (1.3H, m, 2'αβ-Glc*H*), 4.70-4.76 (1.3H, m, 6''αβ-Glc*H*), 4.61 (1H, dd, *J* = 12.0 Hz, 2.0 Hz, 6'α-Glc*H*), 4.47-4.52 (0.6H, m, 6'α-,5'α-Glc*H*), 4.17-4.20 (1H, m, 5'β-Glc*H*), 3.89-3.97 (1.3H, m, 4' αβ-Glc*H*), 2.26 (3H, s, CH_3), 2.25 (3H, s, CH_3), 2.24 (3H, s, CH_3), 2.17 (3H, s, CH_3), 2.13 (3H, s, CH_3), 2.11 (3H, s, CH_3), −2.92

(2H, br s, N*H*). ^{13}C NMR ($CDCl_3$, 125.72 MHz, $CDCl_3$ = 77.0 ppm): δ (ppm) = 170.53 (*C*=O), 170.05 (*C*=O), 169.62 (*C*=O), 168.93 (*C*=O), 147.46−145.48 (2,6-Ph*C*, 3,5-Ph*C*, α-pyrrole*C*), 131.25 (β-pyrrole*C*), 122.12 (4-Ph*C*), 115.51 (1-Ph*C*), 103.81 (meso*C*), 91.49 (1'β-Glc*C*), 75.15 (5'β-Glc*C*), 72.08 (3'β-Glc*C*), 71.77 (2'β-Glc*C*), 63.11 (6'β-Glc*C*), 48.00 (4'β-Glc*C*), 20.86 (*C*H_3), 20.74 (*C*H_3), 20.68 (*C*H_3), 20.63 (*C*H_3). ^{19}F NMR ($CDCl_3$, 470.34 MHz, C*F*$_3$CO$_2$H = −76.05 ppm): δ (ppm) = −132.23 (2F, dd, $J_{F\text{-}F}$ = 24.8 Hz, $J_{F\text{-}F}$ = 11.5 Hz, 3,5-Ph*F*Glc), −136.29 (2F, dd, $J_{F\text{-}F}$ = 23.8 Hz, $J_{F\text{-}F}$ = 11.5 Hz, 2,6-Ph*F*Glc), −136.54 (6F, dd, $J_{F\text{-}F}$ = 24.5 Hz, $J_{F\text{-}F}$ = 10.5 Hz, 3,5-Ph*F*), −151.96 (3F, dd, $J_{F\text{-}F}$ = 21.9 Hz, $J_{F\text{-}F}$ = 21.9 Hz, 4-Ph*F*), −162.04 (6F, dd, $J_{F\text{-}F}$ = 17.2 Hz, $J_{F\text{-}F}$ = 6.9 Hz, 2,6-Ph*F*). UV-Vis (*c* = 5.00 μM, DMSO, path length = 1 cm, 25 °C): λ /nm ($\varepsilon \times 10^{-4}$/M^{-1} cm^{-1}) = 412 (31.58), 505 (2.30), 532 (0.34), 580 (0.76), 631 (0.12).

5-[4-(1,2,3,4-Tetra-O-acetyl-6-thio-D-glucopyranos-6-*S*-yl)-2,3,5,6-tetrafluoro-phenyl)]-10,15,20-tris(2,3,4,5,6-pentafluorophenyl)porphyrin (6Ac). TFPP (100.0 mg, 103 μmol), **6-Ac-S-AcGlc** (127.6 mg, 314 μmol), and DEA (45 μL, 435 μmol) were dissolved in DMF (25 mL). The reaction mixture was stirred at 60ºC for 24h, diluted with CH_2Cl_2 (15 mL) and washed with distilled water (15 mL × 5). The extract was dried over Na_2SO_4 and the solvent was removed under reduced pressure. The crude product was purified by column chromatography (silica gel, CH_2Cl_2 to CH_2Cl_2/EtOAc = 100-90:10) to give TFPP-glucose conjugate **6Ac** (8.5 mg, yield 6.3%) as a deep purplish red solids. Purity (HPLC): >99%. MALDI-TOF high resolution mass spectrometry (HRMS): *m*/*z* for $C_{58}H_{29}N_4O_9F_{19}S$ ($[M]^+$) cacld 1318.13593, found 1318.13464 (error 1.29 mmu, 0.98 ppm). ^{1}H NMR ($CDCl_3$, 499.91 MHz, Si(CH_3)$_4$ = 0 ppm): δ (ppm) = 8.99 (2H, br s, 3,7-β-pyrrole*H*), 8.92 (6H, br s, 2,8,12,13,17,18-β-pyrrole*H*), 5.87 (1H, d, *J* = 8.0 Hz, 1'-Glc*H*), 5.37 (1H, dd, *J* = 9.0 Hz, 9.0 Hz, 4'-Glc*H*), 5.30-5.23 (2H, m, 2',3'-Glc*H*), 4.14-4.11 (1H, m, 5'-Glc*H*), 3.45 (1H, dd, *J* = 9.0 Hz, 9.0 Hz, 6'α-Glc*H*), 3.35 (1H, m, 6"-Glc*H*), 2.16 (3H, s, CH_3), 2.09 (3H,

s, C*H*$_3$), 2.07 (3H, s, C*H*$_3$), 1.87 (3H, s, C*H*$_3$), −2.92 (2H, br s, N*H*). ^{13}C NMR ($CDCl_3$, 125.72 MHz, $CDCl_3$ = 77.0 ppm): δ (ppm) = 170.17 (*C*=O), 169.68 (*C*=O), 169.33 (*C*=O), 168.83 (*C*=O), 147.52−145.46 (2,6-Ph*C*, 3,5-Ph*C*, α-pyrrole*C*), 131.27 (β-pyrrole*C*), 120.43 (4-Ph*C*), 115.51 (1-Ph*C*), 103.57 (meso*C*), 91.72 (1'-Glc*C*), 74.98 (5' -Glc*C*), 72.61 (4'-Glc*C*), 70.68 (3'-Glc*C*), 70.35 (2'-Glc*C*), 35.56 (6'β-Glc*C*), 20.74 (*C*H$_3$), 20.65 (*C*H$_3$), 20.58 (*C*H$_3$), 20.53 (*C*H$_3$). ^{19}F NMR ($CDCl_3$, 470.34 MHz, C*F*$_3$CO$_2$H = −76.05 ppm): δ (ppm) = −133.77 (2F, dd, $J_{F\text{-}F}$ = 24.8 Hz, $J_{F\text{-}F}$ = 12.4 Hz, 3,5-Ph*F*Glc), −137.29 (6F, dd, $J_{F\text{-}F}$ = 23.8 Hz, $J_{F\text{-}F}$ = 11.5 Hz, 3,5-Ph*F*), −138.02 (2F, dd, $J_{F\text{-}F}$ = 25.8 Hz, $J_{F\text{-}F}$ = 12.5 Hz, 2,6-Ph*F*Glc), −152.00 (3F, dd, $J_{F\text{-}F}$ = 33.3 Hz, $J_{F\text{-}F}$ = 21.0 Hz, 4-Ph*F*), −162.05 (6F, dd, $J_{F\text{-}F}$ = 17.2 Hz, $J_{F\text{-}F}$ = 6.9 Hz, 2,6-Ph*F*). UV-Vis (*c* = 5.00 μM, DMSO, path length = 1 cm, 25°C): λ/nm ($\varepsilon \times 10^{-4}$/M^{-1} cm^{-1}) = 412 (36.67), 505 (2.60), 532 (0.33), 580 (0.83), 631 (0.10).

5-[4-(D-Glucopyranosylthio)-1,3,5,6-tetrafluorophenyl)]-10,15,20-tris(2,3,4,5,6-penta-fluorophenyl)porphyrin (2OH). TFPP-Glucose conjugate **2Ac** (48.7mg, 37 μmol) was dissolved in CH_2Cl_2 (20 mL) and MeOH (20 mL). NaOMe was added to adjust the pH to 9. This mixture was heated for 5 min at 40°C, then neutralized with acetic acid. The solvent was removed and the crude product was washed with distilled water (15 mL × 5). The crude product was purified by column chromatography (silica gel, CH_2Cl_2/MeOH = 9/1) and washed with distilled water to give TFPP-glucose conjugate **2OH** (28.3 mg, yield 66.6%) as a deep brownish purple solids. Purity (HPLC): >99%. MALDI-TOF high resolution mass spectrometry (HRMS): *m*/*z* for $C_{50}H_{19}N_4O_4F_{19}S$ ($[M - H_2O]^+$) cacld 1132.08085, found 1132.08181 (error -0.97 mmu, -0.85 ppm). Purity (^{19}F qNMR, 3,5-bis(trifluoromethyl)benzoic Acid): 84.1 wt%. ^{1}H NMR (CD_3OD, 499.91 MHz, C*H*D$_2$OD = 3.30 ppm): δ (ppm) = 9.32, 9.06 (8H, s,β-pyrrole*H*), 5.70 (1H, d, *J* = 2.0 Hz, 1'α-Glc*H*), 5.60 (1H, d, *J* = 4.0 Hz, 1'β-Glc*H*), 4.82 (1H, m, 3'α-Glc*H*), 4.72 (1H, m, 4'α-Glc*H*),

4.68 (1H, m, 6'α-Glc*H*), 4.48 (1H, m, 6''α-Glc*H*), 4.16 (3H, m, 3'β,5'αβ-Glc*H*), 3.54 (4H, m, 2'αβ-,6'β-,6''β-Glc*H*), 3.34 (1H, m, 4'β-Glc*H*). ^{13}C NMR (CD_3OD, 125.72 MHz,CD_3OD = 49.0 ppm): δ (ppm) = 149.06-129.57 (α,β-pyrrole*C*, 2,6-Ph*C* and 3,5-Ph*C*), 122.15 (4-Ph*C*), 116.65 (1-Ph*C*), 105.90, 105.50 (meso*C*), 104.97 (1'β-Glc*C*), 101.23 (1'α-Glc*C*), 90.95 (3'α-Glc*C*), 83.89 (6',6''α-Glc*C*), 81.66 (4'α-Glc*C*), 72.96 (3'β-Glc*C*), 72.49 (5'αβ-Glc*C*), 72.31 (2'α-Glc*C*), 72.30 (4'β-Glc*C*), 59.10 (2'β-Glc*C*), 58.90 (6',6''β-Glc*C*). ^{19}F NMR (CD_3OD, 470.34 MHz, CF_3CO_2H = −76.05 ppm): δ (ppm) = −134.41 (2F, dd, $J_{F\text{-}F}$ = 24.8 Hz, $J_{F\text{-}F}$ = 12.4 Hz, 3,5-Ph*F*Glc), −139.23 (2F, dd, $J_{F\text{-}F}$ = 24.8 Hz, $J_{F\text{-}F}$ = 11.4 Hz, 2,6-Ph*F*Glc), −139.67 (6F, m, $J_{F\text{-}F}$ = 21.9 Hz, 3,5-Ph*F*), −154.86 (3F, t, $J_{F\text{-}F}$ = 35.3 Hz, $J_{F\text{-}F}$ = 18.1 Hz, 4-Ph*F*), −164.47 (6F, dd, $J_{F\text{-}F}$ = 36.2 Hz, $J_{F\text{-}F}$ = 21.0 Hz, 2,6-Ph*F*). UV-Vis (*c* = 4.44 μM, DMSO, path length = 1 cm, 25°C): λ /nm ($\varepsilon \times 10^{-4}$/M^{-1} cm^{-1}) = 412.5 (28.94), 506.0 (1.93), 537.5 (0.03), 582 (0.55). FL (*c* = 4.44μM in DMSO, path length = 1 cm, λ_{ex} = 412.5 nm, 25°C): λ/nm = 637.5, 702.5.

5-[4-(D-glucopyranosylthio)-1,2,5,6-tetrafluorophenyl)]-10,15,20-tris(2,3,4,5,6-penta-fluorophenyl)porphyrin (3OH). A procedure similar to that described for glucosylated TFPP **2OH** was applied to TFPP-glucose conjugate **3Ac** (30.9 mg, 23 μmol) to give TFPP-glucose conjugate **3OH** (10.0 mg, yield 36.7%) as a deep brownish purple solids. Purity (HPLC): >99%. MALDI-TOF high resolution mass spectrometry (HRMS): *m*/*z* for $C_{50}H_{21}N_4O_5F_{19}S$ ([M]$^+$) cacld 1150.09196, found 1150.09238 (error -0.42 mmu, -0.36 ppm). Purity (^{19}F qNMR, 3,5-bis(trifluoromethyl)benzoic Acid): 88.1 wt%. ^{1}H NMR (CD_3OD, 499.91 MHz, C*H*D$_2$OD = 3.30 ppm): δ (ppm) = 9.32, 9.06 (8H, s,β-pyrrole*H*), 5.20 (1H, d, *J* = 4.0 Hz, 1'α-Glc*H*), 4.63 (1H, d, *J* = 8.0 Hz, 1'β-Glc*H*), 4.00-3.93 (2H, m, 4'β-,6'α-Glc*H*), 3.86-3.70 (5H, m, 2'α-,3'α-,4'α-,5'αβ-Glc*H*), 3.60 (1H, dd, *J* = 10.0 Hz, 3'β-Glc*H*), 3.50-3.46 (2H, m, 2'β-,6'β-Glc*H*). ^{13}C NMR (CD_3OD, 125.72 MHz, CD_3OD = 49.0 ppm): δ (ppm) = 148.95-129.60 (α,β-pyrrole*C*, 2,6-Ph*C*

and 3,5-Ph*C*), 121.02 (4-Ph*C*), 116.70 (1-Ph*C*), 106.34, 104.87 (meso*C*), 99.45 (1'α-Glc*C*), 93.72 (1'β-Glc*C*), 80.51 (2'β-Glc*C*), 76.26 (6'β-Glc*C*), 73.94 (3'α-Glc*C*), 73.87 (4'β-Glc*C*), 71.62 (2'α-Glc*C*), 62.85 (4'α-Glc*C*), 62.70 (5'αβ-Glc*C*), 59.37 (3'β-Glc*C*), 56.79 (6'α-Glc*C*). ^{19}F NMR (CD_3OD, 470.34 MHz, CF_3CO_2H = −76.05 ppm): δ (ppm) = −133.72 (2F, dd, $J_{F\text{-}F}$ = 25.8 Hz, $J_{F\text{-}F}$ = 12.4 Hz, 3,5-Ph*F*Glc), −139.67 (6F, m, $J_{F\text{-}F}$ = 15.2 Hz, $J_{F\text{-}F}$ = 6.6 Hz, 3,5-Ph*F*), −140.65 (2F, dd, $J_{F\text{-}F}$ = 24.8 Hz, $J_{F\text{-}F}$ = 11.4 Hz, 2,6-Ph*F*Glc), −154.88 (3F, t, $J_{F\text{-}F}$ = 20.0 Hz, $J_{F\text{-}F}$ = 8.6 Hz, 4-Ph*F*), −164.49 (6F, dd, $J_{F\text{-}F}$ = 22.9 Hz, $J_{F\text{-}F}$ = 6.7 Hz, 2,6-Ph*F*). UV-Vis (c = 4.48 μM, DMSO, path length = 1 cm, 25 °C): λ /nm ($\varepsilon \times 10^{-4}$/M^{-1} cm^{-1}) = 413.0 (30.39), 505.5 (2.13), 537.5 (0.06), 581.0 (0.63). FL (c = 4.48 μM in DMSO, path length = 1 cm, λ_{ex} = 413.0 nm, 25°C): λ/nm = 637.5, 703.0.

5-[4-(D-glucopyranosylthio)-1,2,3,6-tetrafluorophenyl)]-10,15,20-tris(2,3,4,5,6-penta-fluorophenyl)porphyrin (4OH). A procedure similar to that described for TFPP-glucose conjugate **2OH** was applied to TFPP-glucose conjugate **4Ac** (21.4 mg, 16 μmol) to give TFPP-glucose conjugate **4OH** (14.7 mg, yield 78.7%) as a deep brownish purple solids. Purity (HPLC): >99%. MALDI-TOF high resolution mass spectrometry (HRMS): m/z for $C_{50}H_{21}N_4O_5F_{19}S$ ([M]$^+$) cacld 1150.09283, found 1150.09238 (error 0.45 mmu, 0.39 ppm). Purity (^{19}F qNMR, 3,5-bis(trifluoromethyl)benzoic Acid): 80.1 wt%. ^{1}H NMR (CD_3OD, 499.91 MHz, C*H*D$_2$OD = 3.30 ppm): δ (ppm) = 9.32, 9.07 (8H, s,β-pyrrole*H*), 5.27 (1H, d, J = 4.0 Hz, 1'α-Glc*H*), 4.62 (1H, d, J = 8.0 Hz, 1'β-Glc*H*), 4.22-4.16 (2H, m, 6''β-,5'α-Glc*H*), 4.13-4.10 (2H, m, 6',6''α-Glc*H*), 3.98-4.07 (2H, m, 6'β-,4'α-Glc*H*), 3.73-3.69 (2H, m, 3'β-,3'α-Glc*H*), 3.52-3.60 (3H, m, 4'β-,5'β-,2'α-Glc*H*), 3.33 (1H, d, 2'β-Glc*H*). ^{13}C NMR (CD_3OD, 125.72 MHz, CD_3OD = 49.0 ppm): δ (ppm) = 149.07-129.79 (α,β-pyrrole*C*, 2,6-Ph*C* and 3,5-Ph*C*), 121.954-Ph*C*), 116.71(1-Ph*C*), 106.03, 104.93 (meso*C*), 98.12 (1'α-Glc*C*), 94.17 (1'β-Glc*C*), 77.96 (3'α-Glc*C*), 77.88 (3'β-Glc*C*), 77.50 (2'β-Glc*C*), 75.34 (2'α-Glc*C*), 73.51 (4'α-Glc*C*), 72.71 (6''β-Glc*C*), 63.50 (5'α-Glc*C*), 63.496

(6”α-Glc*C*), 63.40 (6’α-Glc*C*), 63.399 (6’β-Glc*C*), 52.76 (4’β-Glc*C*), 52.70 (5’β-Glc*C*). ^{19}F NMR (CD_3OD, 470.34 MHz, CF_3CO_2H = −76.05 ppm): δ (ppm) = −133.03 (2F, dd, $^3J_{F\text{-}F}$ = 24.8 Hz, $^5J_{F\text{-}F}$ = 11.4 Hz, 3,5-Ph*F*Glc), −139.68 (6F, m, $^3J_{F\text{-}F}$ = 24.8 Hz, 3,5-Ph*F*), −139.90 (2F, dd, $^3J_{F\text{-}F}$ = 24.8 Hz, $^5J_{F\text{-}F}$ = 11.5 Hz, 2,6-Ph*F*Glc), −154.87 (3F, t, $^3J_{F\text{-}F}$ = 21.0 Hz, 4-Ph*F*), −164.48 (6F, dd, $^3J_{F\text{-}F}$ = 20.0 Hz, 2,6-Ph*F*). UV-Vis (c = 4.05 μM, DMSO, path length = 1 cm, 25 °C): λ /nm (ε × 10^{-4}/M^{-1} cm^{-1}) = 413.0 (30.15), 506.0 (2.01), 537.5 (0.02), 582.0 (0.57). FL (c = 4.05μM in DMSO, path length = 1 cm, λ_{ex} = 413.0 nm, 25°C): λ/nm = 637.5, 703.0.

5-[4-(D-glucopyranosylthio)-1,2,3,4-tetrafluorophenyl)]-10,15,20-tris(2,3,4,5,6-penta-fluorophenyl)porphyrin (6OH). A procedure similar to that described for TFPP-glucose conjugate **2OH** was applied to TFPP-glucose conjugate **6Ac** (8.5 mg, 6 μmol) to give TFPP-glucose conjugate **6OH** (6.0 mg, yield 80.9%) as a deep brownish purple solid. Purity (HPLC): >99%. MALDI-TOF high resolution mass spectrometry (HRMS): *m*/*z* for $C_{50}H_{21}N_4O_5F_{19}S$ ($[M]^+$) cacld 1150.09181, found 1150.09238 (error -0.57 mmu, -0.49 ppm). Purity (^{19}F qNMR, 3,5-bis(trifluoromethyl)benzoic Acid): 83.7 wt%. ^{1}H NMR (CD_3OD, 499.91 MHz, C*H*D_2OD = 3.30 ppm): δ (ppm) = 9.32, 9.07 (8H, s,β-pyrrole*H*), 5.27 (1H, d, J = 4.0 Hz, 1’α-Glc*H*), 4.62 (1H, d, J = 8.0 Hz, 1’β-Glc*H*), 4.22-4.16 (2H, m, 6”β-,5’α-Glc*H*), 4.13-4.10 (2H, m, 6’,6”α-Glc*H*), 3.98-4.07 (2H, m, 6’β-,4’α-Glc*H*), 3.73-3.69 (2H, m, 3’β-,3’α-Glc*H*), 3.52-3.60 (3H, m, 4’β-,5’β-,2’α-Glc*H*), 3.33 (1H, d, 2’β-Glc*H*). ^{13}C NMR (CD_3OD, 125.72 MHz, CD_3OD = 49.0 ppm): δ (ppm) = 149.07-129.79 (α,β-pyrrole*C*, 2,6-Ph*C* and 3,5-Ph*C*), 121.954-Ph*C*), 116.71(1-Ph*C*), 106.03, 104.93 (meso*C*), 98.12 (1’α-Glc*C*), 94.17 (1’β-Glc*C*), 77.96 (3’α-Glc*C*), 77.88 (3’β-Glc*C*), 77.50 (2’β-Glc*C*), 75.34 (2’α-Glc*C*), 73.51 (4’α-Glc*C*), 72.71 (6”β-Glc*C*), 63.50 (5’α-Glc*C*), 63.496 (6”α-Glc*C*), 63.40 (6’α-Glc*C*), 63.399 (6’β-Glc*C*), 52.76 (4’β-Glc*C*), 52.70 (5’β-Glc*C*). ^{19}F NMR (CD_3OD, 470.34 MHz, CF_3CO_2H = −76.05 ppm): δ (ppm) = −133.03 (2F, dd, $^3J_{F\text{-}F}$ = 24.8

Hz, $^{5}J_{F\text{-}F}$ = 11.4 Hz, 3,5-Ph*F*Glc), −139.68 (6F, m, $^{3}J_{F\text{-}F}$ = 24.8 Hz, 3,5-Ph*F*), −139.90 (2F, dd, $^{3}J_{F\text{-}F}$ = 24.8 Hz, $^{5}J_{F\text{-}F}$ = 11.5 Hz, 2,6-Ph*F*Glc), −154.87 (3F, t, $^{3}J_{F\text{-}F}$ = 21.0 Hz, 4-Ph*F*), −164.48 (6F, dd, $^{3}J_{F\text{-}F}$ = 20.0 Hz, 2,6-Ph*F*). UV-Vis (*c* = 4.19 μM, DMSO, path length = 1 cm, 25°C): λ /nm (ε × 10^{-4}/M^{-1} cm^{-1}) = 412.5 (35.11), 505.5 (2.52), 536.5 (0.06), 581 (0.71). FL (*c* = 4.19μM in DMSO, path length = 1 cm, λ_{ex} = 412.5 nm, 25°C): λ/nm = 637.5, 702.5.

3.5 References

1. Hirohara, S.; Nishida, M.; Sharyo, K.; Obata, M.; Ando, T.; Tanihara, M. *Bioorg. Med. Chem.* **2010**, *18*, 1526.
2. Boyle, R. W.; Dolphin, D. *Photochem. Photobiol.* **1996**, *64*, 469.
3. Kessel, D. *Photodiagn. Photodyn. Ther.* **2004**, *1*, 3.
4. Zhang, Y.; Lovell, J. F. *Theranostics* **2012**, *2*, 905.
5. Bonnett, R. *Chemical Aspects of Photodynamic Therapy*; Gordon and Breach Science Publishers, CRC Press: Boca Raton, FL, 2000.
6. Yano, S.; Hirohara, S.; Obata, M.; Hagiya, Y.; Ogura, S.; Ikeda, A.; Kataoka, H.; Tanaka, M.; Joh, T. *J. Photochem. Photobiol. C: Photohem. Rev.* **2011**, *12*, 46.
7. Moser, J. G. Definition and General Properties of 2nd and 3rd Generation Photosensitizers. In *Photodynamic Tumor Therapy, 2nd and 3rd Generation Photosensitizers*; Moser, J. G., Ed.; Harwood Academic Publishers: The Netherlands, 1998.
8. Wu, J.; Han, H.; Jin, Q.; Li, Z.; Li, H.; Ji, J. *ACS Appl. Mater. Interfaces* **2017**, *9*, 14596.
9. Saenz, C.; Cheruku, R. K.; Ohulchanskyy, T. Y.; Joshi, P.; Tabaczynski, W. A.; Missert, J. R.; Chen, Y.; Pera, P.; Tracy, E.; Marko, A.; Rohrbach, D.; Sunar, U.; Baumann, H.; Pandey, R. K. *ACS Chem. Biol.*, **2017**, *12*, 933.

10. Hirohara, S.; Oka, C.; Totani, M.; Obata, M.; Yuasa, J.; Ito, H.; Tamura, M.; Matsui, H.; Kakiuchi, K.; Kawai, T.; Kawaichi, M.; Tanihara, M. *J. Med. Chem.* **2015**, *58*, 8658.
11. Zheng, G.; Graham, A.; Shibata, M.; Missert, J. R.; Oseroff, O. R.; Dougherty, T. J.; Pandey, R. K. *J. Org. Chem.* **2001**, *66,* 8709.
12. Hirohara, S.; Kawasaki, Y.; Funasako, R.; Yasui, N.; Totani, M.; Alitomo, H.; Yuasa, J.; Kawai, T.; Oka, C.; Kawaichi, M.; Obata, M.; Tanihara, M. *Bioconjugate Chem.* **2012**, *23*, 1881.
13. Zheng, X.; Morgan, J.; Pandey, S. K.; Chen, Y.; Tracy, E.; Baumann, H.; Missert, J. R.; Batt, C.; Jackson, J.; Bellnier, D. A.; Henderson, B. W.; Pandey, R. K. *J. Med. Chem.* **2009**, *52*, 4306.
14. Singh, S.; Aggarwal, A.; Bhupathiraju, N. V. S. D. K.; Arianna, G.; Tiwari, K.; Drain, C. M. *Chem. Rev.* **2015**, *115*, 10261.
15. Tanaka, M.; Kataoka, H.; Mabuchi, M.; Sakuma, S.; Takahashi, S.; Tujii, R.; Akashi, H.; Ohi, H.; Yano, S.; Morita, A.; Joh, T. *Anticancer Res.* **2011**, *31*, 763.
16. Waki, A.; Fujibayashi, Y.; Yokoyama, A. *Nucl. Med. Biol.* **1998**, *25*, 589.
17. Warburg, O. *Science* **1956**, *123*, 309.
18. Ahmed, S.; Davoust, E.; Savoie, H.; Boa, A. N.; Boyle, R. W. *Tetrahedron Lett.* **2004**, *45,* 6045.
19. Sylvain, I.; Zerrouki, R.; Granet, R.; Huang, Y. M.; Lagorce, J. -F.; Guilloton, M.; Blais, J. -C.; Krausza, P. *Bioorg. Med. Chem.* **2002**, *10*, 57.
20. Hirohara, S.; Obata, M.; Saito, A.; Ogata, S.; Ohtsuki, C.; Higashida, S.; Ogura, S.; Okura, I.; Sugai, Y.; Mikata, Y.; Tanihara, M.; Yano, S. *Photochem. Photobiol.* **2004**, 80, 301.
21. Hirohara, S.; Obata, M.; Ogata, S.; Ohtsuki, C.; Higashida, S.; Ogura, S.; Okura, I.; Takenaka, M.; Ono, H.; Sugai, Y.; Mikata, Y.; Tanihara, M.; Yano, S. *J. Photochem. Photobiol. B: Biol.*

2005, *78*, 7.

22. Hirohara, S.; Obata, M.; Ogata, S.; Kajiwara, K.; Ohtsuki, C.; Tanihara, M.; Yano, S. *J. Photochem. Photobiol. B: Biol.* **2006**, *84*, 56.
23. Obata, M.; Hirohara, S.; Sharyo, K.; Alitomo, H.; Kajiwara, K.; Ogata, S.; Tanihara, M.; Ohtsuki, C.; Yano, S. *Biochim. Biophys. Acta* **2007**, *1770*, 1204.
24. Hirohara, S.; Obata, M.; Alitomo, H.; Sharyo, K.; Ogata, S.; Ohtsuki, C.; Yano, S.; Ando, T.; Tanihara, M. *Biol. Pharm. Bull.* **2008**, *31*, 2265.
25. Hirohara, S.; Obata, M.; Alitomo, H.; Sharyo, K.; Ando, T.; Tanihara, M.; Yano, S. *J. Photochem. Photobiol. B: Biol* **2009**, 97, 22.
26. Pasetto, P.; Chen, X.; Drain, C. M.; Franck, R. W. *Chem. Commun.* **2001**, *0*, 81.
27. Chen, X.; Hui, L.; Foster, D. A.; Drain, C. M. *Biochemistry* **2004**, *43*, 10918.
28. Hirohara, S.; Nishida, M.; Sharyo, K.; Obata, M.; Ando, T.; Tanihara, M. *Bioorg. Med. Chem.* **2010**, *18*, 1526.
29. Miljković, M. *Carbohydrates Synthesis, Mechanisms, and Stereoelectronic Effects*; Springer, NY, 2010.
30. Kohata, K.; Higashio, H.; Yamaguchi, Y.; Koketsu, M.; Odashima, T. *Bull. Chem. Soc. Jpn.* **1994**, *67*, 668.
31. Oulmi, D.; Maillard, P.; Guerquin-Kern, J. -L.; Huel, C.; Momenteau, M. *J. Org. Chem.* **1995**, *60*, 1554.
32. Mikata, Y.; Onchi, Y.; Tabata, K.; Ogura, S-I.; Okura, I.; Ono, H.; yano, S. *Tetrahedron Lett.* **1998**, *39*, 4505.
33. Hamazawa, A.; Isamu, K.; Brian, B.; Kiyoshi, I.; Minako, S.; Yasuko, B.; Toyoji, K.; Hirohara, S.; Obata, M.; Mikata, Y.; Yano, S. *Chem. Lett.* **2002**, *3*, 388.

34. Hirohara, S.; Sharyo, K.; Kawasaki, Y.; Totani, M.; Tomotsuka, A.; Funasako, R.; Yasui, N.; Hasegawa, Y.; Yuasa, J.; Nakashima, T.; Kawai, T.; Oka, C.; Kawaichi, M.; Obata, M.; Tanihara, M. *Bull. Chem. Soc. Jpn.* **2013**, *86*, 1295.
35. Roslund, M. U.; Tähtinen, P.; Niemitz, M.; Sjöholm, R. *Carbohydr. Res.* **2008**, *343*, 101.
36. Liu, H.; Celli, J. P. Looking Out The Optical Window: Physical Principles and Instrumentation of Imaging in Photodynamic Therapy. In *Imaging in Photodynamic Therapy*; Hamblin, M. R.; Huang, Y. Eds.; CRC Press:Boca Raton, FL, 2017.
37. Zhu, T. C.; Finlay, J. C. *Med. Phys.* **2008**, 35, 3127.
38. Giovannetti, R. The Use of Spectrophotometry UV-Vis for The Study of Porphyrins. In *Macro To Nano Spectroscopy*; Uddin, J. Ed.; InTech, Rijeka, Croatia, 2012.
39. Rubires, R.; Crusats, J.; El-Hachemi, Z.; Jaramillo, T.; López, M.; Valls, E.; Farrera, J-A.; Ribó, J. M. *New J. Chem.* **1999**, *23*, 189.
40. Gouterman, M. In *The Porphyrins*; Dolphin, D., Ed.; Academic: New York, 1978; Vol. 3, pp 1.
41. Khairutdinov, R. F.; Serpone, N. *J. Phys. Chem. B.* **1999**, *103*, 761.

CHAPTER 4 *In Vitro* Study of Mono-Glycoconjugated Porphyrins

4.1 Introduction

The disadvantages of current PSs should be responded by developing PSs and their PDT characteristics including hydrophilicity-hydrophobicity, reactive oxygen species (ROS) generation, cellular uptake, and selectivity [1-9]. In the previous chapter, the conjugation of 5,10,15,20-tetrakis(pentafluorophenyl)porphyrin (TFPP) with peracetylated thioglucopyranoses have been described to yield acetylated TFPP-glucose conjugates and TFPP-glucose conjugates, along with their characterization. This chapter informs the evaluation of hydrophobicity, ROS generation, cellular uptake, and photocytotoxicity of the resulted TFPP-glucoconjugates **2-4OH** and **6OH**. Next, their cellular uptake test of the TFPP-glucose conjugates was performed on RGK gastric carcinoma mucosal cell line (RGK cells). And finally, the photocytotoxicity TFPP-glucose conjugates were studied along with the results of **1OH** [22].

4.2 Results and Discussion

4.2.1 Hydrophobicity Parameters

Lipophilicity-hydrophobicity is one of the most important intrinsic properties of a compound. This character which is usually associated with polarity and molecular size determines various properties such as solubility and permeability-affinity for biological membranes and, therefore, controls the absorption, distribution, and transport. In PDT application, it is the key factor for transporting the photosensitizers into the cells [10,11].

The hydrophobicity parameter (Log *P*), the logarithmic scale of the partition coefficient between *n*-octanol and water, is closely correlated to the penetration and uptake behavior of drugs through

the cellular membrane [12-15]. Chromatographic method such as reversed-phase thin layer chromatography is an alternative technique for this purpose because the retention indices (R_f) relate with Log*P* value [16-18]. The R_f value is inversely proportional to the capacity factor *k′* in reverse-phase (i.e., partition) chromatography and is in a good-association with the Log*P*. In this experiment, *m*-hydroxybenzaldehyde [19], *p*-fluorobenzaldehyde [19], *m*-fluorobenzaldehyde [19], 5,15-bis-(4-(2-hydroxyethoxy)-2,3,5,6-tetrafluoro-phenyl)-10,20-bis(pentafluorophenyl)-porphyrin [20,21], 5,10-bis(4-(2-hydroxy-ethoxy)-2,3,5,6-tetrafluorophenyl)-15,20-bis(pentafluorophenyl)porphyrin [20,21], and 5,10,15-tris(4-(2-hydroxyethoxy)-2,3,5,6-tetrafluorophenyl)-20-pentafluorophenylporphyrin [20,21] were used as standards to calibrate the RP-TLC system. A good linearity of Log *P* values against Log *k'* values was resulted [20] and their values are tabulated in Table 4.1. The Log *P* values of the synthesized TFPP-glucose conjugates 5-[4-(D-Glucopyranosylthio)-1,3,5,6-tetrafluorophenyl)]-10,15,20-tris(2,3,4,5,6-pentafluorophenyl)porphyrin (**2OH**), 5-[4-(D-glucopyranosylthio)-1,2,5,6-tetrafluorophenyl)]-10,15,20-tris(2,3,4,5,6-penta-fluorophenyl)porphyrin (**3OH**), 5-[4-(D-glucopyranosylthio)-1,2,3,6-tetrafluorophenyl)]-10,15,20-tris(2,3,4,5,6-penta-fluorophenyl)porphyrin (**4OH**), and 5-[4-(D-glucopyranosylthio)-1,2,3,4-tetrafluorophenyl)]-10,15,20-tris(2,3,4,5,6-pentafluoro-phenyl)porphyrin (6OH) (**6OH**) were determined on the basis of this calibration and were compared to previously synthesized 5-[4-(D-Glucopyranosylthio)-2,3,5,6-tetrafluorophenyl)]-10,15,20-tris(2,3,4,5,6-penta-fluorophenyl)porphyrin (**1OH**) [22]. The hydrophobicity increased in the order of **1OH** < **3OH** < **4OH** < **6OH** < **2OH**. This results indicating **2OH** is most hydrophobic and **1OH** is the least hydrophobic in these series mean **3OH** and **4OH** presumably have good amphiphilic properties. **1OH** as the least hydrophobic mono-glycoconjugate among other possesses more hydrophilic character while **2OH** and **6OH** have more hydrophobic tendency.

This hydrophobicity parameter supposedly affects the biological activity of these mono-glycoconjugated porphyrins eventhough the correlation between this parameter with aggregation behavior as explained in Chapter 3 unclear.

Table 4.1 Capacity Factor (*k'*) in RP-TLC (MeOH : H_2O = 9 : 1 v/v) and Hydrophobicity Parameter (Log *P*) of TFPP-glucose conjugates **1-4OH**, and **6OH**.

	R_f	Log k'^a	Log P^b
1OH	0.19	0.72	6.05
2OH	0.11	0.96	6.87
3OH	0.17	0.77	6.21
4OH	0.16	0.80	6.30
6OH	0.14	0.85	6.50

[a] $k' = 1/R_f$. [b] Log P = 3.46 × Log k' + 3.55.

4.2.2 Cellular Uptake

A stomach cancer cell lines, i.e. RGK, gastric carcinoma mucosal cell line (RGK cells) was used as a model cancer cells for the cellular uptake examination. After incubation of this cell lines with **1–4OH**, and **6OH** in the concentration 2.5 μM for 8 and 24 h, the relative cellular uptake can be deduced as shown in the Figure 4.1. The increasing incubation time from 8 to 24 h increased the quantity of the conjugates taken up by the RGK cells, after normalization of the value to that of **1OH** for an 8h incubation. A considerable cellular uptake of **4OH** was shown by the RGK cells among other conjugates. There is correlation between cellular uptake after 8 h incubation with hydrophobicity parameter (Log P) values. **3OH** and **4OH** having intermediate Log P values showed higher uptake than other mono-glycoconjugated porphyrins. The cellular uptake after 8 h incubation increased in the order of **4OH** < **3OH** < **1OH** < **2OH** ≈ **6OH**.

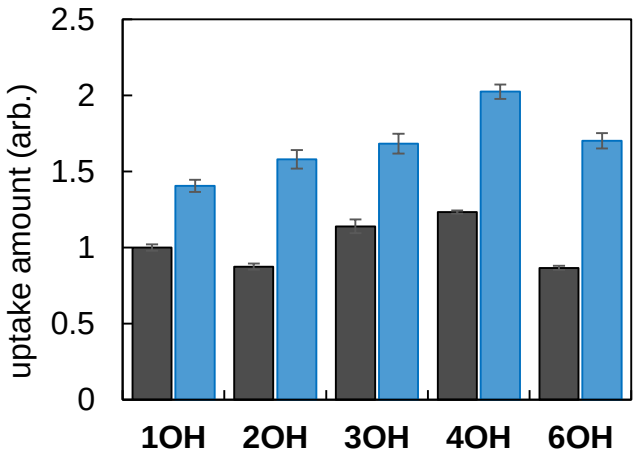

Figure 4.1 Relative uptake amount of TFPP-glucose conjugates **1–4OH**, and **6OH** in RGK-1 cells for 8h (gray stick bars) and 24h (blue stick bars) co-incubation. The concentration of the conjugates was 2.5 μM. Values are the mean ± standard deviation of three replicate experiments.

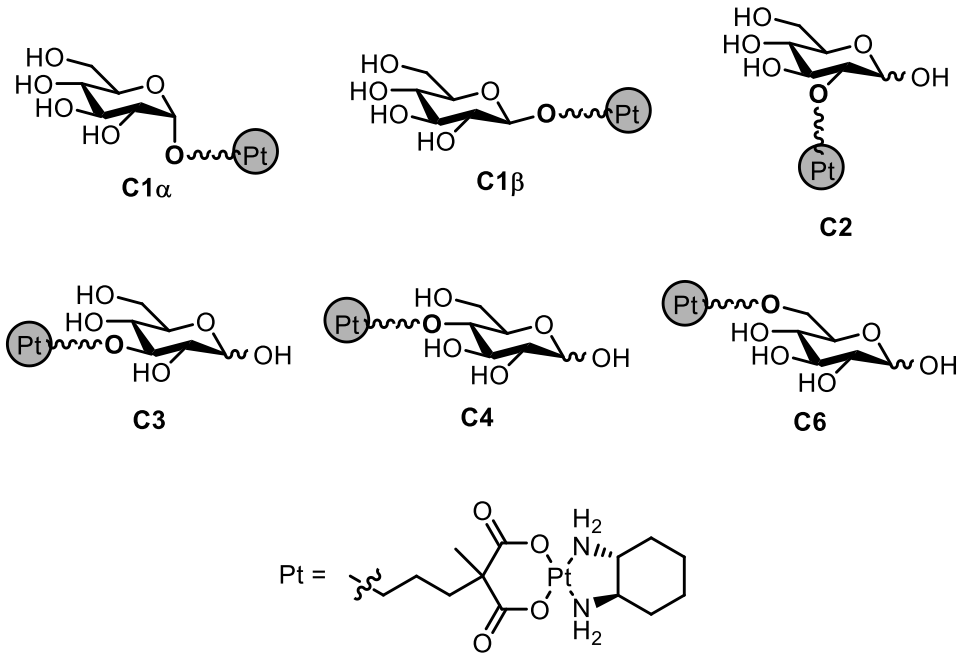

Scheme 4.1 Structure of Pt complex-glucose conjugates[24]

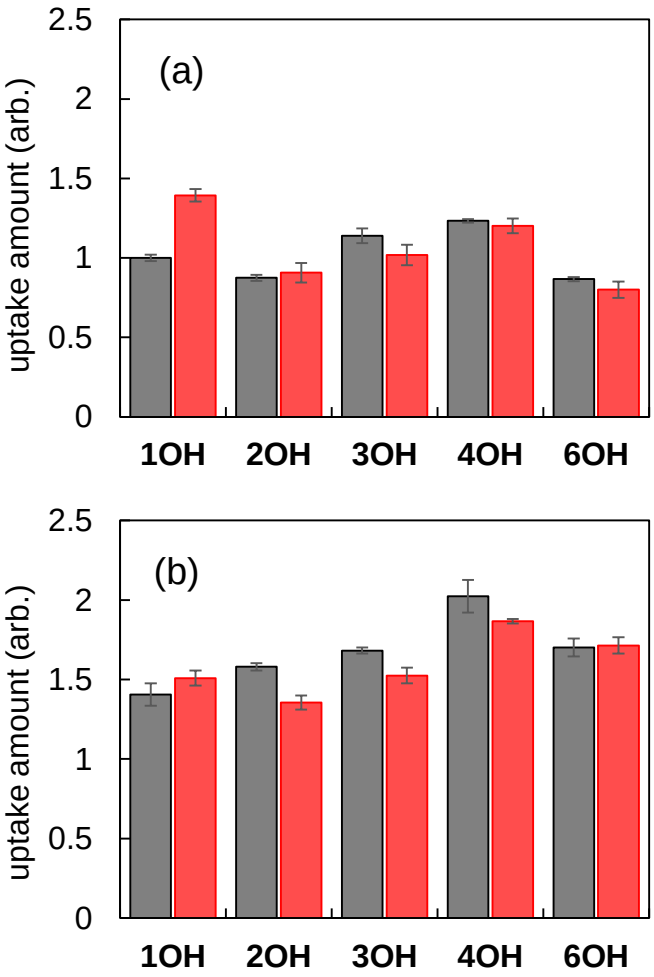

Figure 4.2 Relative uptake amount of TFPP-glucose conjugates **1–4OH**, and **6OH** in RGK cells in the absence (gray stick bars) and presence (red stick bars) of cytochalasin B (c = 50 μM), which is a GLUT1 inhibitor, for 8h (a) and 24h (b) co-incubation. The concentration of the conjugates was 2.5 μM. Values are the mean ± standard deviation of three replicate experiments.

Further investigation on the cellular uptake in RGK cells was carried out in the presence of cytochalasin B, an inhibitor of the membrane-bound glucose transporter (GLUT1) which is usually overexpressed in brain tumors and stomach cancer [23,24], after an 8 and 24 h co-incubation (Figure 4.2). Previous report by Lippard *et al.* stated that a platinum complex Glc-Pt **C2** displayed a high anticancer activity reflected from its high uptake in cancer cells that overexpressed GLUT1 [24]. Study was performed on the cellular uptake of D-glucose with different positions of platinum

complexes (**C1*α***, **C1*β***, **C2**, **C3**, **C4**, and **C6**) (Scheme 4.1) using A2780, A549, and DU 145 cells with 7.5 ~ 72h co-incubation. Figure 4.2 informs that with the occurrence of cytochalasin B the uptake of **2-4OH** by RGK cells was slightly inhibited. This finding implies that GLUT1 partially drives the cellular uptake of these conjugates. A non-specific interaction with cellular membrane probably will be enhanced due to this fact which reflect the small effect of cytochalasin B on the cells. The strong hydrophobic nature of **2-4OH** possibly affects this small influence.

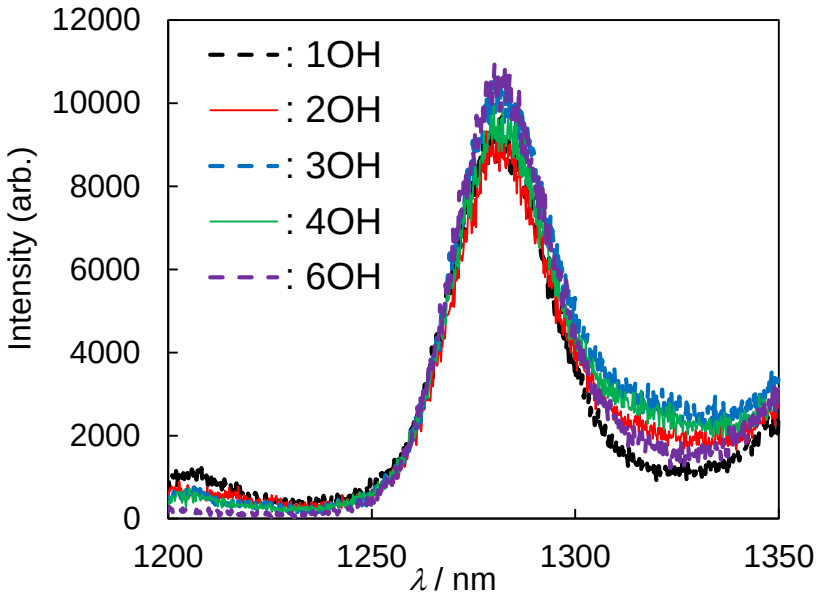

Figure 4.3 Luminescence spectra of $^1O_2$ generated by photosensitization using TFPP-glucose conjugates **1–4OH** and **6OH** in MeOH under O_2 saturated condition. Excitation wavelength was 399.4 nm (**1OH**), 397.6 nm (**2OH**), 395.4 nm (**3OH**), 397.6 nm (**4OH**) and 389.8 nm (**6OH**) (Abs. = 0.2).

4.2.3 Relative Quantum Yield of Singlet Oxygen Generation (Φ_{1O2})

One of the most important factors for the successful PDT application is ROS generation due to the fact that ROS are the key cytotoxic intermediates of PDT [22,26-28]. Photochemical reaction generates ROS during photoabsorption of **2–4OH**, and **6OH** by means of 1) electron transfer generating superoxide anion, hydroxyl radical, etc. (type I reaction) and 2) energy transfer

producing singlet oxygen ($^1O_2$) (type II reaction). Both type of reaction are important for the successful of PDT application [22,29] though it is well known that type II reaction mainly occur during photoabsorption process because of the relatively long lifetime of $^1O_2$.

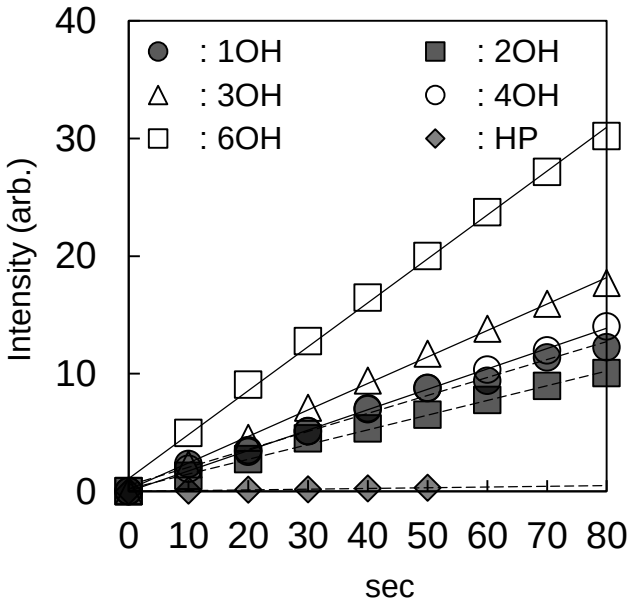

Figure 4.4 The plots of HPF fluorescence intensity of the O_2-saturated PBS solution containing 1% DMSO in the presence of TFPP-glucose conjugates **1–4OH** and **6OH** and HP as a function of the photoirradiation time.

The $^1O_2$ luminescence measurements at 1270 nm in O_2-saturated MeOH for **2–4OH**, and **6OH** was used to measure the relative quantum yield of $^1O_2$ generation (Φ_Δ) (Figure 4.3). This Φ_Δ was normalized to the values for **1OH**. Type I reaction (the relative quantum yields of •OH ($\Phi_{\bullet OH}$)) was evaluated by the rate constant for the increment of the initial rate of hydroxyphenyl fluoresein (HPF)-fluorescence intensity [30] (Figure 4.4) and this value was normalized to the value for hematoporphyrin (HP). Table 4.2 lists the relative Φ_Δ and $\Phi_{\bullet OH}$ values for the TFPP-glucose conjugates. It clearly indicates that there is no differences for all TFPP-glucose conjugates in the Φ_Δ values in methanol. On the other hand, **2–4OH**, and **6OH** generated a higher •OH compared to HP, similar to **1OH** [29]. The order of $\Phi_{\bullet OH}$ values is **2OH** < **1OH** < **4OH** < **3OH** << **6OH**.

This result implies that the $\Phi_{\bullet OH}$ values were dependent, not only on the *S*-glycosylation pattern, but also the specific of D-glucose. It is presumably can be correlated with the different reactivity of thioglucopyranose groups in the mono-glycoconjugated porphyrins. It is known that anomeric position (C1) is the most reactive and C6 is the least reactive among other position (C2, C3, C4). The relative quantum yield of singlet oxygen (Φ_{Δ}) and hydroxyl radical ($\Phi_{\bullet OH}$) of mono-glycoconjugated porphyrins **1-4OH**, and **6OH** also can be evaluated more precisely by using sodium azide and D-mannitol as $^1O_2$ quencer for type II reaction and •OH scavenger for type I reaction, respectively.

Table 4.2 Relative Quantum Yield of Singlet Oxygen (Φ_{Δ}) and Hydroxyl Radical ($\Phi_{\bullet OH}$) of TFPP-glucose conjugates **1-4OH**, and **6OH**.

	$\Phi_{\Delta}{}^a$	$\Phi_{\bullet OH}{}^b$
1OH	1.0	25.0
2OH	1.0	20.5
3OH	1.0	36.9
4OH	1.0	28.4
6OH	1.0	61.2
HP	–	1.0

[a] In O_2-saturated methanol and normalized to the values for **1OH**. The excitation wavelength was 399.4 nm (**1OH**), 397.6 nm (**2OH**), 395.4 nm (**3OH**), 397.6 nm (**4OH**), and 389.8 nm (**6OH**) (Abs = 0.2). [b] The $\Phi_{\bullet OH}$ value in O_2-saturated PBS containing 1 vol% DMSO and normalized to the values for HP.

4.2.4 *In vitro* Study of Photocytotoxicity

The next study is the photocytotoxicity. This experiment was conducted by using a Human cervical cell line (HeLa cells) in the dark and by irradiation together with **1–4OH**, and **6OH** at a concentration of 1.0 μM. A 100 W halogen lamp ($\lambda > 500$ nm) at a light dose of 0 J cm^{-2} (dark) or

16 J cm^{-2} was operated as a light source for this photocytotoxicity evaluation of these conjugates which were incubated with the cells for 24h [31]. The percentage of cell survival (%) was evaluated in terms of the mitochondrial activity of NADH dehydrogenase using the WST-8® reagent from Cell Counting Kit-8 at 24h post-photoirradiation. The value was normalized to the survival rate in the absence of photosensitizer, namely vehicle. These TFPP-glucose conjugates **1–4OH**, and **6OH** showed no cytotoxicity in the dark (Figure 4.5a). Contrastingly, potent photocytotoxicity was

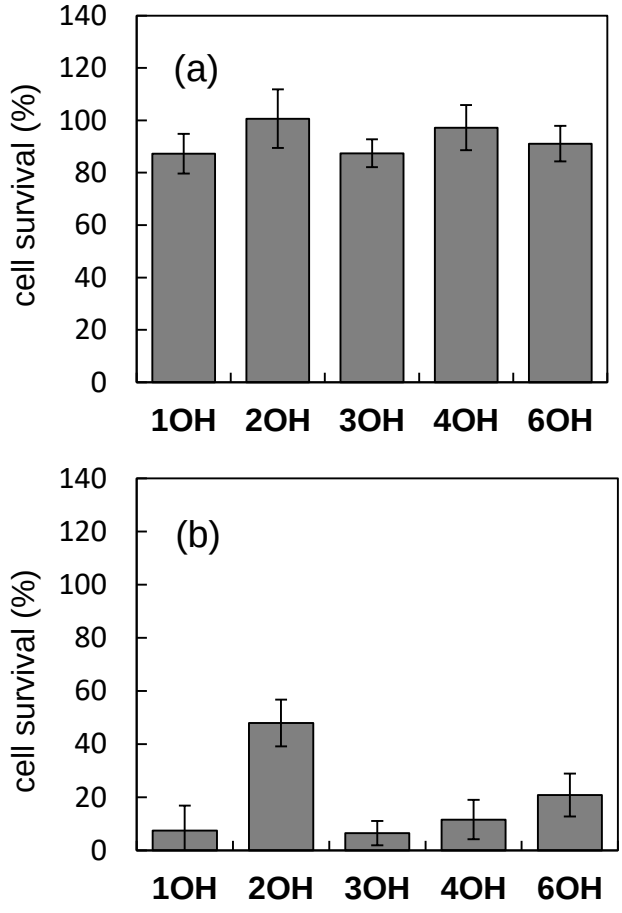

Figure 4.5 Dark (a) and photocytotoxicity (b) of TFPP-glucose conjugates **1–4OH**, and **6OH** in HeLa cells. The concentration of the conjugate was 1.0 μM. The light dose was 0 J cm^{-2} (dark) and 16 J cm^{-2} from a 100 W halogen lamp (λ > 500 nm). Values are the mean ± standard deviation of six replicate experiments.

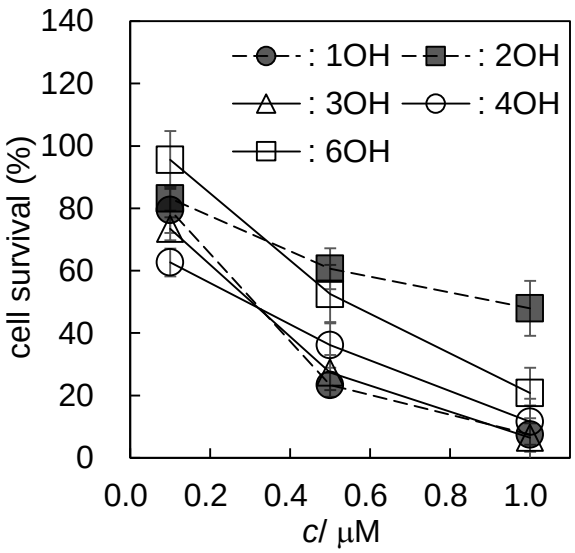

Figure 4.6 Plot of the cell survival rate (%) of HeLa cells treated with TFPP-glucose conjugates **1–4OH**, and **6OH** as a function of the concentration. The light dose was 16 J cm^{-2} from a 100 W halogen lamp (λ > 500 nm). Incubation time with the conjugates was 24 h. Values are the mean ± standard deviation of six replicate experiments.

displayed by all of these conjugates, except for **2OH**, under photoirradiation (Figure 4.5b). These results indicate that the light dose 16 J cm^{-2} was suitable for this photocytotoxicity evaluation. The light dose 16 J cm^{-2} was determined by evaluation of light dependency on the effect of photocytotoxicity of glysocylated porphyrins as previously reported [31]. Briefly, the appropriate light dose was examined by evaluation of HeLa cell survival on irradiation using a halogen lamp (100 W, λ > 500 nm). The results indicated the cell survival decreased from 100.5% to 17.9% as the light dose increased and a lethal dose to 50% of the cell population was found to be 16 J cm^{-2}.

Further photocytotoxicity evaluation was performed in HeLa cells for **1–4OH**, and **6OH** in the concentration range from 0.1 to 1.0 μM (Figure 4.6). A slight higher photocytotoxicity result was shown by **1OH**, **3OH**, and **4OH** with lower concentration needed to induce 50% cell death (EC_{50}) values to some degree compared to the values for **2OH** and **6OH**. The EC_{50} values for **1OH**, **3OH**, and **4OH** are less than 0.5 μM, whereas the EC_{50} values for **2OH** and **6OH** are more than 0.5μM.

It is clear from this result that the cellular uptake after 8 h incubation and photocytotoxicity was parallel for these mono-glycoconjugated porphyrins. The average hydrophobicity of mono-glycoconjugated porphyrins possibly responsible for these results. Besides, under the same conditions as for HeLa cells, the human glioblastoma cell line (U251) and RGK cells were also

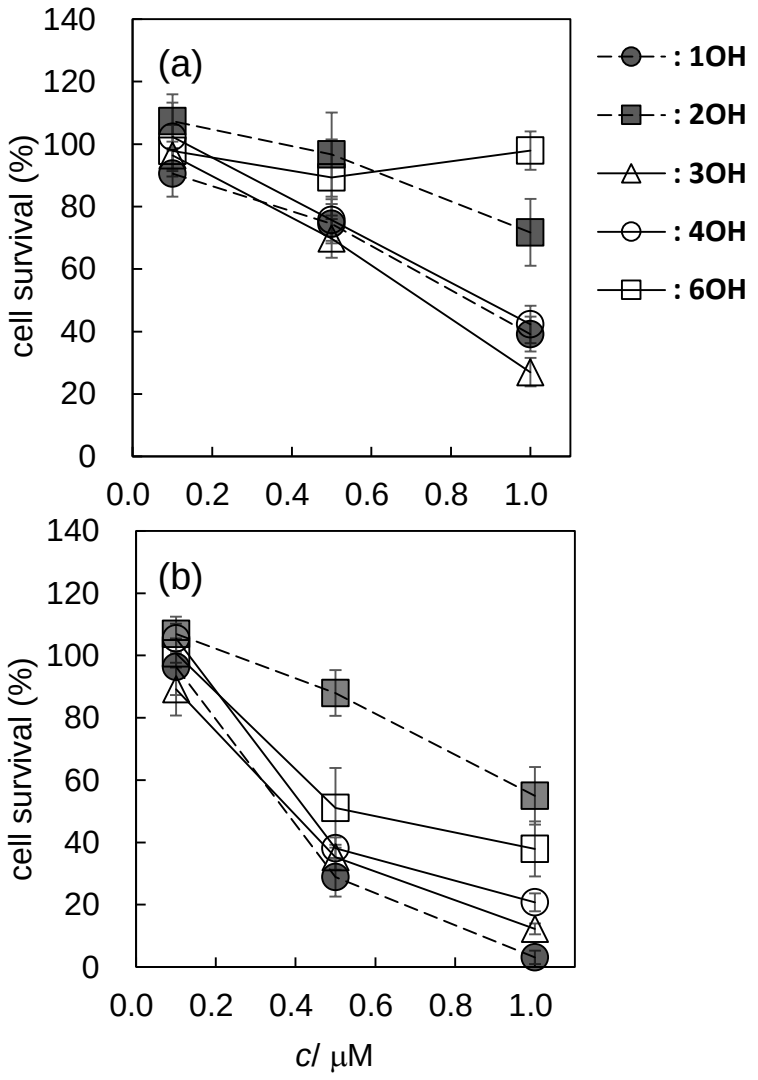

Figure 4.7 Plot of the cell survival rate (%) of U251 cells (a) and RGK cells (b) treated with TFPP-glucose conjugates **1–4OH**, and **6OH** as a function of the concentration. The light dose was 16 J cm^{-2} from a 100 W halogen lamp (λ > 500 nm). Incubation time with the conjugates was 24 h. Values are the mean ± standard deviation of six replicate experiments.

used for the photocytotoxicity test of **1–4OH** and **6OH**. This additional evaluation was carried out due to the fact that PDT has been applied to the treatment of many types of cancer including brain cancer and early gastric cancer [32,33]. A similar outcome to that in HeLa cells for the positional isomers effect in both cells was found for this experiment as illustrated in Figure 4.7. The photocytotoxicity evaluated in U251 cells indicates EC_{50} values for **1OH**, **3OH**, and **4OH** are less than 1.0 μM and the EC_{50} values for **2OH** and **6OH** are more than 1.0 μM. The EC_{50} values resulted from photocytotoxicity evaluation with RGK cells for **1OH**, **3OH**, and **4OH** are less than 0.5 μM and the EC_{50} values for **2OH** and **6OH** are more than 0.5 μM and 0.5 μM, respectively.

4.3 Summary

The hydrophobicity parameter (Log *P*) of TFPP-glucose conjugates was determined by RP-TLC and increased in the order of **1OH** < **3OH** < **4OH** < **6OH** < **2OH**. The cellular uptake examination by RGK cells revealed that the quantity of TFPP-glucose conjugates taken up by the RGK cells linearly correlates with the increasing incubation time. Among them, **4OH** shows a significant cellular uptake. The relative quantum yield of $^1O_2$ generation (Φ_Δ) of **2–4OH**, and **6OH** illustrates that no contrast displayed by all TFPP-glucose conjugates in methanol. **2–4OH**, and **6OH** generated a higher •OH compared to HP, similar to **1OH**. The order of $\Phi_{\bullet OH}$ values is **2OH** < **1OH** < **4OH** < **3OH** << **6OH**. The photocytotoxicity studied in HeLa cells indicates that none of these TFPP-glucose conjugates showed cytotoxicity in the dark, but potent photocytotoxicity was displayed by all of these conjugates, except for **2OH**, under photoirradiation. With detailed photocytotoxicity evaluation in HeLa cells, **1OH**, **3OH**, and **4OH** showed a slight higher photocytotoxicity with lower concentration needed to induce 50% cell death (EC_{50}) values compared to the values for **2OH** and **6OH**. Further photocytotoxicity test using U251 cells and

RGK cells displayed identical results to those in HeLa cells.

4.4 Experiments

Materials and Measurements

Reverse-phase thin layer chromatography (RP-TLC) was carried out using R-18F_{254s} (Merck Japan Ltd., Tokyo, Japan). Luminescence spectra of singlet oxygen sensitized by each compound's solution was recorded using a spectrometer (Jobin Yvon SPEX fluorolog3, HORIBA, Ltd., Kyoto, Japan) equipped with a photomultiplier (NIR-PMT R5509-72, Hamamatsu Photonics K.K., Shizuoka, Japan) cooled to 193 K. The absorbance and the fluorescence intensity of each well were determined using plate readers (Multiscan JX and Fluoroskan Ascent, Thermo Fisher Scientific Co., Yokohama, Japan).

Hydrophobicity Parameters Determined by RP-TLC. The hydrophobicity parameter (logarithm of the partition coefficient between *n*-octanol and water; Log *P*) is well-correlated with the capacity factor *k*′ in reverse-phase (i.e., partition) chromatography as follows:

$$\text{Log } P = a \text{ Log } k' + b \qquad (1)$$

Where *a* and *b* are constants for a given chromatographic system. The capacity factor *k*′ was determined by the R_f value in RP-TLC and a mixture of MeOH and H_2O (9/1, v/v) as the eluent, and calculated as follows:

$$k' = 1 / R_f \qquad (2)$$

m-Hydroxybenzaldehyde (Log *P* = 1.70) [19], *p*-fluorobenzaldehyde (Log *P* = 1.39) [19], *m*-fluorobenzaldehyde (Log *P* = 1.89) [19], 5,15-bis(4-(2-hydroxyethoxy)-2,3,5,6-tetrafluoro-phenyl)-10,20-bis(pentafluorophenyl)porphyrin (Log *P* = 6.5) [20,21], 5,10-bis(4-(2-hydroxy-ethoxy)-2,3,5,6-tetrafluorophenyl)-15,20-bis(pentafluorophenyl)porphyrin (Log *P* = 6.5) [20,21],

and 5,10,15- tris(4-(2-hydroxyethoxy)-2,3,5,6-tetrafluorophenyl)-20-pentafluorophenylporphyrin (Log *P* = 5.4) [20,21] were used as standards to calibrate our RP-TLC system.

ROS Measurements.

Relative quantum yield of singlet oxygen generation (Φ_{1O2}).

Singlet oxygen (Φ_{1O2}). TFPP-glucose conjugates **1OH**, **2OH**, **3OH**, **4OH**, and **6OH** under study was dissolved in MeOH. The absorbance of the solution was adjusted to be 0.2 at an appropriate excitation wavelength (*vide infra*) and purged with oxygen gas for 1 min. Luminescence spectra of singlet oxygen generated by the photoirradiation of the solution were recorded on a spectrophotometer equipped with a photomultiplier cooled at 193 K.

Hydroxyl radical ($\Phi_{\bullet OH}$). **1-4OH**, and **6OH** (c = 1.00 mM), HP (c = 1.00 μM), and HPF (c = 225 nM) were dissolved in PBS containing 0.2% DMSO and placed into a cell. Oxygen gas was introduced to the solution for approximately 1 min prior to photoirradiation. Then, the solution was exposed to light from a 100 W halogen lamp through a Y-50 cutoff filter (λ > 500 nm) at 25°C. The initial rate of fluorescence intensity increments at 510 nm was monitored under the excitation at 490 nm. The rate constant was estimated from the first-order plot of fluorescence intensity increments against photoirradiation time. The relative quantum yield ($\Phi_{\bullet OH}$) was evaluated by the rate constant and was normalized to the value of HP.

***In vitro* studies.**

Cell culture. Human cervical cell line, HeLa (ATCC CCL-2), was obtained from Riken cell bank. Cells were grown in DMEM supplemented with 10% FCS. Human glioblastoma cell lines, U251, were obtained from the American Type Culture Collection. U251 cells were grown in DMEM supplemented with 10% FCS. An *N*-methyl-*N'*-nitro-*N*-nitroso guanidine (MNNG)-induced

mutant of a rat murine RGM gastric carcinoma mucosal cell line, RGK, was kindly provided by Dr. Matsui (Faculty of Medicine, University of Tsukuba). Cells were grown in a 1:1 mixture of DMEM and F12 supplemented with 10% FCS and Antibiotic-Antimycotic.

Cellular uptake inhibition by cytochalasin B. The cellular uptake of **1-4OH**, and **6OH** by RGK cells was examined as follows: Cells (2.5×10^6 cells/well) in 1.5 mL of culture medium were plated in a 6-well plate and incubated for 24 hours (37°C, 5% CO_2). The medium was aspirated, 1.5 mL fresh culture medium with or without cytochalasin B (50 μM final concentration) was added and the cells were incubated for 2h.[24] The medium was aspirated, 1.5 mL of 2.5 μM compound in culture medium containing 1% DMSO was added to each well and the plate was incubated for 8 or 24h. Then, the cells were washed twice with PBS. The cells were lysed in 150 μL of DMSO. The fluorescence intensity of each extract was measured with a plate reader using excitation and an emission wavelengths of 430 and 650 nm, respectively. The concentration of compounds was calculated on the basis of the calibration obtained for each compounds in DMSO. The cellular uptake is given as the means of three replicate experiments.

Photocytotoxicity Test. The photocytotoxicity of **1-4OH**, and **6OH** in these cell lines (HeLa, U251, and RGK cells) was examined as follows: Cells (5×10^3 cells/well) in 100 μL of culture medium were plated in a 96-well plate (Thermo Fisher Scientific Co.) and incubated for 24h (37°C, 5% CO_2). One hundred microliters of a TFPP-glucose conjugates in culture medium containing 2% DMSO was added to each well. The plate was then incubated at 24h in the presence of these compounds. The concentration of these compounds was varied from 0.1 mM to 1 mM in culture medium (final DMSO content was 1% in all cases). The cells were washed twice with PBS and 100 μL of the fresh culture medium was added. The cells were exposed to light from a 100 W halogen lamp equipped with a water jacket and Y-50 cutoff filter (λ>500 nm). The light intensity

was measured by using a UV-vis power meter. The irradiation time was adjusted to obtain the desired light dose of 16 $J \cdot cm^{-2}$. The mitochondrial activity of NADH dehydrogenase of the cells in each well was measured at 24h after photoirradiation using WST-8 reagent (10 μL) from Cell Counting Kit-8 according to the manufacturer's instructions. The absorbance at 450 nm was measured using a plate reader. The percentage cell survival was calculated by normalization with respect to the value for no drug treatment.

4.5 References

1. Konan, Y. N.; Gurny, R.; Allemann, E. *J. Photochem. Photobiol. B Bio.* **2002**, *66*, 89.
2. Mehraban, N.; Freeman, H.S. *Materials* **2015**, *8*, 4421.
3. Bechet, D.; Couleaud, P.; Frochot, C.; Viriot, M. L.; Guillemin, F.; Barberi-Heyob, M. *Trends Biotechnol*. **2008**, *26*, 612.
4. Castano, A. P.; Demidova, T. N.; Hamblin, M. R. *Photodiagnosis Photodyn Ther*. **2004**, *1*, 279.
5. Jain, R. K. *J. Control. Release* **1998**, *53*, 49.
6. Jain, R. K. *Adv. Drug Deliv. Rev.* **2001**, *46*, 149.
7. van Nostrum, C. F. *Adv. Drug Deliv. Rev.* **2004**, *56*, 5.
8. Kessel, D. *Adv. Drug Deliv. Rev.* **2004**, *56*, 7.
9. Cheng, Y.; Burda, C. Nanoparticles for Photodynamic Therapy. In *Comprehensive Nanoscience and Technology*. Vol.2. Andrews, D. L.; Scholes, G. D.; Wiederrecht, G. P. Eds.; Academic Press., San Diego, CA, USA.
10. Zięba, G.; Rojkiewicz, M.; Kozik, V.; Jarzembek, K.; Jarczyk, A.; Sochanik, A.; Kus, P. *Monatsh Chem.* **2012**, *143*, 153.

11. Erić, S.; Pavlović, M.; Popović, G.; Agbaba, D. *J. Chromatogr. Sci.* **2007**, *45*, 140.
12. Yee, K. K. L.; Soo, K. C.; Bay, B. H.; Olivo, M. *Photochem.Photobiol.* **2002**, *76*, 678.
13. Zheng, G.; Potter, W. R.; Camacho, S. H.; Missert, J. R.; Wang, G.; Bellnier, D. A.; Henderson, B. W.; Rodgers, M. A. J.; Dougherty, T. J.; Pandey, R. K. *J. Med. Chem.* **2001**, *44*, 1540.
14. Friberg, E. G.; Čunderlíková, B.; Pettersen, E. O.; Moan, J. *Cancer Lett.* **2003**, *195*, 73.
15. Kępczyński, M.; Pandian, R. P.; Smith, K. M.; Ehrenberg, B. *Photochem. Photobiol.* **2002**, *76*, 127.
16. Cardoso, M. G.; Nelson, D. L.; Amaral, A. T.; Santos, C. D.; Pereira, A. A.; Oliveira, A. C. B. *Int. J. Mol. Sci.* **2002**, *3*, 755.
17. Hirohara, S.; Obata, M.; Ogata, S-i.; Ohtsuki, C.; Higashida, S.; Ogura, S-i.; Okura, I.; Takenaka, M.; Ono, H.; Sugai, Y.; Mikata, Y.; Tanihara, M.; Yano, S. *J. Photochem. Photobiol. B.* **2005**, *78*, 7.
18. Calculated values using Advanced Chemistry Development (ACD/Labs) Software V8.14 for Solaris (©1994-2009 acd/Labs).
19. Obata, M.; Hirohara, S. *J. Photochem. Photobiol. B: Biol.* **2016**, *162*, 324.
20. Hirohara, S.; Kubota, Y.; Akiyama, N.; Obata, M.; Matsui, H.; Kakiuchi, K. Synthesis and Photocytotoxicity of Fluorophenylporphyrin Derivatives having Two Different Functional Groups. In *Spectroscopic Tools for the Diagnosis and Treatment of Cancer*; Pacifichem Symposium, Chapter 10, Miyoshi, N.; Hirakawa, K.; Kundu, S. K. Eds.; Sankeisha, Tokyo, Japan, 2017.
21. Hirohara, S.; Obata, M.; Ogura, S-i.; Okura, I.; Higashida, S.; Ohtsuki, C.; Ogata, S-i.; Nishikawa, Y.; Takenaka, M.; Ono, H.; Mikata, Y.; Yano, S. *J. Porphyrins Phthalocyanines* **2004**, *8*, 1289.

22. Hirohara, S.; Nishida, M.; Sharyo, K.; Obata, M.; Ando, T.; Tanihara, M. *Bioorg. Med. Chem.* **2010**, *18*, 1526.
23. Szablewski, L. *Biochim. Biophys. Acta, Rev. Cancer* **2013**, *1835*, 164.
24. Patra, M.; Awuah, S. G.; Lippard, S. J. *J. Am. Chem. Soc.* **2016**, *138*, 12541.
25. Kessel, D. *Photodiagn. Photodyn. Ther.* **2004**, *1*, 3.
26. Zhang, Y.; Lovell, J. F. *Theranostics* **2012**, *2*, 905.
27. Bonnett, R. *Chemical Aspects of Photodynamic Therapy*; Gordon and Breach Science Publishers, CRC Press: Boca Raton, FL, 2000.
28. Yano, S.; Hirohara, S.; Obata, M.; Hagiya, Y.; Ogura, S.; Ikeda, A.; Kataoka, H.; Tanaka, M.; Joh, T. *J. Photochem. Photobiol. C: Photohem. Rev.* **2011**, *12*, 46.
29. Hirohara, S.; Sharyo, K.; Kawasaki, Y.; Totani, M.; Tomotsuka, A.; Funasako, R.; Yasui, N.; Hasegawa, Y.; Yuasa, J.; Nakashima, T.; Kawai, T.; Oka, C.; Kawaichi, M.; Obata, M.; Tanihara, M. *Bull. Chem. Soc. Jpn.* **2013**, *86*, 1295.
30. Setsukinai, K-i.; Urano, Y.; Kakinuma, K.; Majima, H. J.; Nagano, T. *J. Biol. Chem.* **2003**, *278*, 3170.
31. Hirohara, S.; Obata, M.; Saito, A.; Ogata, S-i.; Ohtsuki, C.; Higashida, S.; Ogura, S-i.; Okura, I.; Sugai, Y.; Mikata, Y.; Tanihara, M.; Yano, S. *Photochem. Photobiol.* **2004**, *80*, 301.
32. Ethirajan, M.; Chen, Y.; Joshi, P.; Pandey, R. K. *Chem. Soc. Rev.* **2011**, *40*, 340.
33. MacDonald, I. J.; Dougherty, T. J. *J. Porphyrins Phthalocyanines* **2001**, *5*, 105.

CHAPTER 5 Synthesis of Multi-Glycoconjugated Porphyrins

5.1 Introduction

Carbohydrate modified porphyrins have been investigated as PSs in PDT [1]. Conjugation of porphyrins to sugars produces mono-, bis- (*cis*- and *trans*-), tri-, and tetra-substituted glycoconjugates. Previous study on tetraphenylporphyrin sulfonic acid (TPPS) reported that bis *cis*-substituted conjugate has the highest uptake and photocytoxicity among other conjugates (mono-, bis *trans*-, tri-, and tetra-sulfonic acids) [2]. Whereas, bis *trans*- glucose derivatives of 5,10,15,20-tetrakis(pentafluorophenyl)porphyrin (TFPP) displayed the top one on photocytotoxicity compared to other derivatives as described on other papers [3,4]. These findings imply that the number of substituent and their pattern of substitution are important factors for the development of photosensitizers. It was reported on chapter 4 that **3OH** and **4OH** showed potent photocytotoxicity and concentration inducing 50% cell death (EC_{50}) values of gastric carcinoma mucosal cell line (RGK cells), Human cervical cell line (HeLa cells), and human glioblastoma cell line (U251). In line with this and in order to search more active PSs, this chapter accounts the synthesis of bis *cis*-, bis *trans*-, tri-, and tetra-substituted conjugates TFPP with tetraacetyl 3-thio glucose (**3-Ac-S-AcGlc**) and tetraacetyl 4-thio glucose (**4-Ac-S-AcGlc**).

5.2 Results and Discussion

In order to examine the influence of the number of thioglucoses and their pattern of substitution on the properties of glycoconjugates for photosensitizers, acetylated TFPP-glucose conjugates from conjugation of TFPP with **3-Ac-S-AcGlc** and **4-Ac-S-AcGlc** were synthesized. aromatic nucleophilic substitution reactions were employed to couple TFPP with **3-Ac-S-AcGlc** and **4-Ac-S-AcGlc**, and this reaction was performed in *N*,*N*-dimethylormamide (DMF) with the addition of

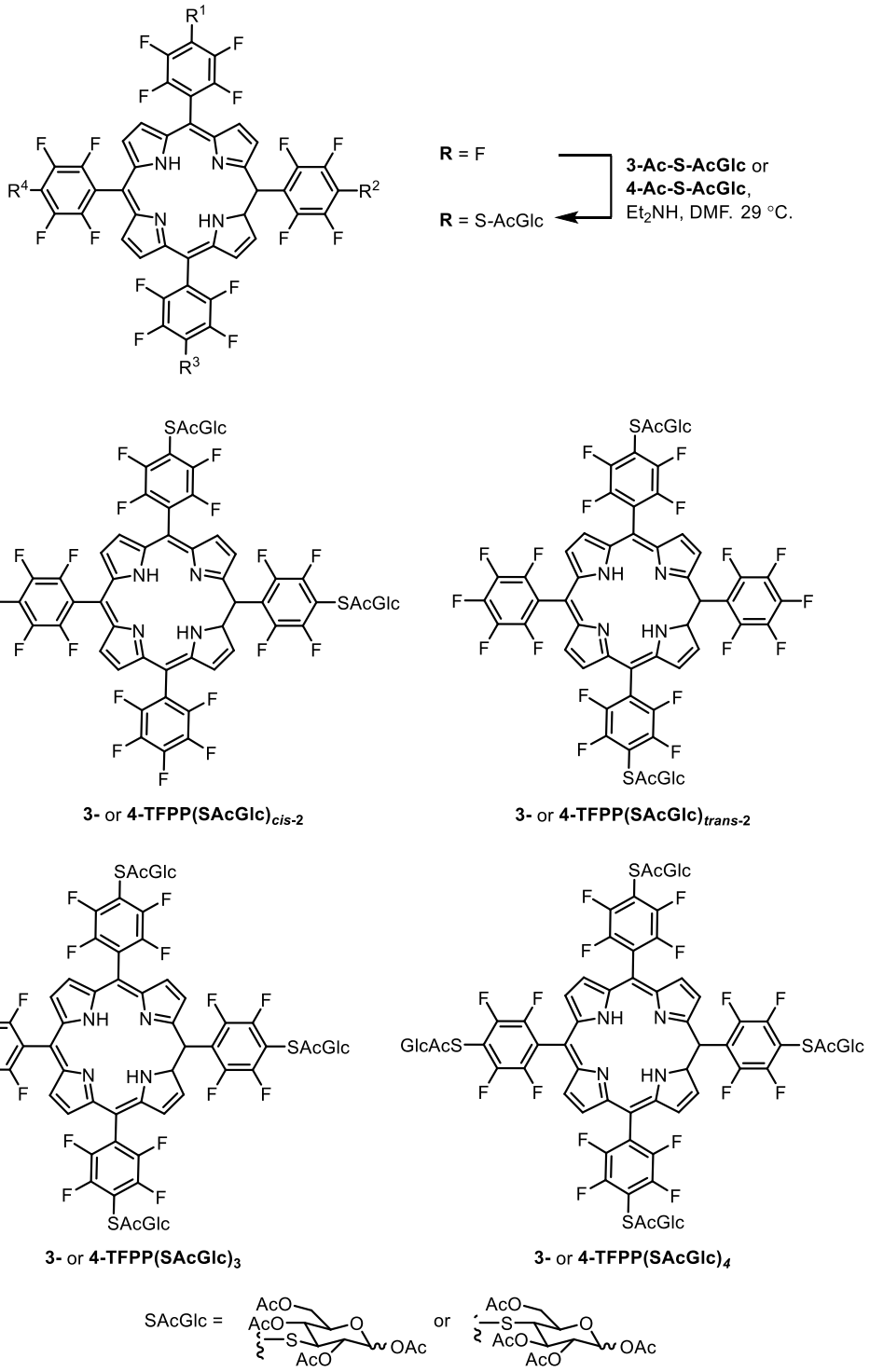

Scheme 5.1 Synthesis of acetylated TFPP-glucose conjugates

diethylamine (Scheme 5.1) [5]. The reaction was conducted at 29 ºC for 48 h since this reaction involved C3 and C4 position of thiosugars (**3-Ac-S-AcGlc** and **4-Ac-S-AcGlc**) which have different reactivity compared to anomeric position [6]. The reaction was conducted by using more TFPP and **3-Ac-S-AcGlc** and **4-Ac-S-AcGlc** ratio (TFPP : **3-Ac-S-AcGlc** = 1 : 4, TFPP :**4-Ac-S-AcGlc** = 1 : 5) as compared to mono-glycoconjugated porphyrins synthesis. After several times of purification using conventional column chromatography, the acetylated conjugates **3-TFPP(SAcGlc)$_{2mix}$**, **3-TFPP(SAcGlc)$_3$**, **4-TFPP(SAcGlc)$_{trans\text{-}2}$**, **4-TFPP(SAcGlc)$_{cis\text{-}2}$**, **4-TFPP(SAcGlc)$_3$**, and **4-TFPP(SAcGlc)$_4$** were isolated.

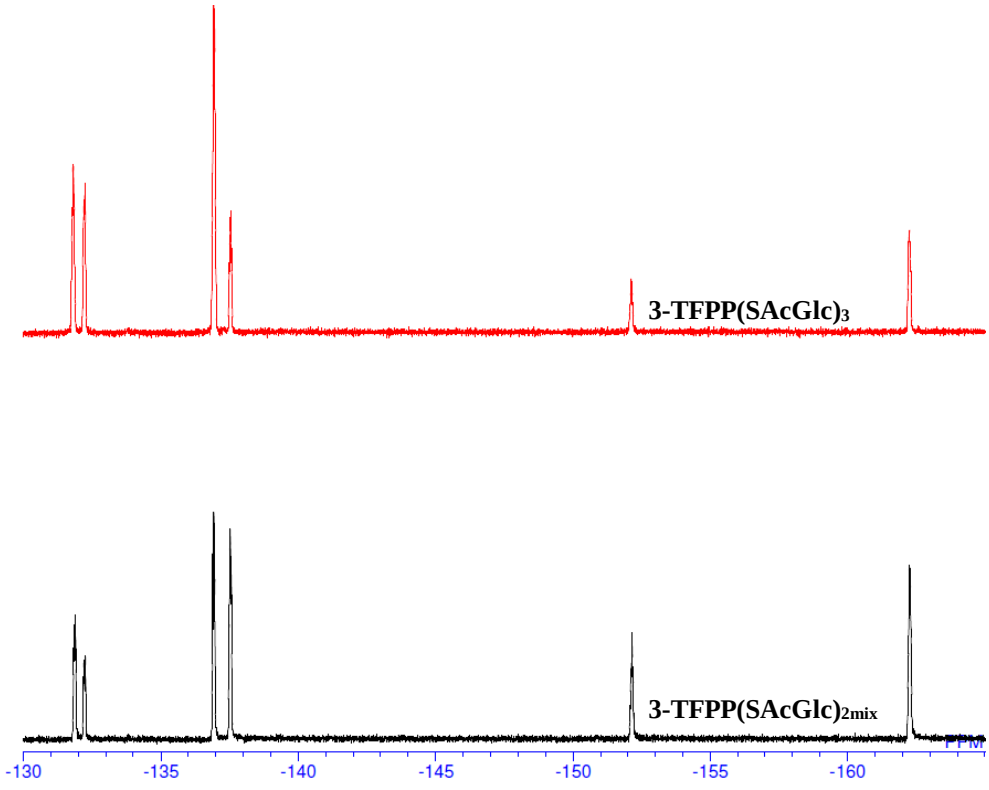

Figure 5.1 Selected ^{19}F NMR of **3-TFPP(SAcGlc)$_{2mix}$** and **3-TFPP(SAcGlc)$_3$**

Identification of the isolated conjugates **3-TFPP(SAcGlc)$_{2mix}$**, **3-TFPP(SAcGlc)$_3$**, **4-TFPP(SAcGlc)$_{trans\text{-}2}$**, **4-TFPP(SAcGlc)$_{cis\text{-}2}$**, **4-TFPP(SAcGlc)$_3$**, and **4-TFPP(SAcGlc)$_4$** were roughly carried out by examining their TLC profile. **3-TFPP(SAcGlc)$_{trans\text{-}2}$**, **3-TFPP(SAcGlc)$_{cis\text{-}2}$**, and **3-TFPP(SAcGlc)$_3$** have *Rf* value of 0.68, 0.60, and 0.54, respectively. The retention factor (*Rf*) values for **4-TFPP(SAcGlc)$_{trans\text{-}2}$**, **4-TFPP(SAcGlc)$_{cis\text{-}2}$**, **4-TFPP(SAcGlc)$_3$**, and **4-TFPP(SAcGlc)$_4$** are 0.68, 0.60, 0.54, and 0.43. This *Rf* values order are consistent with the high-performance liquid chromatography (HPLC) retention time values and sequence of mono-, di-, tri-, and tetra-glucosylated fluorophenylporphyrins from 1-thioglucose [5].

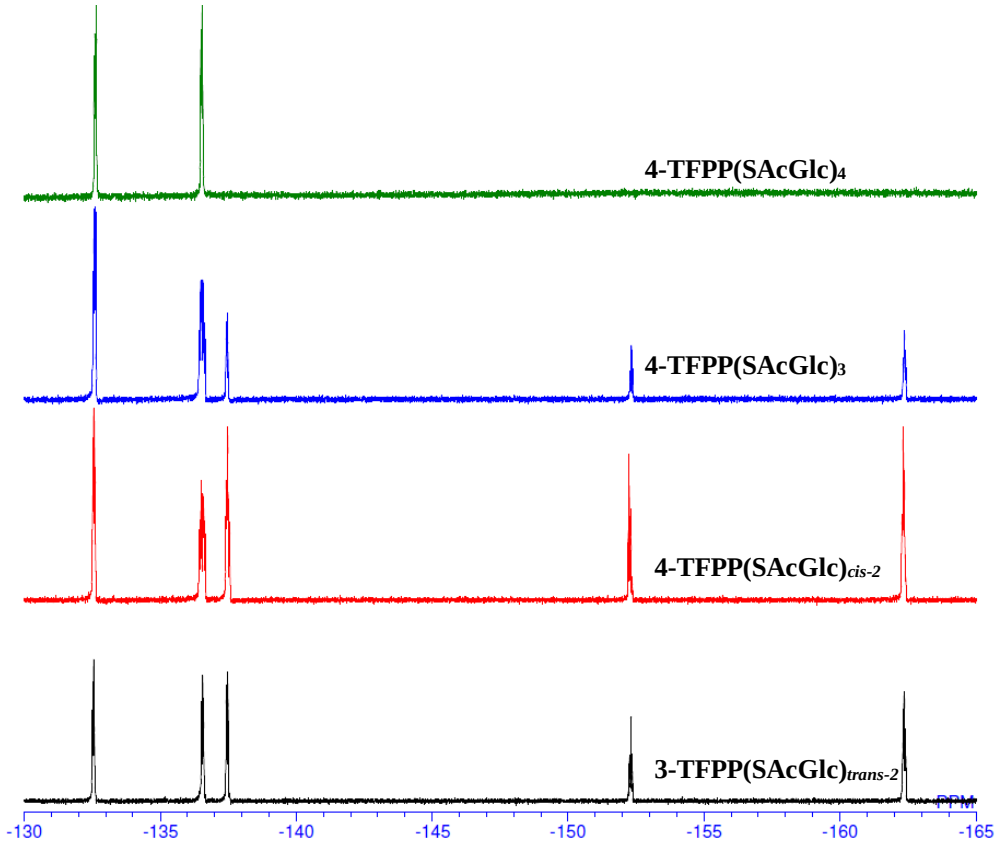

Figure 5.2 Selected ^{19}F NMR of **4-TFPP(SAcGlc)$_{trans\text{-}2}$**, **4-TFPP(SAcGlc)$_{cis\text{-}2}$**, **4-TFPP(SAcGlc)$_3$**, and **4-TFPP(SAcGlc)$_4$**

The ^{19}F NMR spectra supports this identification since ^{19}F has similar abundance and spin number [7] (Figure 5.1 and Figure 5.2). The integration value and multiplicity definitely distinguish all conjugates. The ^{19}F NMR spectra of all conjugates showed two double-doublet peaks with a typical AA'XX' spin coupling ($J_{F\text{-}F}$ = 24-27 Hz and $J_{F\text{-}F}$ = 11-14 Hz), clearly indicating *para*-substitution of the tetrafluorophenyl groups [8-11]. The ^{19}F NMR spectra also showed two sets of two peaks conforming the 2,6- and 3,5-F nucleus of glucose-conjugated perfluorophenyl group. Detailed study on the ^{19}F NMR spectra clearly indicates that the 4-F nucleus of the pentafluorophenyl groups remains in the porphyrin ring.

5.3 Summary

The **3-TFPP(SAcGlc)$_{2mix}$**, **3-TFPP(SAcGlc)$_3$**, **4-TFPP(SAcGlc)$_{trans\text{-}2}$**, **4-TFPP(SAcGlc)$_{cis\text{-}2}$**, **4-TFPP(SAcGlc)$_3$**, and **4-TFPP(SAcGlc)$_4$** were synthesized and isolated. This research part of doctoral thesis is in progress and will be completed soon.

5.4 Experiments

Materials and Measurements

The purities of peracetyrated TFPP-Glucose conjugates **3-TFPP(SAcGlc)$_{2mix}$**, **3-TFPP(SAcGlc)$_3$**, **4-TFPP(SAcGlc)$_{trans\text{-}2}$**, **4-TFPP(SAcGlc)$_{cis\text{-}2}$**, **4-TFPP(SAcGlc)$_3$**, and **4-TFPP(SAcGlc)$_4$** were determined on an HPLC system (Jasco PU-2086 Plus Intelligent pump, Jasco Co., Ltd., Tokyo, Japan) equipped with a UV-vis detector (UV-2075 Plus, Jasco Co., Ltd.) and a silica gel column (COSMOSIL 5SL-II packed column, 4.6 mmϕ × 150 mm, Nacalai Tesque, Inc., Kyoto, Japan) using a mixture of CH_2Cl_2 and ethyl acetate (9/1, v/v) at 30 °C. NMR spectra were recorded using an AVANCE III HD (500 MHz; Bruker Biospin K.K., Yokohama, Japan) and a NMR-DD2 500PS

(500 MHz; Agilent Technologies, CA, USA).

5,10-Bis[4-(1,2,4,6-tetra-*O*-acetyl-3-thio-D-glucopyranos-3-*S*-yl)-2,3,5,6-tetrafluorophenyl)]-15,20-bis(2,3,4,5,6-pentafluorophenyl)porphyrin, 5,15-Bis[4-(1,2,4,6-tetra-*O*-acetyl-3-thio-D-glucopyranos-3-*S*-yl)-2,3,5,6-tetrafluoro-phenyl)]-10,20-bis(2,3,4,5,6-pentafluorophenyl)-porphyrin (3-TFPP(SAcGlc)$_{2mix}$). TFPP (189.6 mg, 195 μmol), **3-Ac-S-AcGlc** (330.6 mg, 813 μmol), and diethylamine (DEA, 80.6 μL, 779 μmol) were dissolved in DMF (60 mL). The reaction mixture was stirred at 29 ºC for 48 h, diluted with CH_2Cl_2/ AcOEt (1/1, v/v, 100 mL) and washed with distilled water (100 mL × 5). The extract was dried over Na_2SO_4 and the solvent was removed under reduced pressure. The crude product was separated by column chromatography (silica gel, CH_2Cl_2 to CH_2Cl_2/EtOAc = 100–70:30) to give **3-TFPP(SAcGlc)$_{2mix}$** (+ **3-Ac-S-AcGlc**) (219 mg) as dark red solids. R_f value 0.68 (**3-TFPP(SAcGlc)$_{trans\text{-}2}$**), 0.60 (**3-TFPP(SAcGlc)$_{cis\text{-}2}$**) (CH_2Cl_2 : EtOAc = 8 : 2). ^{19}F NMR ($CDCl_3$, 470.34 MHz, CF_3CO_2H = −76.05 ppm): δ (ppm) = −132.03 (4F, dd, $J_{F\text{-}F}$ = 24.9 Hz, $J_{F\text{-}F}$ = 11.3 Hz, 3,5-Ph*F*Glc), −136.92 (4F, dd, $J_{F\text{-}F}$ = 24.9 Hz, $J_{F\text{-}F}$ = 11.8 Hz, 2,6-Ph*F*Glc), −137.52 (4F, dd, $J_{F\text{-}F}$ = 21.2 Hz, $J_{F\text{-}F}$ = 15.5 Hz, 3,5-Ph*F*), −152.15 (2F, m, 4-Ph*F*), −162.25 (4F, m, 2,6-Ph*F*).

5,10,15-Tris[4-(1,2,4,6-tetra-*O*-acetyl-3-thio-D-glucopyranos-3-*S*-yl)-2,3,5,6-tetrafluoro-phenyl)]-20-(2,3,4,5,6-pentafluorophenyl)porphyrin (3-TFPP(SAcGlc)$_3$). TFPP (189.6 mg, 195 μmol), **3-Ac-S-AcGlc** (330.6 mg, 813 μmol), and diethylamine (DEA, 80.6 μL, 779 μmol) were dissolved in DMF (60 mL). The reaction mixture was stirred at 29 ºC for 48 h, diluted with CH_2Cl_2/ AcOEt (1/1, v/v, 100 mL) and washed with distilled water (100 mL × 5). The extract was dried over Na_2SO_4 and the solvent was removed under reduced pressure. The crude product was separated by column chromatography (silica gel, CH_2Cl_2 to CH_2Cl_2/EtOAc = 100–70:30) to give

3-TFPP(SAcGlc)$_3$ (62 mg) as dark red solids. R_f value 0.54 (CH_2Cl_2 : EtOAc = 8 : 2). ^{19}F NMR ($CDCl_3$, 470.34 MHz, CF_3CO_2H = −76.05 ppm): δ (ppm) = −132.00 (6F, dd, $J_{F\text{-}F}$ = 23.1 Hz, $J_{F\text{-}F}$ = 13.6 Hz, 3,5-Ph*F*Glc), −136.92 (6F, m, 2,6-Ph*F*Glc), −137.53 (2F, dd, $J_{F\text{-}F}$ = 22.6 Hz, $J_{F\text{-}F}$ = 7.5 Hz, 3,5-Ph*F*), −152.12 (1F, m, 4-Ph*F*), −162.24 (2F, m, 2,6-Ph*F*).

5,15-Bis[4-(1,2,3,6-tetra-*O*-acetyl-4-thio-D-glucopyranos-4-*S*-yl)-2,3,5,6-tetrafluoro-phenyl)]-10,20-bis(2,3,4,5,6-pentafluorophenyl)porphyrin (4-TFPP(SAcGlc)$_{trans\text{-}2}$). TFPP (300.9 mg, 309 μmol), **4-Ac-S-AcGlc** (618.2 mg, 1521 μmol), and diethylamine (DEA, 129 μL, 1247μmol) were dissolved in DMF (60 mL). The reaction mixture was stirred at 29 ºC for 48 h, diluted with CH_2Cl_2/ AcOEt (1/1, v/v, 100 mL) and washed with distilled water (100 mL × 5). The extract was dried over Na_2SO_4 and the solvent was removed under reduced pressure. The crude product was separated by column chromatography (silica gel, CH_2Cl_2 to CH_2Cl_2/EtOAc = 100–50:50) to give **4-TFPP(SAcGlc)$_{trans\text{-}2}$** (+ **4-Ac-S-AcGlc**) (204 mg) as dark red solids. R_f value 0.68 (CH_2Cl_2 : EtOAc = 8 : 2). ^{19}F NMR ($CDCl_3$, 470.34 MHz, CF_3CO_2H = −76.05 ppm): δ (ppm) = −132.53 (4F, dd, $J_{F\text{-}F}$ = 24.9 Hz, $J_{F\text{-}F}$ = 13.9 Hz, 3,5-Ph*F*Glc), −136.55 (4F, dd, $J_{F\text{-}F}$ = 26.8 Hz, $J_{F\text{-}F}$ = 13.6 Hz, 2,6-Ph*F*Glc), −137.46 (4F, dd, $J_{F\text{-}F}$ = 24.5 Hz, $J_{F\text{-}F}$ = 7.5 Hz, 3,5-Ph*F*), −152.31 (2F, dd, $J_{F\text{-}F}$ = 21.2 Hz, $J_{F\text{-}F}$ = 21.2 Hz, 4-Ph*F*), −162.36 (4F, m, 2,6-Ph*F*).

5,10-Bis[4-(1,2,3,6-tetra-*O*-acetyl-4-thio-D-glucopyranos-4-*S*-yl)-2,3,5,6-tetrafluoro-phenyl)]-15,20-bis(2,3,4,5,6-pentafluorophenyl)porphyrin (4-TFPP(SAcGlc)$_{cis\text{-}2}$). TFPP (300.9 mg, 309 μmol), **4-Ac-S-AcGlc** (618.2 mg, 1521 μmol), and diethylamine (DEA, 129 μL, 1247μmol) were dissolved in DMF (60 mL). The reaction mixture was stirred at 29 ºC for 48 h, diluted with CH_2Cl_2/ AcOEt (1/1, v/v, 100 mL) and washed with distilled water (100 mL × 5). The extract was dried over Na_2SO_4 and the solvent was removed under reduced pressure. The crude product was separated by column chromatography (silica gel, CH_2Cl_2 to CH_2Cl_2/EtOAc = 100–

50:50) to give **4-TFPP(SAcGlc)$_{cis\text{-}2}$** (83 mg) as dark red solids. R_f value 0.60 (CH_2Cl_2 : EtOAc = 8 : 2). ^{19}F NMR ($CDCl_3$, 470.34 MHz, CF_3CO_2H = −76.05 ppm): δ (ppm) = −132.56 (4F, dd, $J_{F\text{-}F}$ = 24.9 Hz, $J_{F\text{-}F}$ = 11.8 Hz, 3,5-Ph*F*Glc), −136.51 (4F, dd, $J_{F\text{-}F}$ = 24.9 Hz, $J_{F\text{-}F}$ = 11.8 Hz, 2,6-Ph*F*Glc), −137.46 (4F, m, 3,5-Ph*F*), −152.26 (2F, dd, $J_{F\text{-}F}$ = 20.7 Hz, 4-Ph*F*), −162.32 (4F, m, 2,6-Ph*F*).

5,10,15-Tris[4-(1,2,3,6-tetra-*O*-acetyl-4-thio-D-glucopyranos-4-*S*-yl)-2,3,5,6-tetrafluoro-phenyl)]-20-(2,3,4,5,6-pentafluorophenyl)porphyrin (4-TFPP(SAcGlc)$_3$). TFPP (300.9 mg, 309 μmol), **4-Ac-S-AcGlc** (618.2 mg, 1521 μmol), and diethylamine (DEA, 129 μL, 1247μmol) were dissolved in DMF (60 mL). The reaction mixture was stirred at 29 ºC for 48 h, diluted with CH_2Cl_2/ AcOEt (1/1, v/v, 100 mL) and washed with distilled water (100 mL × 5). The extract was dried over Na_2SO_4 and the solvent was removed under reduced pressure. The crude product was separated by column chromatography (silica gel, CH_2Cl_2 to CH_2Cl_2/EtOAc = 100–50:50) to give **4-TFPP(SAcGlc)$_3$** (128 mg) as dark red solids. R_f value 0.54 (CH_2Cl_2 : EtOAc = 8 : 2). ^{19}F NMR ($CDCl_3$, 470.34 MHz, CF_3CO_2H = −76.05 ppm): δ (ppm) = −132.57 (6F, dd, $^3J_{F\text{-}F}$ = 24.5 Hz, $^5J_{F\text{-}F}$ = 11.2 Hz, 3,5-Ph*F*Glc), −136.54 (6F, m, 2,6-Ph*F*Glc), −137.45 (2F, dd, $^3J_{F\text{-}F}$ = 22.6 Hz, $^5J_{F\text{-}F}$ = 7.5 Hz, 3,5-Ph*F*), −152.33 (1F, dd, $^3J_{F\text{-}F}$ = 20.7 Hz, $^5J_{F\text{-}F}$ = 20.7 Hz, 4-Ph*F*), −162.37 (2F, dd, $^3J_{F\text{-}F}$ = 23.1 Hz, $^5J_{F\text{-}F}$ = 8.0 Hz, 2,6-Ph*F*).

5,10,15,20-Tetra[4-(1,2,3,6-tetra-*O*-acetyl-4-thio-D-glucopyranos-4-*S*-yl)-2,3,5,6-tetrafluoro-phenyl)]-2,3,4,5,6-pentafluorophenylporphyrin (4-TFPP(SAcGlc)$_4$). TFPP (300.9 mg, 309 μmol), **4-Ac-S-AcGlc** (618.2 mg, 1521 μmol), and diethylamine (DEA, 129 μL, 1247μmol) were dissolved in DMF (60 mL). The reaction mixture was stirred at 29 ºC for 48 h, diluted with CH_2Cl_2/ AcOEt (1/1, v/v, 100 mL) and washed with distilled water (100 mL × 5). The extract was dried over Na_2SO_4 and the solvent was removed under reduced pressure. The crude product was

separated by column chromatography (silica gel, CH_2Cl_2 to CH_2Cl_2/EtOAc = 100–50:50) to give **4-TFPP(SAcGlc)$_4$** (64 mg) as dark red solids. R_f value 0.43 (CH_2Cl_2 : EtOAc = 8 : 2). ^{19}F NMR ($CDCl_3$, 470.34 MHz, C*F*$_3$CO$_2$H = −76.05 ppm): δ (ppm) = −132.61 (8F, dd, $^3J_{F\text{-}F}$ = 24.9 Hz, $^2J_{F\text{-}F}$ = 11.3 Hz, 3,5-Ph*F*Glc), −136.52 (8F, dd, $^3J_{F\text{-}F}$ = 24.9 Hz, $^5J_{F\text{-}F}$ = 11.3 Hz, 2,6-Ph*F*Glc).

5.5 References

1. Moylan, C.; Scanlan, E. M.; Senge, M. O. *Curr. Med. Chem.* **2015**, *19*, 2238.
2. Kessel, D.; Thompson, P.; Saatio, K.; Nantwi, K. D. *Photochem. Photobiol.* **1987**, *45*, 787.
3. Hirohara, S.; Nishida, M.; Sharyo, K.; Obata, M.; Ando, T. Tanihara, M. *Bioorg. Med. Chem.* **2010**, *18*, 1526.
4. Hirohara, S.; Sharyo, K.; Kawasaki, Y.; Totani, M.; Tomotsuka, A.; Funasako, R.; Yasui, N.; Hasegawa, Y.; Yuasa, J.; Nakashima, T.; Kawai, T.; Oka, C.; Kawaichi, M.; Obata, M.; Tanihara, M. *Bull. Chem. Soc. Jpn.* **2013**, *86*, 1295.
5. Hirohara, S.; Nishida, M.; Sharyo, K.; Obata, M.; Ando, T.; Tanihara, M. *Bioorg. Med. Chem.* **2010**, *18*, 1526.
6. Miljković, M. *Carbohydrates Synthesis, Mechanisms, and Stereoelectronic Effects*; Springer, NY, 2010.
7. Sylvestein, R. M.; Webster, F. X.; Kiemle, D. J. Spectrometric Identification of organic Compounds seventh edition, John Wiley & Sons, 2005, New York, USA. pp. 323.
8. Hirohara, S.; Obata, M.; Alitomo, H.; Sharyo, K.; Ando. T.; Tanihara, M.; Yano, S. *J. Photchem. Photobiol B: Bio.* **2009**, *97*, 22.
9. Hirohara, S.; Obata, M.; Alitomo, H.; Sharyo, K.; Ando. T.; Tanihara, M.; Yano, S. *Bioconjugate Chem.* **2009**, *20*, 944.

10. Petrakis, L.; Sederholm, C. H. *J. Chem. Phys.* **1961**, *35*, 1243.

11. Castillo, N.; Matta, C. F.; Boyd, R. J. *J. Chem. Inf. Model.* **2005**, *45*, 354.

CHAPTER 6 Summary

Commenced with commercially available carbohydrates, deoxy 2-, 3-, 4-, and 6-thioglucoses with acetyl group protection were synthesized. Starting with D-mannose, tetraacetyl 2-thio glucose as a β-anomer was obtained. 3-Thiolated derivative was synthesized from diacetone D-glucose as α/β-anomeric mixture. The 4-thio glucose as α/β-anomeric mixture was prepared from D-galactose. The 6-thio glucose as β-anomer was obtained from D-glucose. Introduction of acetylthio groups were performed by S_N2 reaction with the appropriate surfonylated carbohydrates.

The S_NAr reactions of TFPP with peracetylated thioglucopyranoses gave acetylated TFPP-glucose conjugates. Deprotection of acetyl groups produces the TFPP-glucose conjugates with >99% purities. While **synthesized conjugates** have phyllo-type UV-vis spectra with one intense peak of Soret band and three Q bands in DMSO, they have a broad peak in the UV-vis spectra recorded in PBS containing 1 vol% DMSO and displayed a red-shifted Soret band.

The hydrophobicity parameter (Log *P*) of TFPP-thioglucose conjugates was determined by RP-TLC and increased in the order of 1-thio Glc < 3-thio Glc < 4-thio Glc < 6-thio Glc < 2-thio Glc. The cellular uptake examination by RGK cells revealed that the quantity of TFPP-glucose conjugates taken up by the RGK cells linearly correlates with the increasing incubation time. Among them, 4-thio Glc conjugate shows a significant cellular uptake. The relative quantum yields of $^1O_2$ generation (Φ_Δ) illustrate that no contrast displayed by all TFPP-glucose conjugates in methanol. The prepared conjugates generated higher amount of •OH species compared to HP, similar to previously synthesized 1-thio Glc conjugate. The order of $\Phi_{\bullet OH}$ values is 2-thio Glc < 1-thio Glc < 4-thio Glc < 3-thio Glc << 6-thio Glc. The photocytotoxicity studied in HeLa cells indicates that none of these TFPP-glucose conjugates showed cytotoxicity in the dark, but potent

photocytotoxicity was displayed by all of these conjugates, except for 2-thio Glc conjugate, under photoirradiation. With detailed photocytotoxicity evaluation in HeLa cells, 1-, 3- and 4-thio Glc conjugates showed a slight higher photocytotoxicity with lower concentration needed to induce 50% cell death (EC_{50}) values compared to the values for 2- and 6-thio Glc materials. Further photocytotoxicity test using U251 cells and RGK cells displayed an identical result to that in HeLa cells.

The di- (including *cis* and *trans* substitution), tri-, and tetrasubstituted TFPP with deoxythioglucoses were synthesized and isolated.

From the previous chapter results, mono-glycoconjugated porhyrins has a possibility to enhance the photosensitizers activity as shown by mono-glycoconjugated porphyrins resulted from 3-thio Glc and 4-thio Glc.

In the future, this research will be continued in order to find the effective PDT photosensitizers. The future development includes metalation of the obtained mono-glycoconjugated porphyrins followed by their photophysical properties and biological evaluation. The intermediate acetylated multi-glycoconjugated porphyrins will be separated and purified to yield the multi-glycoconjugated porphyrins. Their photophysical properties and biological activity then will be evaluated. The multi-glycoconjugated porphyrins will also be metallated and their photophysical properties and biological activity will be studied.

Acknowledgements

In the name of God, the Most Gracious, the Most Merciful. All praises and thanks be to Him, for only with His blessings and graces this thesis can be finished.

First and foremost, I would like to convey my utmost gratitude to my beloved parents, parents in law, my wife with my daughter and my son, my sister, and my brothers for their everlasting love, pray, encouragement, and understanding so that I can finish my study.

My sincere gratitude goes to Prof. Kiyomi Kakiuchi for giving me an opportunity to join his group and for his guidance and continuous support for this study. My sincere gratitude also goes to Prof. Shiho Hirohara of Ube National College of Technology (UNCT). I am extremely indebted to her. It is impossible to finish this study without her.

I would like to express my profound and sincere appreciation to Assoc. Prof. Tsumoru Morimoto for his continuous support especially during the difficult time of this study, Asst. Prof. Hiroki Tanimoto and Asst. Prof. Yasuhiro Nishiyama for invaluable discussion and excellent technical helps and assistance during daily experiment. I also wish to express my sincere thanks to Prof. Hiroko Yamada and Assoc. Prof. Tsuyoshi Ando for their valuable discussion and advices as doctoral supervising committee.

I would like to thank our lab's secretary, Ms Hisayo Fujiki, for her finest technical helps and continuous support during the difficult time of this study. My thanks also goes to all past and present members of Synthetic Organic Chemistry Laboratory of NAIST and Bioorganic Chemistry Laboratory of UNCT for their help, friendship, and enjoyable environment.

I am deeply appreciate The Hitachi Global Foundation for providing the financial support for study and living in Japan.

Supporting Information

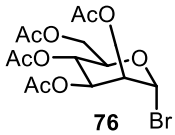

76

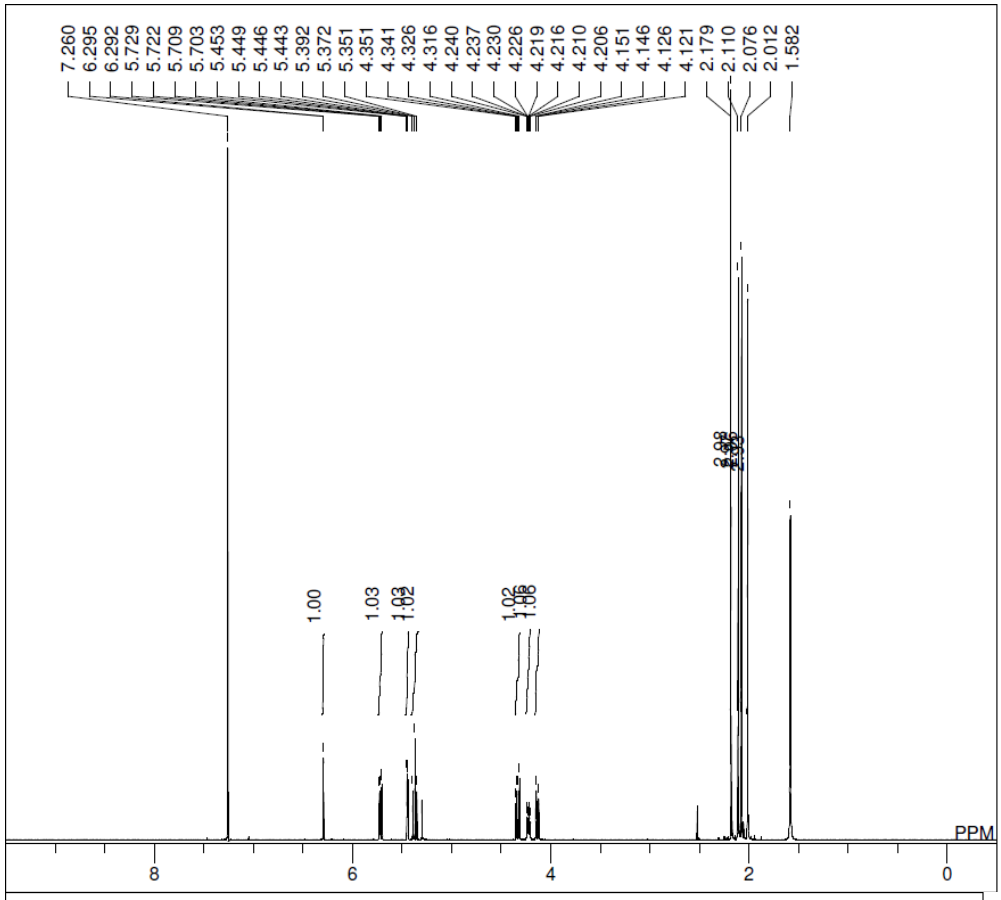

DFILE _AF_02_051b proton-1-1.als
COMNT AF_02_051b proton
DATIM 2015-11-04 21:43:58
OBNUC 1H
EXMOD proton.jxp
OBFRQ 500.16 MHz
OBSET 2.41 KHz
OBFIN 6.01 Hz
POINT 13107
FREQU 7507.51 Hz
SCANS 8
ACQTM 1.7459 sec
PD 5.0000 sec
PW1 7.20 usec
IRNUC 1H
CTEMP 16.8 c
SLVNT CDCL3
EXREF 7.26 ppm
BF 0.10 Hz
RGAIN 34

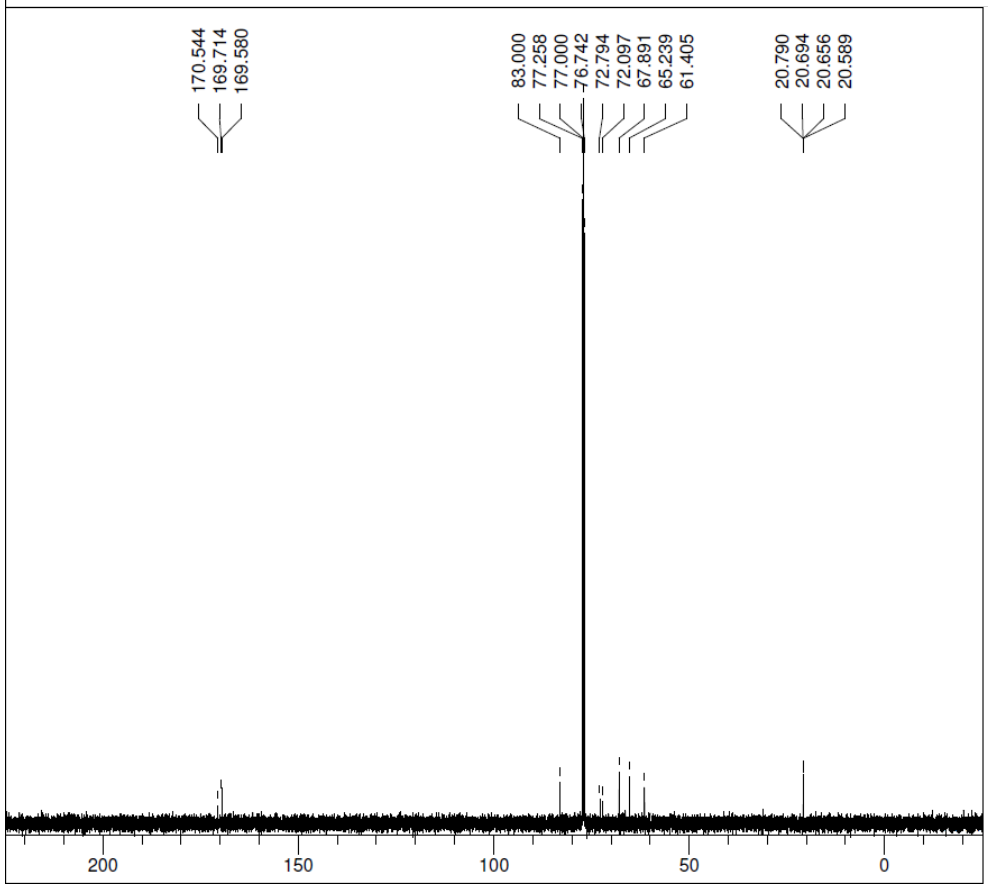

DFILE _AF_02_051 carbon-1-1.als
COMNT AF_02_051 carbon
DATIM 2015-11-04 14:28:42
OBNUC 13C
EXMOD carbon.jxp
OBFRQ 125.77 MHz
OBSET 7.87 KHz
OBFIN 4.21 Hz
POINT 26214
FREQU 31446.54 Hz
SCANS 358
ACQTM 0.8336 sec
PD 2.0000 sec
PW1 4.00 usec
IRNUC 1H
CTEMP 17.7 c
SLVNT CDCL3
EXREF 77.00 ppm
BF 0.10 Hz
RGAIN 60

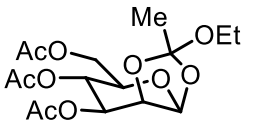

77

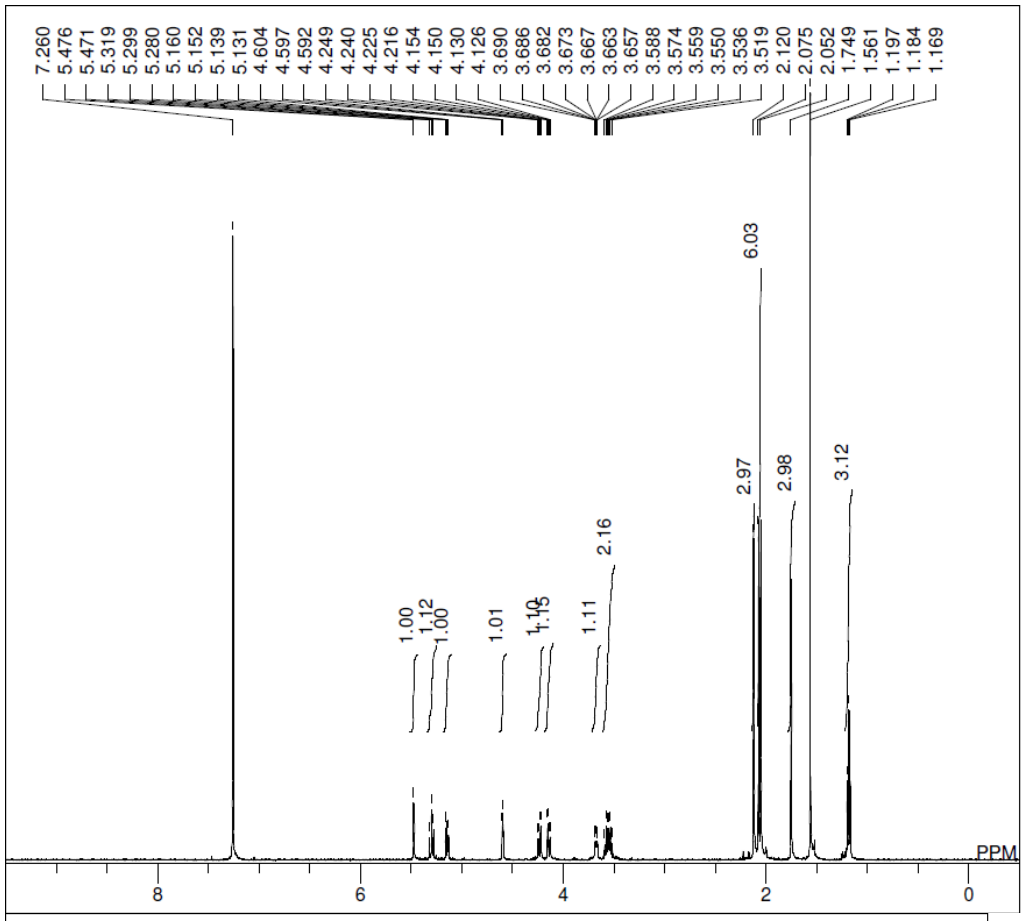

DFILE _AF_02_014 2a proton-1-1.als
COMNT AF_02_014 2a proton
DATIM 2015-07-28 12:03:07
OBNUC 1H
EXMOD proton.jxp
OBFRQ 500.16 MHz
OBSET 2.41 KHz
OBFIN 6.01 Hz
POINT 13107
FREQU 7507.51 Hz
SCANS 8
ACQTM 1.7459 sec
PD 5.0000 sec
PW1 6.22 usec
IRNUC 1H
CTEMP 19.6 c
SLVNT CDCL3
EXREF 7.26 ppm
BF 0.10 Hz
RGAIN 52

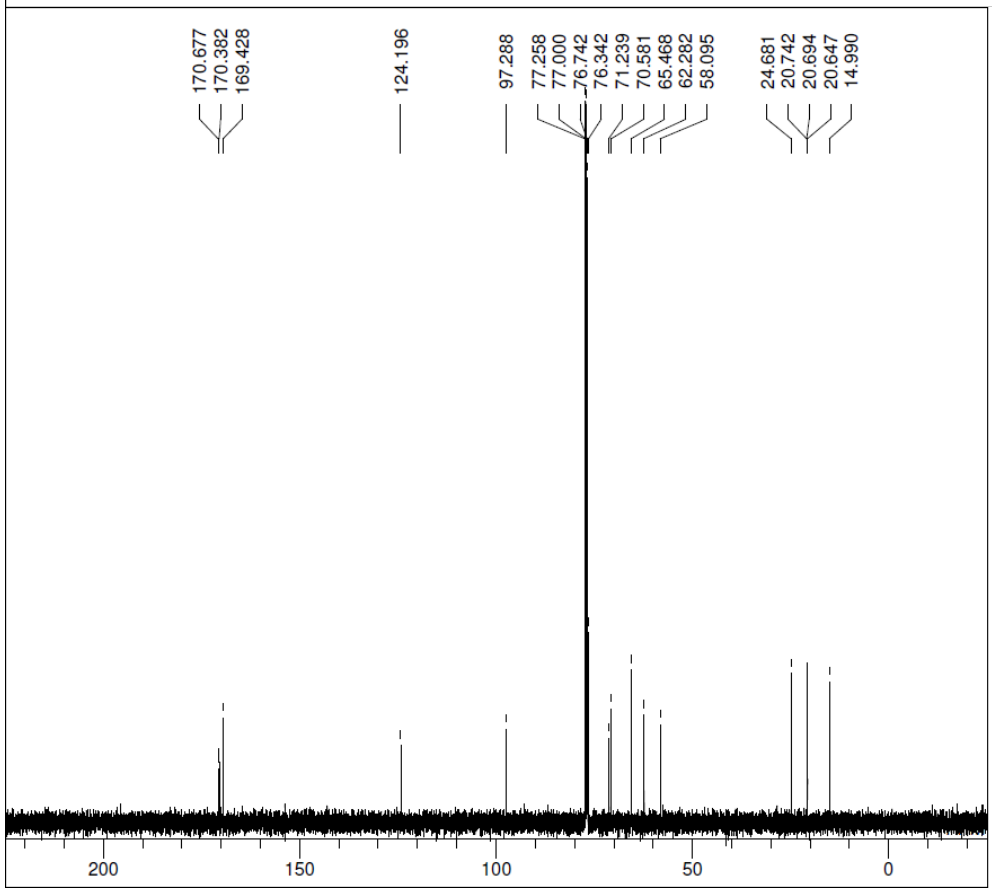

DFILE _AF_02_014 2a b carbon-1-1.als
COMNT AF_02_014 2a carbon
DATIM 2015-07-28 14:03:55
OBNUC 13C
EXMOD carbon.jxp
OBFRQ 125.77 MHz
OBSET 7.87 KHz
OBFIN 4.21 Hz
POINT 26214
FREQU 31446.54 Hz
SCANS 246
ACQTM 0.8336 sec
PD 2.0000 sec
PW1 3.12 usec
IRNUC 1H
CTEMP 20.1 c
SLVNT CDCL3
EXREF 77.00 ppm
BF 0.10 Hz
RGAIN 56

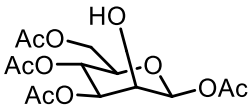

78

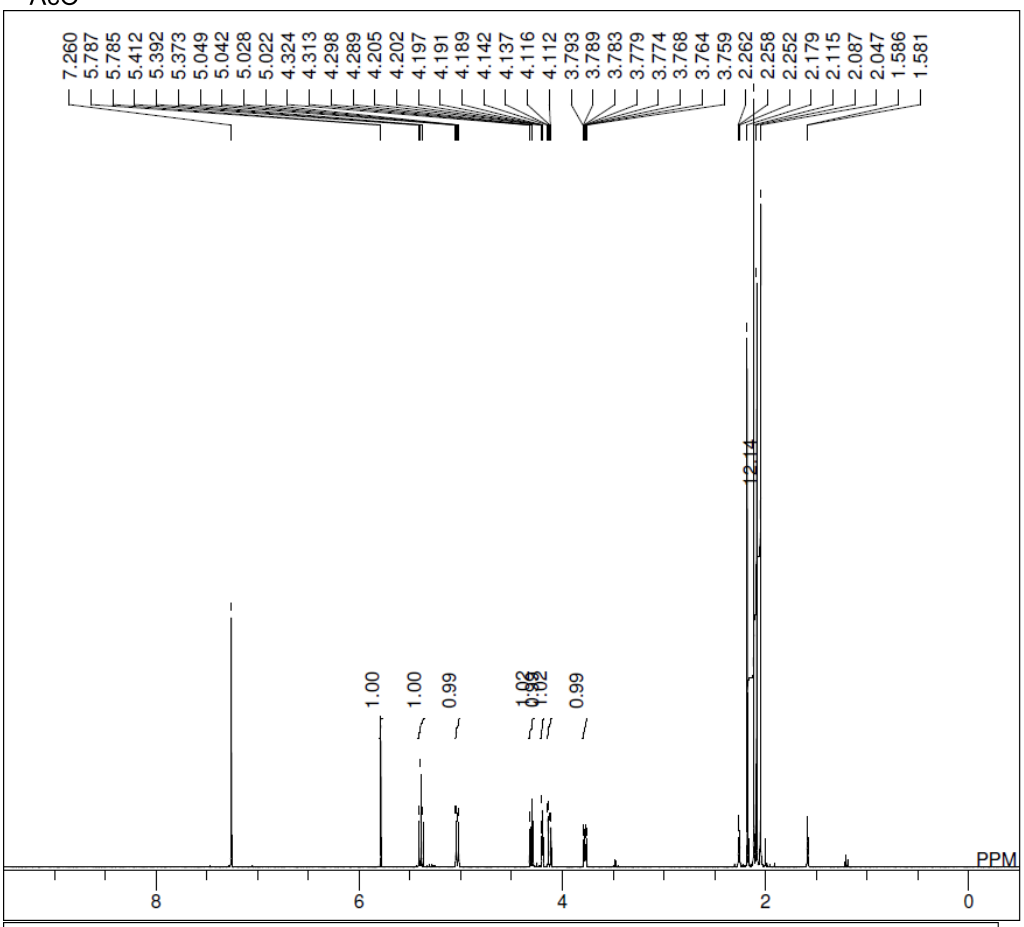

DFILE	_AF_02_061 proton-1-1.als
COMNT	AF_02_061 proton
DATIM	2015-11-30 14:16:32
OBNUC	1H
EXMOD	proton.jxp
OBFRQ	500.16 MHz
OBSET	2.41 KHz
OBFIN	6.01 Hz
POINT	13107
FREQU	7507.51 Hz
SCANS	8
ACQTM	1.7459 sec
PD	5.0000 sec
PW1	7.20 usec
IRNUC	1H
CTEMP	20.4 c
SLVNT	CDCL3
EXREF	7.26 ppm
BF	0.10 Hz
RGAIN	34

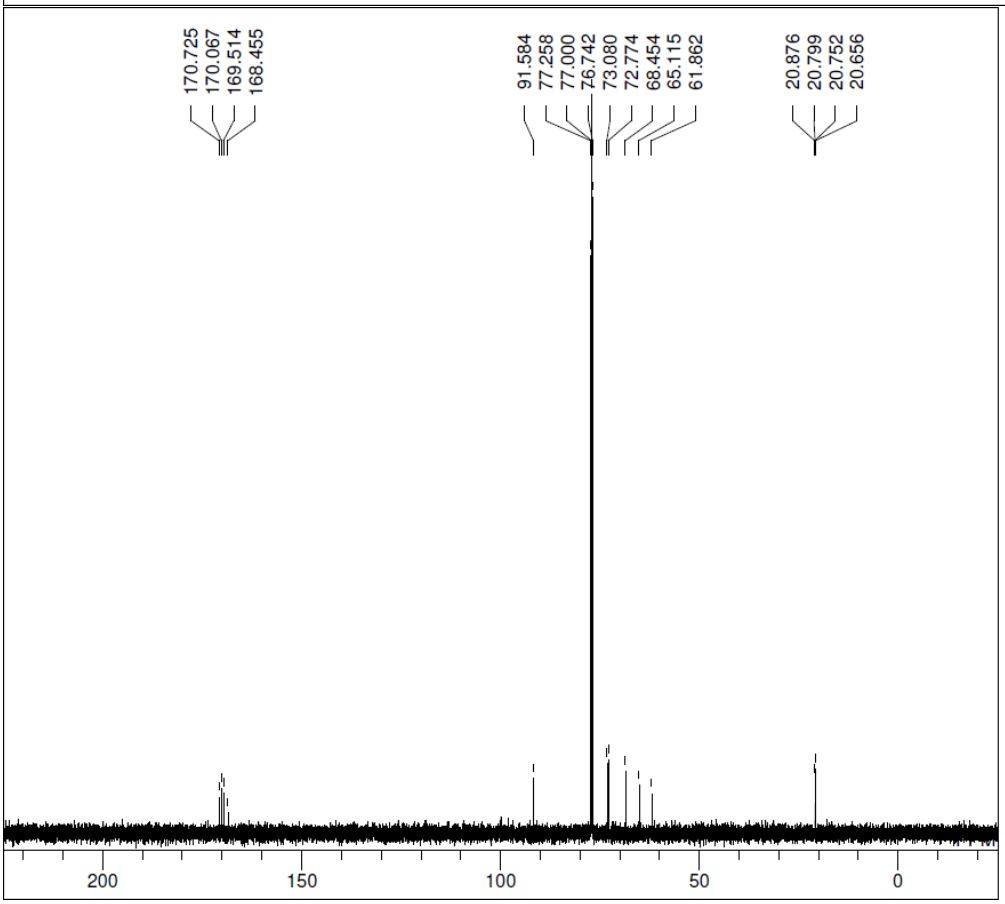

DFILE	_AF_02_061 carbon-1-1.als
COMNT	AF_02_061 carbon
DATIM	2015-11-30 14:36:22
OBNUC	13C
EXMOD	carbon.jxp
OBFRQ	125.77 MHz
OBSET	7.87 KHz
OBFIN	4.21 Hz
POINT	26214
FREQU	31446.54 Hz
SCANS	303
ACQTM	0.8336 sec
PD	2.0000 sec
PW1	4.00 usec
IRNUC	1H
CTEMP	20.7 c
SLVNT	CDCL3
EXREF	77.00 ppm
BF	0.10 Hz
RGAIN	60

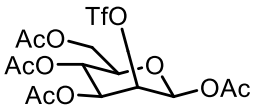

2-Tf-O-AcMan

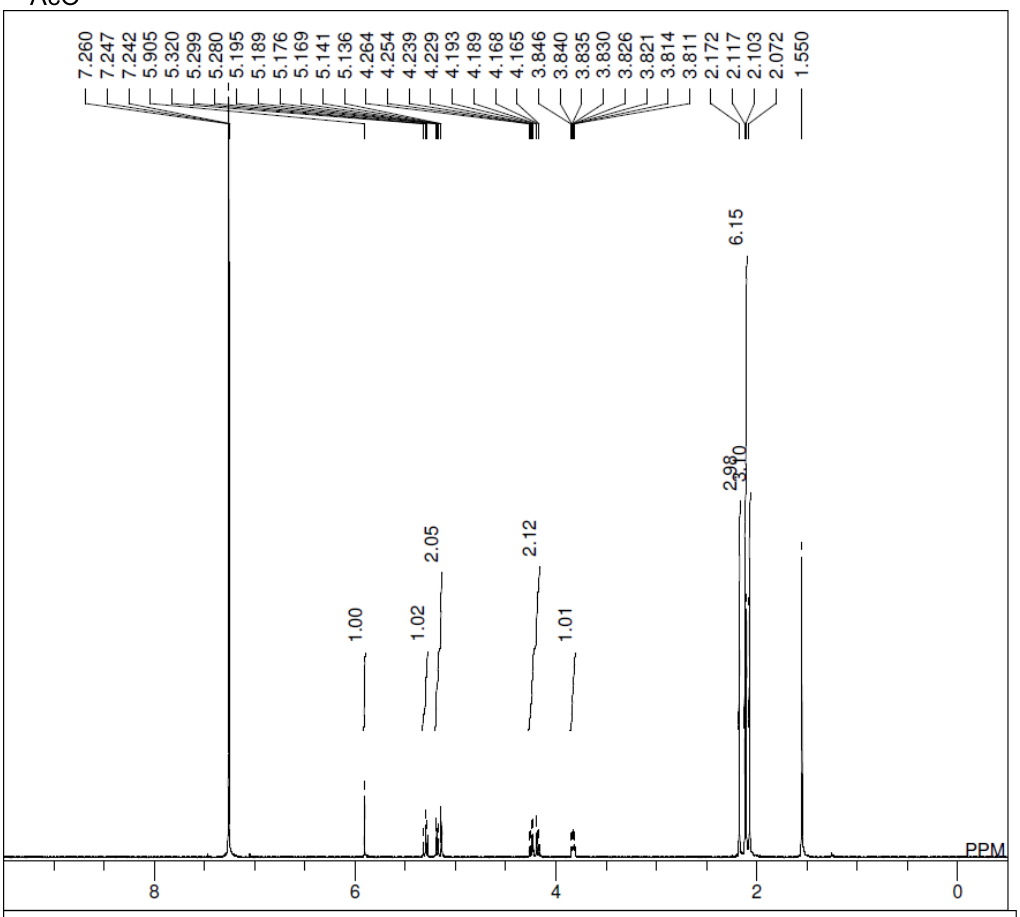

DFILE	_AF_01_120 proton-1-1 b.als
COMNT	AF_01_120 proton
DATIM	2015-06-23 11:44:31
OBNUC	1H
EXMOD	proton.jxp
OBFRQ	500.16 MHz
OBSET	2.41 KHz
OBFIN	6.01 Hz
POINT	13107
FREQU	7507.51 Hz
SCANS	8
ACQTM	1.7459 sec
PD	5.0000 sec
PW1	6.22 usec
IRNUC	1H
CTEMP	19.1 c
SLVNT	CDCL3
EXREF	7.26 ppm
BF	0.10 Hz
RGAIN	58

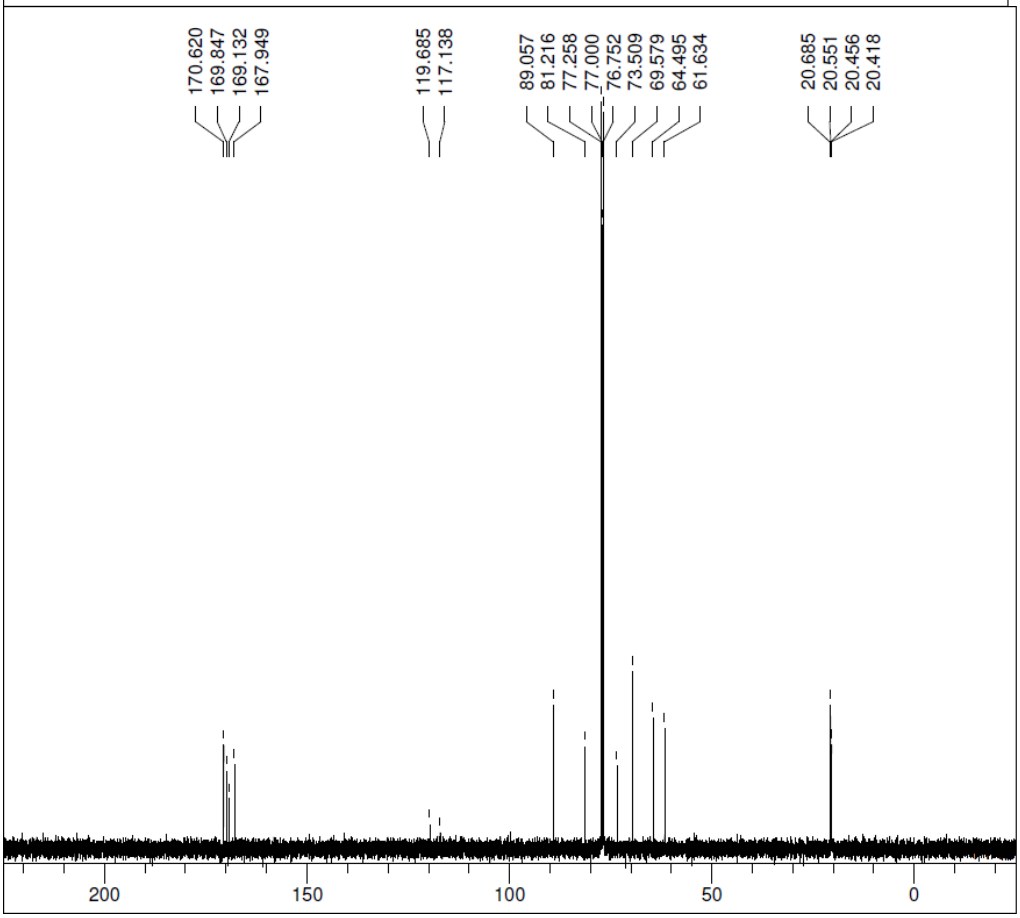

DFILE	_AF_02_047 carbon-1-1.als
COMNT	AF_02_047 carbon
DATIM	2015-12-09 21:27:48
OBNUC	13C
EXMOD	carbon.jxp
OBFRQ	125.77 MHz
OBSET	7.87 KHz
OBFIN	4.21 Hz
POINT	26214
FREQU	31446.54 Hz
SCANS	484
ACQTM	0.8336 sec
PD	2.0000 sec
PW1	4.00 usec
IRNUC	1H
CTEMP	20.3 c
SLVNT	CDCL3
EXREF	77.00 ppm
BF	0.10 Hz
RGAIN	60

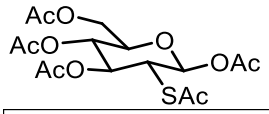

2-Ac-S-AcGlc

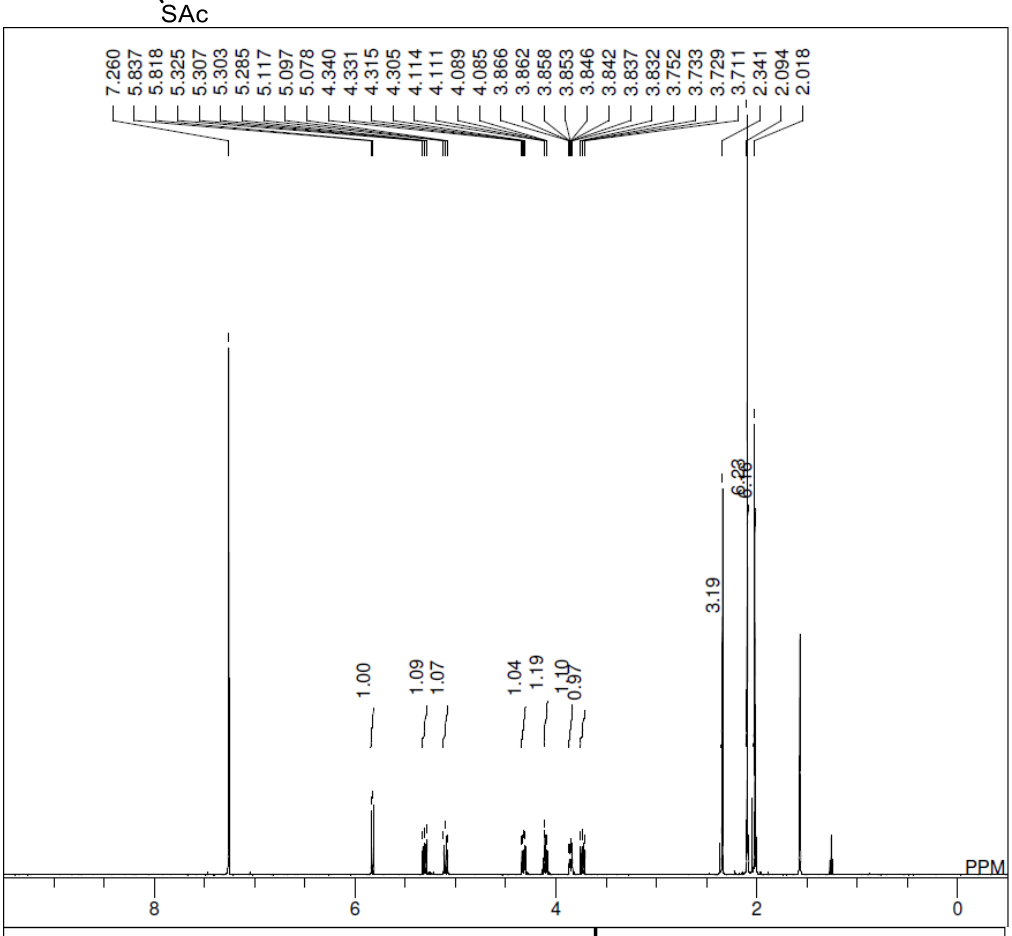

DFILE _AF_02_148 d proton-1-1.als
COMNT AF_02_148 c proton
DATIM 2016-07-13 21:45:17
OBNUC 1H
EXMOD proton.jxp
OBFRQ 500.16 MHz
OBSET 2.41 KHz
OBFIN 6.01 Hz
POINT 13107
FREQU 7507.51 Hz
SCANS 8
ACQTM 1.7459 sec
PD 5.0000 sec
PW1 6.22 usec
IRNUC 1H
CTEMP 18.9 c
SLVNT CDCL3
EXREF 7.26 ppm
BF 0.10 Hz
RGAIN 46

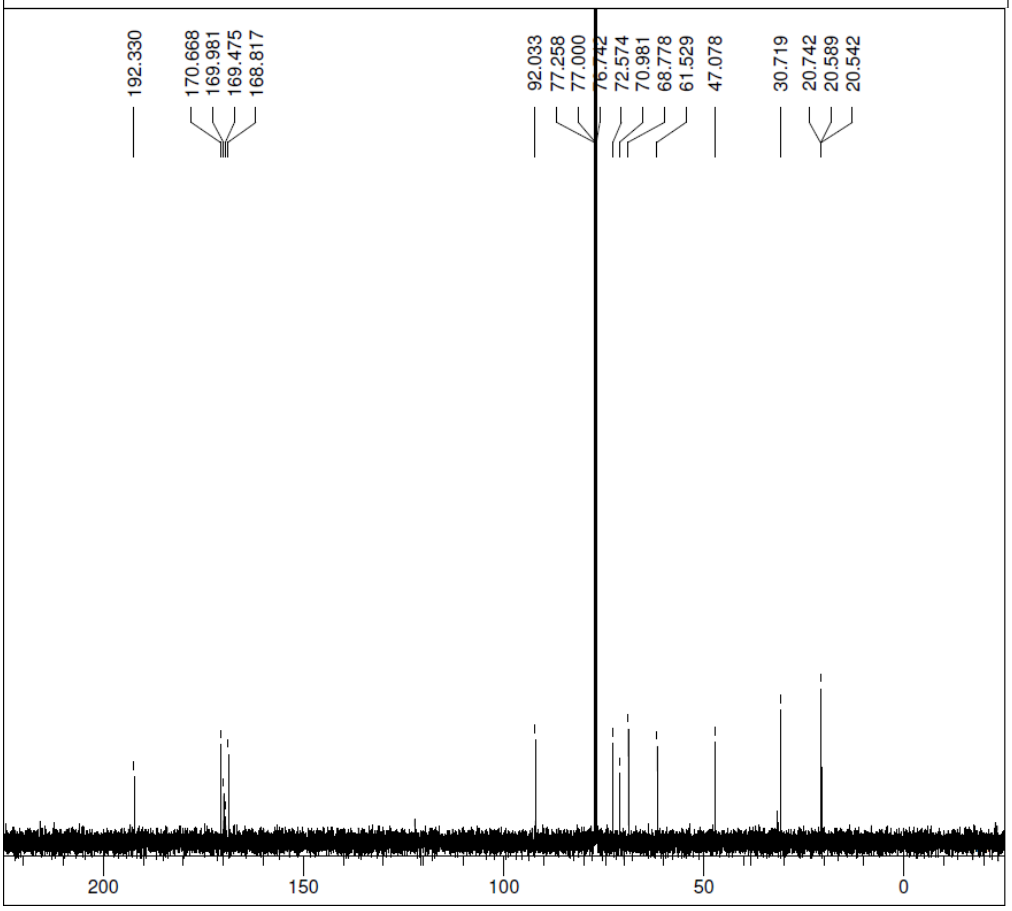

DFILE _AF_02_148 b carbon-1-1.als
COMNT AF_02_148 b carbon
DATIM 2016-07-05 11:36:05
OBNUC 13C
EXMOD carbon.jxp
OBFRQ 125.77 MHz
OBSET 7.87 KHz
OBFIN 4.21 Hz
POINT 26214
FREQU 31446.54 Hz
SCANS 250
ACQTM 0.8336 sec
PD 2.0000 sec
PW1 3.12 usec
IRNUC 1H
CTEMP 19.3 c
SLVNT CDCL3
EXREF 77.00 ppm
BF 0.10 Hz
RGAIN 58

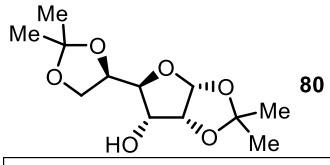

80

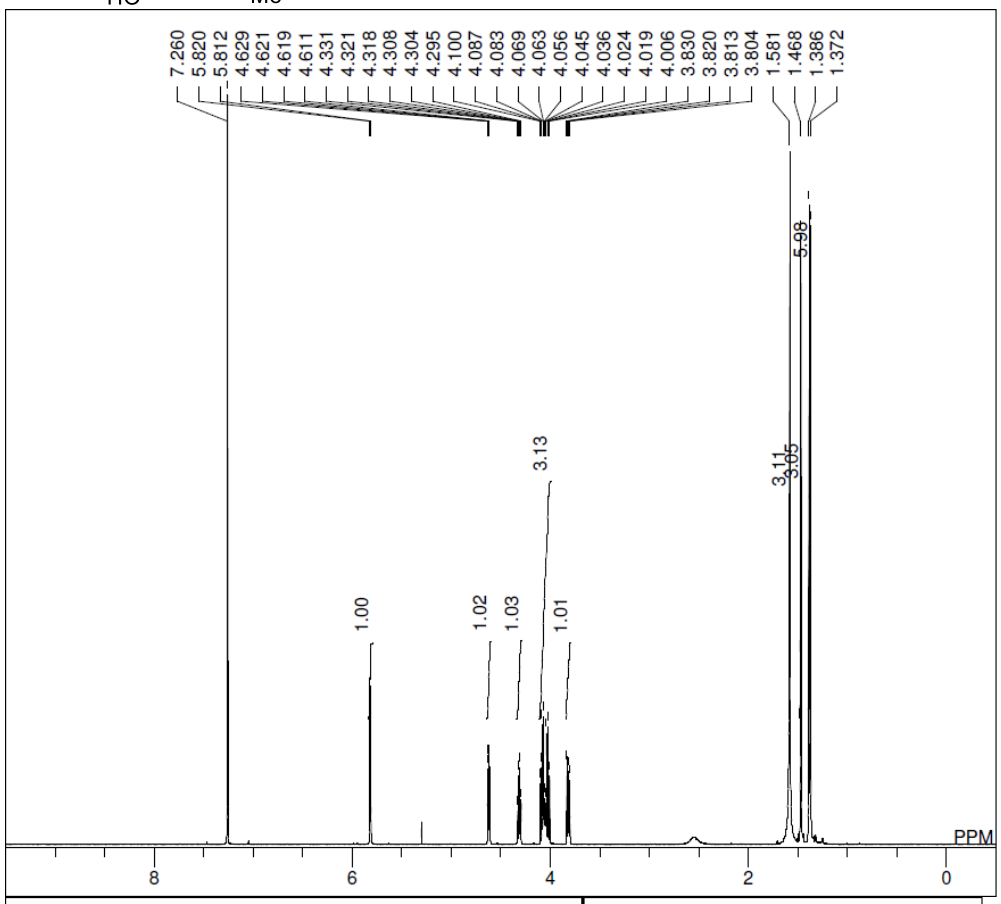

DFILE	_AF_02_131-1-1.als
COMNT	AF_02_131
DATIM	2016-06-15 22:14:54
OBNUC	1H
EXMOD	proton.jxp
OBFRQ	500.16 MHz
OBSET	2.41 KHz
OBFIN	6.01 Hz
POINT	13107
FREQU	7507.51 Hz
SCANS	8
ACQTM	1.7459 sec
PD	5.0000 sec
PW1	6.22 usec
IRNUC	1H
CTEMP	18.4 c
SLVNT	CDCL3
EXREF	7.26 ppm
BF	0.10 Hz
RGAIN	46

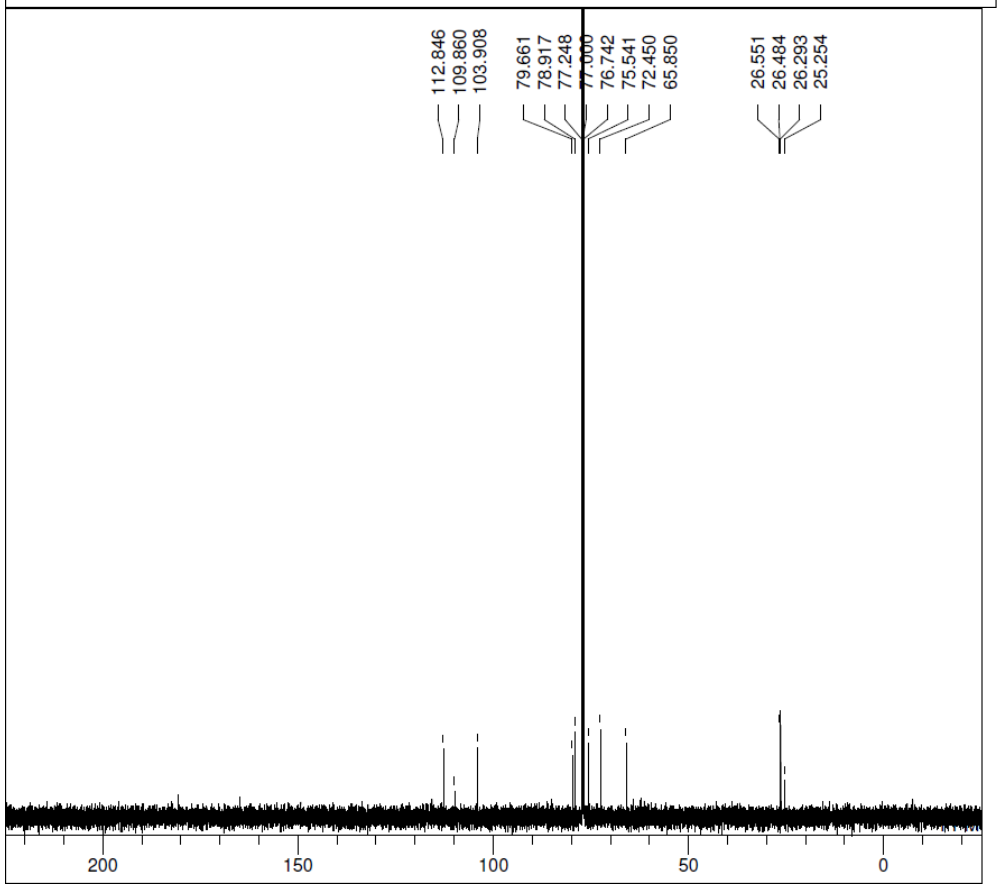

DFILE	_AF_02_131 C-1-1.als
COMNT	AF_02_131
DATIM	2016-06-15 22:32:39
OBNUC	13C
EXMOD	carbon.jxp
OBFRQ	125.77 MHz
OBSET	7.87 KHz
OBFIN	4.21 Hz
POINT	26214
FREQU	31446.54 Hz
SCANS	250
ACQTM	0.8336 sec
PD	2.0000 sec
PW1	3.12 usec
IRNUC	1H
CTEMP	19.3 c
SLVNT	CDCL3
EXREF	77.00 ppm
BF	0.10 Hz
RGAIN	60

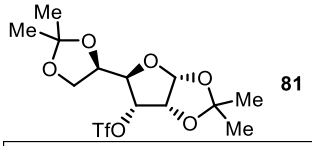

81

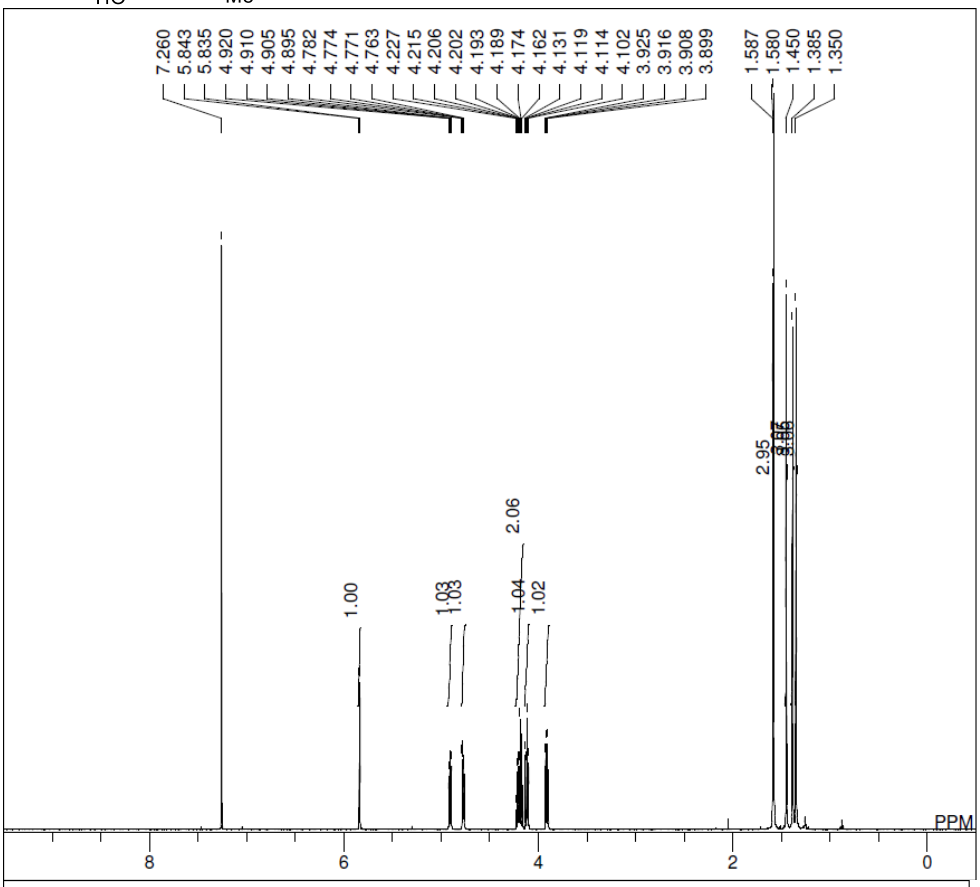

DFILE	_AF_02_132-1-1.als
COMNT	AF_02_132
DATIM	2016-06-17 14:12:05
OBNUC	1H
EXMOD	proton.jxp
OBFRQ	500.16 MHz
OBSET	2.41 KHz
OBFIN	6.01 Hz
POINT	13107
FREQU	7507.51 Hz
SCANS	8
ACQTM	1.7459 sec
PD	5.0000 sec
PW1	6.22 usec
IRNUC	1H
CTEMP	17.9 c
SLVNT	CDCL3
EXREF	7.26 ppm
BF	0.10 Hz
RGAIN	44

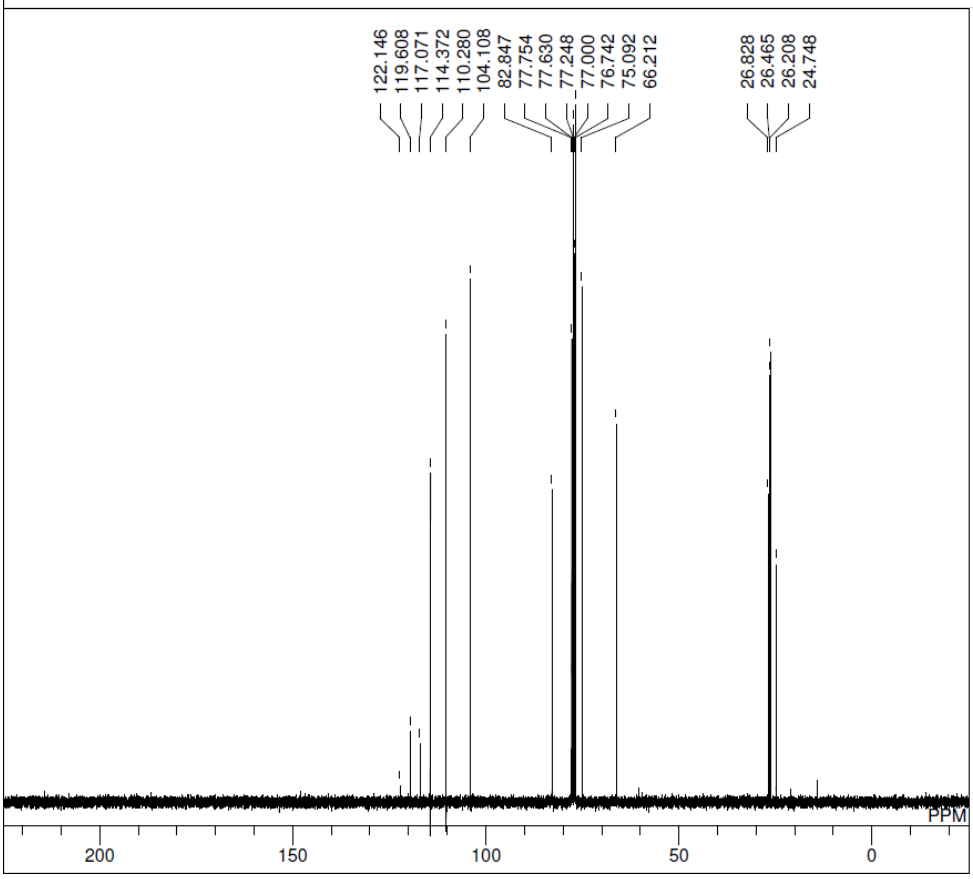

DFILE	_AF_02_132 b carbon-1-1.als
COMNT	AF_02_132 b carbon
DATIM	2016-06-17 16:43:45
OBNUC	13C
EXMOD	carbon.jxp
OBFRQ	125.77 MHz
OBSET	7.87 KHz
OBFIN	4.21 Hz
POINT	26214
FREQU	31446.54 Hz
SCANS	250
ACQTM	0.8336 sec
PD	2.0000 sec
PW1	3.12 usec
IRNUC	1H
CTEMP	19.2 c
SLVNT	CDCL3
EXREF	77.00 ppm
BF	0.10 Hz
RGAIN	60

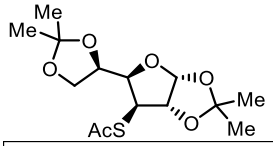

Diacetone-3-deoxy-Ac-S-Glc

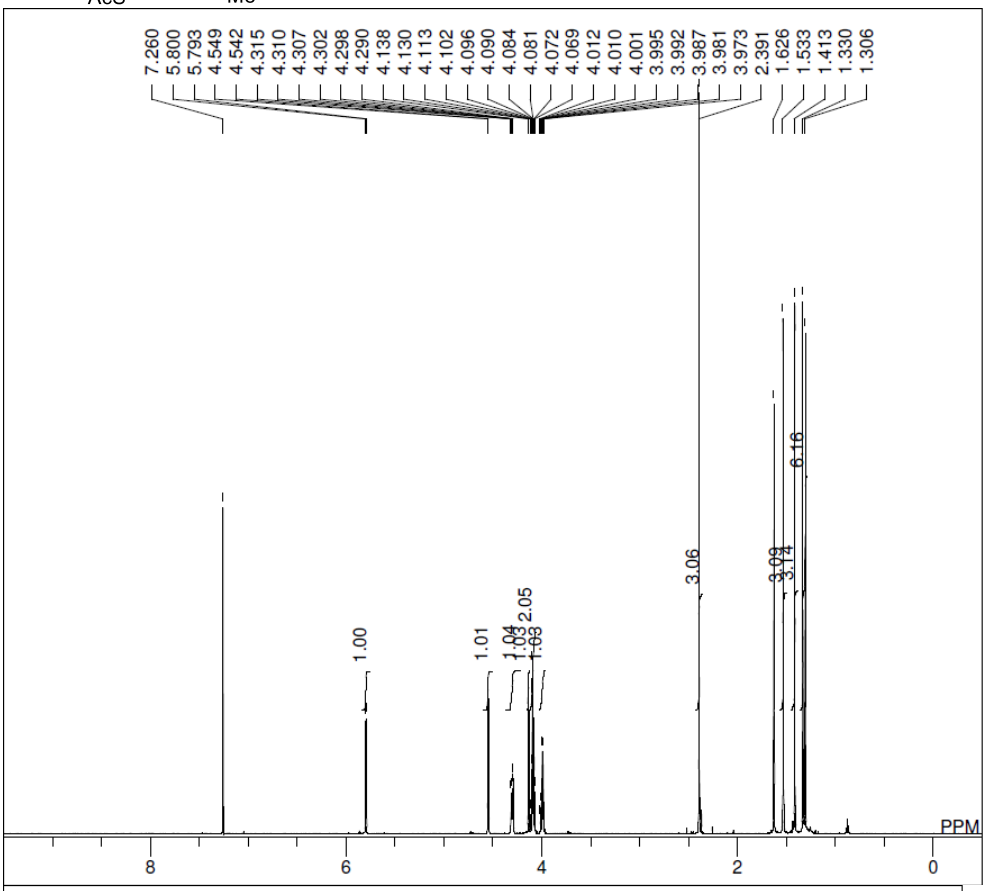

DFILE _AF_02_145 45 proton-1-1.als
COMNT AF_02_145 45 proton
DATIM 2016-07-01 09:36:30
OBNUC 1H
EXMOD proton.jxp
OBFRQ 500.16 MHz
OBSET 2.41 KHz
OBFIN 6.01 Hz
POINT 13107
FREQU 7507.51 Hz
SCANS 8
ACQTM 1.7459 sec
PD 5.0000 sec
PW1 6.22 usec
IRNUC 1H
CTEMP 18.4 c
SLVNT CDCL3
EXREF 7.26 ppm
BF 0.10 Hz
RGAIN 40

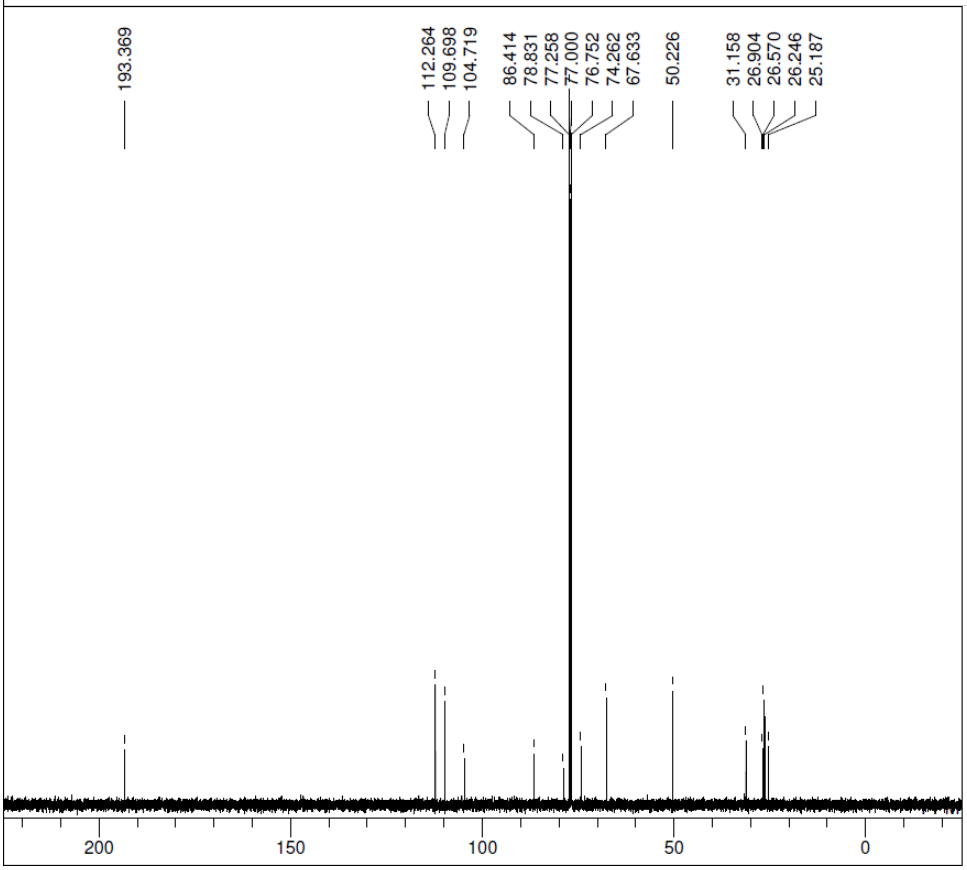

DFILE _AF_02_145 45 carbon-1-1.als
COMNT AF_02_145 45 carbon
DATIM 2016-07-01 09:55:04
OBNUC 13C
EXMOD carbon.jxp
OBFRQ 125.77 MHz
OBSET 7.87 KHz
OBFIN 4.21 Hz
POINT 26214
FREQU 31446.54 Hz
SCANS 250
ACQTM 0.8336 sec
PD 2.0000 sec
PW1 3.12 usec
IRNUC 1H
CTEMP 18.7 c
SLVNT CDCL3
EXREF 77.00 ppm
BF 0.10 Hz
RGAIN 58

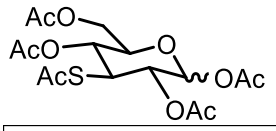

3-Ac-S-AcGlc

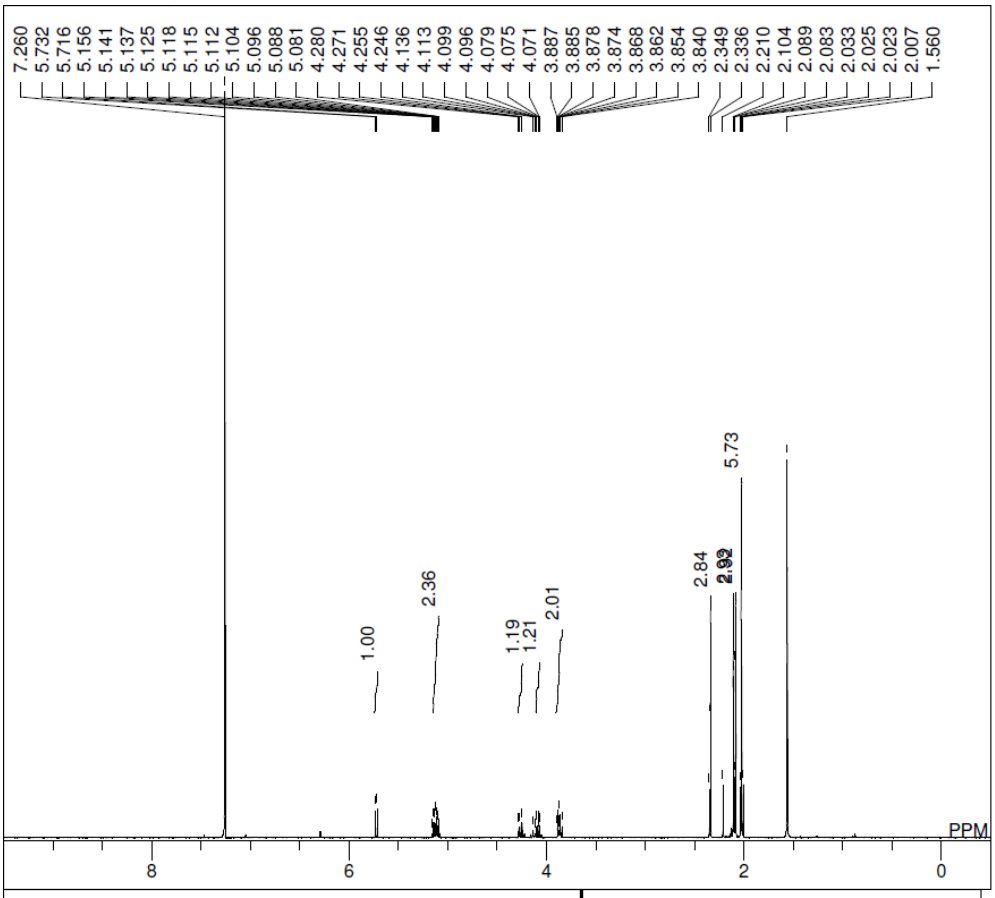

DFILE	_AF_03_001 b proton-1-1.als
COMNT	AF_03_001 b proton
DATIM	2016-07-12 11:08:32
OBNUC	1H
EXMOD	proton.jxp
OBFRQ	500.16 MHz
OBSET	2.41 KHz
OBFIN	6.01 Hz
POINT	13107
FREQU	7507.51 Hz
SCANS	8
ACQTM	1.7459 sec
PD	5.0000 sec
PW1	6.22 usec
IRNUC	1H
CTEMP	18.6 c
SLVNT	CDCL3
EXREF	7.26 ppm
BF	0.10 Hz
RGAIN	48

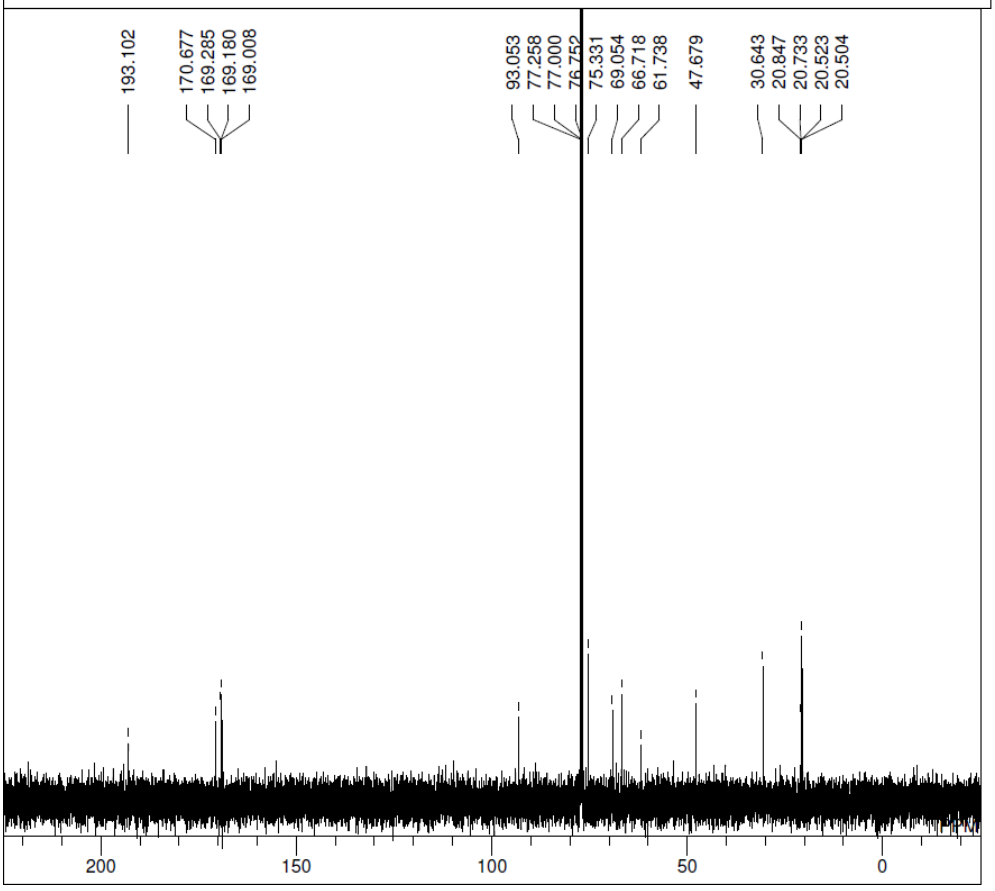

DFILE	_AF_02_146 carbon-1-1.als
COMNT	AF_02_146 carbon
DATIM	2016-07-04 17:50:08
OBNUC	13C
EXMOD	carbon.jxp
OBFRQ	125.77 MHz
OBSET	7.87 KHz
OBFIN	4.21 Hz
POINT	26214
FREQU	31446.54 Hz
SCANS	250
ACQTM	0.8336 sec
PD	2.0000 sec
PW1	3.12 usec
IRNUC	1H
CTEMP	19.4 c
SLVNT	CDCL3
EXREF	77.00 ppm
BF	0.10 Hz
RGAIN	58

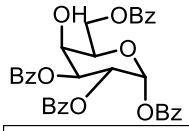

83

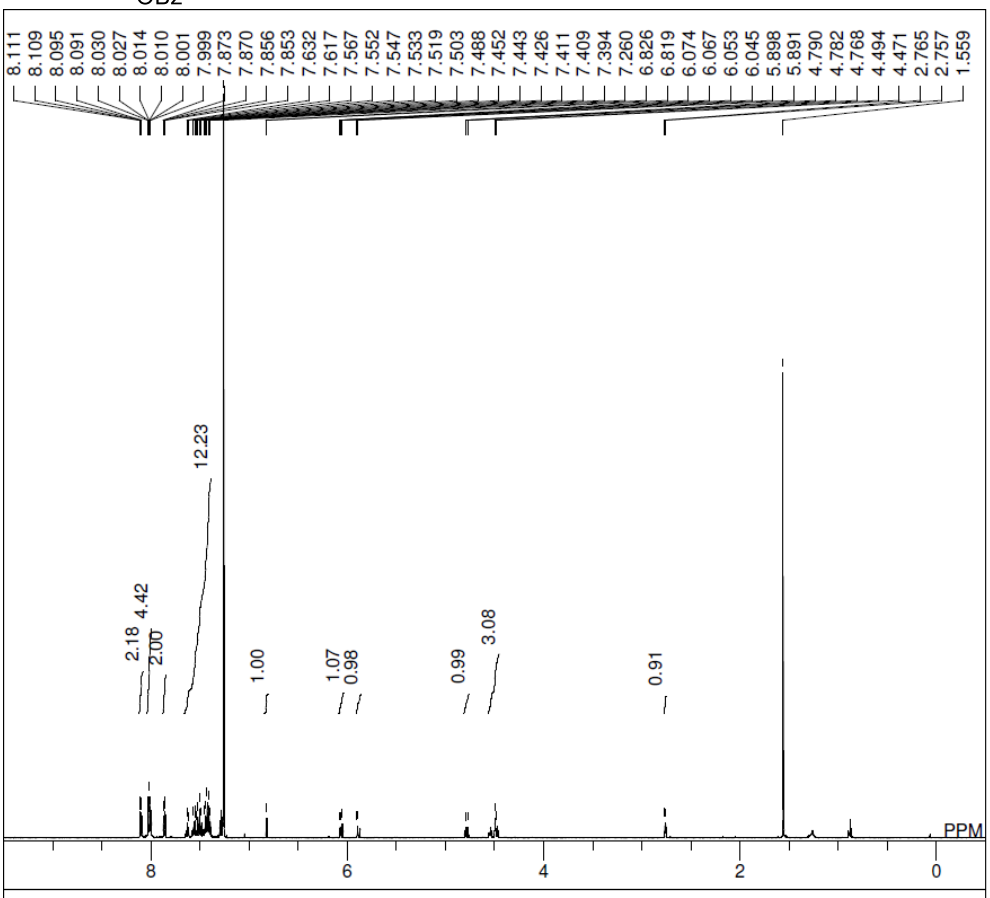

DFILE _AF_03_105 2743 proton-1-1.als
COMNT AF_03_105 2743 proton
DATIM 2017-02-07 20:29:44
OBNUC 1H
EXMOD proton.jxp
OBFRQ 500.16 MHz
OBSET 2.41 KHz
OBFIN 6.01 Hz
POINT 13107
FREQU 7507.51 Hz
SCANS 8
ACQTM 1.7459 sec
PD 5.0000 sec
PW1 6.85 usec
IRNUC 1H
CTEMP 17.7 c
SLVNT CDCL3
EXREF 7.26 ppm
BF 0.10 Hz
RGAIN 50

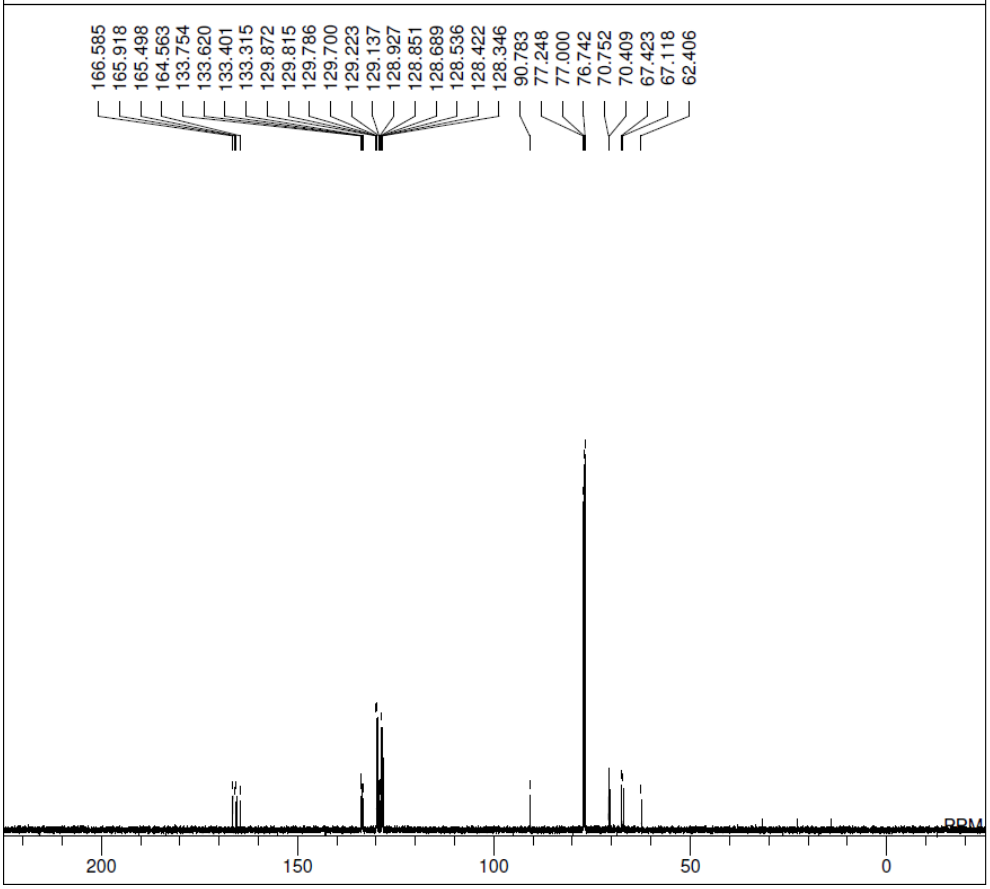

DFILE _AF_03_105 2743c carbon-1-1.als
COMNT AF_03_105 2743c carbon
DATIM 2017-02-08 13:41:36
OBNUC 13C
EXMOD carbon.jxp
OBFRQ 125.77 MHz
OBSET 7.87 KHz
OBFIN 4.21 Hz
POINT 26214
FREQU 31446.54 Hz
SCANS 400
ACQTM 0.8336 sec
PD 2.0000 sec
PW1 3.12 usec
IRNUC 1H
CTEMP 18.4 c
SLVNT CDCL3
EXREF 77.00 ppm
BF 0.10 Hz
RGAIN 60

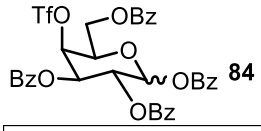

84

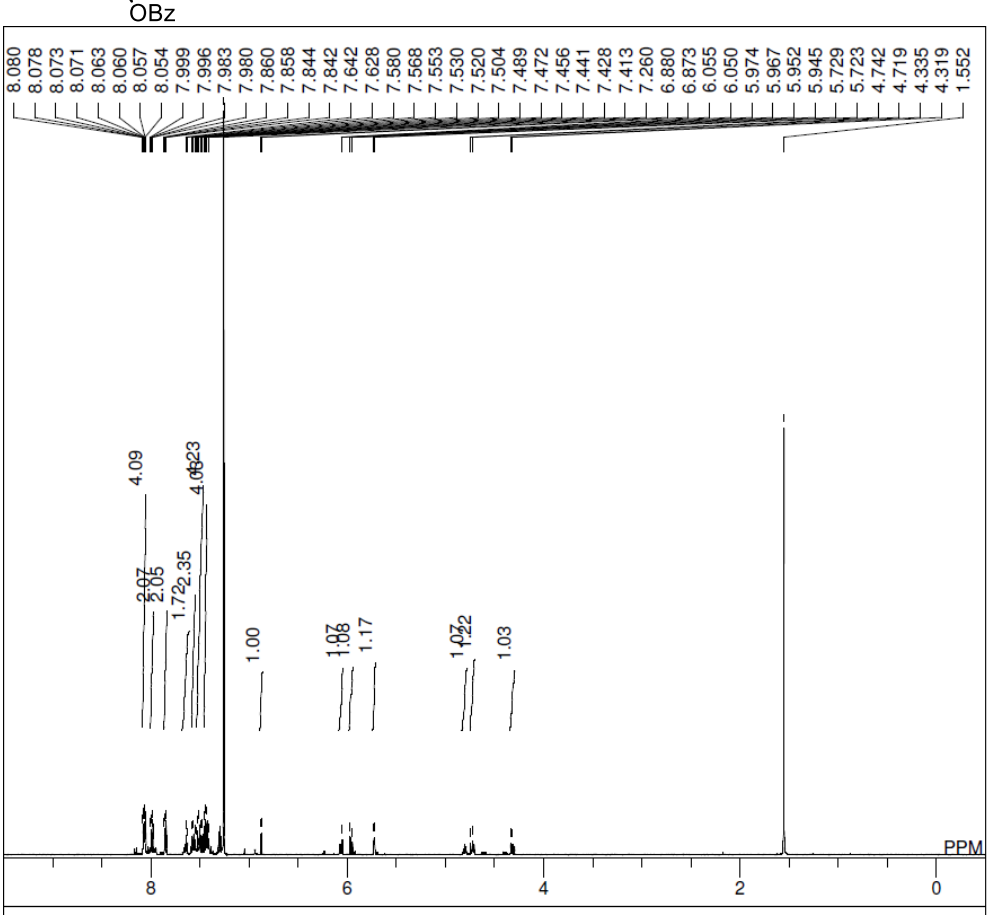

DFILE	_AF_03_092 221 GPC1b proton-1
COMNT	AF_03_092 221 GPC1b proton
DATIM	2017-02-16 14:34:29
OBNUC	1H
EXMOD	proton.jxp
OBFRQ	500.16 MHz
OBSET	2.41 KHz
OBFIN	6.01 Hz
POINT	13107
FREQU	7507.51 Hz
SCANS	8
ACQTM	1.7459 sec
PD	5.0000 sec
PW1	6.85 usec
IRNUC	1H
CTEMP	19.0 c
SLVNT	CDCL3
EXREF	7.26 ppm
BF	0.10 Hz
RGAIN	48

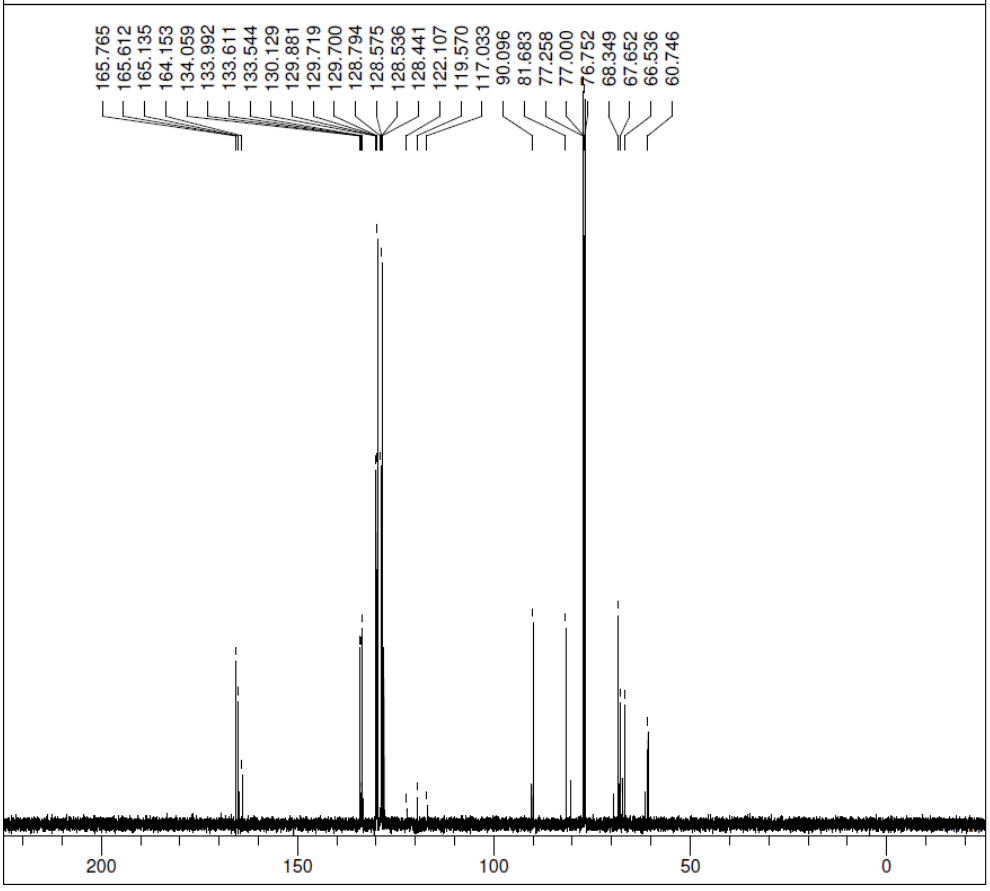

DFILE	_AF_03_092 221 GPC1 carbon-1-
COMNT	AF_03_092 221 GPC1 carbon
DATIM	2017-02-16 16:24:23
OBNUC	13C
EXMOD	carbon.jxp
OBFRQ	125.77 MHz
OBSET	7.87 KHz
OBFIN	4.21 Hz
POINT	26214
FREQU	31446.54 Hz
SCANS	250
ACQTM	0.8336 sec
PD	2.0000 sec
PW1	3.12 usec
IRNUC	1H
CTEMP	20.3 c
SLVNT	CDCL3
EXREF	77.00 ppm
BF	0.10 Hz
RGAIN	60

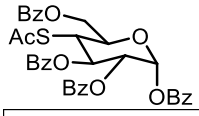

4-Ac-S-Bz-Glc

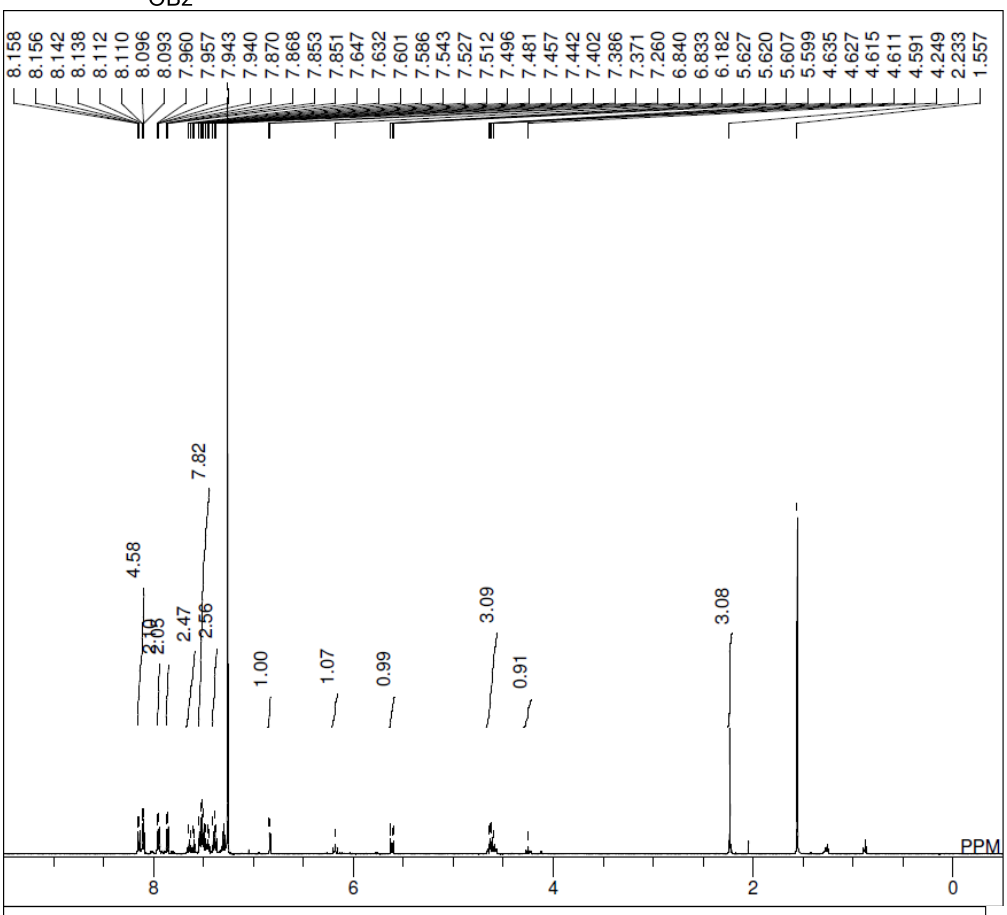

DFILE _AF_03_122 54126b proton-1-1.al
COMNT AF_03_122 54126b proton
DATIM 2017-02-07 21:15:13
OBNUC 1H
EXMOD proton.jxp
OBFRQ 500.16 MHz
OBSET 2.41 KHz
OBFIN 6.01 Hz
POINT 13107
FREQU 7507.51 Hz
SCANS 8
ACQTM 1.7459 sec
PD 5.0000 sec
PW1 6.85 usec
IRNUC 1H
CTEMP 17.6 c
SLVNT CDCL3
EXREF 7.26 ppm
BF 0.10 Hz
RGAIN 50

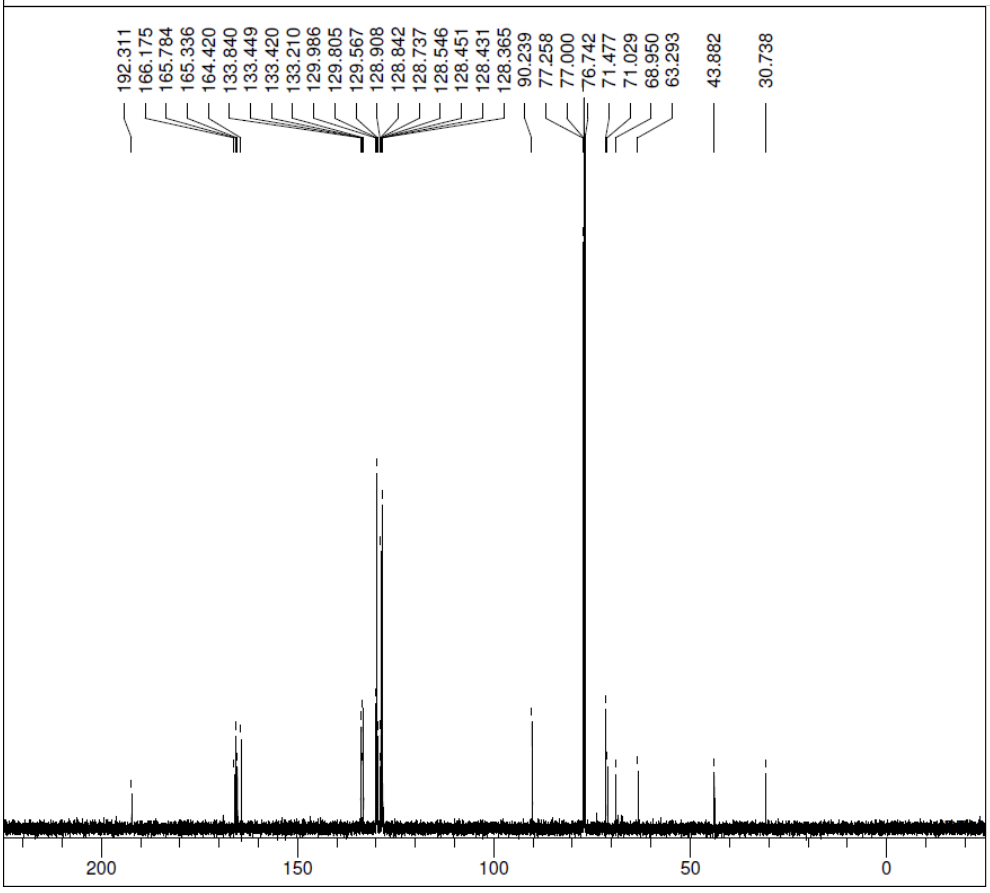

DFILE _AF_03_122 54126c carbon-1-1.a
COMNT AF_03_122 54126c carbon
DATIM 2017-02-10 14:53:56
OBNUC 13C
EXMOD carbon.jxp
OBFRQ 125.77 MHz
OBSET 7.87 KHz
OBFIN 4.21 Hz
POINT 26214
FREQU 31446.54 Hz
SCANS 250
ACQTM 0.8336 sec
PD 2.0000 sec
PW1 3.12 usec
IRNUC 1H
CTEMP 17.7 c
SLVNT CDCL3
EXREF 77.00 ppm
BF 0.10 Hz
RGAIN 60

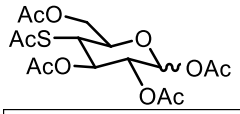

4-Ac-S-AcGlc

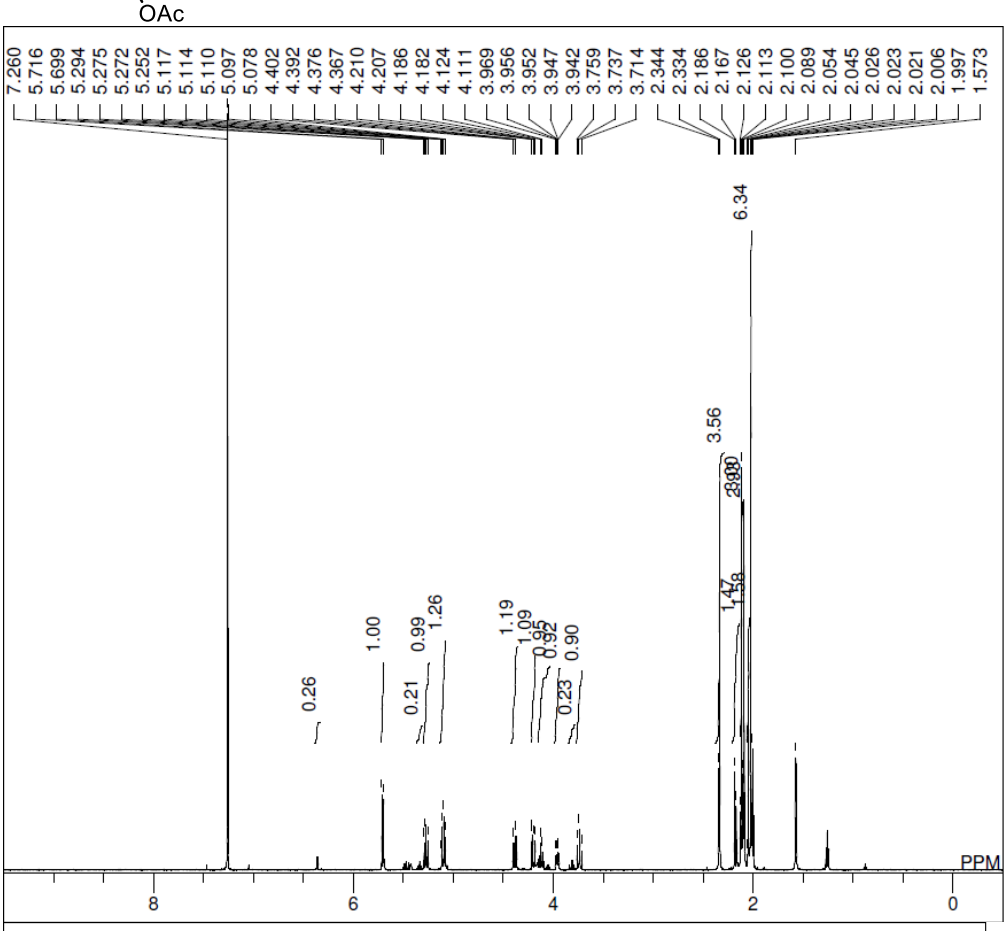

DFILE _AF_03_127 1457 proton-1-1.als
COMNT AF_03_127 1457 proton
DATIM 2017-02-10 17:36:16
OBNUC 1H
EXMOD proton.jxp
OBFRQ 500.16 MHz
OBSET 2.41 KHz
OBFIN 6.01 Hz
POINT 13107
FREQU 7507.51 Hz
SCANS 8
ACQTM 1.7459 sec
PD 5.0000 sec
PW1 6.85 usec
IRNUC 1H
CTEMP 17.1 c
SLVNT CDCL3
EXREF 7.26 ppm
BF 0.10 Hz
RGAIN 46

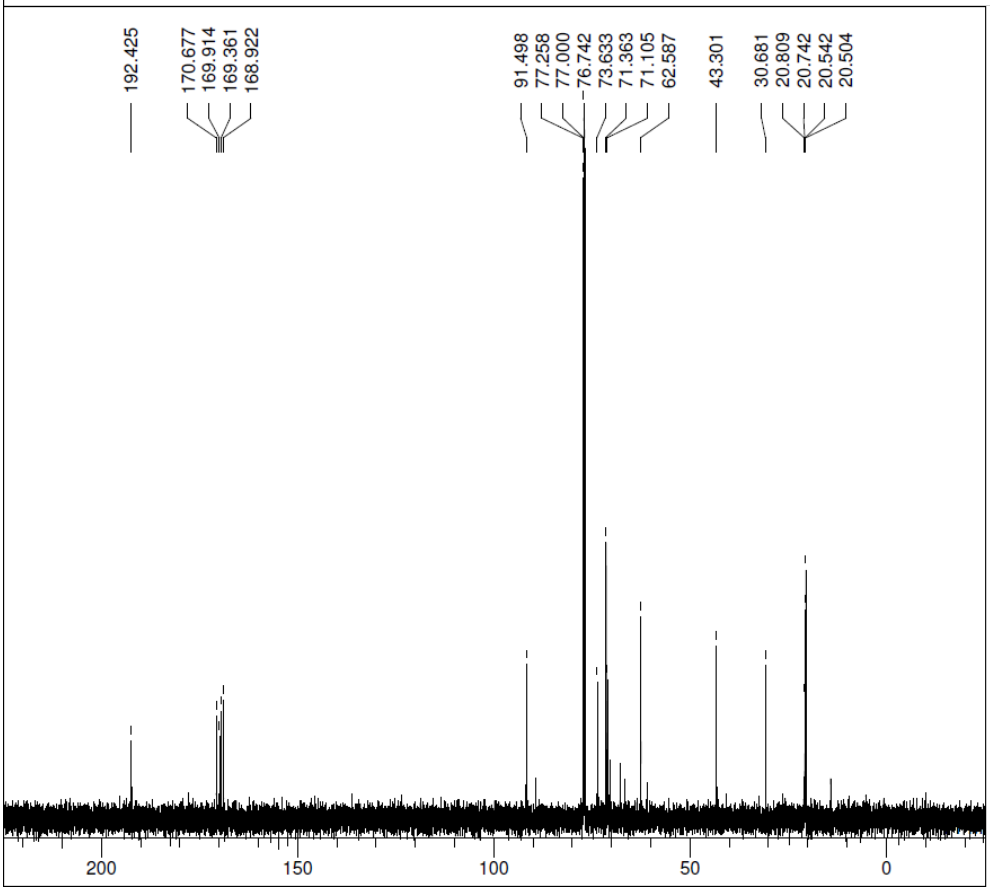

DFILE _AF_03_127 1457 carbon-1-1.als
COMNT AF_03_127 1457 carbon
DATIM 2017-02-14 09:52:18
OBNUC 13C
EXMOD carbon.jxp
OBFRQ 125.77 MHz
OBSET 7.87 KHz
OBFIN 4.21 Hz
POINT 26214
FREQU 31446.54 Hz
SCANS 250
ACQTM 0.8336 sec
PD 2.0000 sec
PW1 3.12 usec
IRNUC 1H
CTEMP 16.6 c
SLVNT CDCL3
EXREF 77.00 ppm
BF 0.10 Hz
RGAIN 60

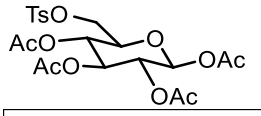

6-Ts-O-Ac-Glc

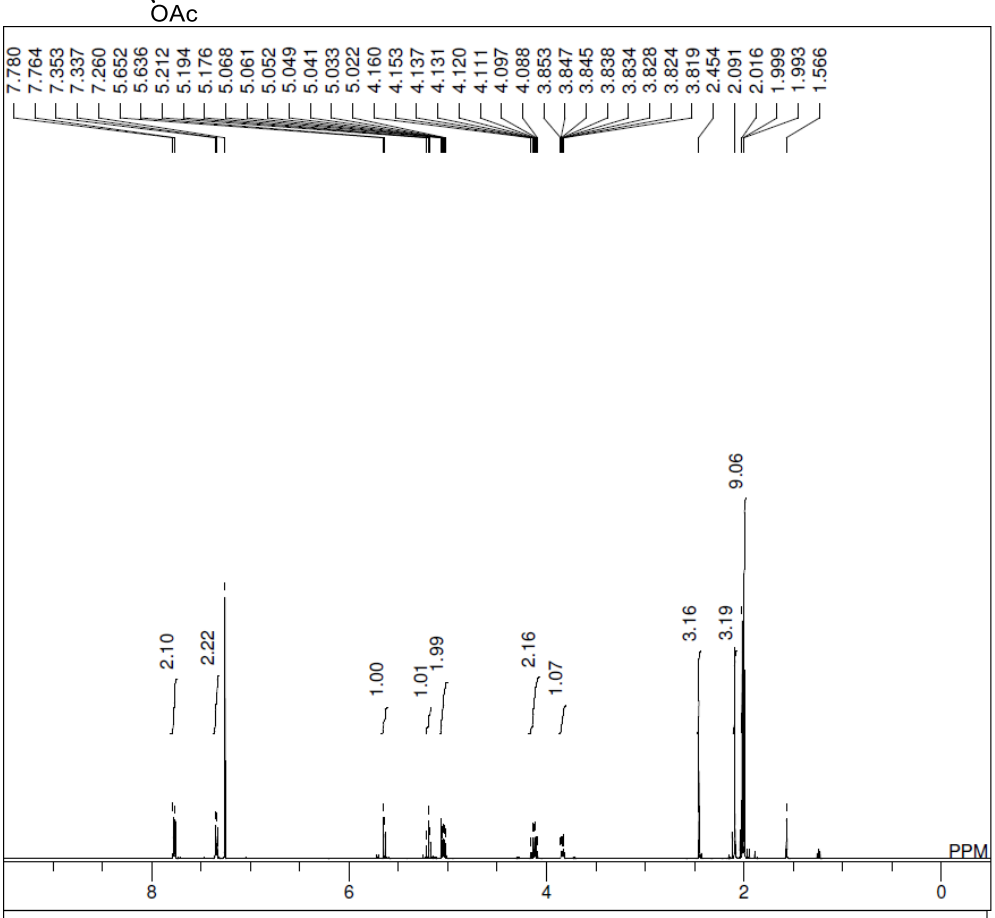

DFILE	_AF_03_023 b proton-1-1.als
COMNT	AF_03_023 b proton
DATIM	2017-02-15 20:23:50
OBNUC	1H
EXMOD	proton.jxp
OBFRQ	500.16 MHz
OBSET	2.41 KHz
OBFIN	6.01 Hz
POINT	13107
FREQU	7507.51 Hz
SCANS	8
ACQTM	1.7459 sec
PD	5.0000 sec
PW1	6.85 usec
IRNUC	1H
CTEMP	17.4 c
SLVNT	CDCL3
EXREF	7.26 ppm
BF	0.10 Hz
RGAIN	44

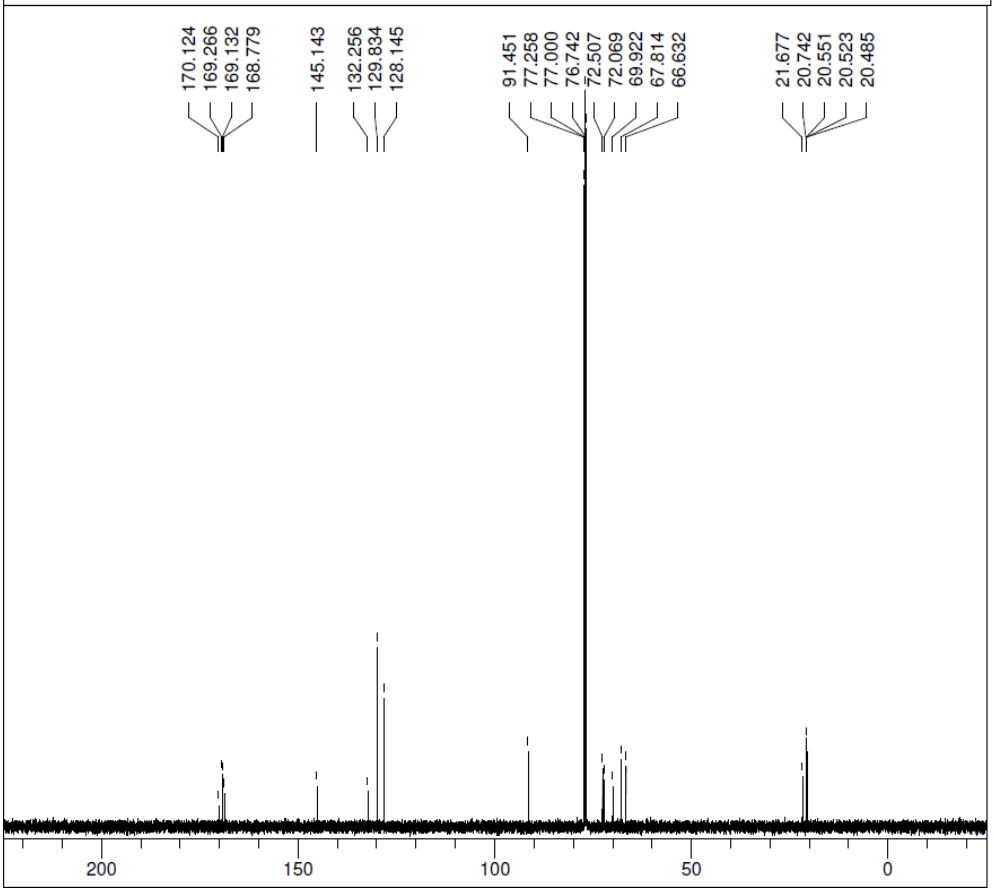

DFILE	_AF_03_023 b carbon-1-1.als
COMNT	AF_03_023 b carbon
DATIM	2017-02-16 09:48:25
OBNUC	13C
EXMOD	carbon.jxp
OBFRQ	125.77 MHz
OBSET	7.87 KHz
OBFIN	4.21 Hz
POINT	26214
FREQU	31446.54 Hz
SCANS	425
ACQTM	0.8336 sec
PD	2.0000 sec
PW1	3.12 usec
IRNUC	1H
CTEMP	17.3 c
SLVNT	CDCL3
EXREF	77.00 ppm
BF	0.10 Hz
RGAIN	60

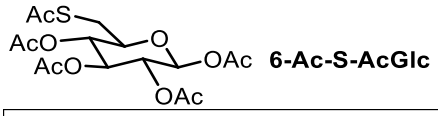

6-Ac-S-AcGlc

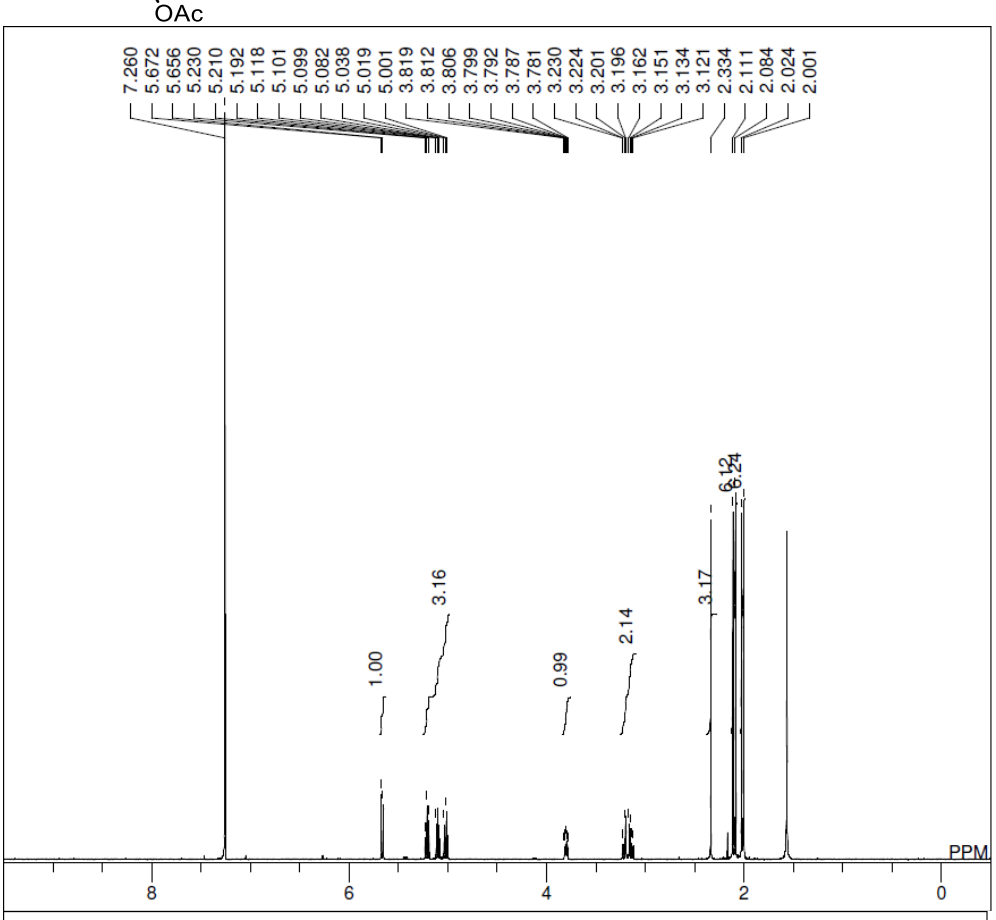

DFILE	_AF_03_017 c proton-1-1.als
COMNT	AF_03_017 c proton
DATIM	2016-07-29 11:27:11
OBNUC	1H
EXMOD	proton.jxp
OBFRQ	500.16 MHz
OBSET	2.41 KHz
OBFIN	6.01 Hz
POINT	13107
FREQU	7507.51 Hz
SCANS	8
ACQTM	1.7459 sec
PD	5.0000 sec
PW1	6.22 usec
IRNUC	1H
CTEMP	19.5 c
SLVNT	CDCL3
EXREF	7.26 ppm
BF	0.10 Hz
RGAIN	50

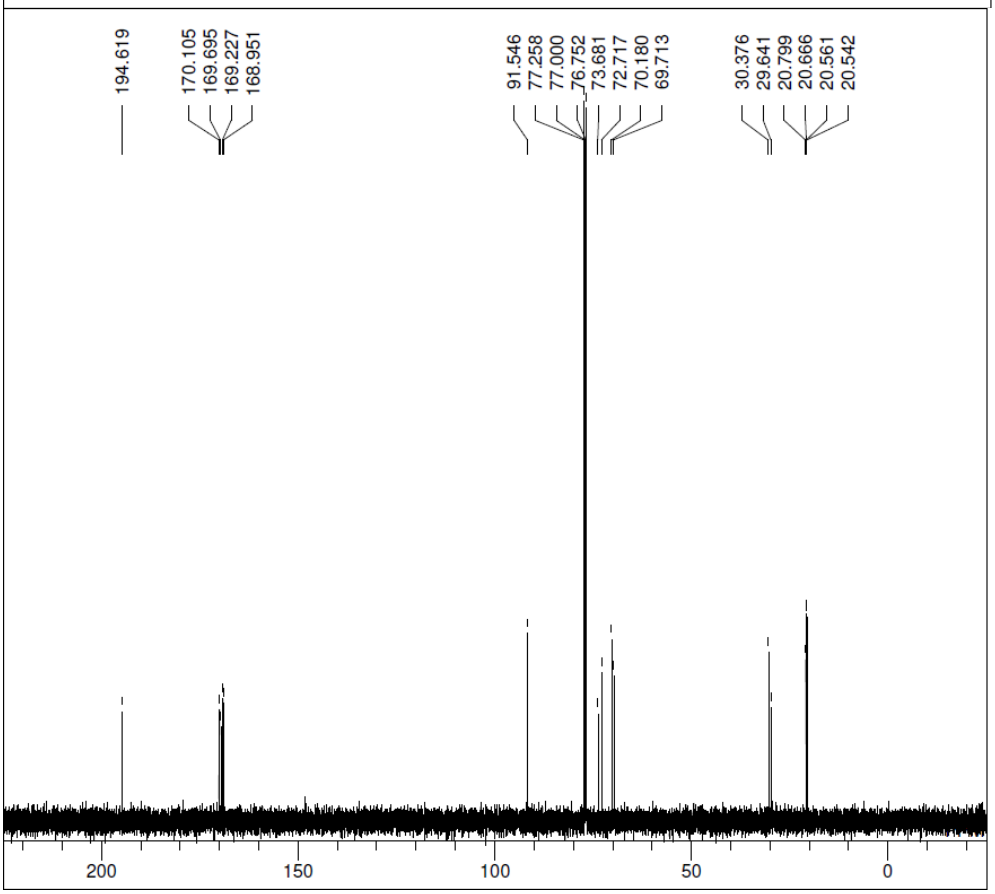

DFILE	_AF_03_017 d carbon-1-1.als
COMNT	AF_03_017 d carbon
DATIM	2016-07-29 15:24:02
OBNUC	13C
EXMOD	carbon.jxp
OBFRQ	125.77 MHz
OBSET	7.87 KHz
OBFIN	4.21 Hz
POINT	26214
FREQU	31446.54 Hz
SCANS	250
ACQTM	0.8336 sec
PD	2.0000 sec
PW1	3.12 usec
IRNUC	1H
CTEMP	20.1 c
SLVNT	CDCL3
EXREF	77.00 ppm
BF	0.10 Hz
RGAIN	58

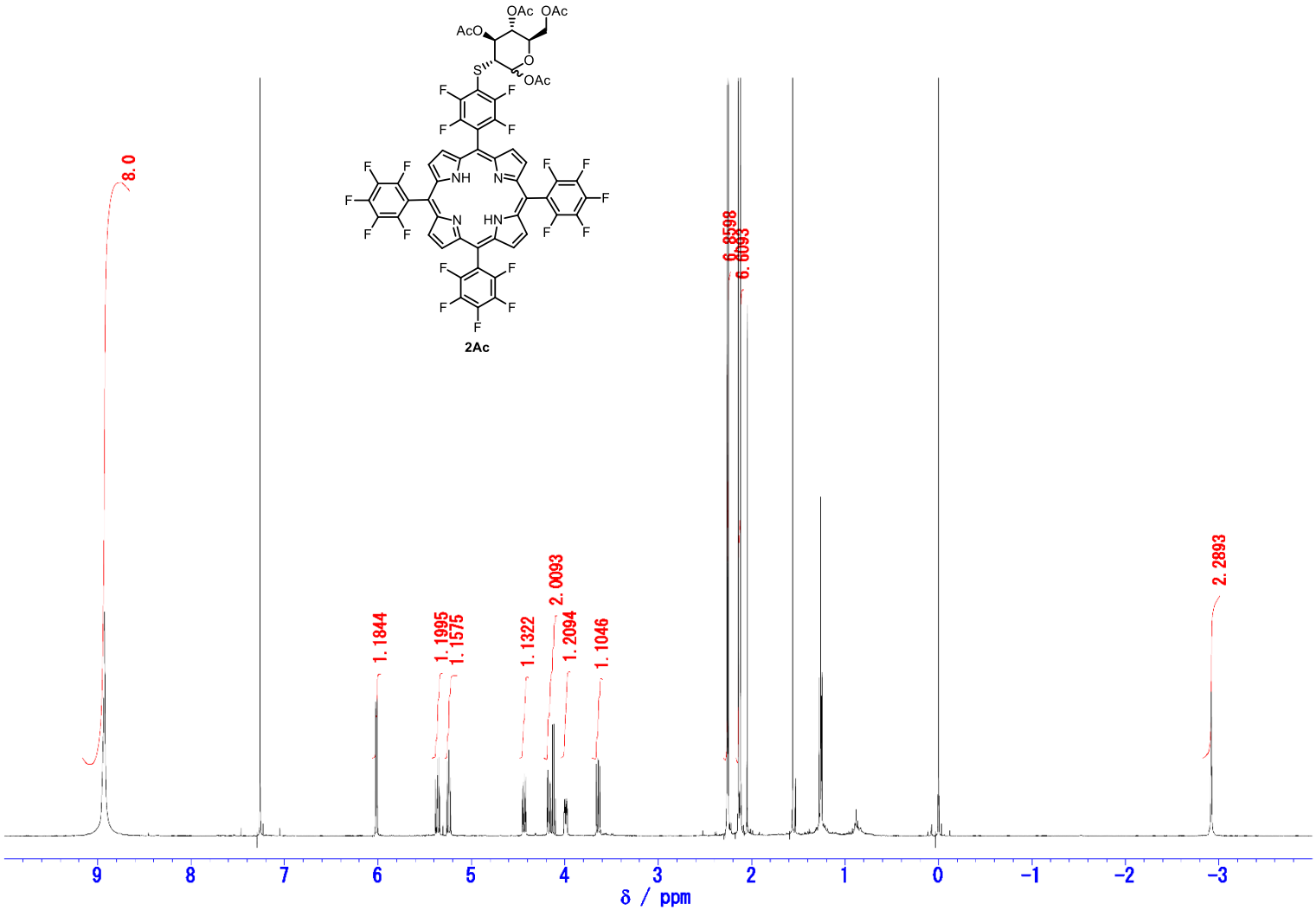

Figure ^{1}H NMR spectrum of **2Ac** in $CDCl_3$. (499.91 MHz)

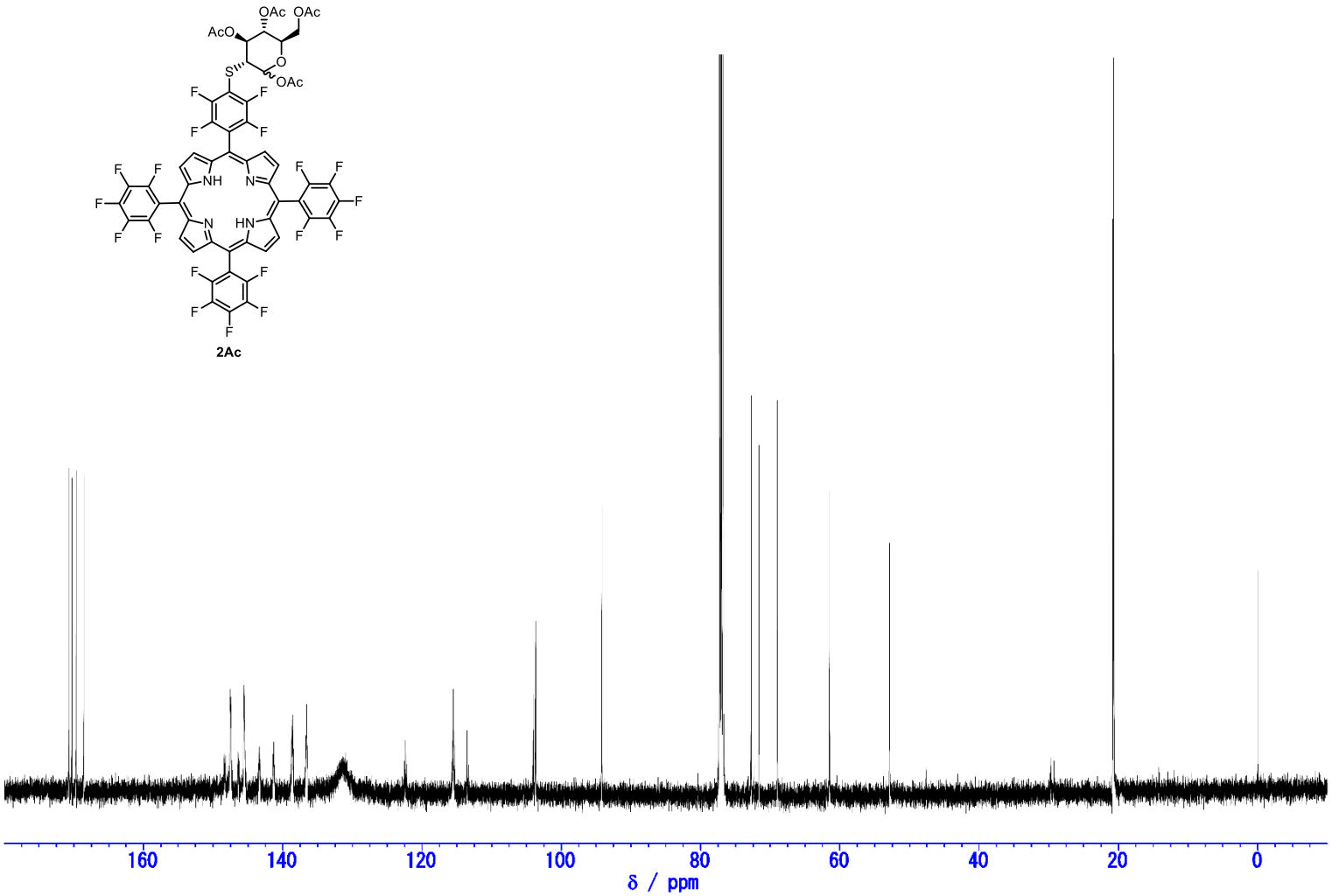

Figure ^{13}C NMR spectrum of **2Ac** in $CDCl_3$. (125.72 MHz)

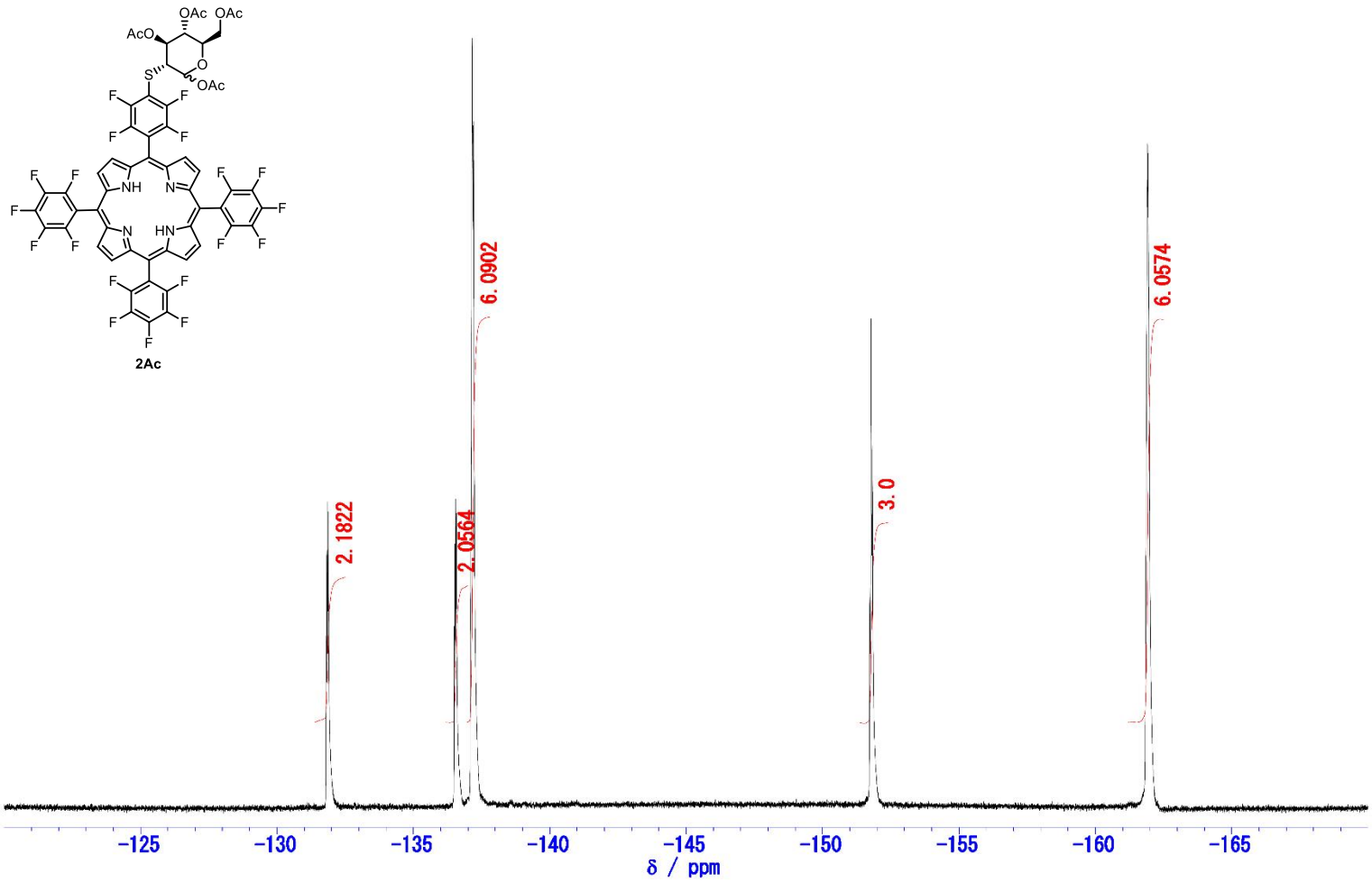

Figure ^{19}F NMR spectrum of **2Ac** in $CDCl_3$. (470.34 MH)

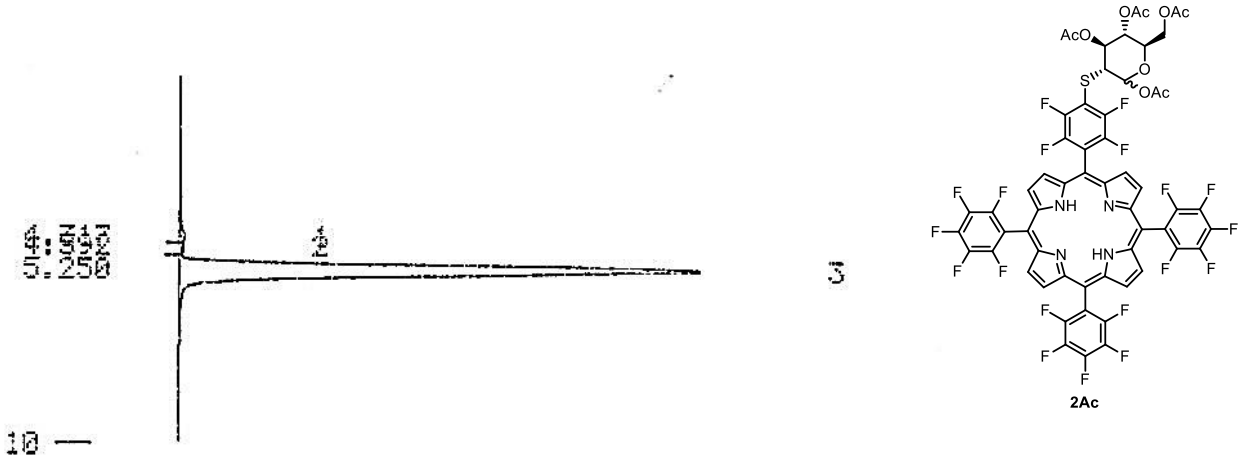

-- % CALCULATION RESULT --

WINDOW = 0 % SCALE FACTOR = 1.0000 PEAK AREA

PEAK#	RT(min)	AREA	HEIGHT	MK	AREA%
1	4.317	34994	1811	LV	0.8270
2	4.592	18515	1248	LV	0.4376
3	5.250	4177745	216498	LLL	98.7354
	TOTAL	4231254	219557		100.0000

Figure Chromatogram of **2Ac** on NP-HPLC. The conditions of **2Ac** was as follows: elution solvent, CH_2Cl_2/ AcOEt (9/1, v/v), column, 4.6 mm I.D.×150 mm; temperature, 30°C; flow rate, 0.75 mL/ min; detector, 410 nm.

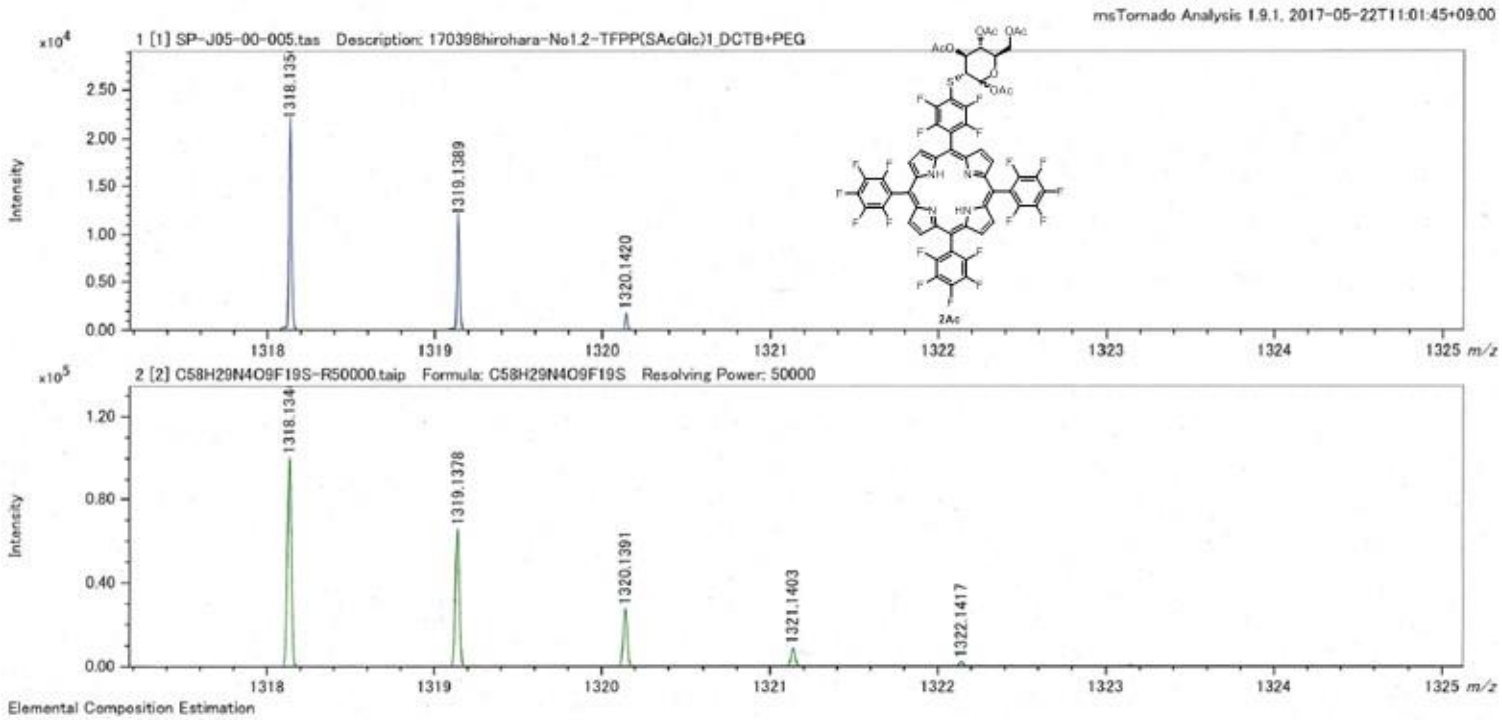

Figure Mass spectrum of **2Ac**. (HRMS)

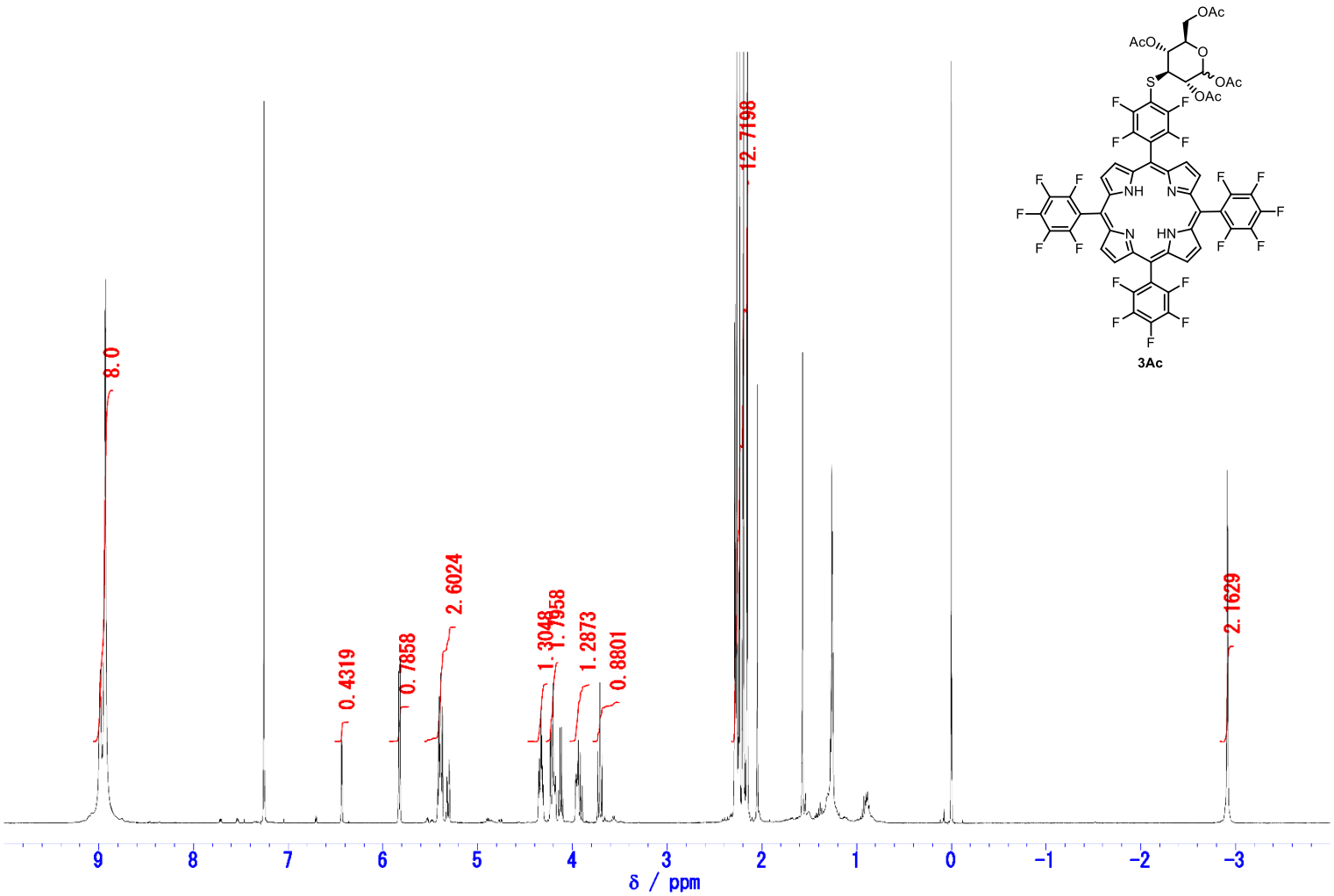

Figure ^{1}H NMR spectrum of **3Ac** in $CDCl_3$. (499.91 MHz)

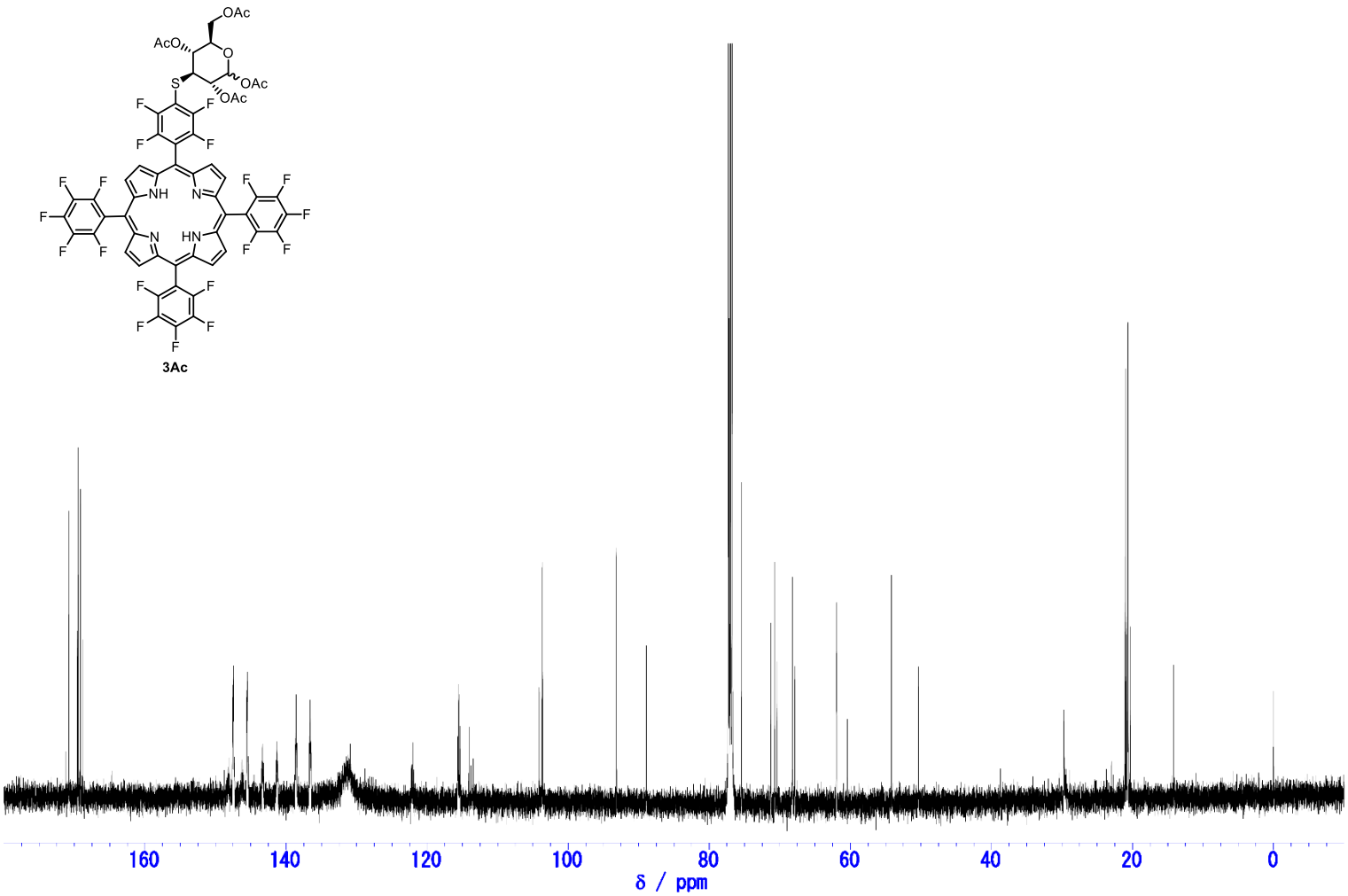

Figure ^{13}C NMR spectrum of **3Ac** in $CDCl_3$. (125.72 MHz)

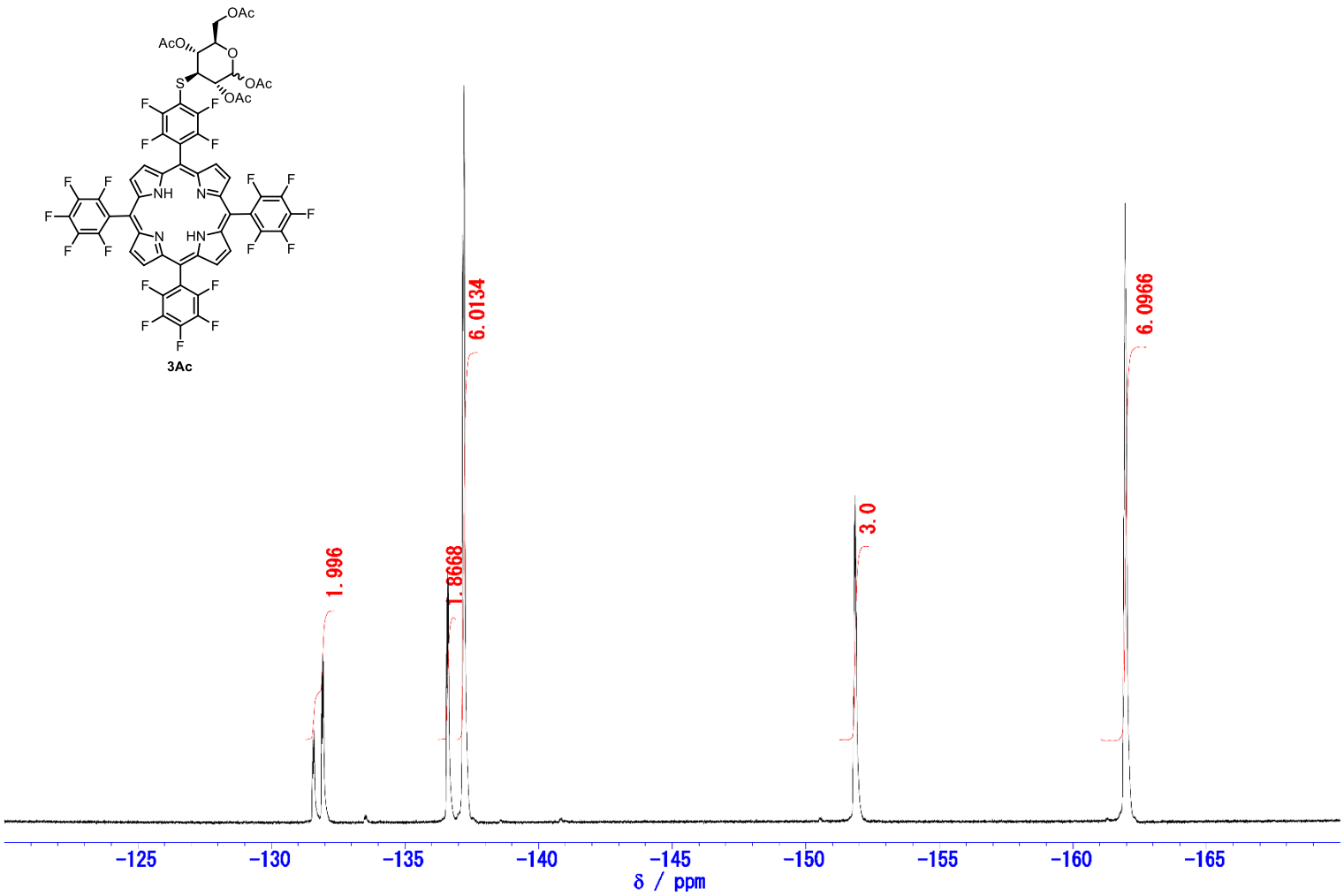

Figure ^{19}F NMR spectrum of **3Ac** in $CDCl_3$. (470.34 MHz)

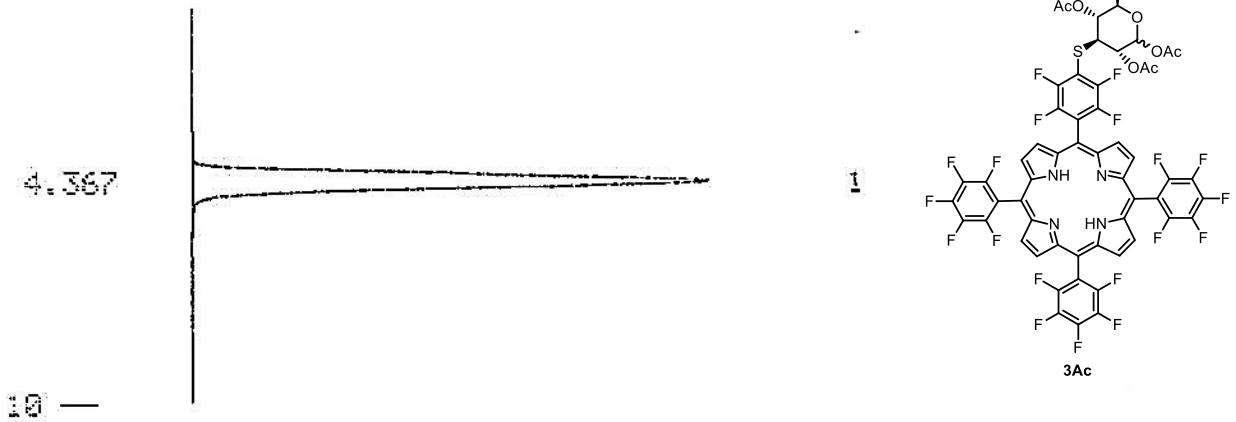

-- % CALCULATION RESULT --

WINDOW = 0 % SCALE FACTOR = 1.0000 PEAK AREA

PEAK#	RT(min)	AREA	HEIGHT	MK	AREA%
1	4.367	4892944	200945		100.0000
	TOTAL	4892944	200945		100.0000

Figure Chromatogram of **3Ac** on NP-HPLC. The conditions of **3Ac** was as follows: elution solvent, CH_2Cl_2/ AcOEt (9/1, v/v), column, 4.6 mm I.D.×150 mm; temperature, 30ºC; flow rate, 0.75 mL/ min; detector, 410 nm.

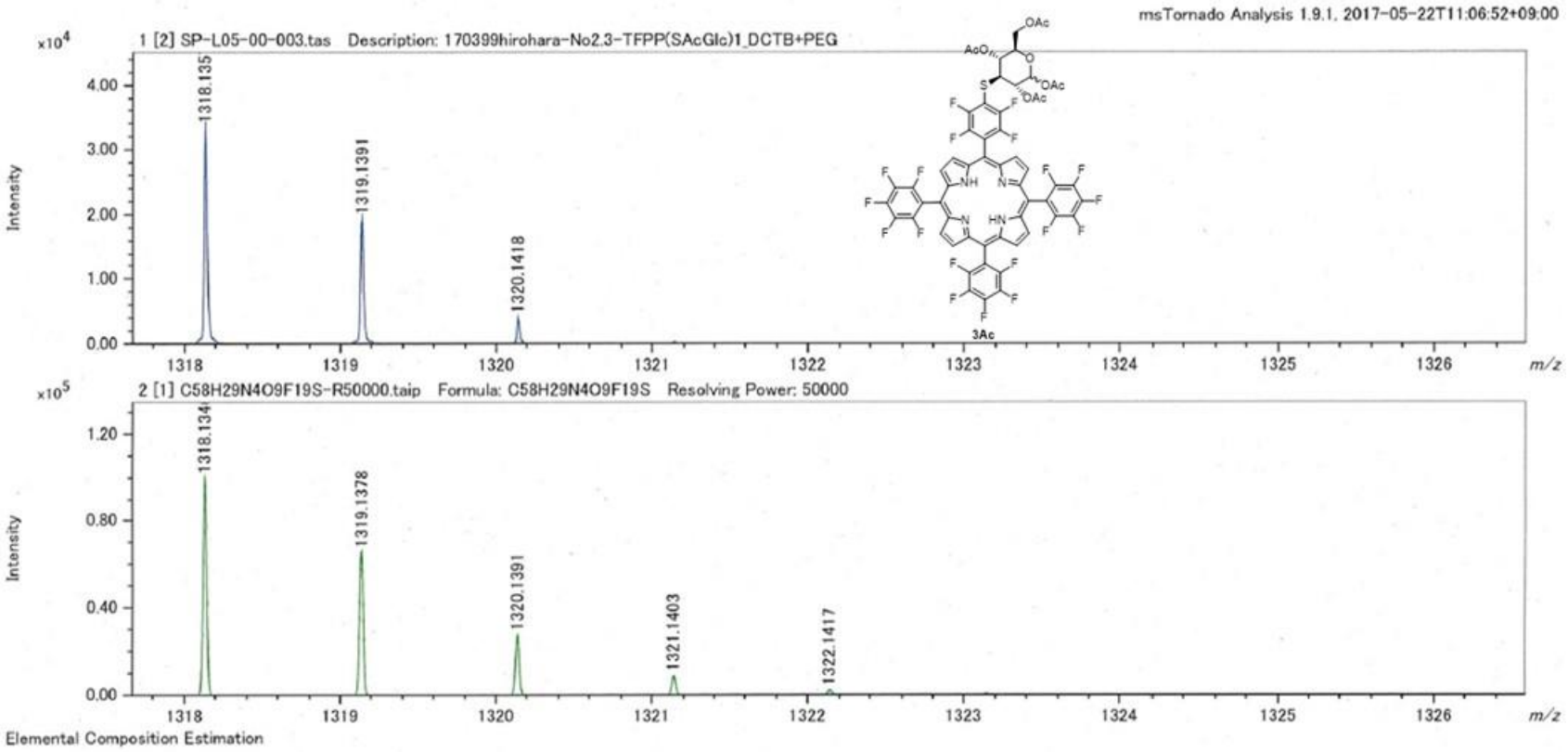

Elemental Composition Estimation

Parameters:

Mass	Tolerance	Electron Mode	Charge	DBE Range	Max Results
1318.13569 ± 0.00659	5.0 ppm	Odd/Even	+1	-0.5 – 200.0	100

Elements

C	H	N	O	F	S
0 – 60	0 – 30	0 – 4	0 – 9	0 – 19	0 – 1

Results:

#	Formula	Mass	DBE	Abs. Error (u)	Error (u)	Error (ppm)
1	C58 H29 N4 O9 F19 S	1318.13464	37.0	0.00105	0.00105	0.80

Figure Mass spectrum of **3Ac**. (HRMS)

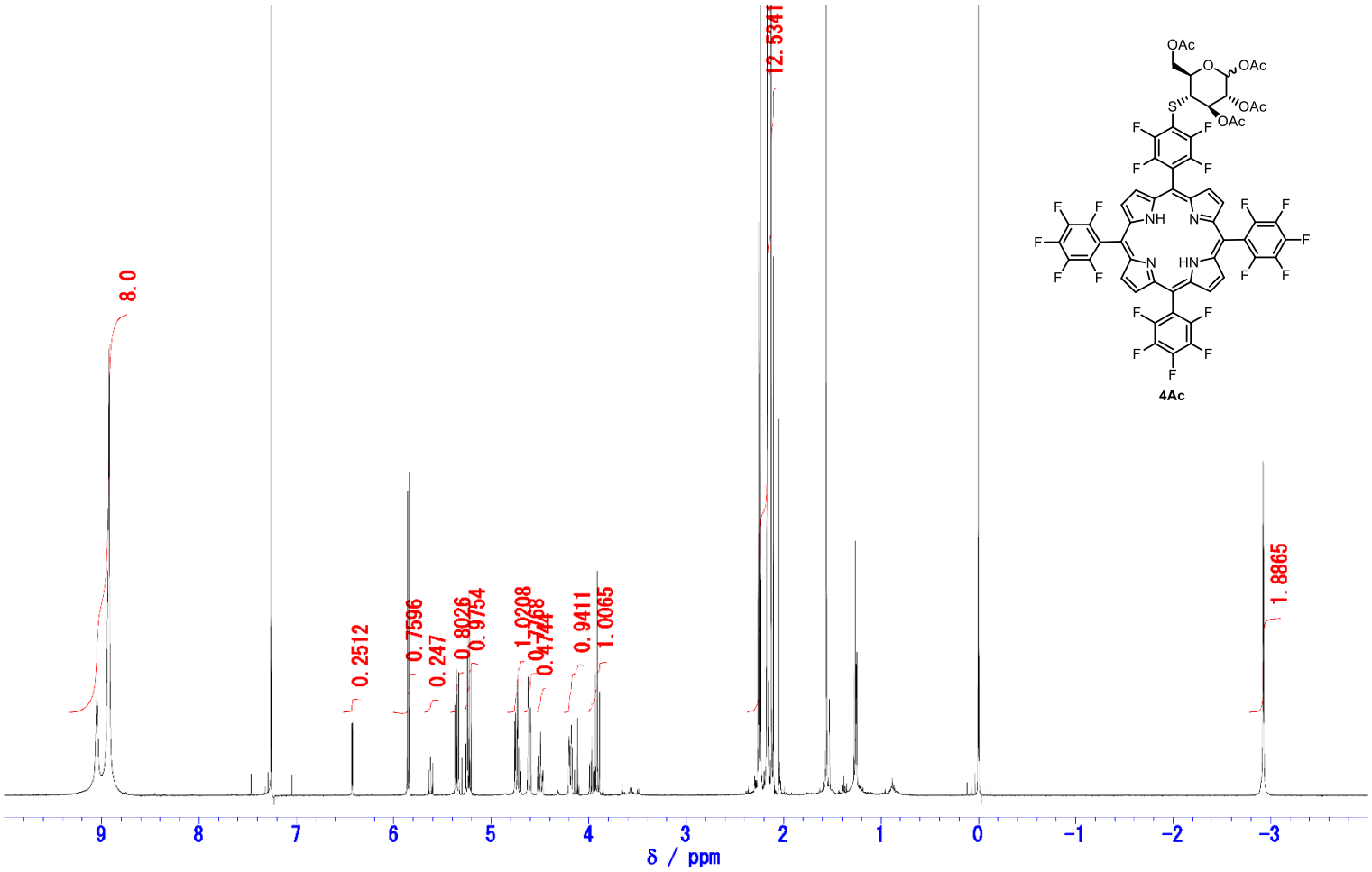

Figure ^{1}H NMR spectrum of **4Ac** in $CDCl_3$. (499.91 MHz)

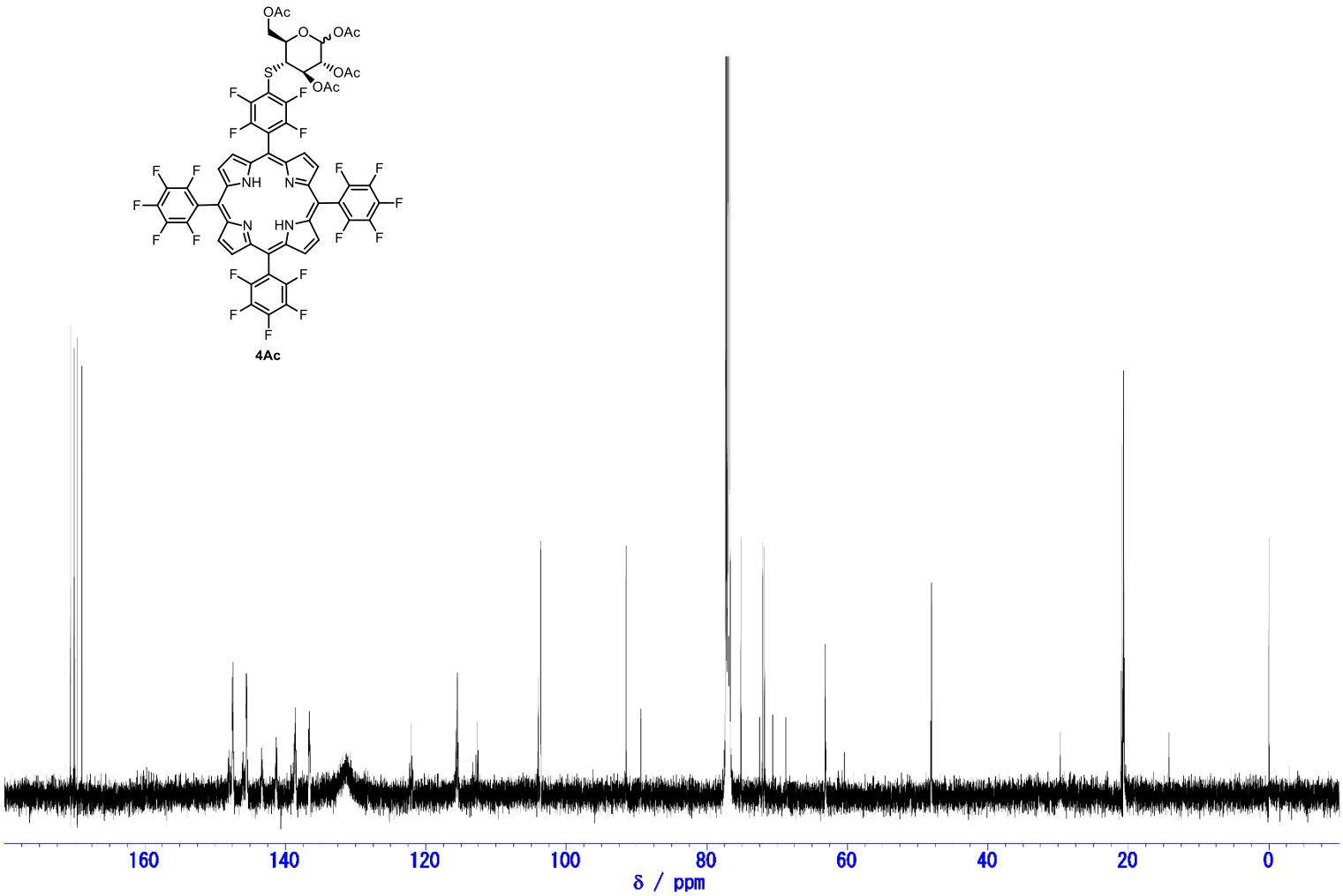

Figure ^{13}C NMR spectrum of **4Ac** in $CDCl_3$. (125.72 MHz)

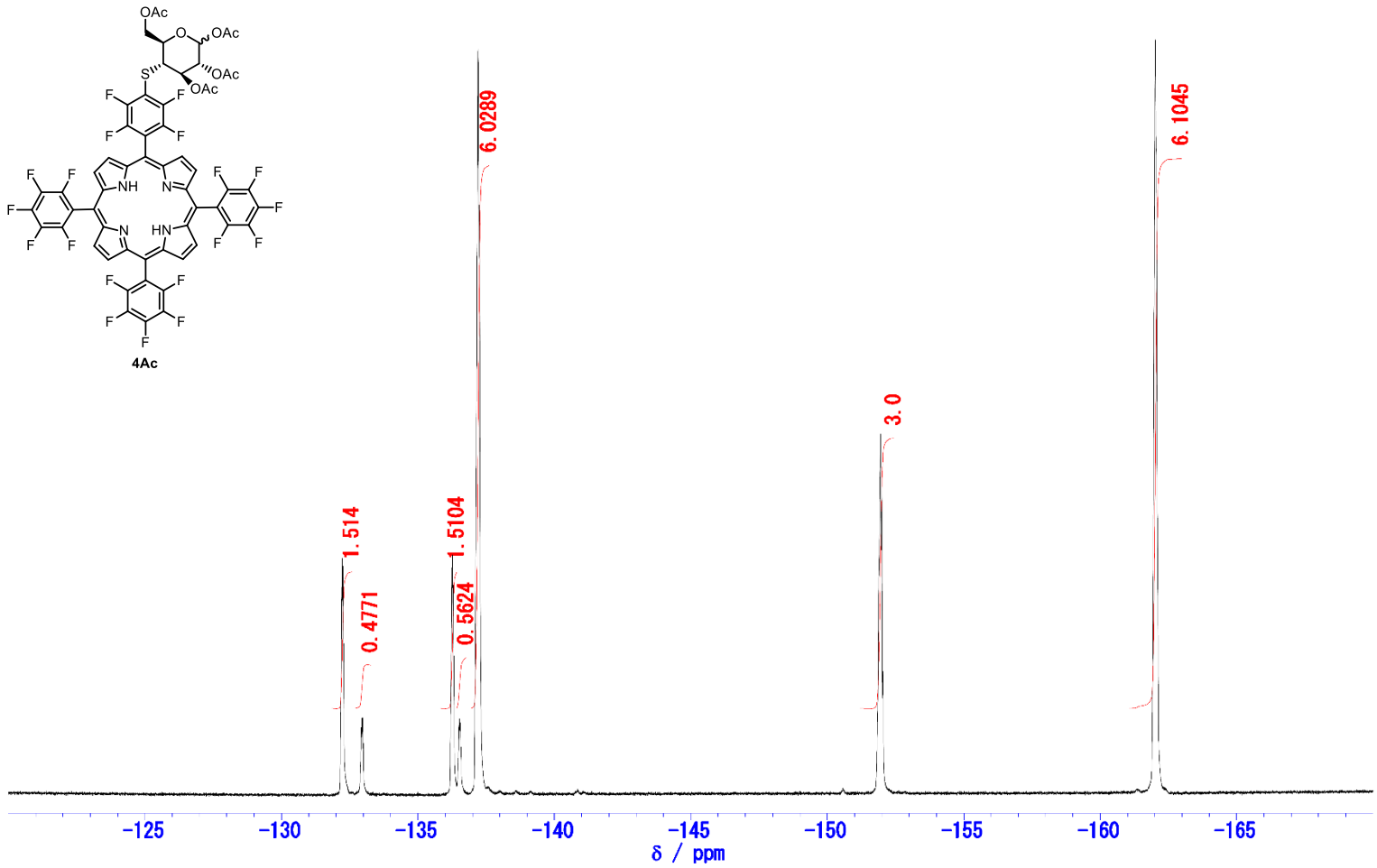

Figure ^{19}F NMR spectrum of **4Ac** in $CDCl_3$. (470.34 MHz)

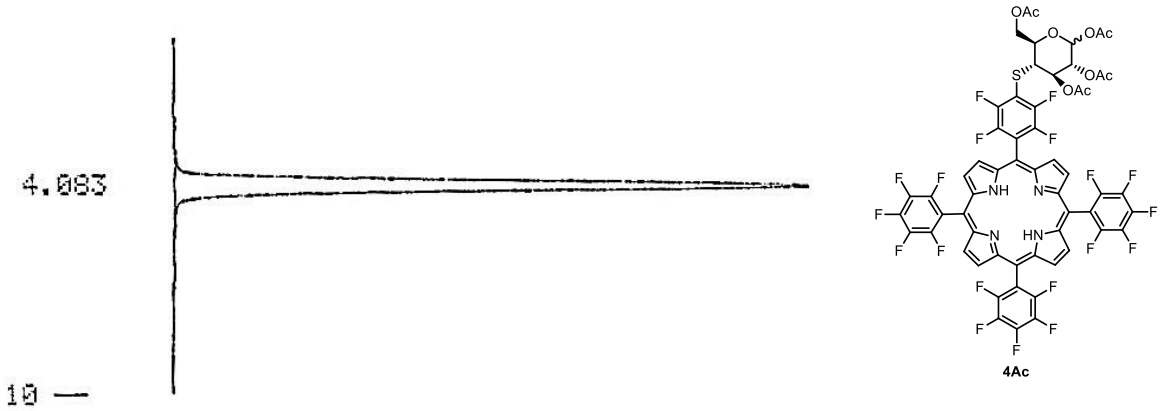

-- % CALCULATION RESULT --

WINDOW = 0 % SCALE FACTOR = 1.0000 PEAK AREA

PEAK#	RT(min)	AREA	HEIGHT	MK	AREA%
1	4.083	2695084	136683		100.0000
	TOTAL	2695084	136683		100.0000

Figure Chromatogram of **4Ac** on NP-HPLC. The conditions of **4Ac** was as follows: elution solvent, CH_2Cl_2/ AcOEt (9/1, v/v), column, 4.6 mm I.D.×150 mm; temperature, 30ºC; flow rate, 0.75 mL/ min; detector, 410 nm.

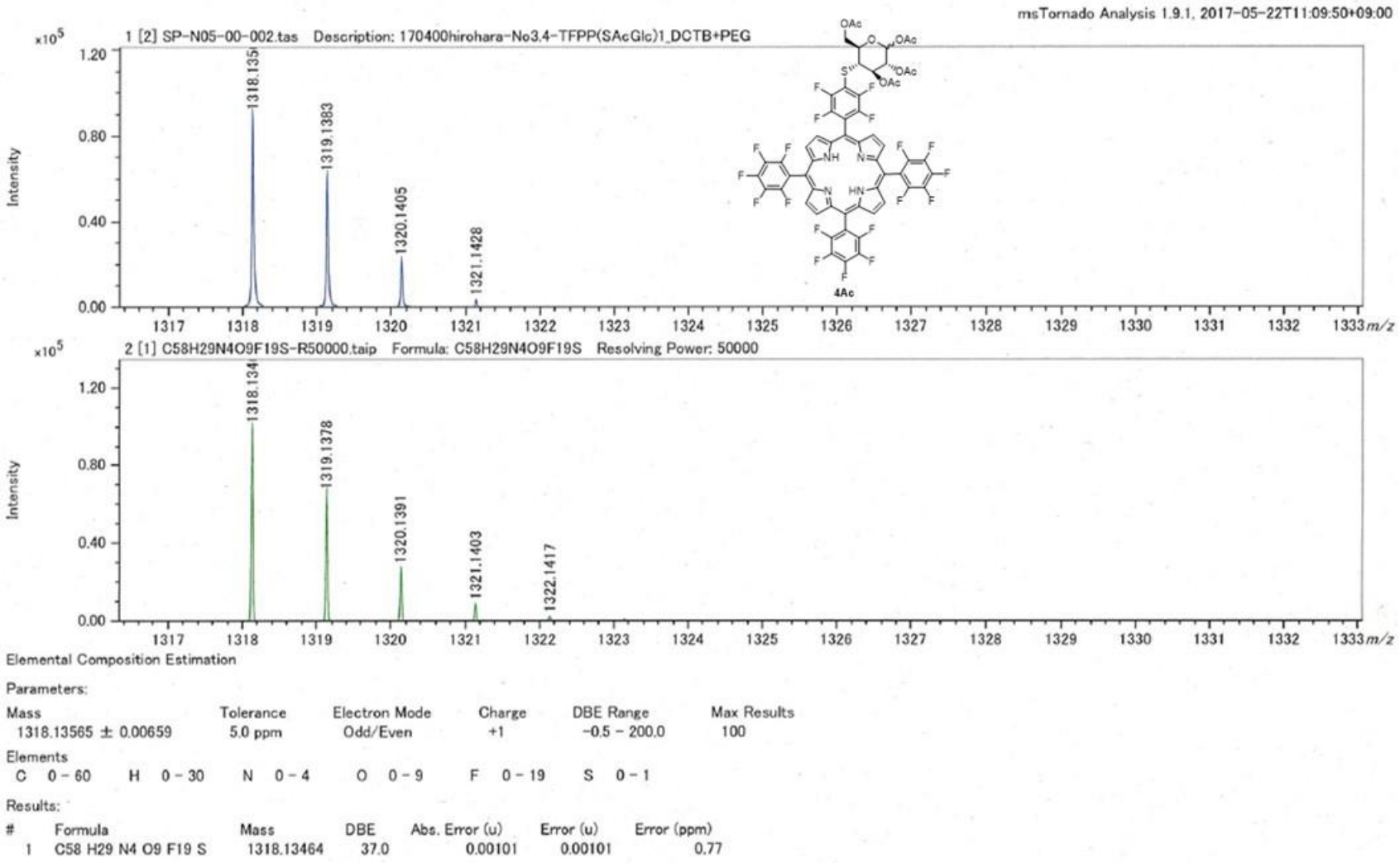

Elemental Composition Estimation

Parameters:

Mass	Tolerance	Electron Mode	Charge	DBE Range	Max Results
1318.13565 ± 0.00659	5.0 ppm	Odd/Even	+1	-0.5 - 200.0	100

Elements

C	H	N	O	F	S
0 - 60	0 - 30	0 - 4	0 - 9	0 - 19	0 - 1

Results:

#	Formula	Mass	DBE	Abs. Error (u)	Error (u)	Error (ppm)
1	C58 H29 N4 O9 F19 S	1318.13464	37.0	0.00101	0.00101	0.77

Figure Mass spectrum of **4Ac**. (HRMS)

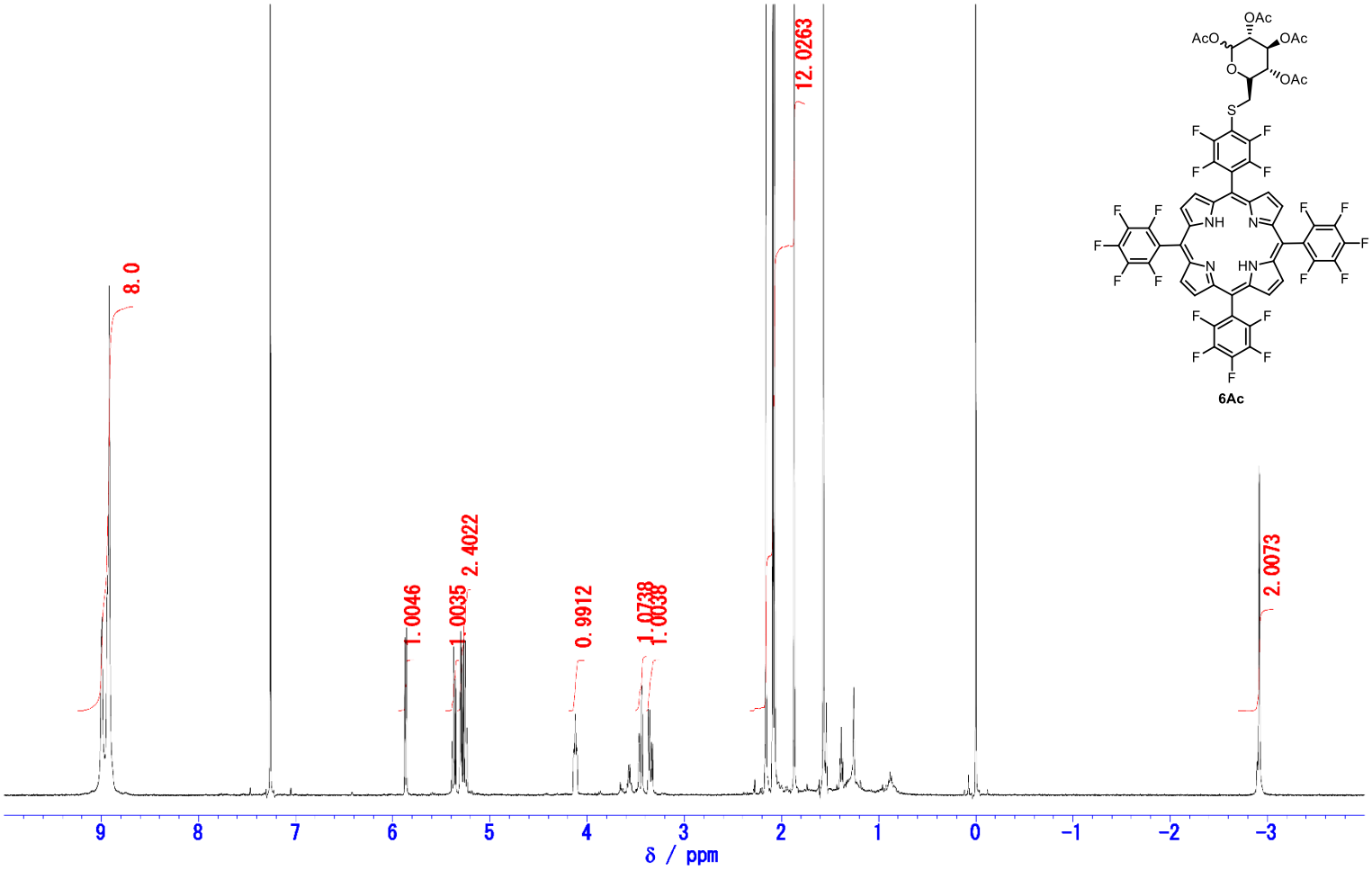

Figure ^{1}H NMR spectrum of **6Ac** in $CDCl_3$. (499.91 MHz)

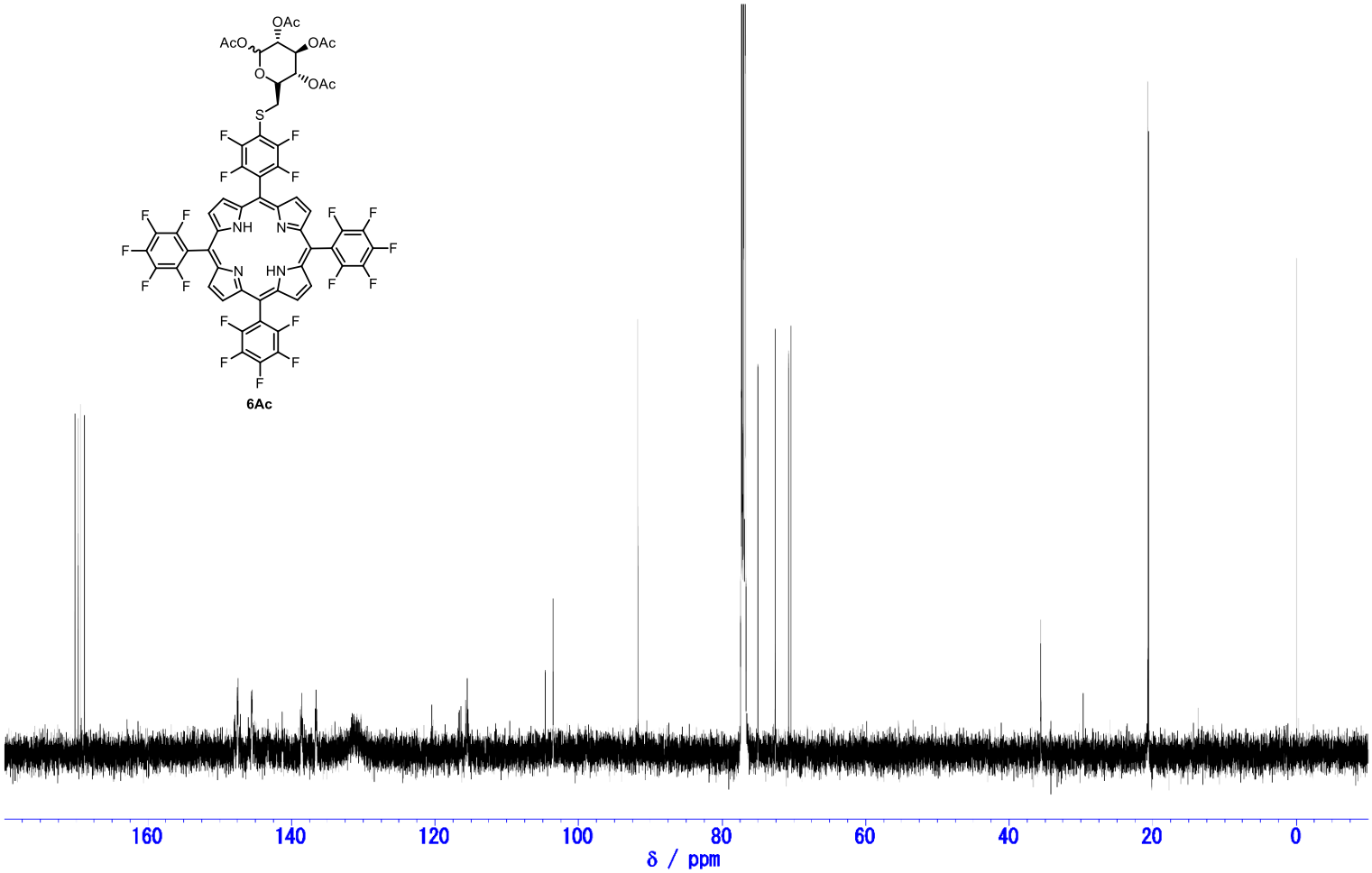

Figure ^{13}C NMR spectrum of **6Ac** in $CDCl_3$. (125.72 MHz)

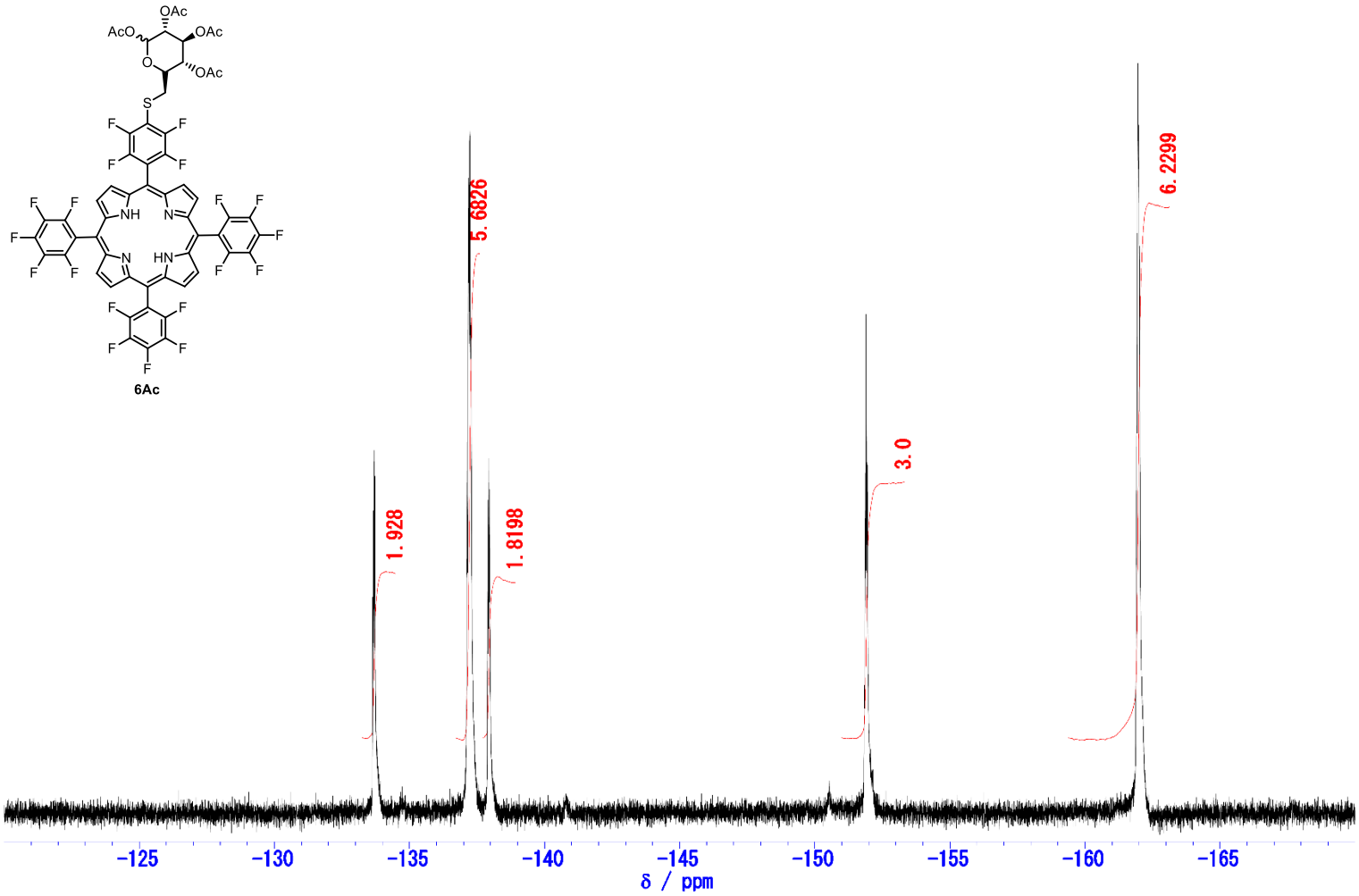

Figure ^{19}F NMR spectrum of **6Ac** in $CDCl_3$. (470.34 MHz)

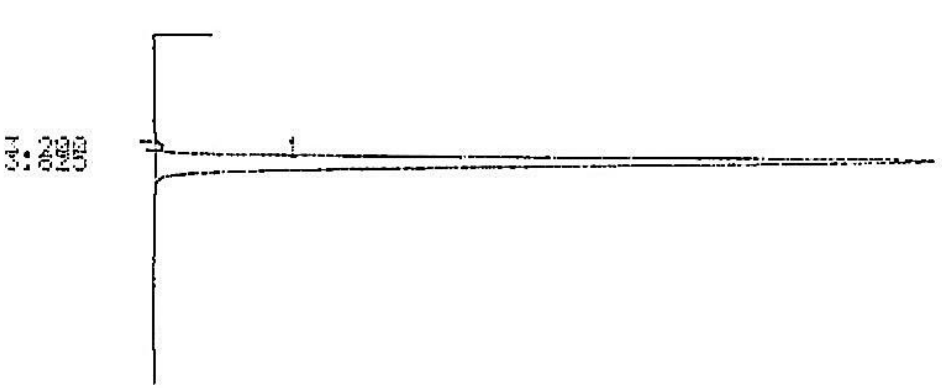

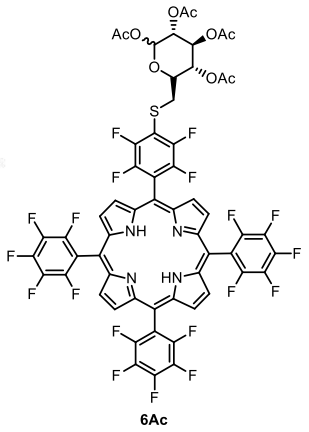

-- % CALCULATION RESULT --

WINDOW = 0 % SCALE FACTOR = 1.0000 PEAK AREA

PEAK#	RT(min)	AREA	HEIGHT	MK	AREA%
1	3.200	3981	407	L	0.2628
2	3.625	1510885	85187	LLL	99.7372
	TOTAL	1514865	85594		100.0000

Figure Chromatogram of **6Ac** on NP-HPLC. The conditions of **6Ac** was as follows: elution solvent, CH_2Cl_2/ AcOEt (9/1, v/v), column, 4.6 mm I.D.×150 mm; temperature, 30°C; flow rate, 0.75 mL/ min; detector, 410 nm.

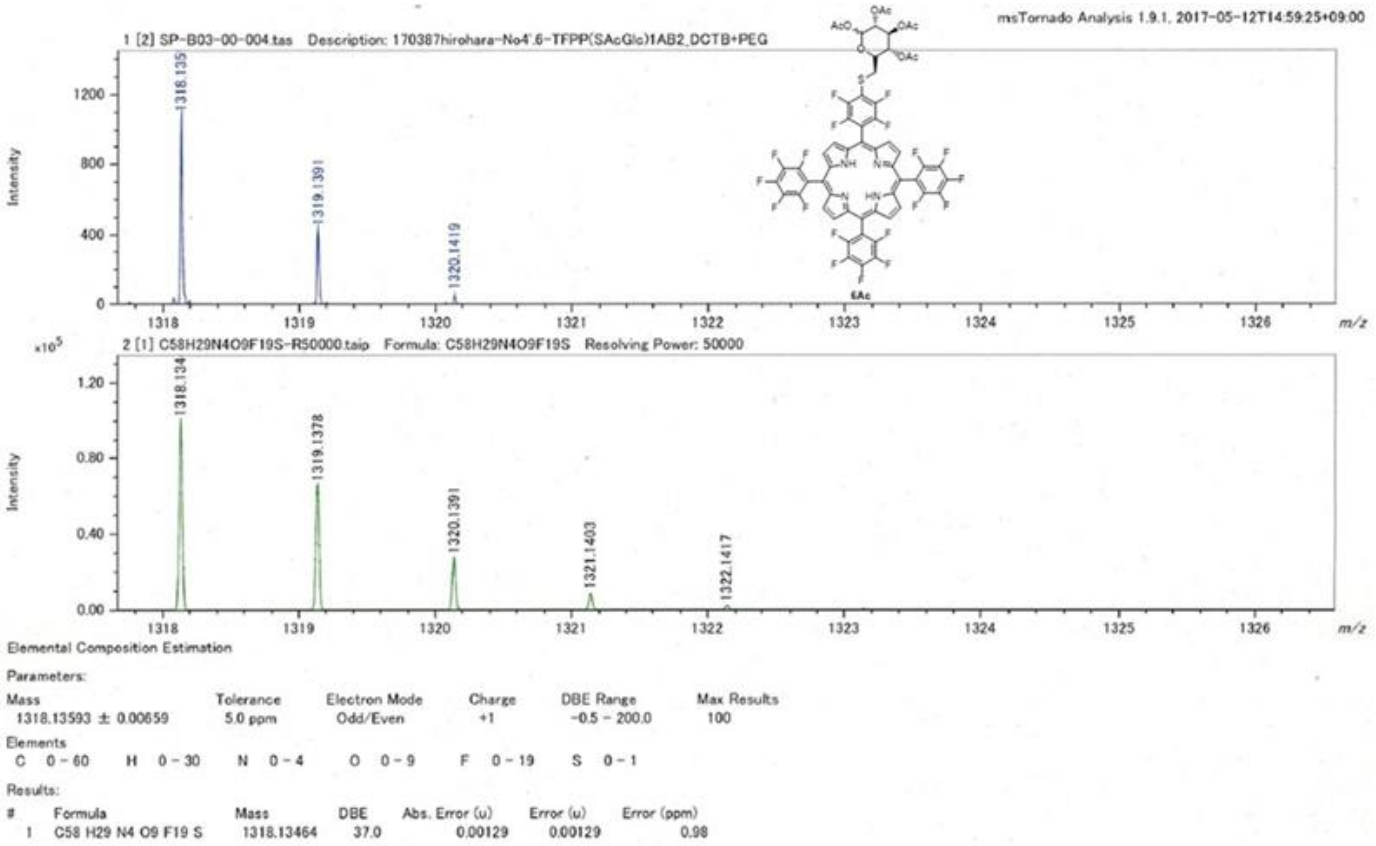

Figure Mass spectrum of **6Ac**. (HRMS)

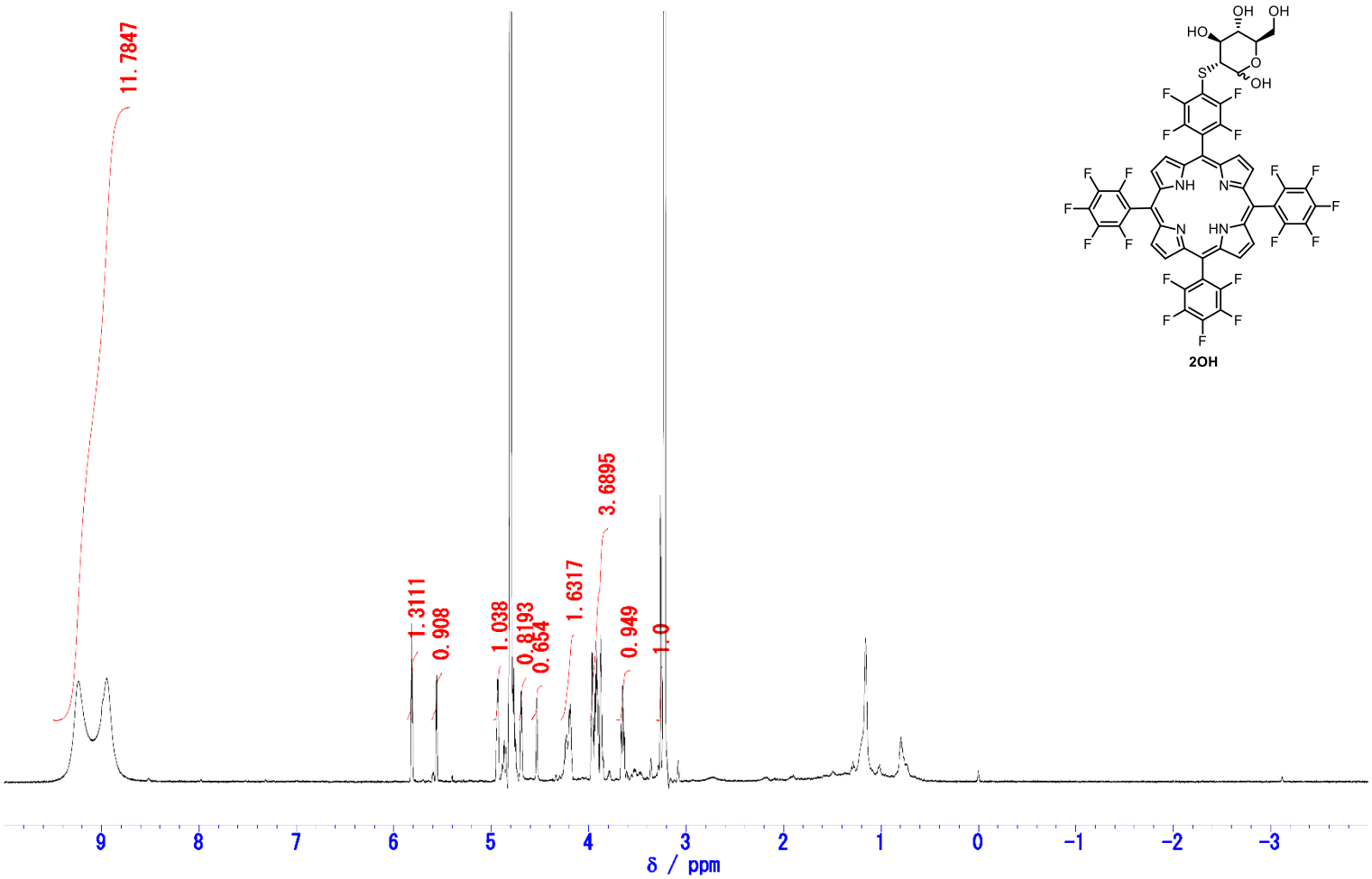

Figure ^{1}H NMR spectrum of **2OH** in CD_3OD. (499.91 MHz)

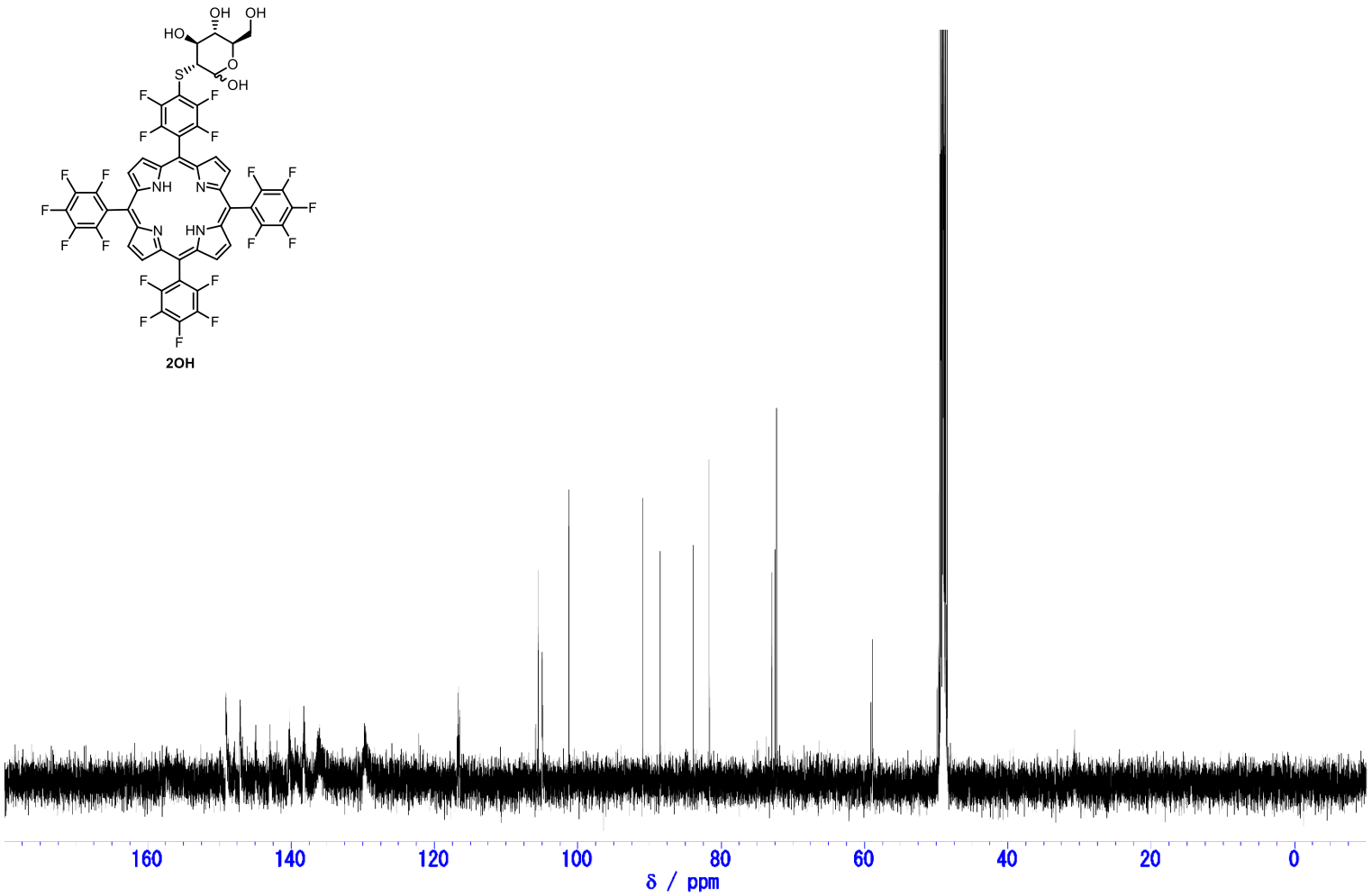

Figure ^{13}C NMR spectrum of **2OH** in CD_3OD. (125.72 MHz)

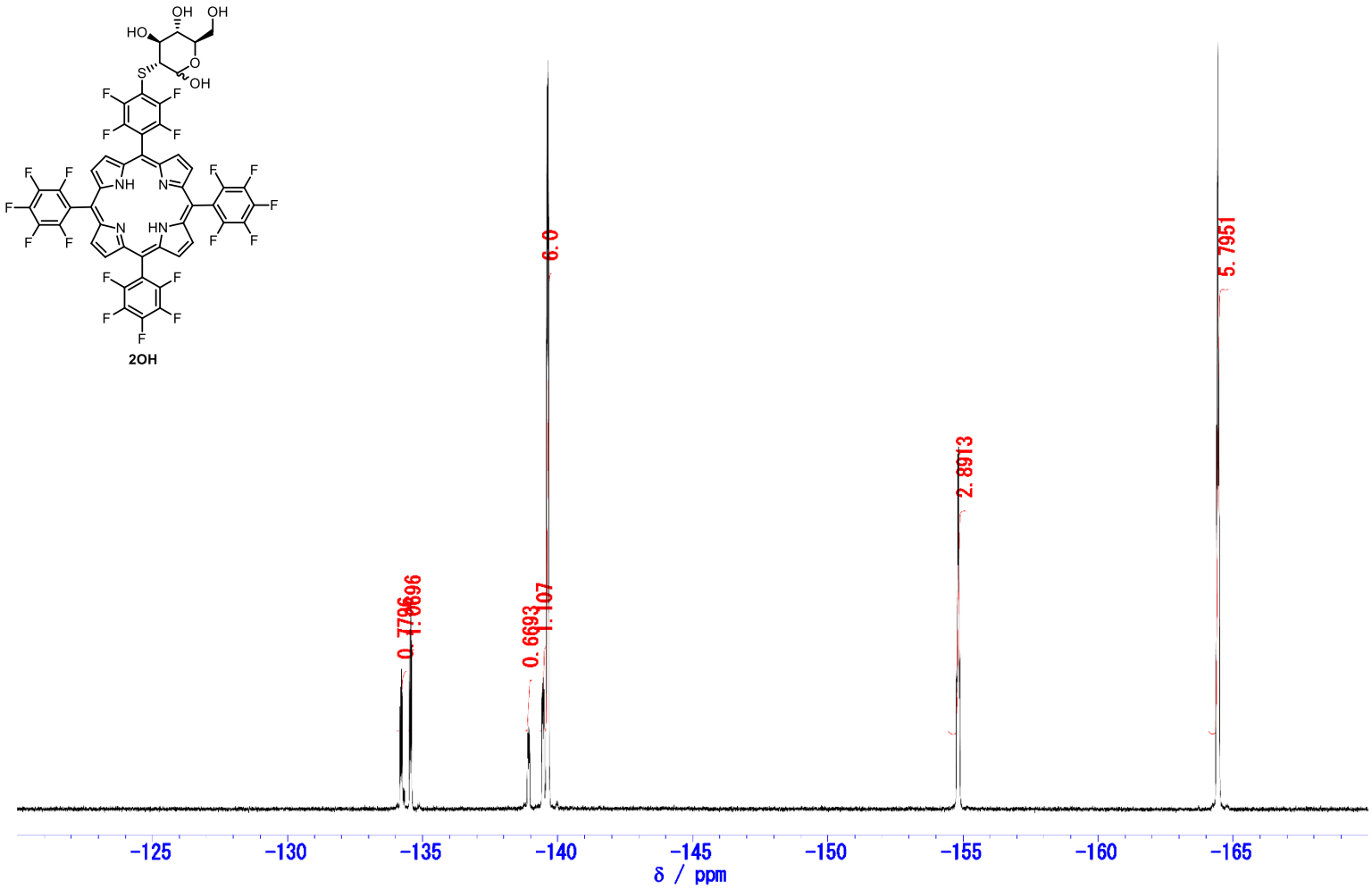

Figure ^{19}F NMR spectrum of **2OH** in CD_3OD. (470.34 MHz)

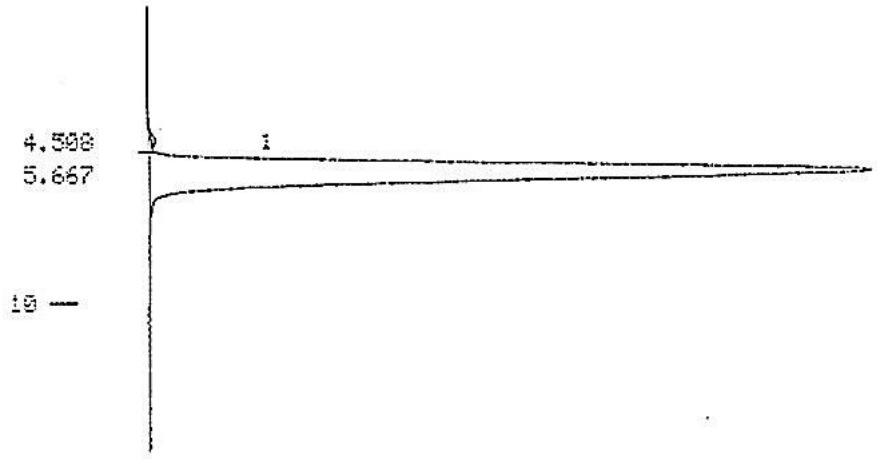

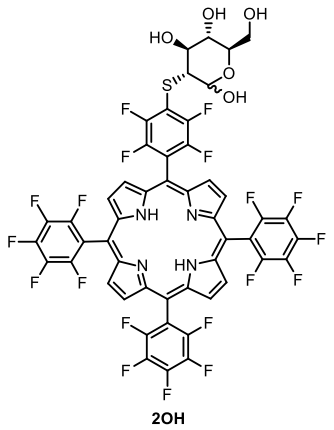

-- % CALCULATION RESULT --

WINDOW = 0 % SCALE FACTOR = 1.0000 PEAK AREA

PEAK#	RT(min)	AREA	HEIGHT	MK	AREA%
1	4.508	14831	674	L	0.4063
2	5.667	3635220	93635	LLL	99.5937
	TOTAL	3650051	94309		100.0000

Figure Chromatogram of **2OH** on NP-HPLC. The conditions of **2OH** was as follows: elution solvent, CH_2Cl_2/ MeOH (9/1, v/v), column, 4.6 mm I.D.×150 mm; temperature, 30ºC; flow rate, 0.5 mL/ min; detector, 410 nm.

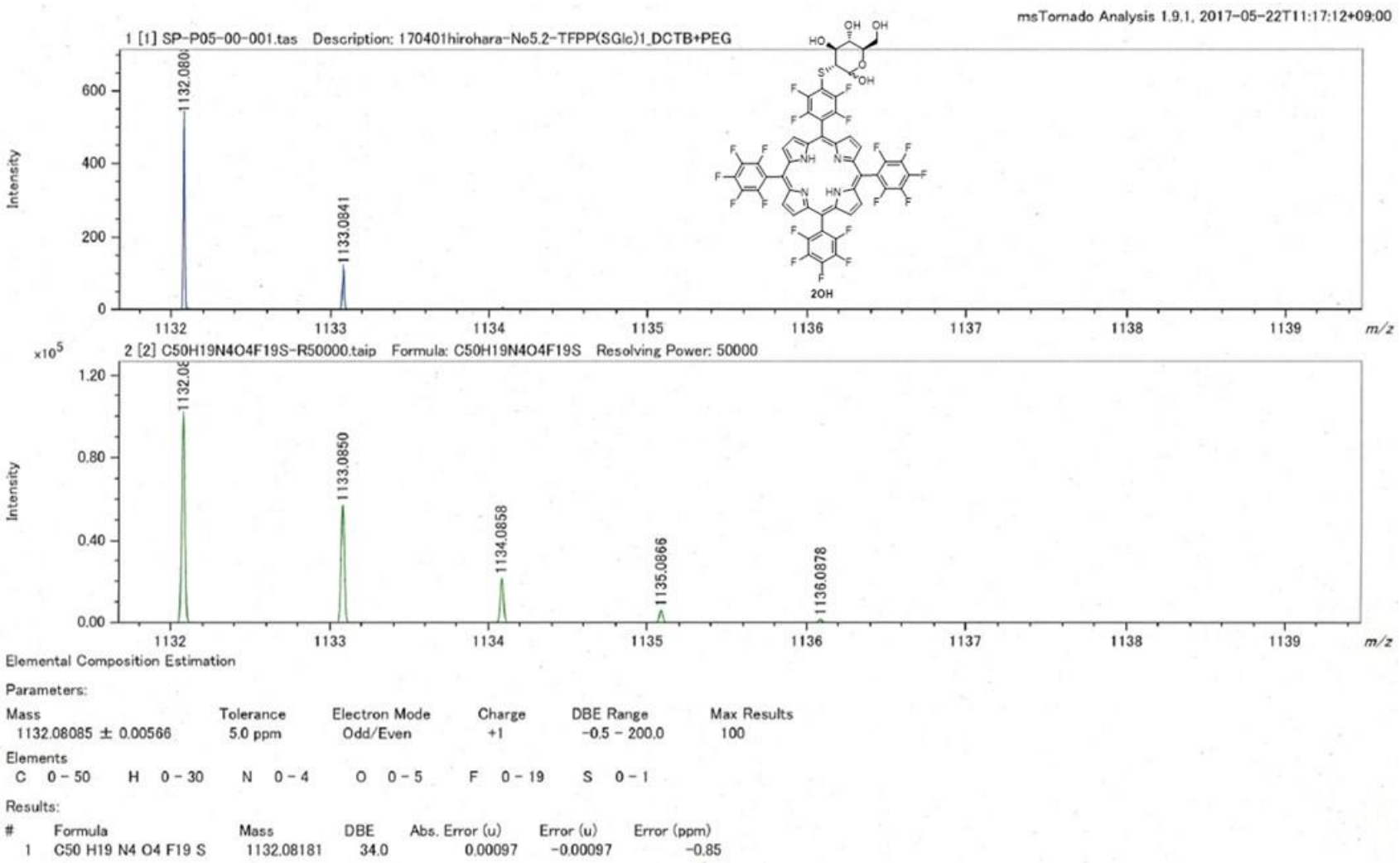

Figure Mass spectrum of **2OH**. (HRMS)

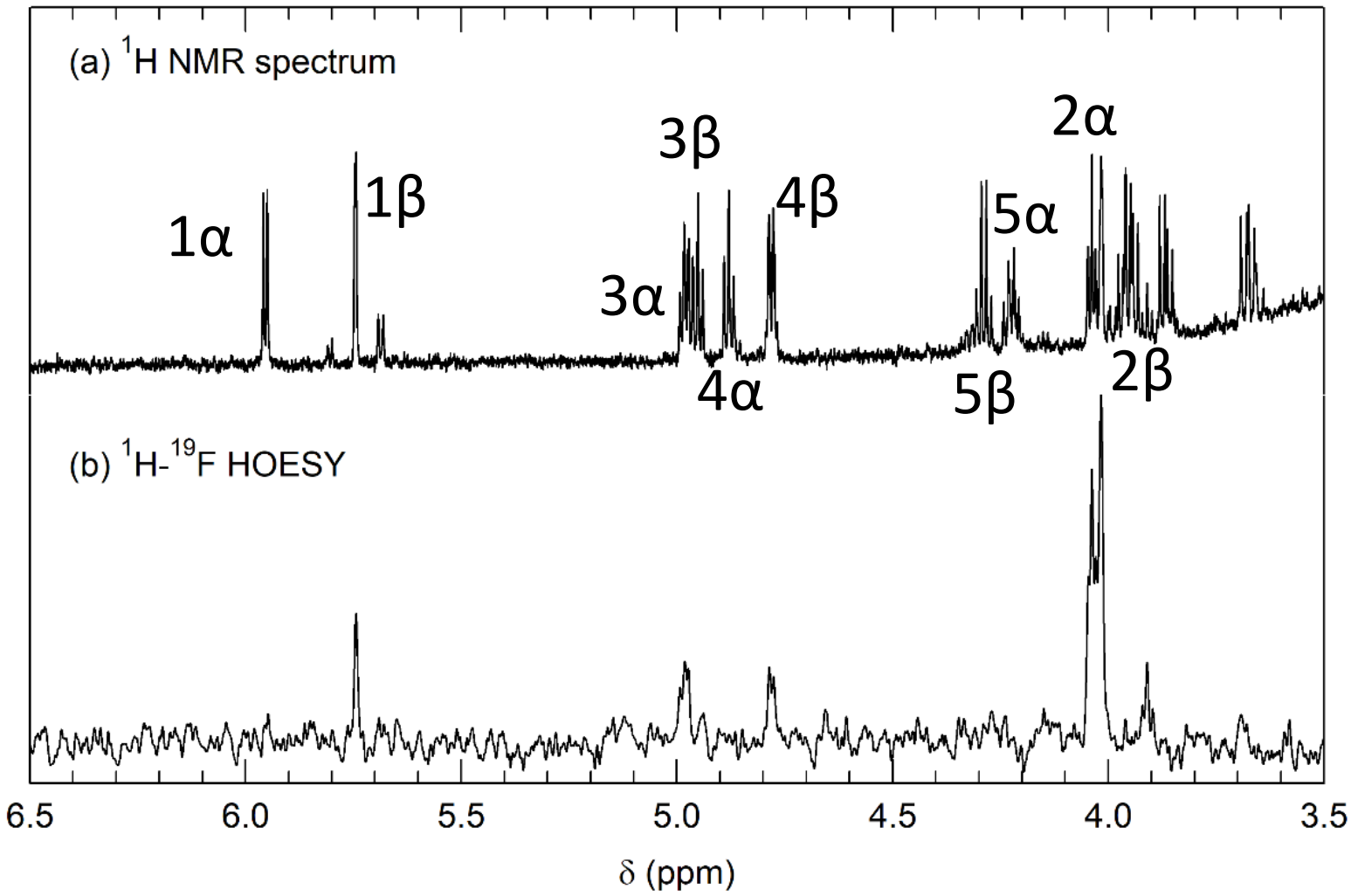

Figure ^{1}H NMR and ^{1}H-^{19}F HOESY spectra of **2OH** in acetone-d_6.

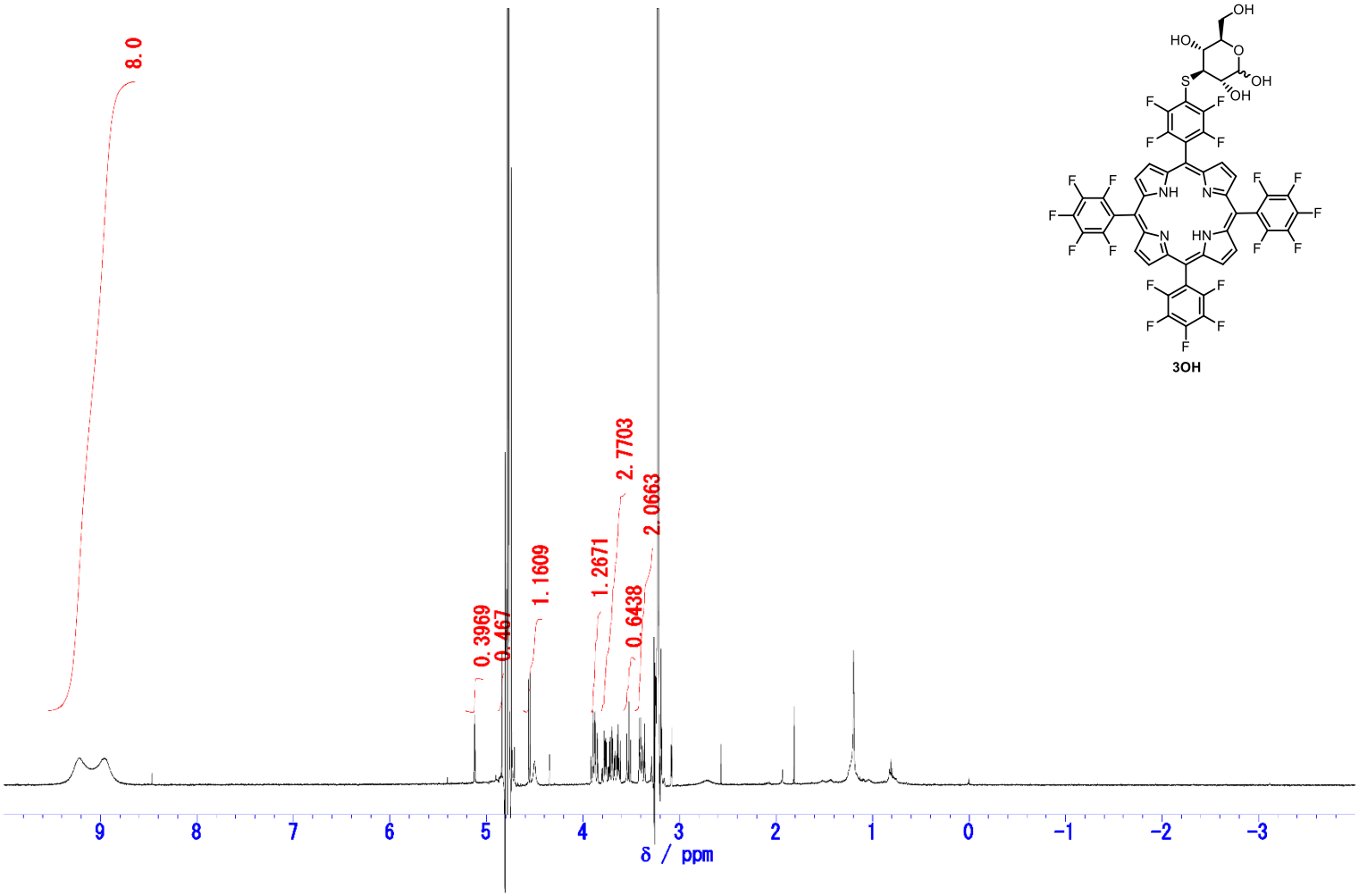

Figure ^{1}H NMR spectrum of **3OH** in CD_3OD. (499.91 MHz)

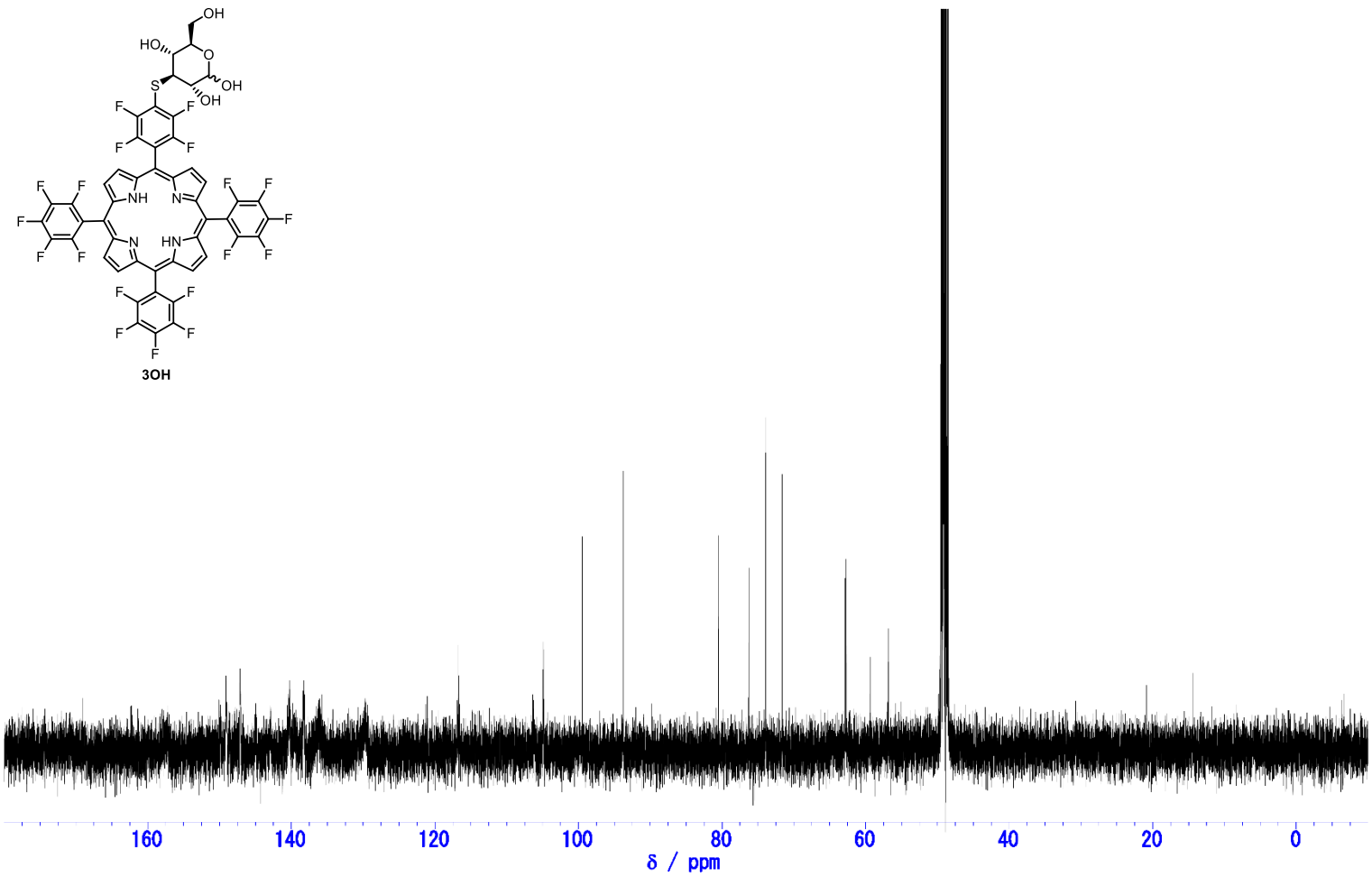

Figure ^{13}C NMR spectrum of **3OH** in CD_3OD. (125.72 MHz)

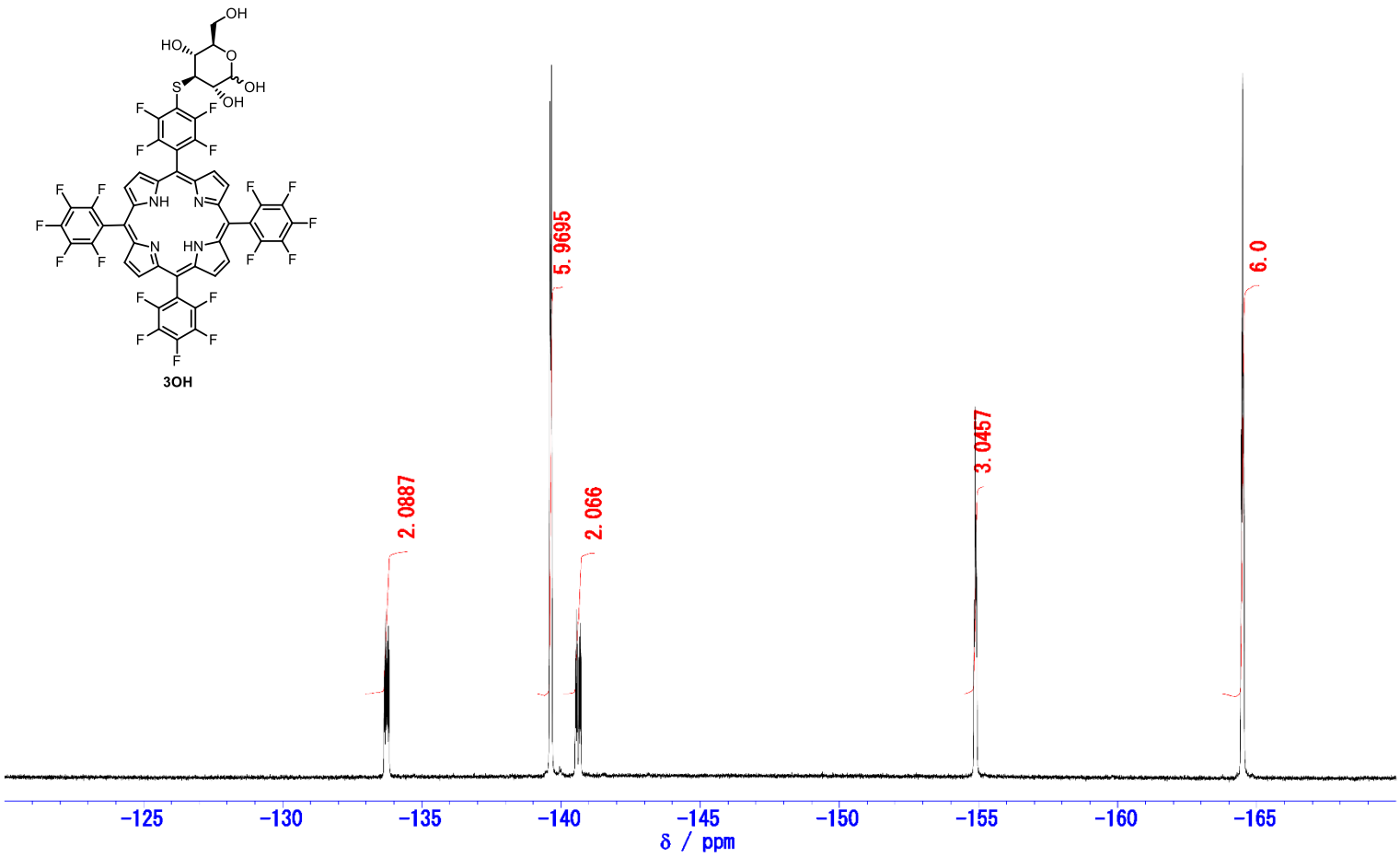

Figure ^{19}F NMR spectrum of **3OH** in CD_3OD. (470.34 MHz)

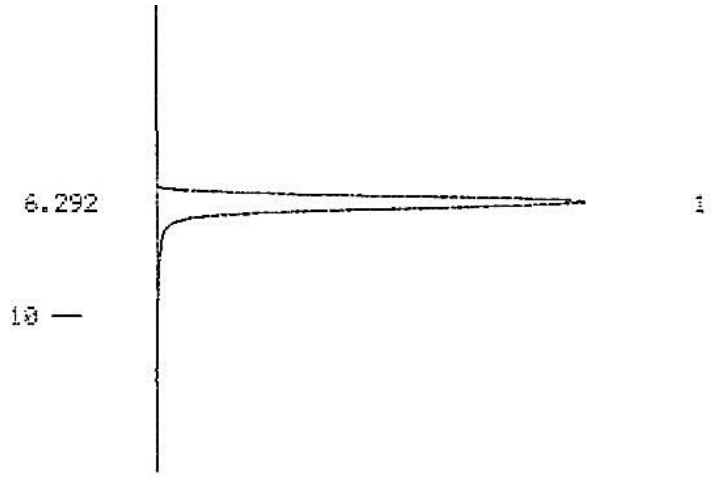

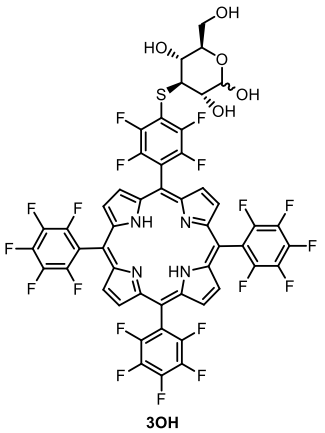

-- % CALCULATION RESULT --

WINDOW = 0 % SCALE FACTOR = 1.0000 PEAK AREA

PEAK#	RT(min)	AREA	HEIGHT	MK	AREA%
1	6.292	1591287	52986		100.0000
	TOTAL	1591287	52986		100.0000

Figure Chromatogram of **3OH** on NP-HPLC. The conditions of **3OH** was as follows: elution solvent, CH_2Cl_2/ MeOH (9/1, v/v), column, 4.6 mm I.D.×150 mm; temperature, 30ºC; flow rate, 0.5 mL/ min; detector, 410 nm.

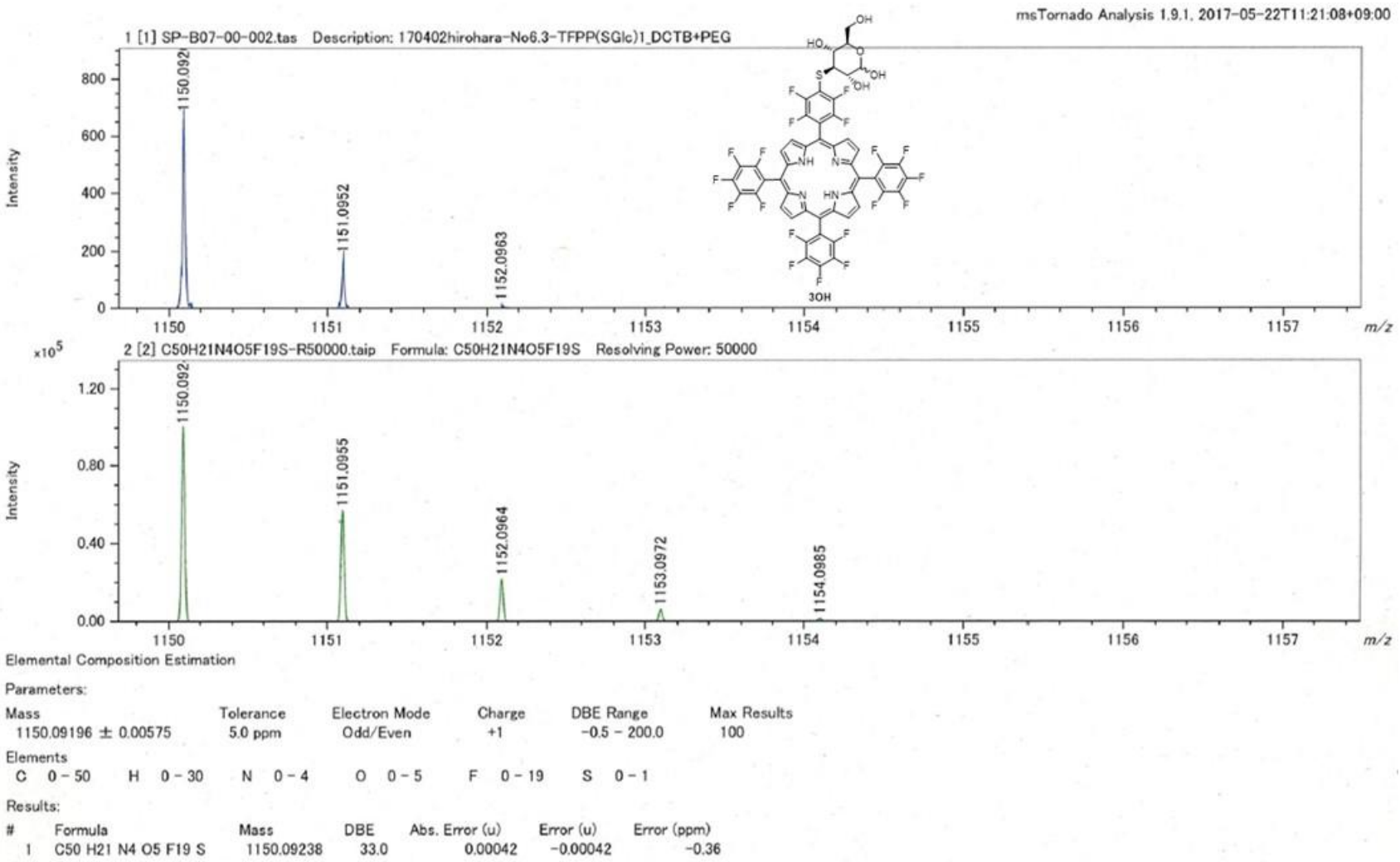

Figure Mass spectrum of **3OH**. (HRMS)

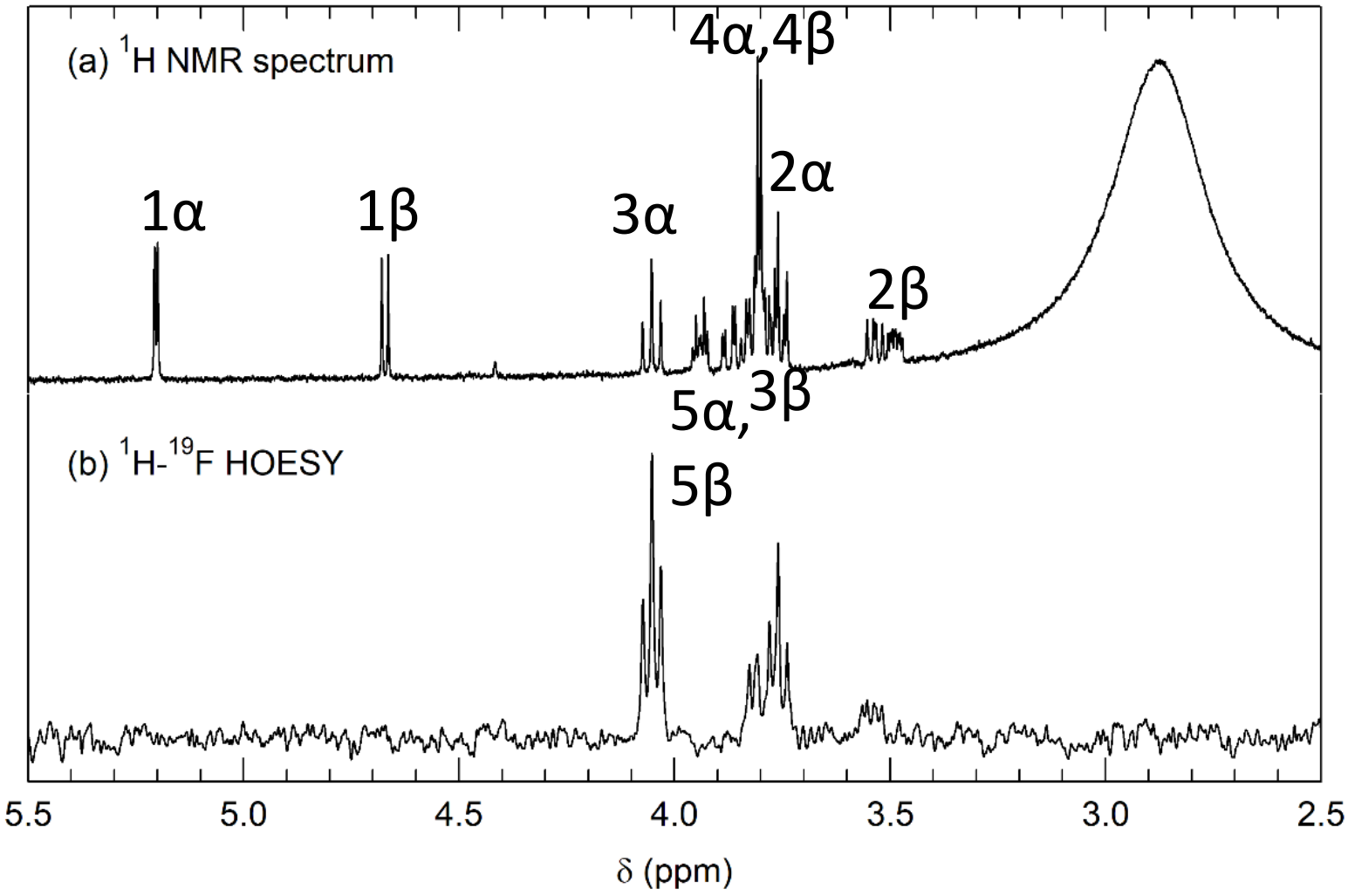

Figure ^{1}H NMR and ^{1}H-^{19}F HOESY spectra of **3OH** in acetone-d_6.

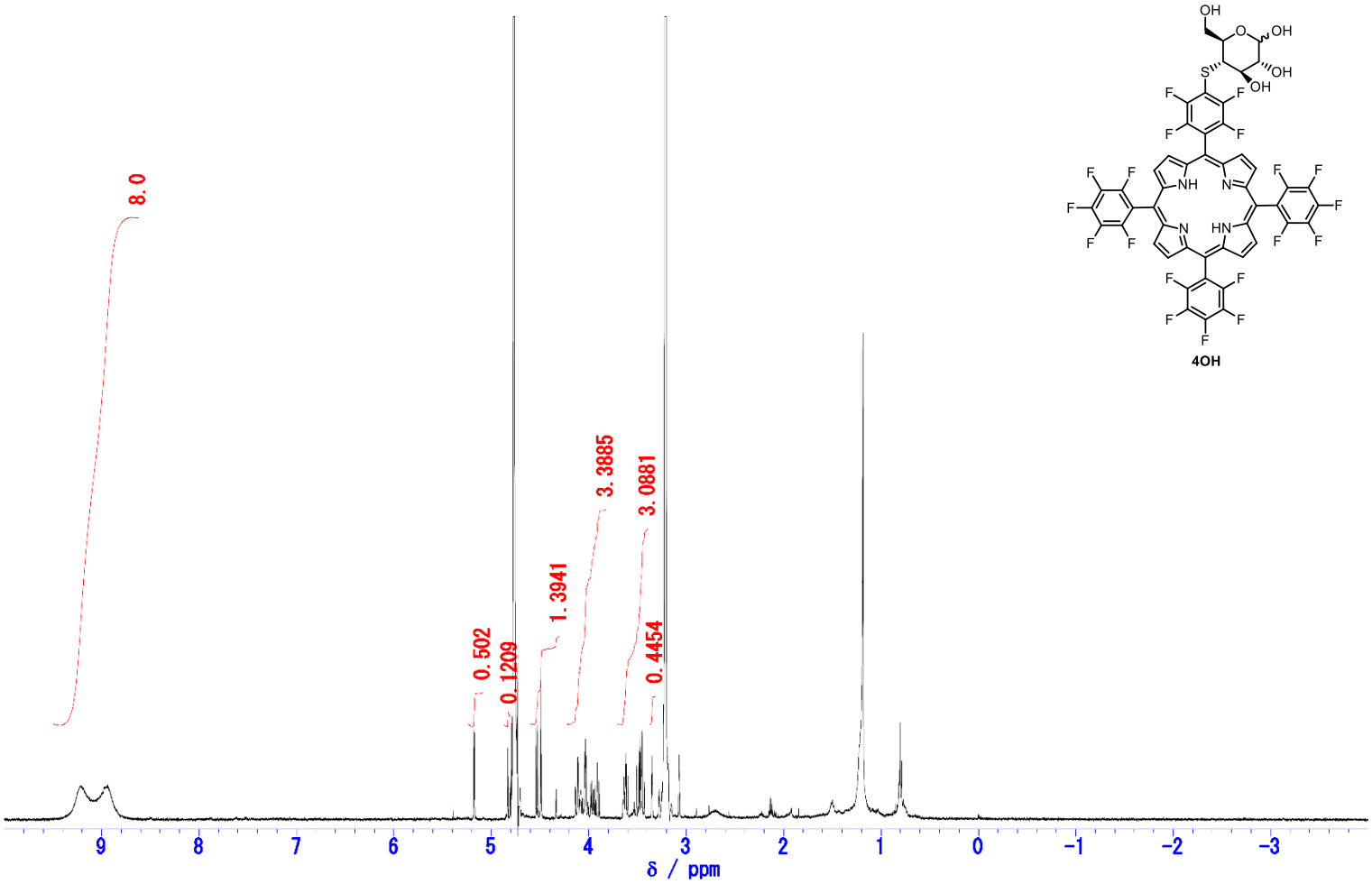

Figure ^{1}H NMR spectrum of **4OH** in CD_3OD. (499.91 MHz)

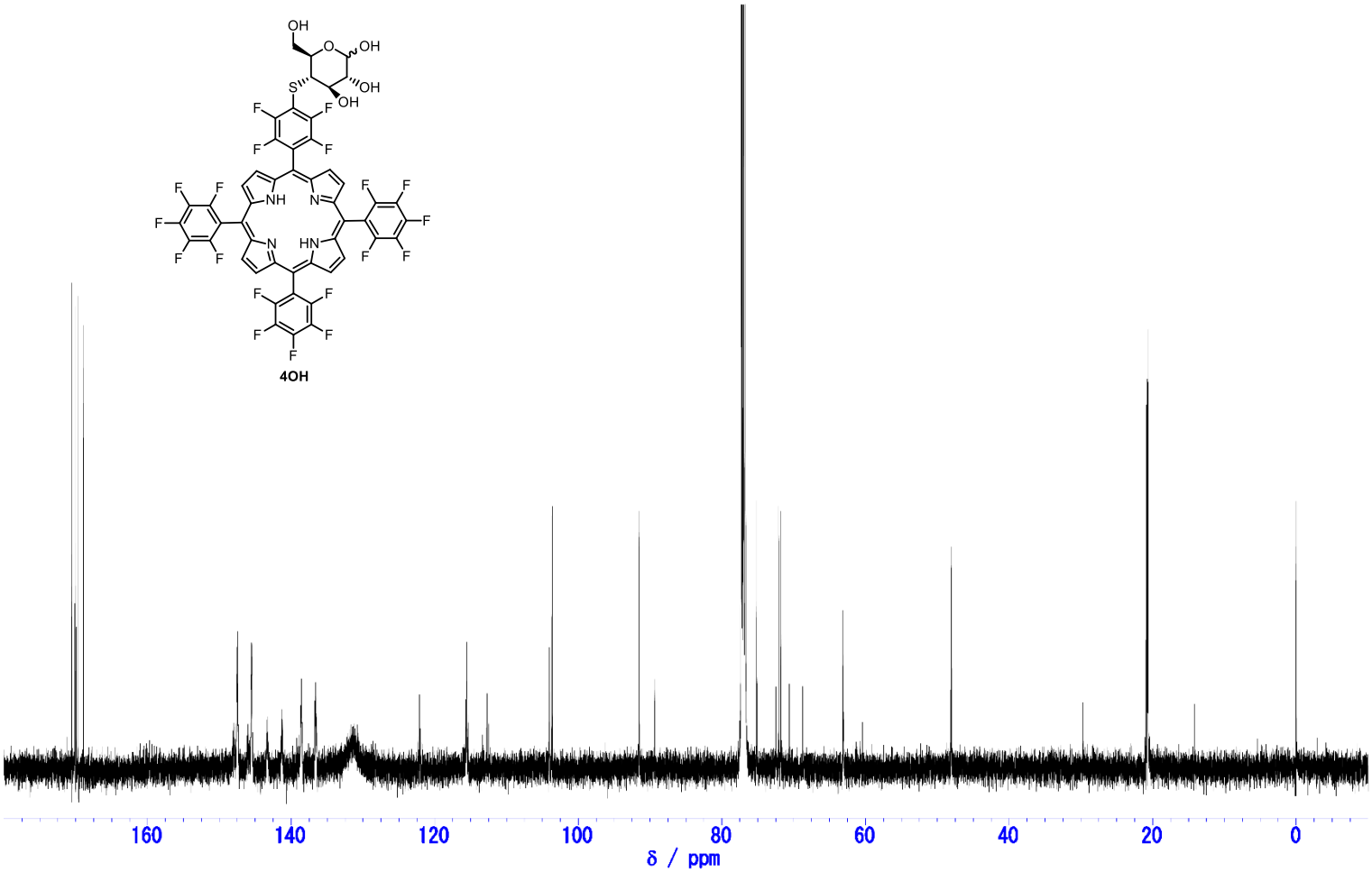

Figure ^{13}C NMR spectrum of **4OH** in CD_3OD. (125.72 MHz)

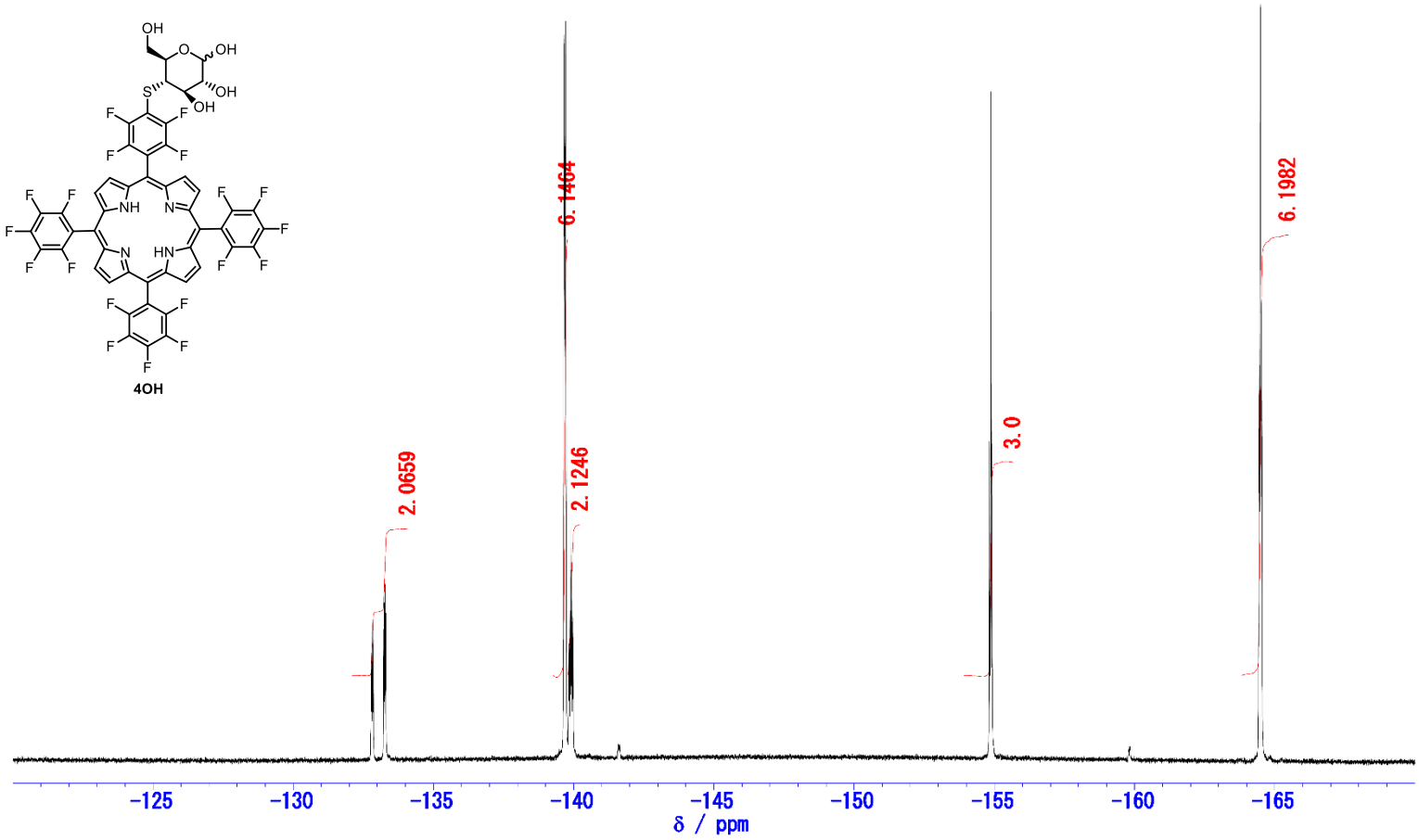

Figure ^{19}F NMR spectrum of **4OH** in CD_3OD. (470.34 MHz)

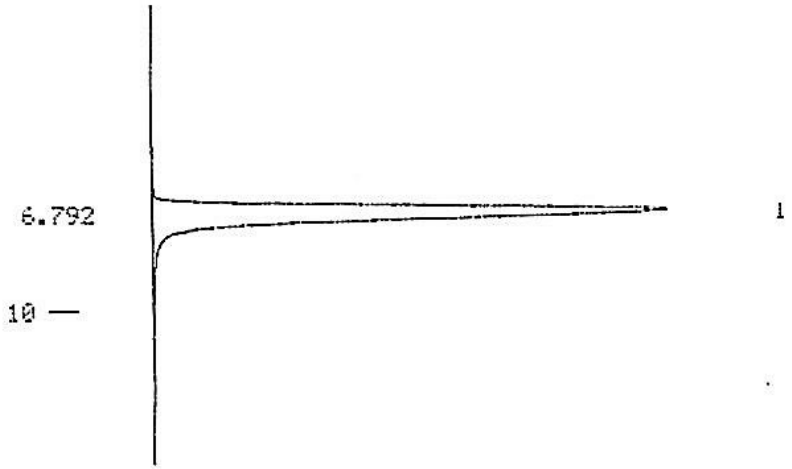

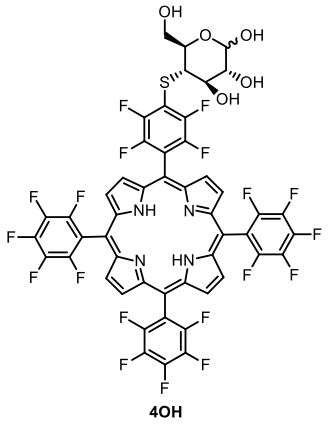

-- % CALCULATION RESULT --

WINDOW = 0 % SCALE FACTOR = 1.0000 PEAK AREA

PEAK#	RT(min)	AREA	HEIGHT	MK	AREA%
1	6.792	8028796	256890		100.0000
	TOTAL	8028796	256890		100.0000

Figure Chromatogram of **4OH** on NP-HPLC. The conditions of **4OH** was as follows: elution solvent, CH_2Cl_2/ MeOH (9/1, v/v), column, 4.6 mm I.D.×150 mm; temperature, 30°C; flow rate, 0.5 mL/ min; detector, 410 nm.

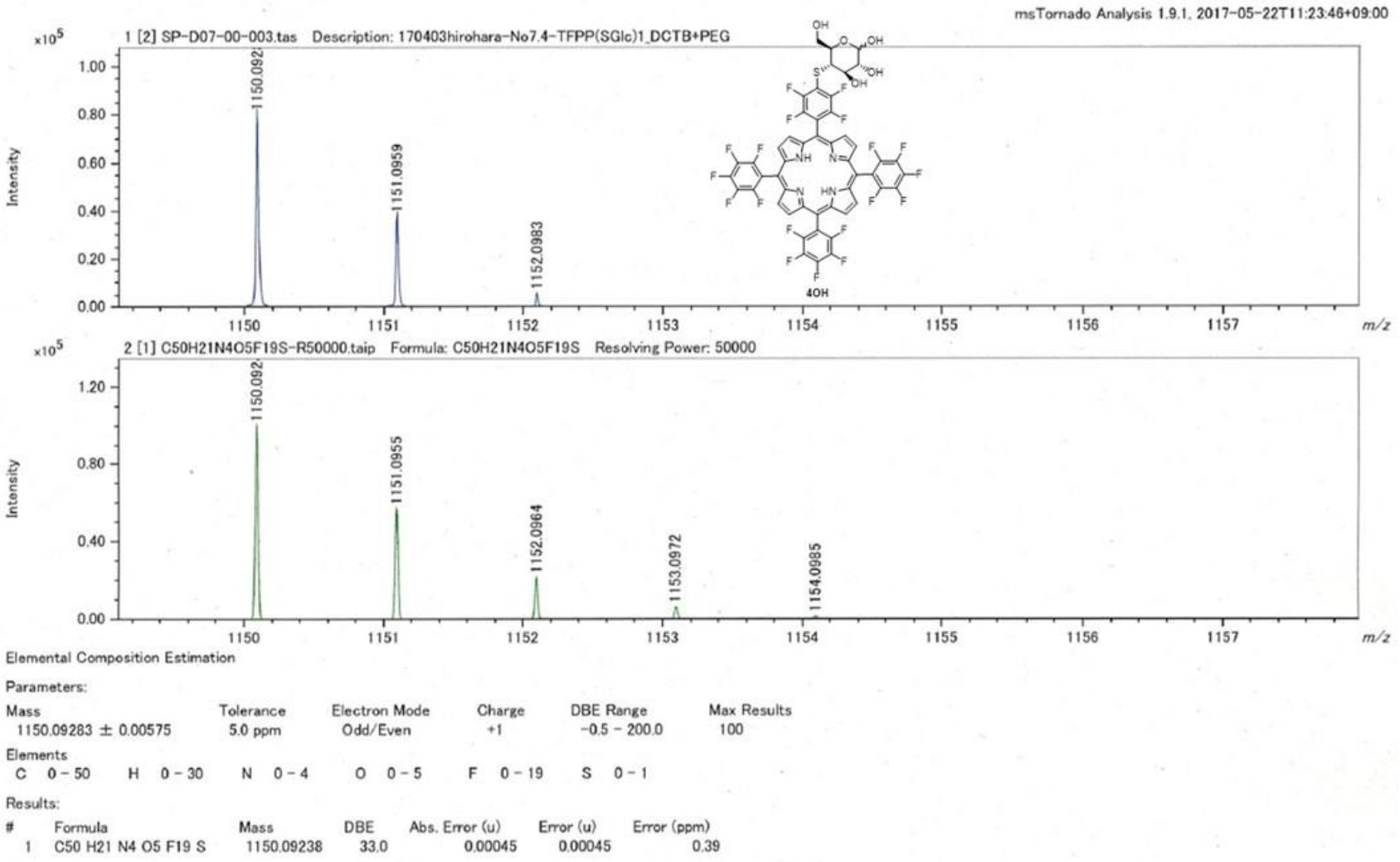

Figure Mass spectrum of **4OH**. (HRMS)

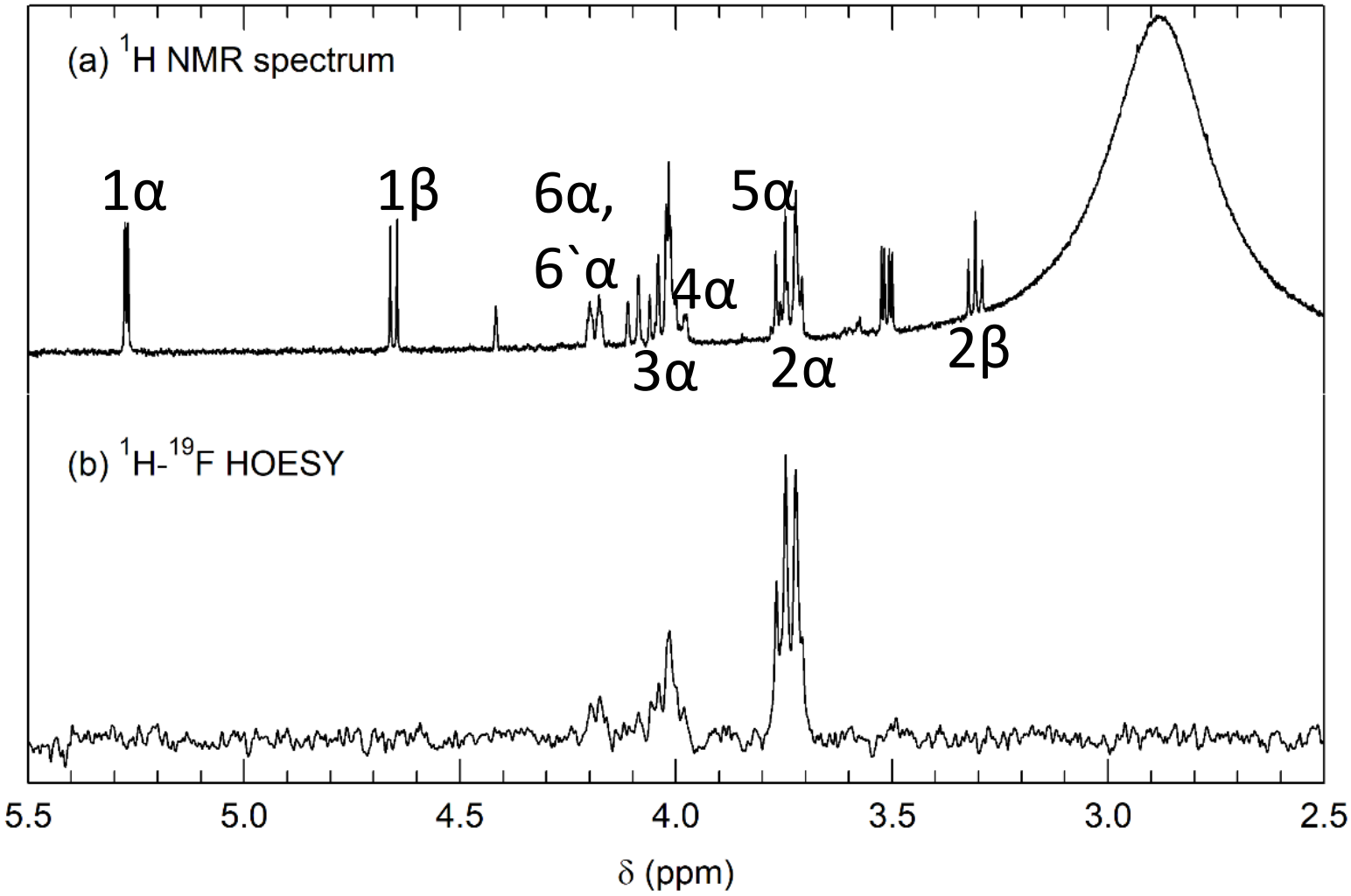

Figure ^{1}H NMR and ^{1}H-^{19}F HOESY spectra of **4OH** in acetone-d_6.

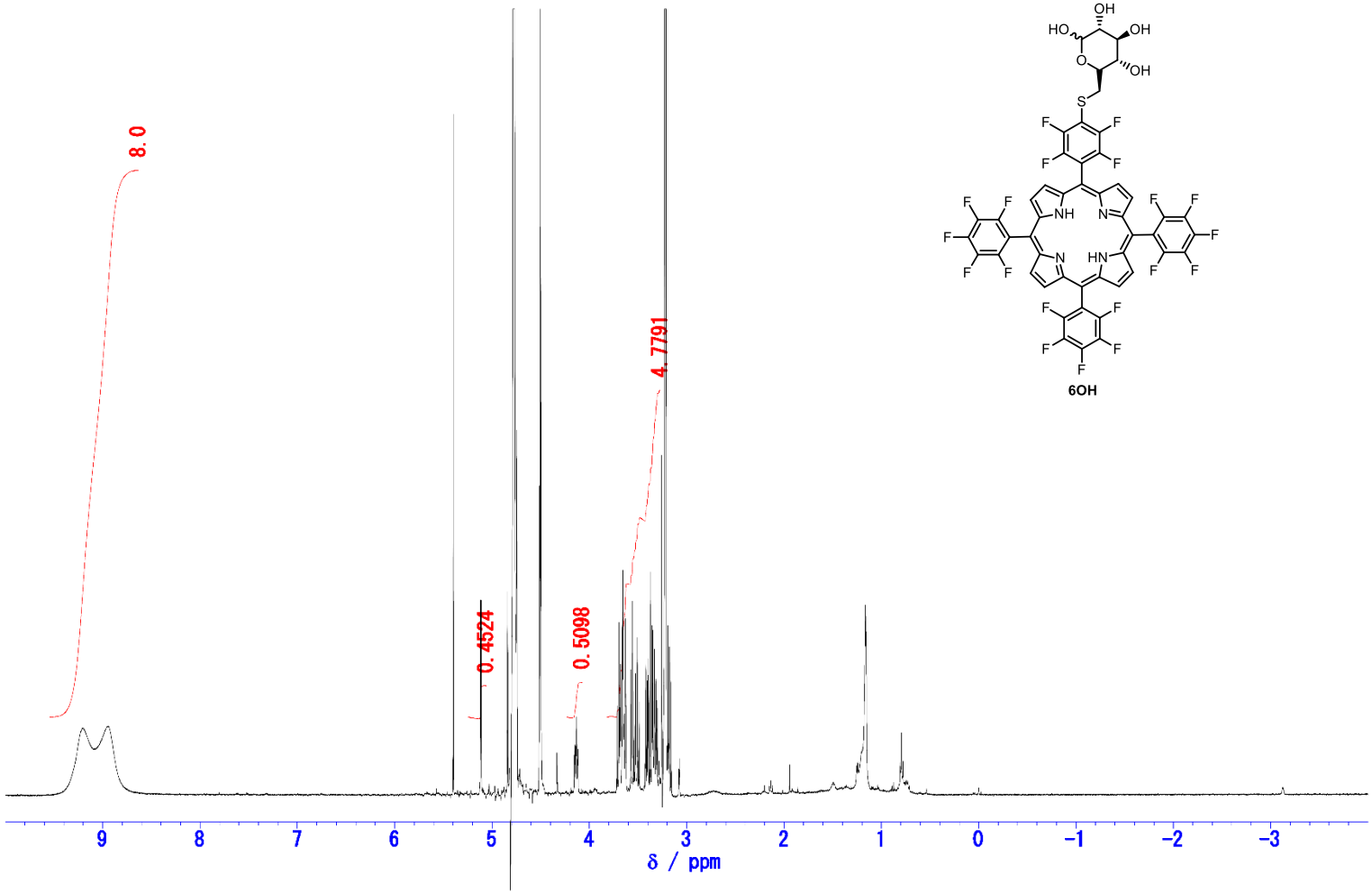

Figure ^{1}H NMR spectrum of **6OH** in CD_3OD. (499.91 MHz)

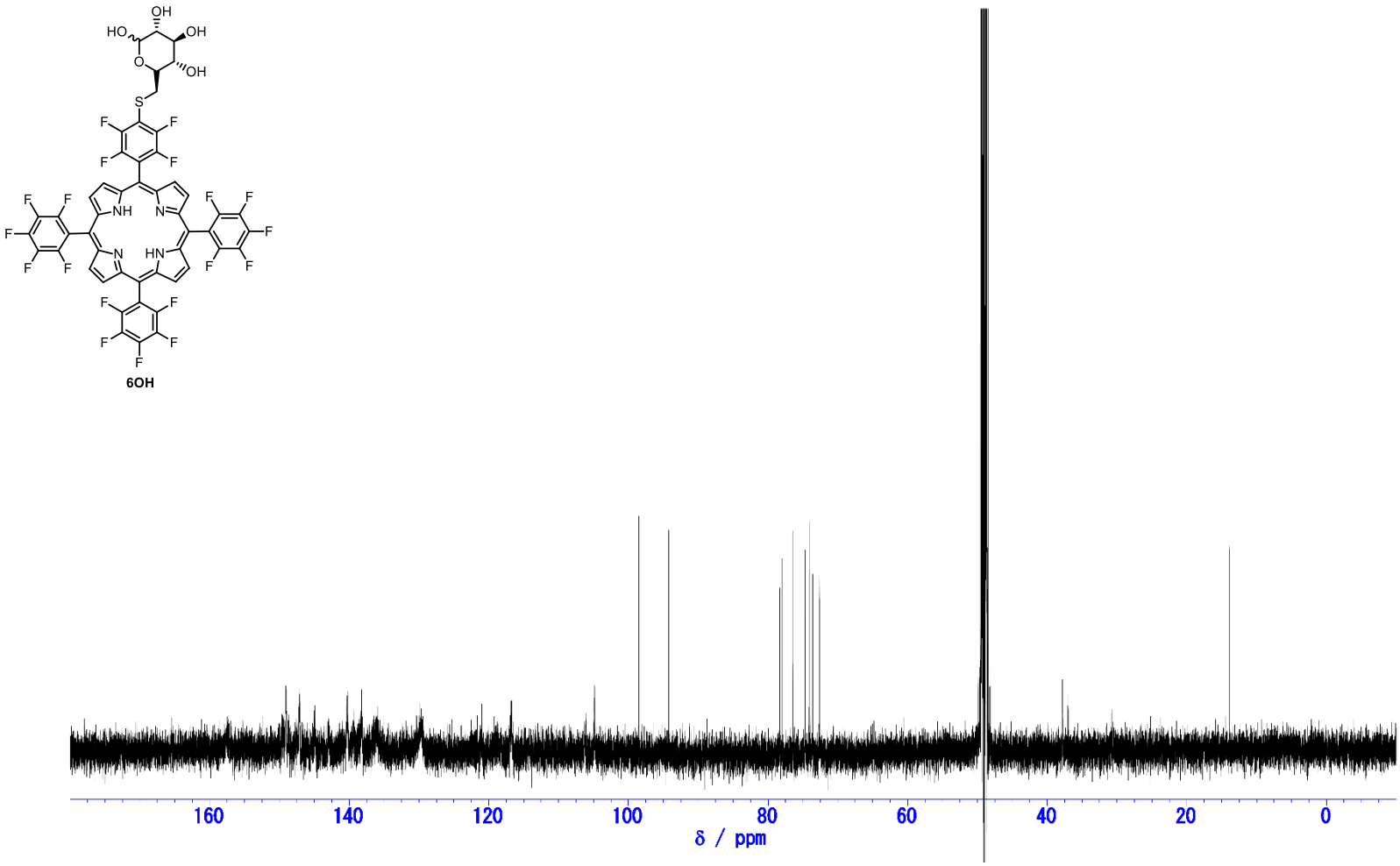

Figure ^{13}C NMR spectrum of **6OH** in $CDCl_3$. (125.72 MHz)

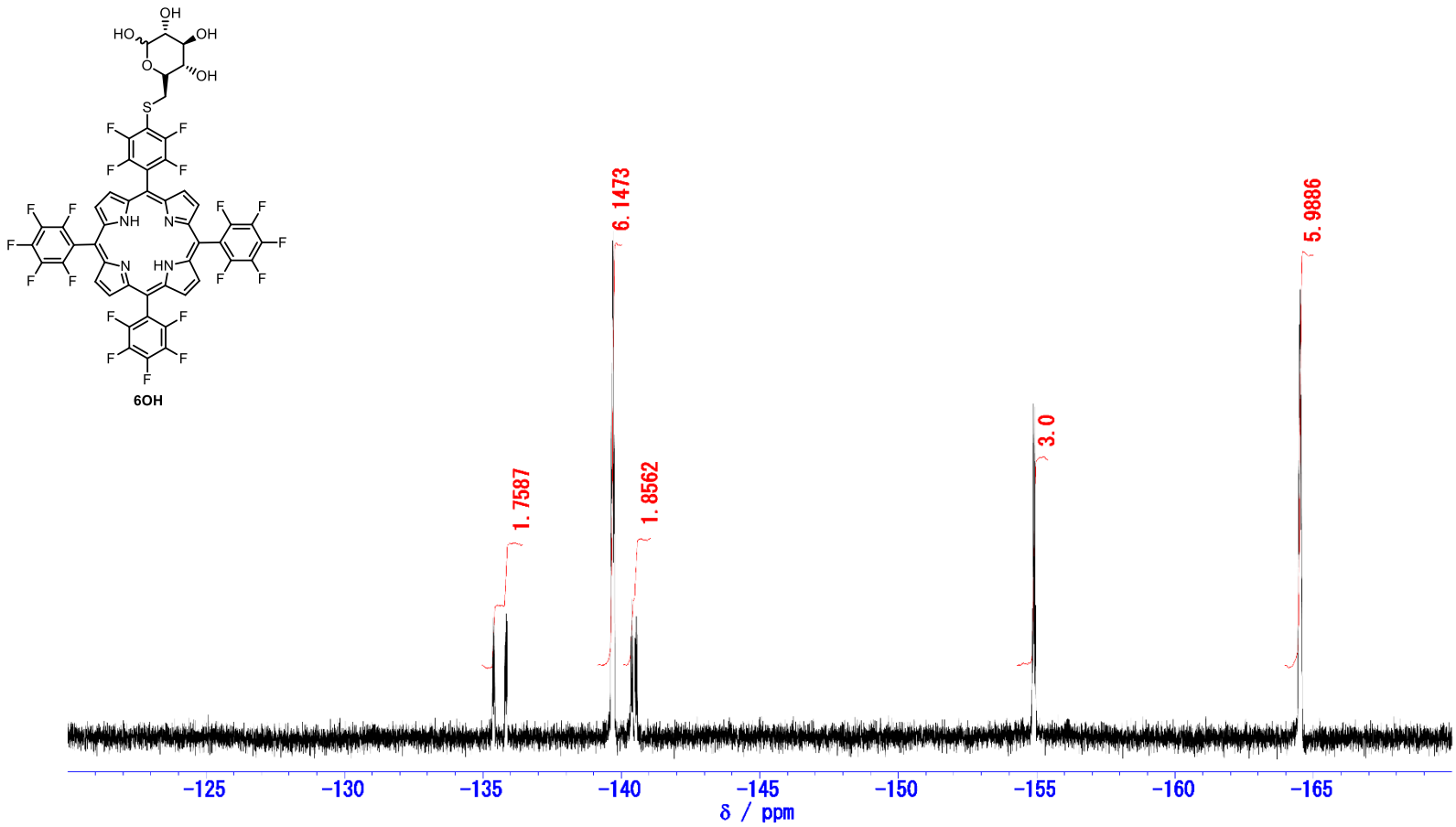

Figure ^{19}F NMR spectrum of **6OH** in CD_3OD. (470.34 MHz)

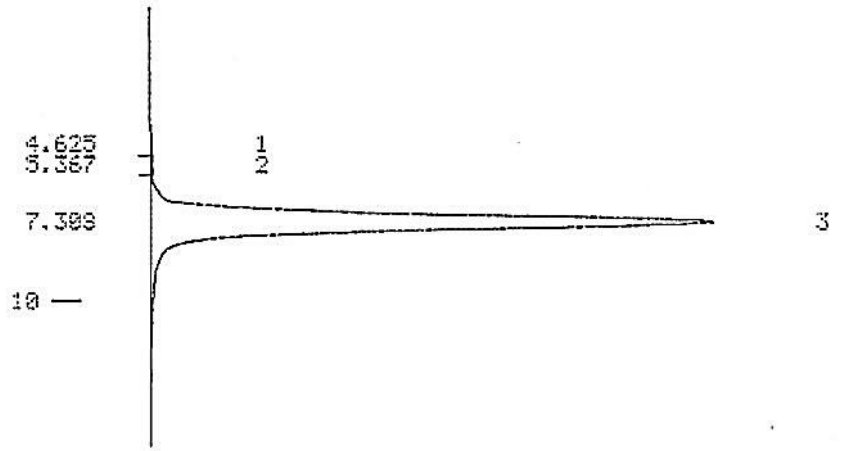

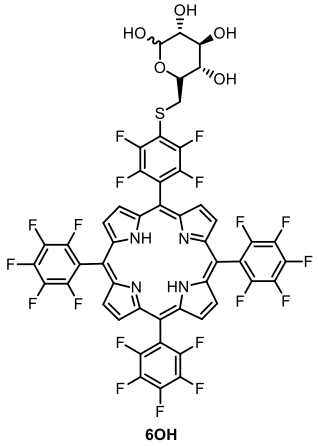

-- % CALCULATION RESULT --

WINDOW = 0 % SCALE FACTOR = 1.0000 PEAK AREA

PEAK#	RT(min)	AREA	HEIGHT	MK	AREA%
1	4.625	52668	1562	LV	0.2237
2	5.367	27320	1127	LV	0.1160
3	7.308	23462807	588916	LLL	99.6602
TOTAL		23542795	591604		100.0000

Figure Chromatogram of **6OH** on NP-HPLC. The conditions of **6OH** was as follows: elution solvent, CH_2Cl_2/ MeOH (9/1, v/v), column, 4.6 mm I.D.×150 mm; temperature, 30ºC; flow rate, 0.5 mL/ min; detector, 410 nm.

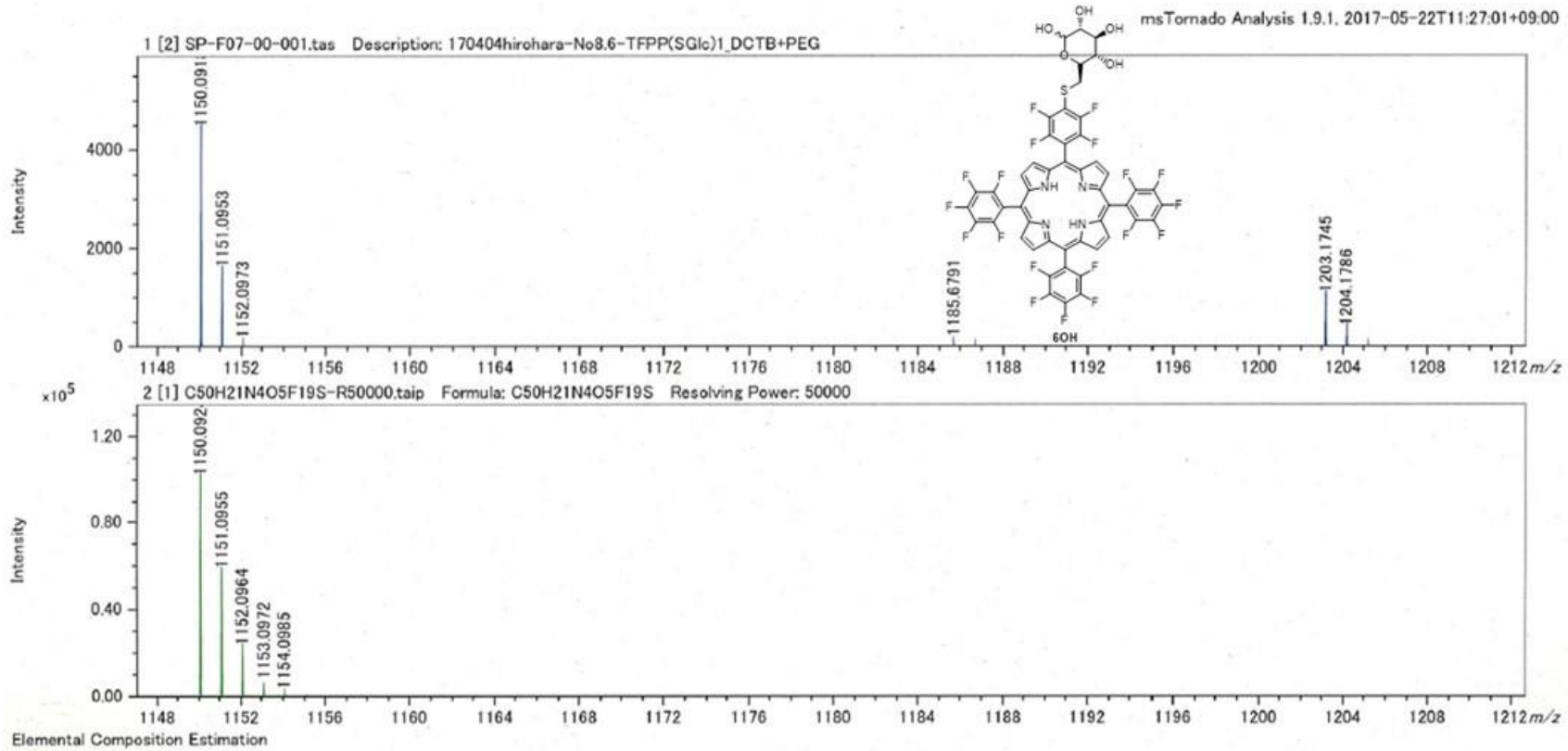

Elemental Composition Estimation

Parameters:

Mass	Tolerance	Electron Mode	Charge	DBE Range	Max Results
1150.09181 ± 0.00575	5.0 ppm	Odd/Even	+1	-0.5 – 200.0	100

Elements

C	H	N	O	F	S
0 – 50	0 – 30	0 – 4	0 – 5	0 – 19	0 – 1

Results:

#	Formula	Mass	DBE	Abs. Error (u)	Error (u)	Error (ppm)
1	C50 H21 N4 O5 F19 S	1150.09238	33.0	0.00057	-0.00057	-0.49

Figure Mass spectrum of **6OH**. (HRMS)

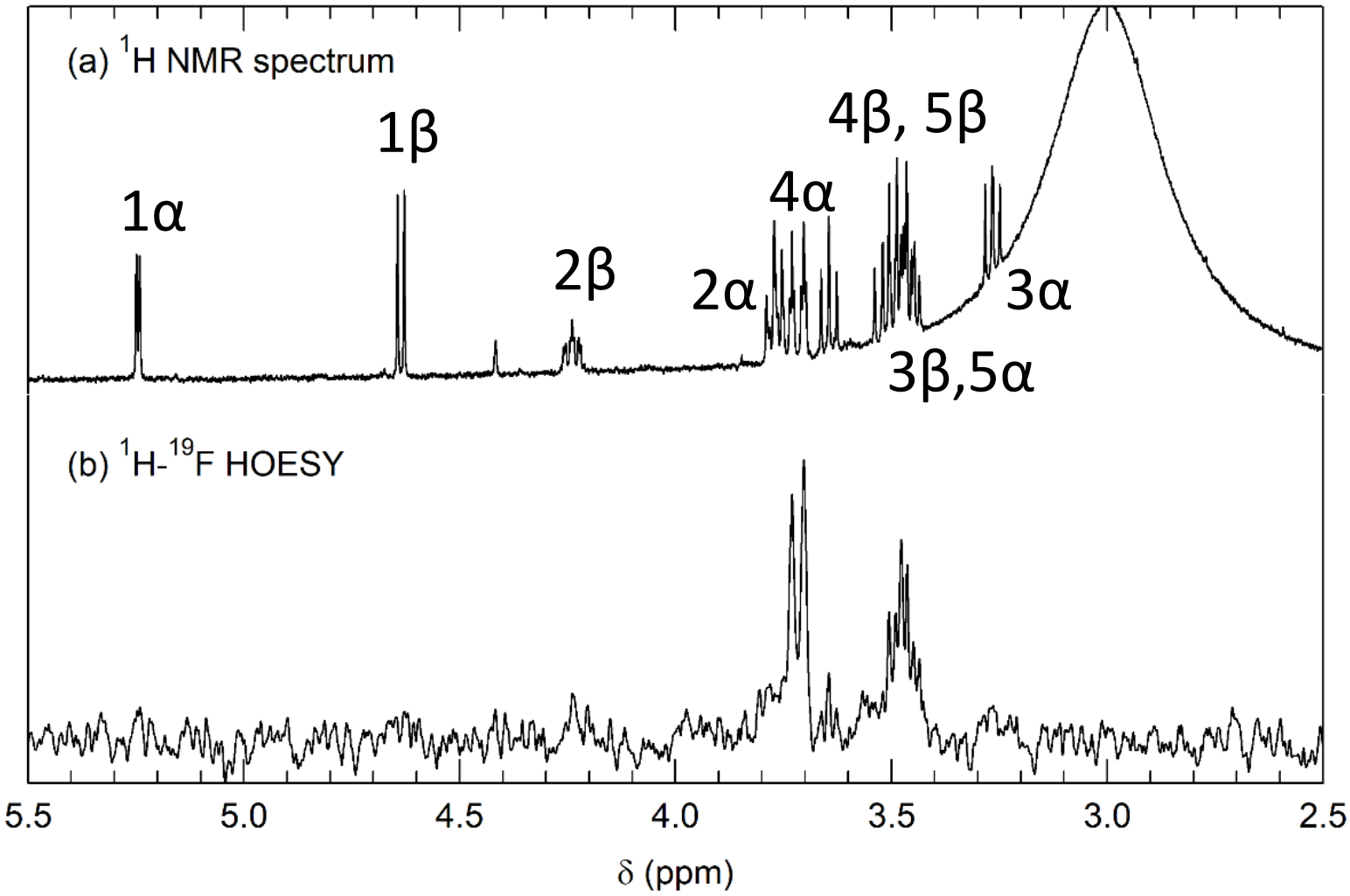

Figure ^{1}H NMR and ^{1}H-^{19}F HOESY spectra of **6OH** in acetone-d_6.

Quantitative ^{19}F NMR Analysis

The purities of TFPP-glucose conjugates were evaluated by quantitaive ^{19}F NMR. 3,5-Bis(trifluoromethyl)benzoic acid (certified reference materials obtained from National Metrology Institute of Japan) was used as a standard material. A precisely weighted TFPP-glucose conjugates and the standard material were dissolved in acetone-d_6. The ^{19}F NMR spectrum of the mixture was recorded on AVANCE III HD (500 MHz; Bruker Biospin K.K., Yokohama, Japan) using flip angle of 90° and relaxation time of 60 s. The transmittance frequency was adjusted the center of two peaks, which used in the calculation to minimize the offset effect. The chamical shift was adjusted using trifluoromethylbenzene (−63.72 ppm) as an external standard.

The absolute weight of TFPP-glucose conjugates can be calculated from the following equation:

$$W_{\mathrm{S}} = W_{\mathrm{R}} \times \frac{A_{\mathrm{R}}}{A_{\mathrm{S}}} \times \frac{M_{\mathrm{R}}}{M_{\mathrm{S}}} \times \frac{N_{\mathrm{S}}}{N_{\mathrm{R}}}$$

W_{S} and W_{R} are the absolute weight of sample (TFPP-glucose conjugates) and reference (standard material), respectively. A_{S} and A_{R} are the peak area of fluorine at 2,6-position of pentafluorophenyl group (approximately −140 ppm) and fluorine of standard material (at −64.5 ppm). M_{S} and M_{R} are molar mass of TFPP-glucose conjugates (1150.7602) and standard material (258.1165). N_{S} and N_{R} are the number of fluorine at 2,6-position of pentafluorophenyl group (8) and fluorine of standard materials (6).

Table Summary of Quantitative ^{19}F qNMR Analysis

	2OH	**3OH**	**4OH**	**6OH**
W (mg)	1.079	1.281	1.307	1.460
W_R (mg)	1.607	1.030	1.181	1.004
A_R	6.000	6.000	6.000	6.000
A_S	1.014	1.968	1.591	2.186
W_S (mg)	0.9081	1.1296	1.0471	1.2231
Purity (wt%)	84.1	88.1	80.1	83.7

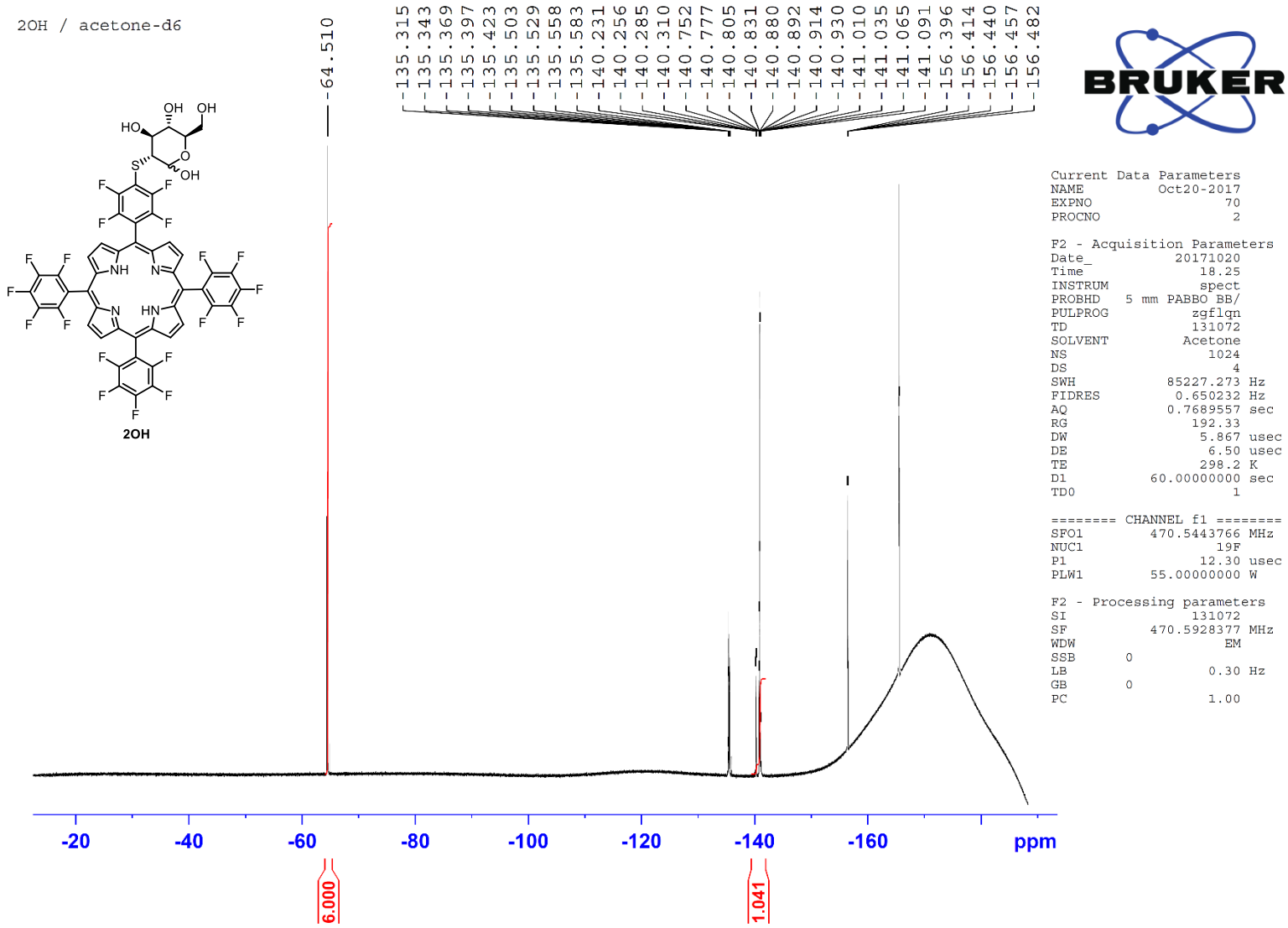

Figure ^{19}F qNMR spectra of **2OH** in acetone-d_6. (470.54 MHz, 3,5-bis(trifluoromethyl)benzoic acid = -64.2 ppm)

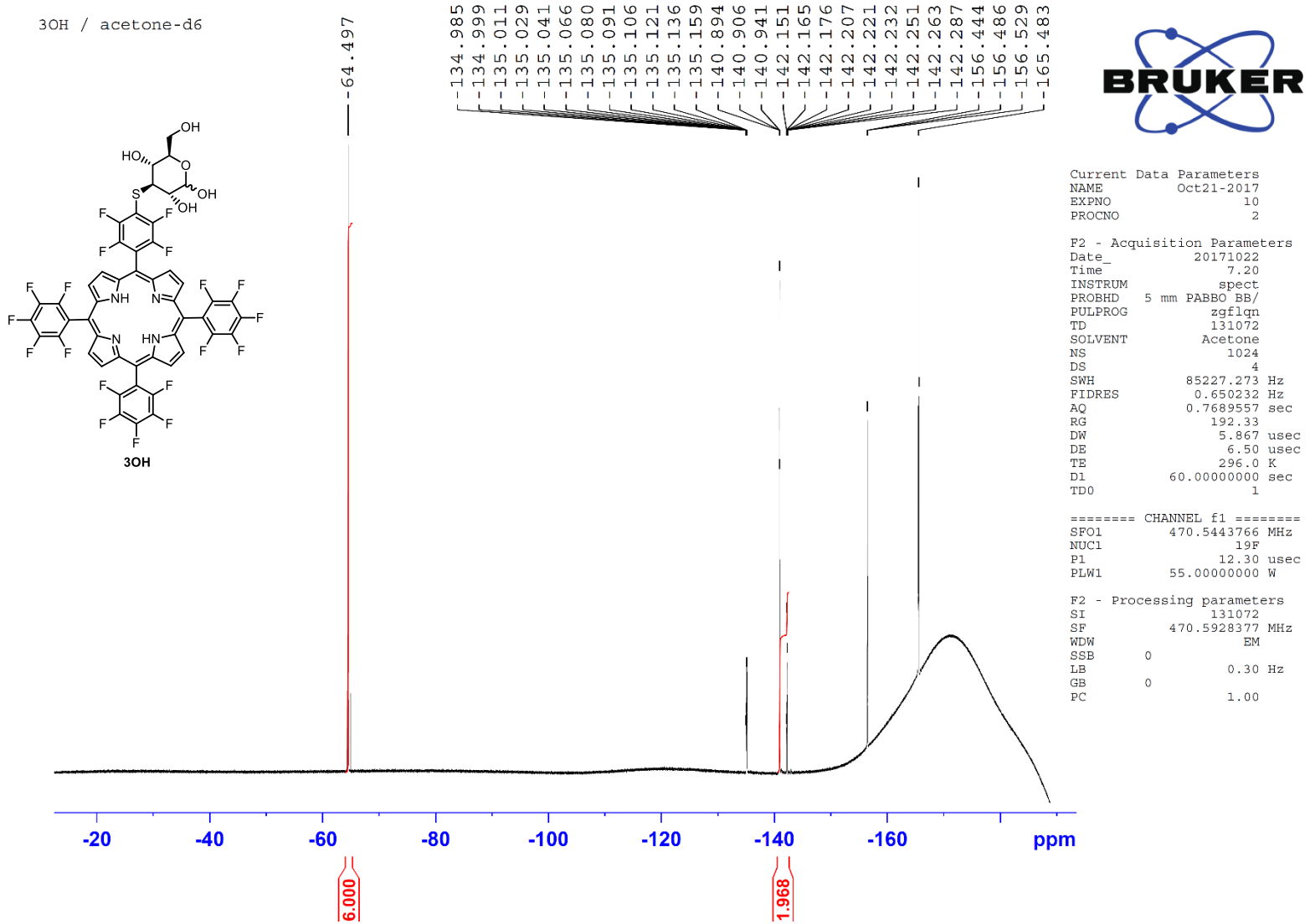

Figure ^{19}F qNMR spectra of **3OH** in acetone-d_6. (470.54 MHz, 3,5-bis(trifluoromethyl)benzoic acid = -64.2 ppm)

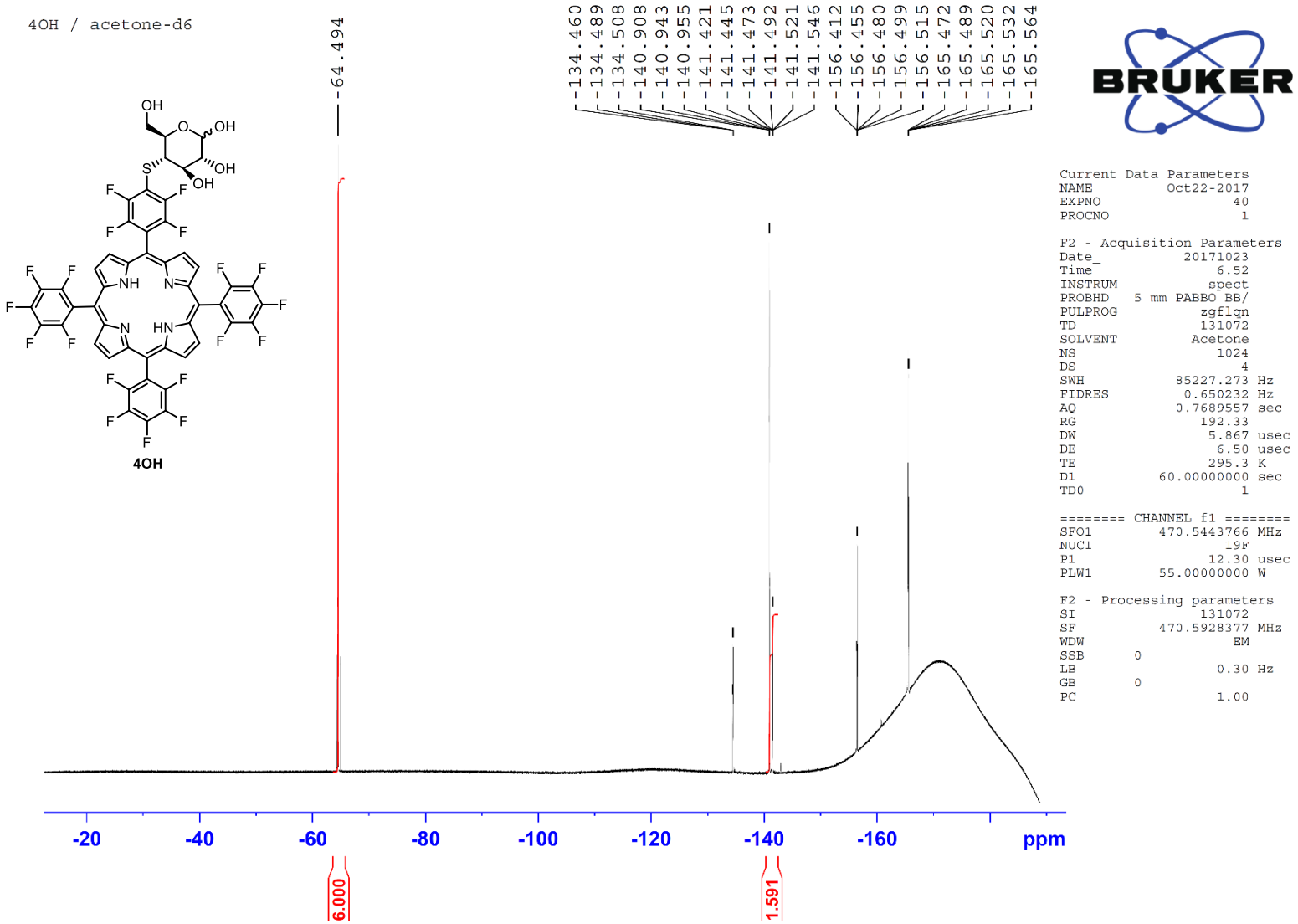

Figure ^{19}F qNMR spectra of **4OH** in acetone-d_6. (470.54 MHz, 3,5-bis(trifluoromethyl)benzoic acid = -64.2 ppm)

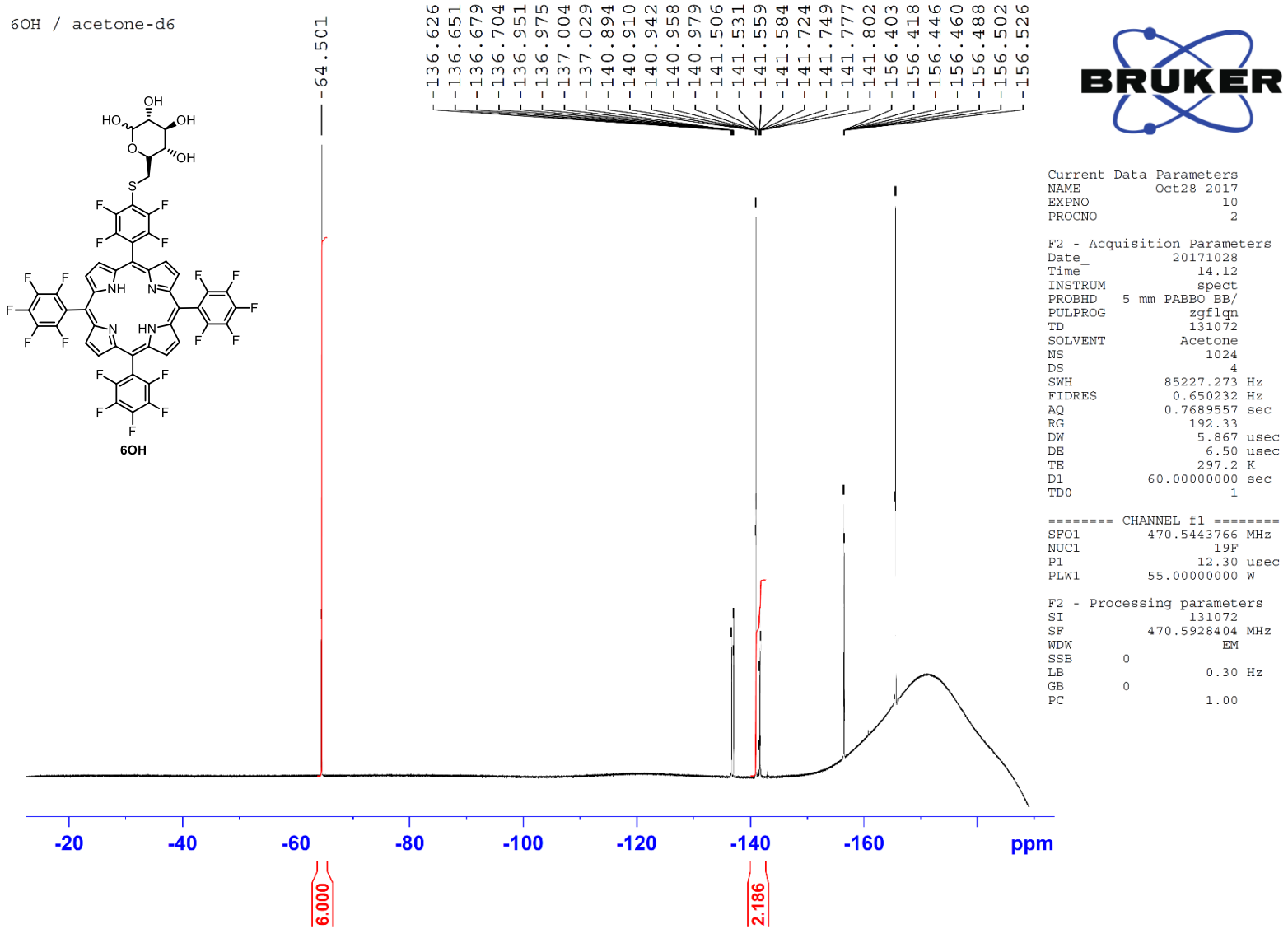

Figure ^{19}F qNMR spectra of **6OH** in acetone-d_6. (470.54 MHz, 3,5-bis(trifluoromethyl)benzoic acid = -64.2 ppm)

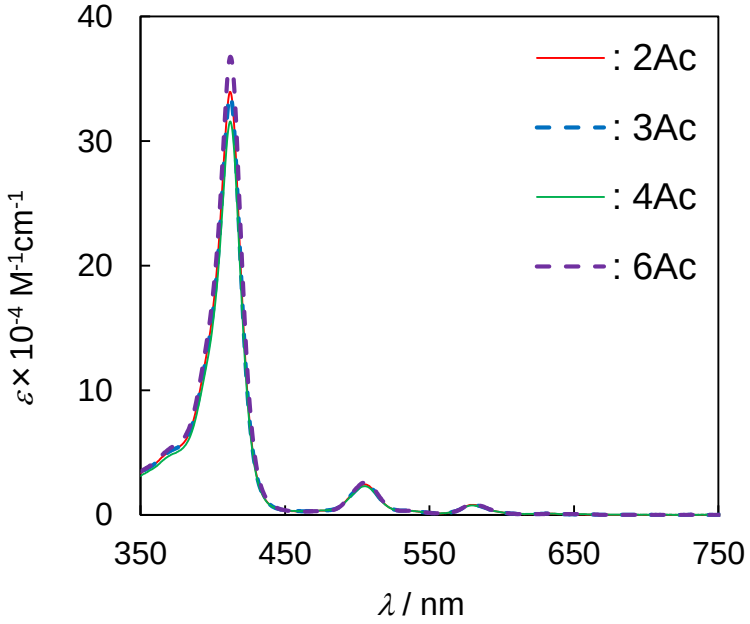

Figure UV-vis spectra of TFPP-glucose conjugates **2Ac**, **3Ac**, **4Ac** and **6Ac** in DMSO at 25°C. [TFPP-Glucose conjugates]= 5.00 μM.

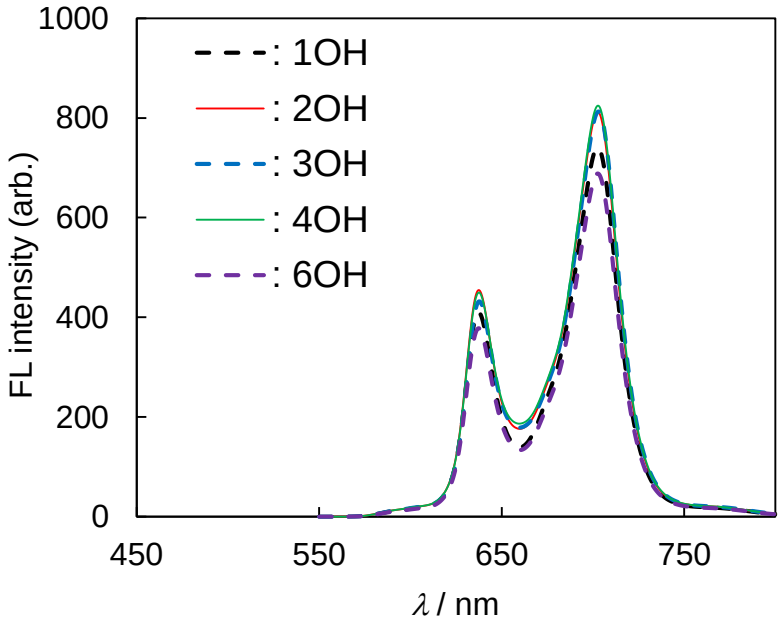

Figure Steady-state luminescence spectra of TFPP-glucose conjugates **1OH**, **2OH**, **3OH**, **4OH** and **6OH** in DMSO at 25°C. [TFPP-Glucose conjugates]= 5.00 μM. The excitation wavelength was adjusted to the maximum absorption wavelength of the Soret band.

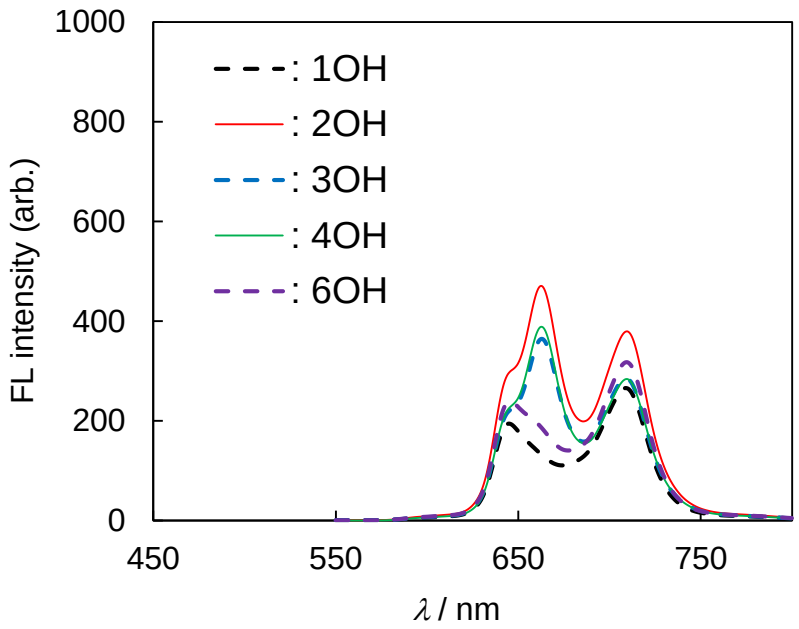

Figure Steady-state luminescence spectra of TFPP-glucose conjugates **1OH**, **2OH**, **3OH**, **4OH** and **6OH** in PBS solution containing 1% DMSO at 25°C. [TFPP-Glucose conjugates]= 5.00 μM. The excitation wavelength was adjusted to the maximum absorption wavelength of the Soret band.

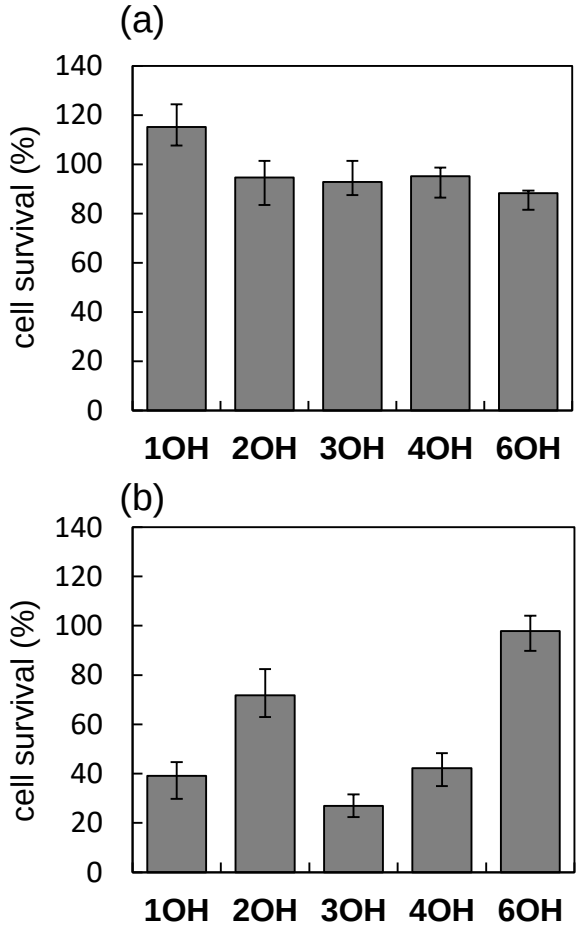

Figure Dark (a) and photocytotoxicity (b) of TFPP-glucose conjugates **1OH**, **2OH**, **3OH**, **4OH** and **6OH** in U251 cells. [Glucosylated porphyrin]= 1.0 μM. The light dose was 16 J cm^{-2} from a 100 W halogen lamp (λ > 500 nm). Incubation time: 24h. Values are the mean ± standard deviation of six replicate experiments.

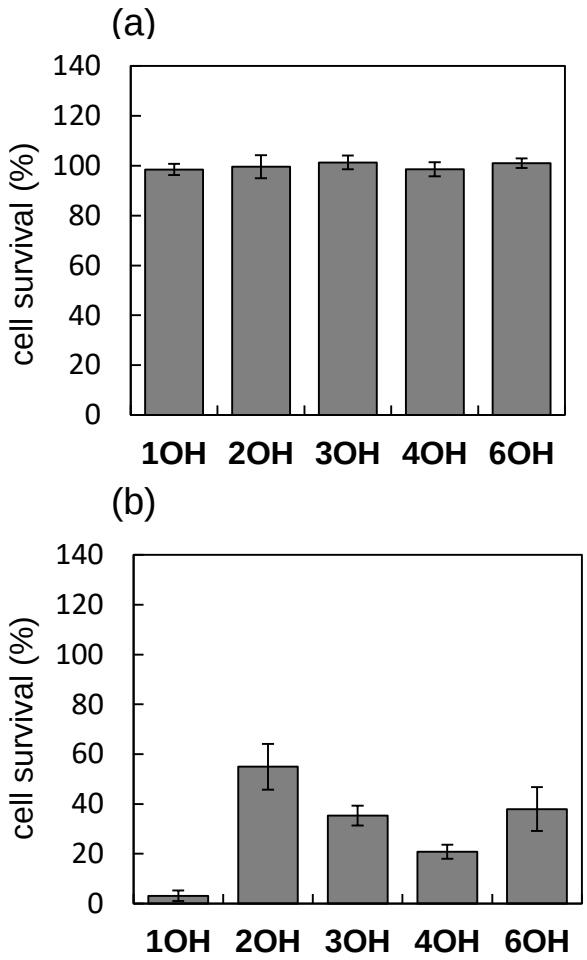

Figure Dark (a) and photocytotoxicity (b) of TFPP-glucose conjugates **1OH**, **2OH**, **3OH**, **4OH** and **6OH** in RGK cells. [Glucosylated porphyrin]= 1.0 μM. The light dose was 16 J cm^{-2} from a 100 W halogen lamp (λ > 500 nm). Incubation time: 24h. Values are the mean ± standard deviation of six replicate experiments.

3-TFPP(SAcGlc)$_{2mix}$

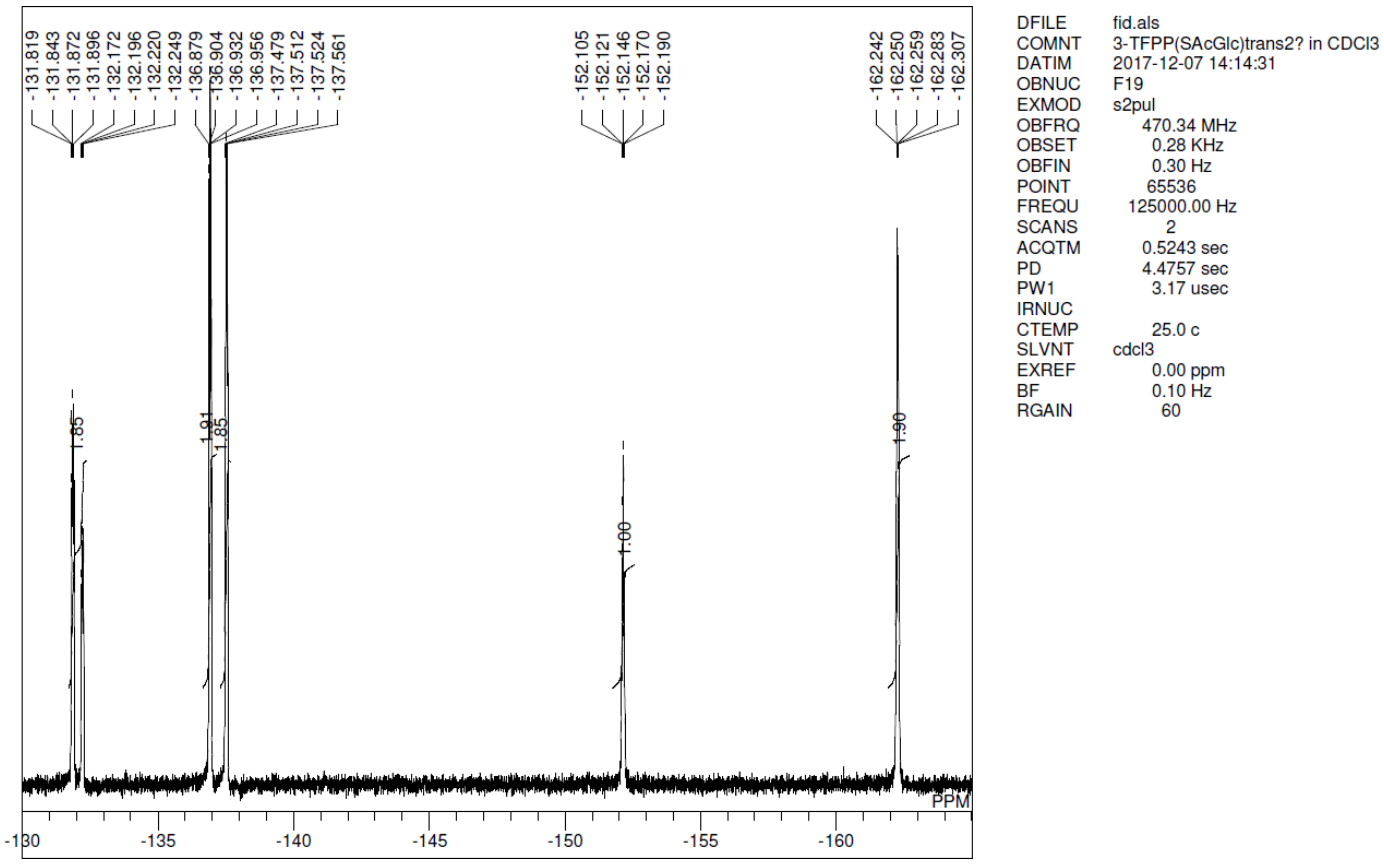

Figure ^{19}F NMR spectrum of **3-TFPP(SAcGlc)$_{2mix}$** in $CDCl_3$. (470.34 MH)

3-TFPP(SAcGlc)$_3$

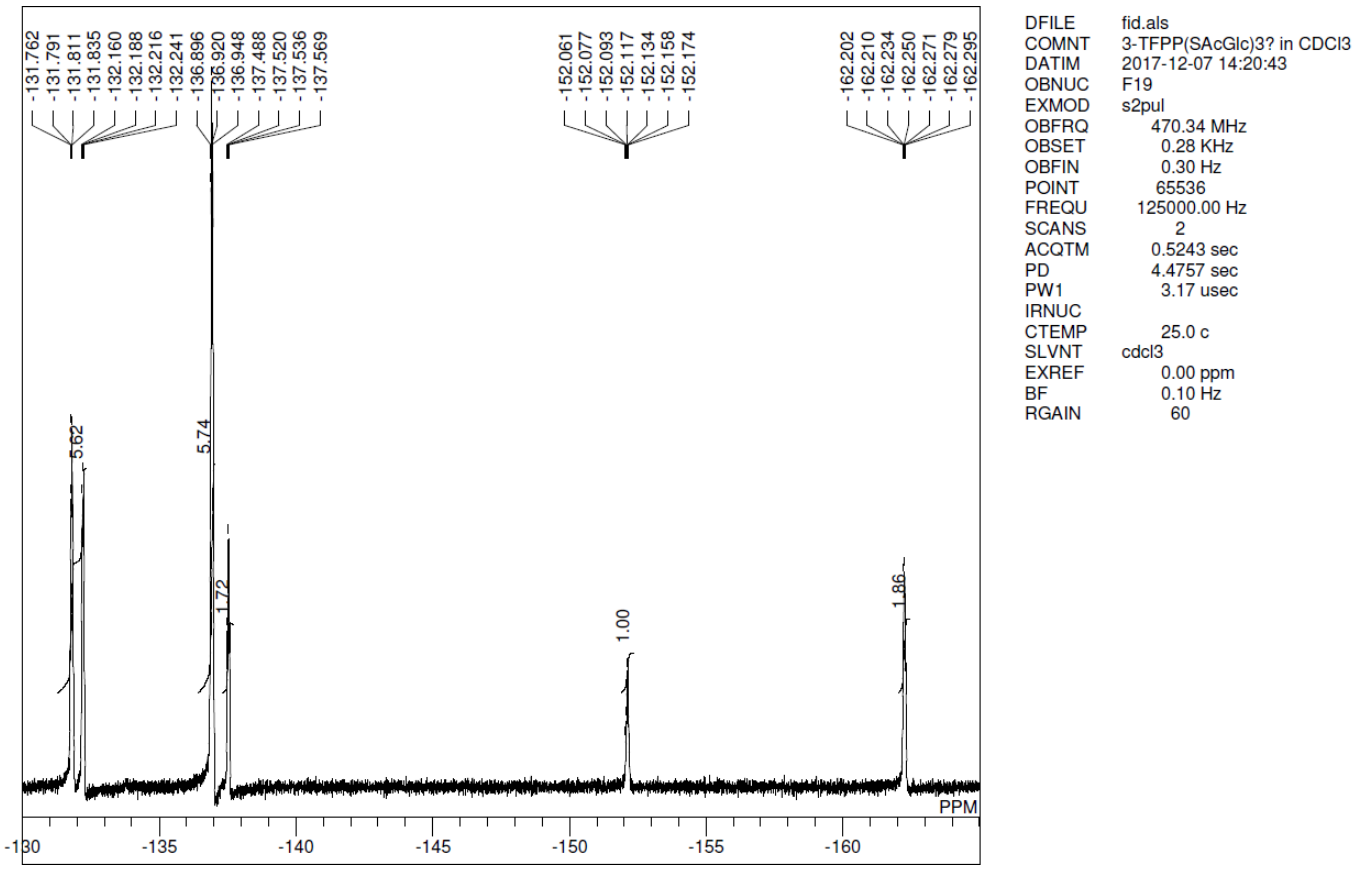

Figure ^{19}F NMR spectrum of **3-TFPP(SAcGlc)$_3$** in $CDCl_3$. (470.34 MH)

4-TFPP(SAcGlc)*cis*-2

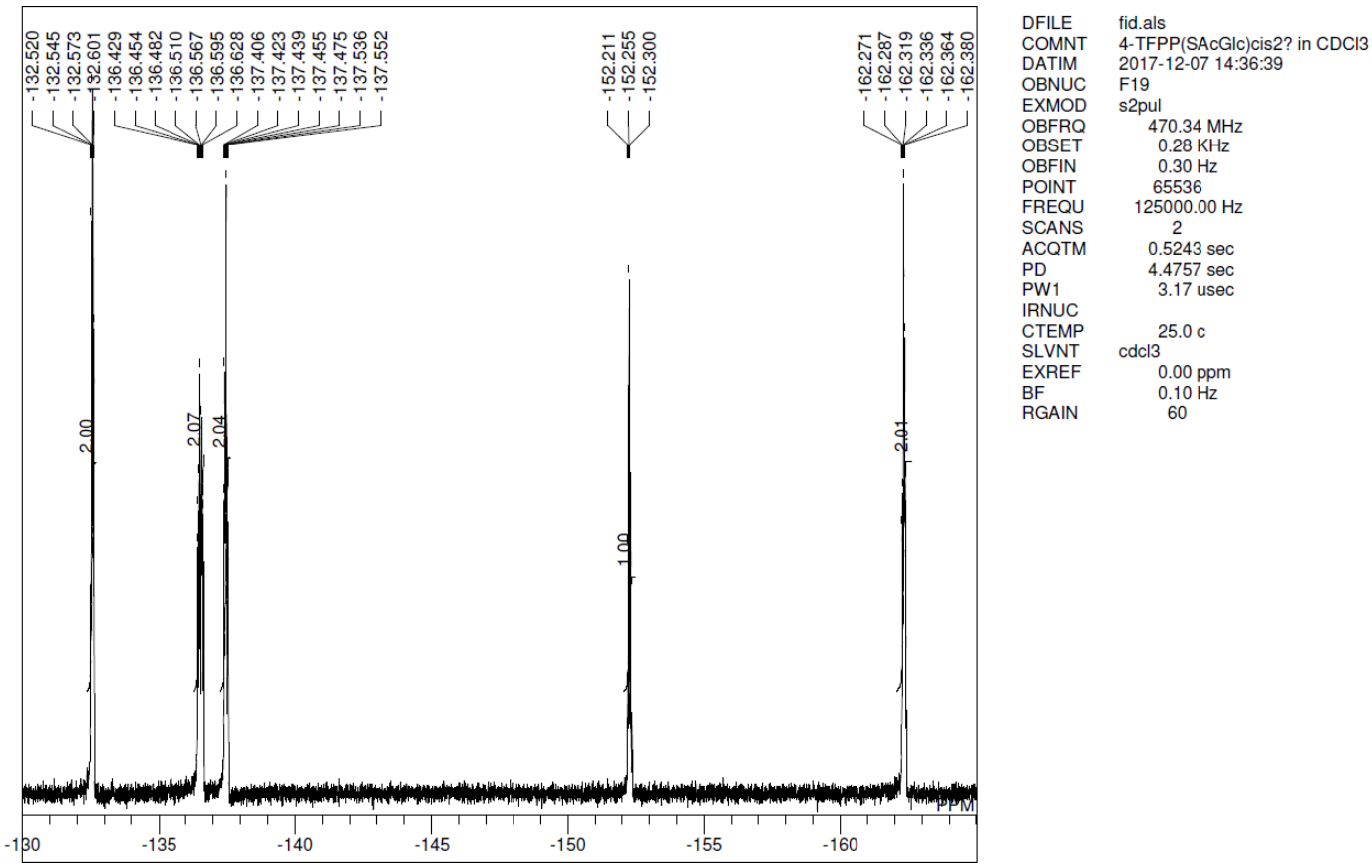

Figure ^{19}F NMR spectrum of **4-TFPP(SAcGlc)*cis*-2** in $CDCl_3$. (470.34 MH)

4-TFPP(SAcGlc)*trans*-2

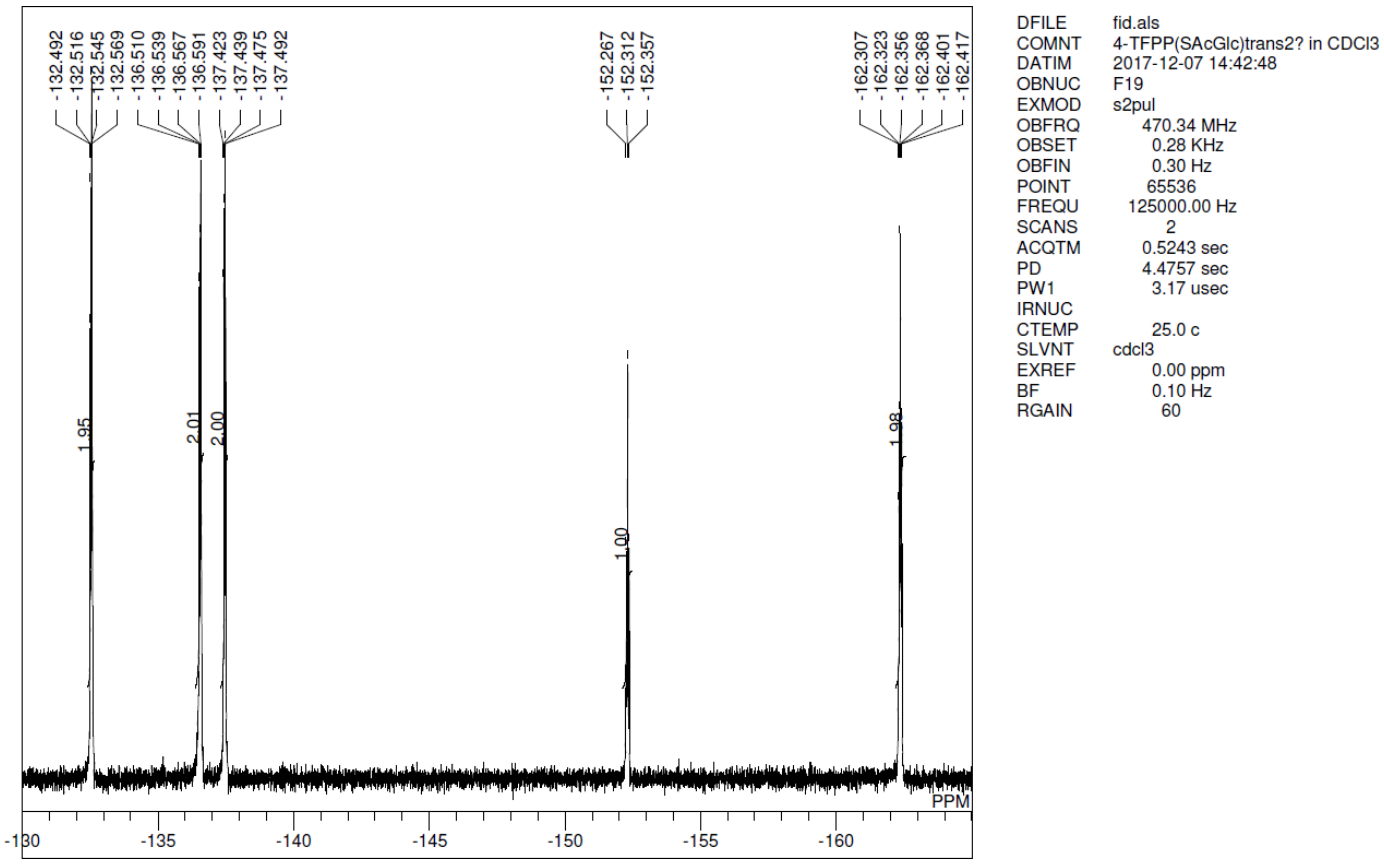

Figure ^{19}F NMR spectrum of **4-TFPP(SAcGlc)*trans*-2** in $CDCl_3$. (470.34 MH)

4-TFPP(SAcGlc)$_3$

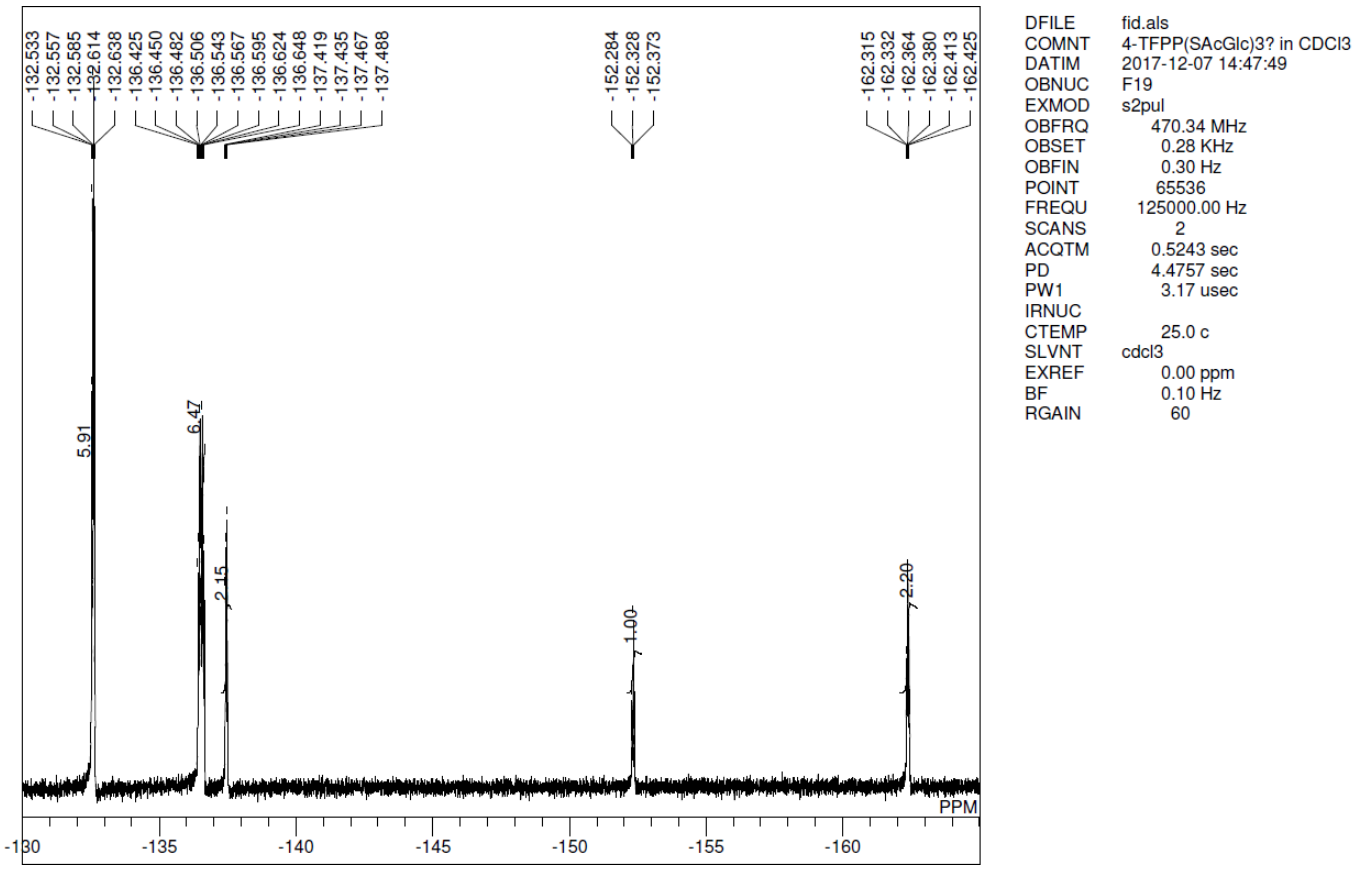

Figure ^{19}F NMR spectrum of **4-TFPP(SAcGlc)$_3$** in $CDCl_3$. (470.34 MH)

4-TFPP(SAcGlc)$_4$

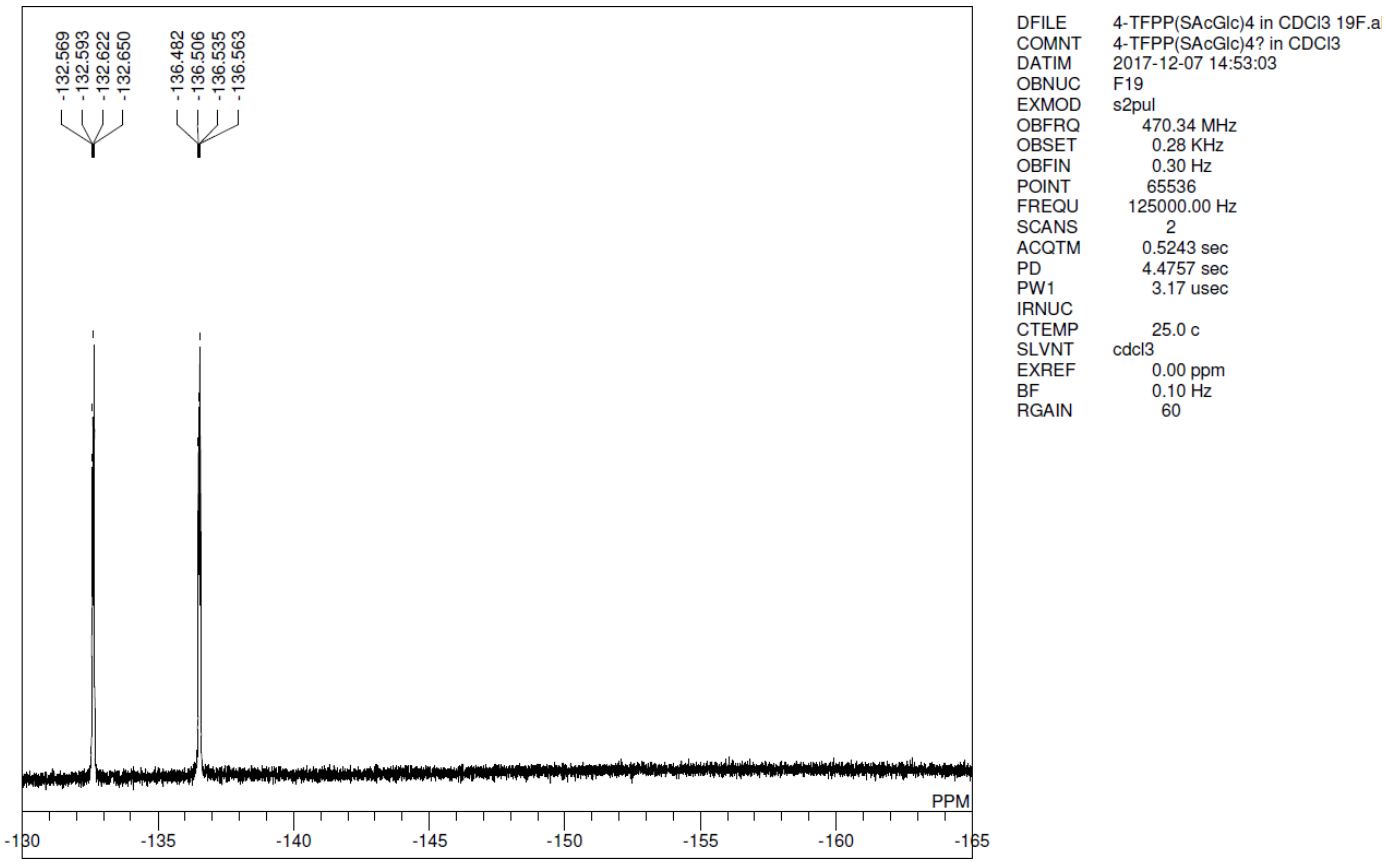

Figure ^{19}F NMR spectrum of **4-TFPP(SAcGlc)$_4$** in $CDCl_3$. (470.34 MH)